"STUDY TO EXPLORE INCLUSION COMPLEXATIONS AND ASSORTED INTERACTIONS OF SOME INDUSTRIALLY AND BIOLOGICALLY SIGNIFICANT MOLECULES IN DIVERSE SYSTEMS"

A thesis submitted to the

UNIVERSITY OF NORTH BENGAL

For the award of

DOCTOR OF PHILOSOPHY (Ph.D.)

In

CHEMISTRY

By

SAMAPIKA RAY, *M.Sc. in Chemistry*

Under the supervision and guidance of

DR. MAHENDRA NATH ROY

Professor of Chemistry

Department of Chemistry

University of North Bengal

Darjeeling, PIN– 734013, WB, INDIA

March

2022

This Thesis is dedicated

To

My beloved Parents, Sister

and

My Husband

DECLARATION

I declare that the thesis entitled "**STUDY TO EXPLORE INCLUSION COMPLEXATIONS AND ASSORTED INTERACTIONS OF SOME INDUSTRIALLY AND BIOLOGICALLY SIGNIFICANT MOLECULES IN DIVERSE SYSTEMS**" has been prepared by me under the guidance of Dr. Mahendra Nath Roy, Professor of Chemistry, University of North Bengal. No part of this thesis has formed the basis for the award of any degree or fellowship previously.

Samapika Ray.

Samapika Ray

Research Scholar

Department of Chemistry

University of North Bengal

Darjeeling – 734013

West Bengal, India

Date: 07.03.2022

UNIVERSITY OF NORTH BENGAL

Prof (Dr.) M. N. Roy,
Awardee of One Time Grant from UGC,
Prof. Suresh C. Ameta awarde from ICS,
Shiksha Ratna by Govt. of West Bengal
and
Bronze Medal from CRSI
Department of Chemistry
E-mail: *mahendraroy2002@yahoo.co.in*

उत्तर बंग
विश्वविद्यालय

Phone : 0353 2776381
Mobile: 09434496154
Fax: 91 353 2699001
Darjeeling 734 013, INDIA
March, 2022

CERTIFICATE

I certify that Smt. Samapika Ray has prepared the thesis entitled "**STUDY TO EXPLORE INCLUSION COMPLEXATIONS AND ASSORTED INTERACTIONS OF SOME INDUSTRIALLY AND BIOLOGICALLY SIGNIFICANT MOLECULES IN DIVERSE SYSTEMS**" for the award of Ph.D. degree of the University of North Bengal, under my guidance. She has carried out the research work at the Department of Chemistry, University of North Bengal.

Mahendra Nath Roy

DR. MAHENDRA NATH ROY

Professor of Chemistry

Department of Chemistry

University of North Bengal

Darjeeling – 734013

West Bengal, India

Prof. (Dr.) M.N. Roy
FRSC (London), UK
Department of Chemistry
University of North Bengal
Darjeeling-734013, India

Date: 07-03-2022

Curiginal

Document Information

Analyzed document	Samapika Ray_Chemistry.pdf (D127905595)
Submitted	2022-02-15T06:20:00.0000000
Submitted by	University of North Bengal
Submitter email	nbuplg@nbu.ac.in
Similarity	8%
Analysis address	nbuplg.nbu@analysis.urkund.com

Sources included in the report

W	URL: http://www.rsc.org/suppdata/c5/ra/c5ra24102b/c5ra24102b1.pdf Fetched: 2021-07-06T00:52:56.3270000	11
W	URL: https://www.ncbi.nlm.nih.gov/pmc/articles/PMC6115366/ Fetched: 2021-12-27T12:04:25.8170000	14
W	URL: https://pubs.rsc.org/en/content/getauthorversionpdf/C4RA07877B Fetched: 2022-01-11T08:35:45.9200000	8
W	URL: https://ir.nbu.ac.in/bitstream/123456789/2854/17/17_chapter%205.pdf Fetched: 2022-02-15T06:21:35.1930000	16
W	URL: http://14.139.211.59/bitstream/123456789/2648/16/16_chapter%204.pdf Fetched: 2022-02-15T06:21:35.2370000	6
W	URL: https://openresearchlibrary.org/ext/api/media/8585e356-73a7-4173-a2d8-425b0bdc1dcd/assets/external_content.pdf Fetched: 2021-04-14T07:31:38.2330000	10
W	URL: https://www.ijiesr.com/liebrary/e14/911425989.pdf Fetched: 2022-02-15T06:21:35.4800000	3
W	URL: https://www.nature.com/articles/s41598-018-31373-x Fetched: 2019-11-30T13:19:15.0370000	1
W	URL: https://innovareacademics.in/journals/index.php/ajpcr/article/download/15164/9522 Fetched: 2022-02-15T06:21:47.5130000	1

Samapika Ray

Signature of the Candidate

Mala Dr. Nath Roy

Signature of the Supervisor

Prof. (Dr.) M.N. Roy
FRSC (London), UK
Department of Chemistry
University of North Bengal
Darjeeling-734013, India

ACKNOWLEDGEMENT

Research is not just to explore new ideas but also to change the perspectives of life. During the course of my research I have come across many people and their contribution throughout the journey is irreplaceable.

Firstly I would like to thanks my honourable supervisor Prof.(Dr.) Mahendra Nath Roy, Dept. of Chemistry, University of North Bengal. I have received constant guidance, important suggestions and inspiration from him all the way through my research work. The motivational words, constant encouragement and support are truly the milestones of my journey of research. It would not have been possible to construct the thesis without his invaluable guidance and support.

My vote of thanks to the Honourable head of the department of Chemistry, NBU and all the respected faculty members, dept. of Chemistry, NBU for their support and assistance. I am thankful to university for supplying me necessary laboratory facilities and University Instrumentation Centre, University of North Bengal for their instrumental supports.

My deepest gratitude to my parents Sri Upen Chandra Ray and Smt. Mamata Ray ; without whom I would have never been able to pursue my research. My special thanks to my sister Miss Sanchita Ray for being my biggest supporter. I would also like to convey my gratitude to my father-in-law, Sri Manoranjan Barman and mother-in-law, Smt. Sabitri Barman for their unbelievable support. The wholehearted cooperation that I got from my husband Mr. Mithun Barman can't be expressed in words.

I would like to thank my lab mates for their constant support and suggestions.

The numerous books, research articles and computer websites have helped me a lot for making my thesis.

Finally, I would like to acknowledge University Grants Commission 'ONE TIME GRANT' Ref No. F4-10/2010(BSR),UGC, New Delhi for financial support.

Samapika Ray.

Samapika Ray
Research Scholar
Department of Chemistry
University of North Bengal
Darjeeling-734013,WB,India

Date: 07.03.2022

PREFACE

The work in the thesis entitled "**STUDY TO EXPLORE INCLUSION COMPLEXATIONS AND ASSORTED INTERACTIONS OF SOME INDUSTRIALLY AND BIOLOGICALLY SIGNIFICANT MOLECULES IN DIVERSE SYSTEMS"** was initiated under the supervision of Dr. Mahendra Nath Roy, Prof. of Chemistry in the Department of Chemistry, University of North Bengal.

The overall work is an endeavour to explore the host – guest inclusion complexation of some industrially as well as biologically significant molecules with cyclodextrins. The work also includes the study of molecular interactions between two bioactive molecules by some physicochemical methodologies.

During my research work, I got opportunities to participate in several meets and seminars across the country. I felt highly motivated by listening and interacting with eminent experts and scientists.

In executing general practice of reporting scientific observation, due acknowledgement has been made whenever the work described was based on the findings of the other investigators. I must take the responsibility of any unintentional oversights and errors, which might have crept in spite of precautions.

I am hoping that all the learning outcomes that I have gathered during the course of my research will definitely make me stronger to take challenges.

ABSTRACT

The research work based on host-guest inclusion complexations and assorted interactions in solution phase of some significant molecules both industrially and biologically. A number of physicochemical and spectroscopic techniques were applied to establish our findings.

The host-guest inclusion complexation actually refers to cyclodextrin molecules as host (we have chosen cyclodextrins) and small or modest size molecules are taken as guest, having biological and industrial value.

The study of inclusion lies on- first the establishment of the inclusion phenomenon i.e. whether the inclusion occurs or not and secondly what changes can be expected after the completion of the overall process of inclusion and also sometimes its execution in biological systems with the help of cell viability or cytotoxicity study between the IC and the pure molecule.

Now in accordance with the title of the thesis, establishment of the formation of inclusion complex is of main concern here as it can cause several modifications in the properties of the guest molecule, which may lead to lessen the toxicity, increase its solubility, stability even it can enhance the bioavailability and decrease the side effects especially for drugs. Drugs that are metabolised before going to the target site , cyclodextrins can be used as carriers for those drugs as CDs are natural, biodegradable and non-toxic.

The research works also includes the study of the interaction of bioactive molecules in solution phase (ternary system). The bioactive molecules that have considerable role in cell functioning were getting into the solution phase to study their interactions through some physicochemical and spectroscopic methods like density measurement, viscosity measurement, refractive indexmeasurement etc. by varying the temperature. The interactions (between solute-solute, solute-solvent and solvent-solvent) that make the changes in the various physicochemical parameters involvehydrogen bonding, ion-ion, hydrophobic-hydrophobic, hydrophobic-hydrophilic, ion-dipole, dipole-dipole etc.

The temperature dependent limiting apparent molar volume gives us the limiting molar expansibility and the value of Hepler constant tells us about the structure making and breaking tendency of solute molecules in solution. The viscosity A and B coefficients deliver a variety of information about the behaviour of solutes or ions.

The characterization of the inclusion complex has been done with numerous spectroscopic techniques; these are NMR (1H, 2D NOESY, ROESY), FTIR, Fluorescence, UV-Vis etc. Other studies were also done for the characterisation of the IC ; PXRD, SEM, ITC and cell viability study.

Indigosulfonic acid dipotassium salt is a derivative of natural dye indigo. It has various applications in different industrial fields. The dye has been incorporated into the cavity of β –CD to reduce its toxicity.

DL-Aminoglutethimide, a drug can cause aromatase inhibition. It possesses the efficiency of inhibiting the synthesis of certain hormones that are responsible for breast cancer and prostate cancers. So it can be used in medical adrenalectomy which is drug induced rather than surgical one. This drug is proved to be an effective medication for the patients having metastatic breast carcinoma. By suppressing estrogen, it inhibits the growth of the hormone-dependent tumors. The inclusion complex of the drug DL-AGT and β –CD is of massive importance in different fields of chemistry.

The guanidine diuretic amiloride hydrochloride has a unique capability of restoring potassium while eliminating sodium with extra fluid from our body. The inclusion phenomena of this drug with α and β-CD have been studied.

Alibendol is an important component of maximum choleretic and cholekinetic drugs. It is also an antispasmodic ,helps to relax muscles. In biliary insufficiency, it shows effective results.

Both uracil and gallic acid are the biologically essential molecules. The nucleobase that present in RNA is uracil. Through bonding with phosphates and riboses, it helps in synthesizing many enzymes in our body; thus facilitates cell functioning. On the other hand, gallic acid acts as an antioxidant and present in many plants and fruits. It accumulates a variety of applications.

Summary of work done:

Chapter I: The chapter includes the scope, application and most importantly the objectives of the research work. It consists of the names of the biologically and industrially significant molecules and the reason behind choosing them as the parts of our work.

Chapter II: This chapter contains the review of the earlier works about the host guest inclusion and the phenomena of solution. Detailed description of the theories of investigation of all the interactions in solution including equations and different studies that have been done during the research work are included in this chapter. The studies are NMR, FTIR, fluorescence, ITC, PXRD, UV-Vis, SEM, HRMS, density, viscosity, refractive index etc.

Chapter III: It covers the experimental section i.e. details of the samples and the working principles of the instrument used throughout the research work. The source, purity, application and physical properties of the drugs, dye, bioactive molecules and cyclodextrin molecules have been thoroughly discussed in this chapter. The instrumental details are covered in this particular chapter.

Chapter IV: Here, the solution behaviour of two bioactive molecules uracil and gallic acid has been studied. With the help of different physicochemical parameters like apparent molar volume, limiting apparent volume, viscosity, refractive index data of the two concerned molecules in solution; a definite idea of their interactions in solution have been received. This will be helpful for future researches.

Chapter V: Here in this chapter we have studied the inclusion phenomenon of the drug alibendol with β-CD with the help of different spectroscopic techniques. The host-guest inclusion has been done so that the side effects of the drug can be reduced to some extent. Job's plot(from Uv-visible study) reveals the stoichiometry of complexation as 1:1. Binding constants at three different temperatures supplied information about the interaction between alibendol and β-CD and the cross peaks present in the 2D ROESY spectra is an authentication of the formation of inclusion complex.

Chapter VI: The chapter includes the study of incorporation of a diuretic drug amiloride hydrochloride inside the hydrophobic cavity of α and β-cyclodextrin. Various characterization techniques have been applied for the establishment of the IC e.g. UV-Vis, ^{1}HNMR, HRMS etc. Theoretical studies showed that the encapsulation of the drug for α-CD is partial and for β-CD is complete and this finding is also satisfied by the values of association constants obtained from Uv-visible study. The antimicrobial activity shown by the complexes formed is commendable than the drug itself.

Chapter VII: The host-guest inclusion complex of DL-Aminoglutethimide and β-CD has been characterised by ^{1}HNMR, FTIR, SEM, PXRD, UV-vis, molecular docking study. The cell viability study has also been done for the IC, which appeared to be nontoxic in comparison to the drug. The inclusion process will be thoughtful in transforming the drug of low toxicity.

Chapter VIII: The encapsulation of a dye molecule Indigosulfonic acid dipotassium salt with β- CD has been studied with certain spectroscopic and calorimetric studies. These were ^{1}H NMR, 2D NOESY NMR, SEM, FTIR, UV-vis, Fluorescence and ITC study. The stoichiometry was found to be 1:1 and all the experimental results suggest the occurrence of inclusion within β- CD. The inclusion complex might be effective in reducing the toxicity of the dye.

Chapter IX: This chapter contains concluding remarks of the research works included in the thesis.

TABLE OF CONTENTS

LIST OF TABLES

LIST OF FIGURES

CHAPTERS	FIGURES	PAGE NO.
	Fig.2: Job plot of β-Cyclodextrin (β-CD) and Indigosulfonic Acid dipotassium salt (ISD) system at λ_{max} (Indigosulfonic Acid Dipotassium Salt) = 289 nm **Fig.4:** Benesi-Hildebrand double reciprocal plot for the effect of β-CD on the absorbance of ISD at three different temperatures 293.15 K, 303.15 K and 313.15 K. **Fig.5 :** Plot of logK_a vs 1/T for the interaction of β-CD with ISD. **Fig.6**: Plot of 1/ΔF (ΔF is the absorbance difference of guest in presence and absent of CD) Vs 1/[CD] ([CD] is the concentration of CD) from the Stern-Volmer equation and fluorescence spectra of Indigosulfonic Acid Dipotassium salt and β-Cyclodextrin at different molar concentration. **Fig.7:** Representative ITC(Isothermal Titrtion Calorimetry) profiles for the titration of ISD(Indigosulfonic Acid Dipotassium salt) (500mM) with β-CD (50 mM) at 298.15 K. figure above represent the raw data for the continuous injection of β-CDs(β-Cyclodextrin) into the ISD(Indigosulfonic Acid dipotassium Salt), after correction of heat of dilution. Figure below is the binding isotherm fitted to the raw data and the bottom panels show the integrated heat data after correction of heat of dilution. **Fig.8:** FT-IR spectra of β-Cyclodextrin, pure Indigosulfonic acid dipotassium salt and ISD-β-Cyclodextrin inclusion complex. **Fig.9**: ^{1}H NMR spectra of β-Cyclodextrin, pure Indigosulfonic acid dipotassium salt and β-CD-ISD inclusion complex. **Fig.10**:2D NOESY NMR spectra of ISD-β-Cyclodextrin inclusion complex.	

CHAPTERS	FIGURES	PAGE NO.
	Fig 11: Structures of Indigosulfonic Acid Dipotassium Salt and β-Cyclodextrin and their schematic representation of inclusion. **Fig.12**: SEM images of (A) pure β-Cyclodextrin, (B) pure Indigosulfonic acid Dipotassium Salt and (C) ISD.β-CD inclusion complex.	

LIST OF SCHEMES

APPENDIX A

LIST OF PUBLICATIONS

1. Probing Inclusion Complex of a Dye (ISD) with Cyclic Oligosaccharide for Minimizing Harmful Effects.

(Included in Thesis)

Journal of Chemical, Biological and Physical Sciences. JCBPS; Section A; February 2021

–April 2021, Vol. 11, No. 2; 304-323,

2. Assorted Interactions Prevalent in Uracil and Aqueous Gallic Acid Solution Explored by Physicochemical Contrivance

(Included in Thesis)

Journal of Advanced Chemical Sciences J. Adv. Chem. Sci. – Volume 6 Issue 1 (2020) 667–670

3. Exploring Existence of Host-Guest Inclusion Complex of β-Cyclodextrin of a Biologically Active Compound with the Manifestation of Diverse Interactions

Emerging Science Journal Vol. 2, No. 5, October, 2018

4. Physicochemical and computational investigations of some food chemicals prevalent in aqueous 1-butyl-1-methyl-pyrrolidinium chloride solutions with the manifestation of solvation consequences

Journal of Molecular Liquids

Available online 21 February 2022, 118800

In Press,

5. Synthesis and Characterization of Inclusion Complex of DL-Aminoglutethimide with β-Cyclodextrin and Its Innovative Application in Biological System: Computational and Experimental Investigations

(Included in Thesis)

***Accepted in ACS OMEGA**

APPENDIX B

List of Seminar/Conference/Workshop attended

1. International Seminar on 'International Year of the Periodic Table of Chemical Elements-2019. 22nd-23rd November 2019. Organized by Dept. of Chemistry. University of North Bengal. (Poster Presentation)

2. SERB sponsored National Conference on 'Green Chemistry: An Alternative of Conventional Chemistry' Organized by: Dept of Chemistry, CBPBU,Cooch Behar, West Bengal, India In association with Indian Chemical Society, Kolkata. Co-Sponsored by: ANTON PAAR INDIA PVT. LTD Date:20th-21st September,2019. (Poster Presentation)

3. National Seminar on ''Frontiers in Chemistry-2020" March 5, 2020, Organized by Dept. of Chemistry, University of North Bengal.

4. TWO DAYS NATIONAL WEB-BASED CONFERENCE ON "ENVIRONMENTAL DETERMINISM, DIVERSE POLLUTIONS, SOURCES AND CONTROLLING MANAGEMENT THROUGH SCIENCES AND HUMANITIES" .22nd and 23rd March, 2021. Organized by Alipurduar University. (Oral Presentation)

CHAPTER I

NECESSITY OF THE RESEARCH WORK

I.1. OBJECT, SCOPE AND APPLICATION OF THE RESEARCH WORK

Research is a continuous effort of exploring new ideas, new definitions where all the new dimensions arise in a broader way. It can be done in any field. In the field of science research based ideas are of immense importance. Scientific research comprises of collecting data and establishing new facts with evidences. It's not only developing concepts, perceptions but also help in diminishing faulty beliefs. Research is a construction of new base. It is a practice to understand the human race and to find out how this understanding can be made beneficial for the whole world. For the betterment/growth of science researches are going on in every field of science especially in medicinal/pharmaceutical chemistry.

Nowadays supramolecular chemistry based researches are enforcing great impact in biomedical science unlike conventional chemistry. Supramolecular assemblies consist of discrete number of molecules by non-covalent interactions . There are enormous applications in the area of host-guest supramolecular chemistry, likewise drug delivery, catalysis, pharmaceutical and nano technologies. The exceptional noncovalent interactions between guest and the complementary host molecule result unbelievable outcomes ;that is why it is also termed as molecular recognition. Molecular self assembly can be constructed in order to get a pre-planned stoichiometry by taking a biologically potent or chemically reactive entity and a template which can be made according to requirements of the chemistry we are looking for. Modern approaches are progressing in the same technique. In making of larger structures e.g. vesicles, micelles, nano rods, membranes etc. this technique is somewhat difficult to maintain as they are not energetically favourable in such situations.

Inclusion complexation is an inevitable part of the host-guest chemistry. It is possible to explicate their structures by monitoring their type of interactions or attachments. The association constant of the above type of binding can be determined by

studying the thermodynamics of the complexation process. The main benefit of host-guest supramolecular chemistry is in the manufacture of functionalised biomimetic systems. It has great biomedical advantages. Targeted drug delivery and controlled release of the drug by using supramolecular systems reduce the side effects of the drug and make it more efficient in its therapeutic activity. Other important advantages in cell biology applying supramolecular designs are of utmost credit. The stability of the typical host-guest inclusion complex depends on a number of non-bonding interactions e.g. hydrogen bonding, van der Waals forces, hydrophobic forces and some electrostatic interactions.

Cyclic macromolecules introduce innovative thoughts in host-guest chemistry associated researches. Basically they don't have any end group. Porphyrins, cyclodextrins, crown ethers, calixarenes are the standard examples of macrocycles or macromolecules. They all have molecular hollow space. Among a lot of these macromolecules cyclodextrins are quite fascinating due to various reasons. Cyclodextrins have hydrophobic interior cavity with hydrophobic exterior which makes them soluble in water and by choosing specific guest molecules, they are competent enough to make inclusion structures.

Cyclodextrin-tailored nano particles are presenting great influence to improve the features of the consequential systems, such as conductance, electronic, thermal, and catalytic actions. A number of molecular architects have been planned to advance the efficacy of certain macromolecular systems. These are proved to be effectual in making different type of molecular machines, nanosensing, nanotubes etc. [1] [2] [3] [4] [5]

Host-guest inclusion complexation including cyclodextrins or cycloamyloses covered a huge region in advanced science. They have vast application starting from food, chemical industries, cosmetics ,drug delivery, pharmaceutical to environmental and agricultural sciences.[6] CDs can be produced by the enzymatic degradation of starch. There are three types of CDs in nature such as α ,β and $^{\gamma}$ CDs with 6,7,8 glucopyranose units. Due to the toroidal cone shaped CDs can completely or partially trap hydrophobic molecules into the cavity. The moderate cavity diameter of β- CD is suitable for encapsulating the guest or the entering molecule. Inclusion complexes of CDs are acceptable worldwide due to various reasons e.g. CDs have low production cost, water

soluble, low toxicity and appropriate cavity diameter. The host molecules that are taken here are α and β-cyclodextrins. The properties of the entering guest molecule have been changed greatly after complexation. These include solubility, permeability, stability, effectiveness, bioavailabiity, taste etc. Several bioactive molecules are being entrapped inside the CD moiety to improve their physical and chemical properties. [7, 8]

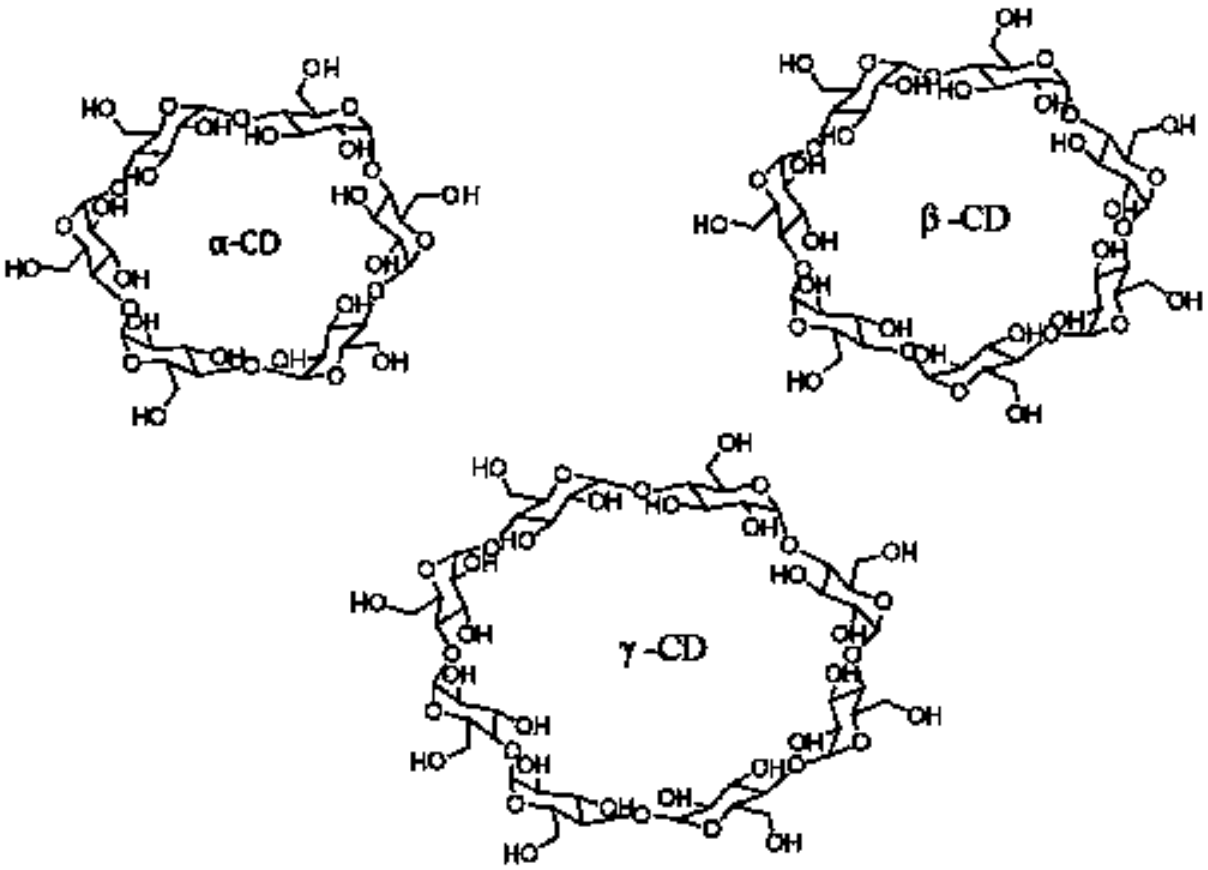

Fig.I.1. Structures of the Cyclodextrin molecules

To understand the chemistry of solution one need to understand the change in properties of an entity when it is dissolved in a new substance i.e. one needs to have a clear idea about the nature of solute and solvent molecules. What changes are taking place after they get into solution phase and also what kind of interactions are going on etc. should be taken into consideration . There will always be some anomaly when different solutes and solvents are mixed together. Studies of the aqueous solution of different molecules have given a variety of information regarding various thermodynamic properties. The contribution of a lot of intermolecular forces are there in

the process of solvation, these are dipole-dipole,ion-dipole,H-bonding, van der Waals forces. [9] The solute-solute interaction of uracil and gallic acid has been studied here.

In pharmacology, sustained release of the drug molecules is a very crucial thing. These types of bioactive molecules can be protected by encapsulating them inside the cavity of cyclodextrins to retain their therapeutic activity and to lessen their adverse effects. Moreover, it is also important to confirm that the inclusion complex has been formed between the host and the guest molecules. In order to achieve such goals inclusion complex of some biologically potent molecules with α and β cyclodextrins have been investigated. The concerned bioactive molecules are DL-Aminoglutethimide, Amiloride hydrochloride, Alibendol. On the other hand to minimize the harmful effects of certain dyes, complexation of the dye with cyclodextrin is considered to be a unique approach. Here complexation of Indigosulfonic Acid Dipotassium Salt with β-CD has been studied.

The synthesis of inclusion complex of the dye, Indigosulfonic acid dipotassium salt (ISD) and β- CD has been done along with characterization by different types of spectroscopic studies and calorimetric study. ISD is a derivative of indigo which is a natural dye. The application of dyes are vast including colouring food, textiles, medicinal products, cosmetics and they generally have complicated aromatic chemical structures. [10] Because of intramolecular H-bonds ISD seems to have high melting point. Moreover every synthetic dye must have some toxicity likewise ISD shows some toxicity when consumed. Whereas, β-CD has very low toxicity. So, formation of inclusion complex makes the overall moiety less toxic. The inclusion phenomenon of ISD and β-CD was studied to reduce the toxic effect of the dye. [11-14] [14-17]

The encapsulation of the drug DL-AGT and β-CD was investigated both in solid and liquid phase and it was also examined by the cell viability study that the inclusion complex is non-toxic. DL-Aminoglutethimide (DL-AGT) is an aromatase inhibitory drug. Formerly it was used as an anticonvulsant in United States but soon withdrawn from market due to some unanticipated side effects. It showed unusual side effects on various endocrine organs particularly adrenal. It restricts quite a lot of enzymes in the adrenal cortex. Its anomalous side effect turned out to be a blessing in the endocrine therapy. Hormone dependent human breast neoplasms are generally stimulated by estrogen

hormone can generate hormone dependent breast carcinoma. It can be possible to suppress the estrogen level by the use of some aromatase inhibitory drug and for that DL-AGT has been seemed to be effective. The antitumor efficacy of DL-AGT by suppressing estrogen found to be more productive in drug induced medical adrenalectomy than surgical adrenalectomy for the treatment of advanced breast cancer. Besides all these benefits DL-AGT has lack of specificity and side effects that are not linked to deprivation of estrogen. To make the drug more specific in its therapeutic activity and to decrease the side effects of it, an inclusion process has been done between the drug and a cyclic oligosaccharide β- CD. [18] [19] [20] [21]

There are already diverse pharmacological applications of the drug Amiloride hydrochloride (AMHCl) in literature. AMHCl is a guanidine diuretic, having an unlikeable taste ,synthesized first withinside the lab of Merck, Sharp and Dohme. It is 3,5 diamino-N-(aminoiminomethyl)-6-Chloropyrazine carboxamide. It has minor natriuretic, diuretic effects. It can expel sodium, holding potassium and used as a remedy in hypokalemia. AMHCl is used for the treatment of congestive heart collapse or high blood pressure. As the extra sodium is discarded in conjunction with excess water from the body, the blood pressure automatically reduced. Being a BCS drug of class III it possesses high solubility and less permeability.

The administration of any drug orally includes an array of limitations due to enzymatic degradation and first pass metabolism in the GI tract. Most of the drugs are metabolised in the gastrointestinal tract and thus the effective dose for the activity of the drug decreases i.e. its bioavailability decreases. Due to belonging to a BCS class III drug AMHCl has less efficient to pass through biological membrane. Now a days buccal routes are considered to be the smartest way for the drug to be orally administered. The drugs that can't be administered due to unpleasant odour can be taken as a form of mucoadhesive films as reported in the literature .

The inclusion complexation of the drug AMHCl with α and β-CDs not yet been discussed so far our knowledge is concerned. The approach may lead to various chemical advantages of the drug. The inclusion complex may diminish its side effects and increase its bioavailability or can be orally administered without any risk of hepatic first pass metabolism. [22, 23] [24]

2-hydroxy-*N*-(2-hydroxyethyl)-3-methoxy-5-(2-propenyl)benzamide or alibendol is of important pharmaceutical interest due to its activity in the field of medicinal chemistry. It has the formula of $C_{13}H_{17}NO_4$ and melting point of 95^0C and can be prepared by mixing ethyl ester of 2-hydroxy-3-methoxy-5-allyl-benzoic acid and ethanolamine under suitable experimental condition. The number of patents for the synthesis of alibendol is very little even the mentioning of alibendol is very less in literature.

The maximum choleretic, antispasmodic and cholekinetic drugs use alibendol in their composition as an active component. In biliary insufficiency it shows outstanding activity i.e. in dyspepsia, other uses are in alimentary intolerance and in hepatic origin constipation.

But as an active ingredient in antispasmodics it must have some sort of side effect such as vomiting, headache, dizziness, nervousness, irritation and in some cases allergic reactions. To consume such drugs may cause allergic reactions.

Alibendol included β –CD inclusion complex has not been studied earlier. We have studied the inclusion system with the help of some spectroscopic investigations. The pronounced inclusion system may decrease the limitations of the drug either by increasing bioavailability or by decreasing its side effects. [25] [26]

The pyrimidines and nitrogen heterocycles are mostly seen in a number of bio-active molecules and exhibit substantial therapeutic efficacy. Among these pyrimidine is found to be the most suitable architect in the chemistry of nucleic acid . The common natural derivative of pyrimidine is uracil. Uracil is the necleobase present in RNA but absent in DNA or it can be said that it is dimethylated in DNA, which is thymine. Uracil linked to the nucleobase adenine through two hydrogen bonds in RNA. It is reported earlier that uracil can be generated from pyrimidine by the action of UV light.

Uracil has a very little acidity. It can go through tautomeric shifts into amide-imidic acid due to nuclear unsteadiness which may occur owing to loss of aromaticity. The amide tautomer is the lactam structure and the imidic acid tautomer is the lactim structure. Generally uracil is more common in the lactum structure. Uracil has a variety of

application in drug discovery. Most of the synthesized drugs having antitumor, anticancer efficiency include uracil moiety in them.[27]

Gallic acid is a polyphenolic compound having tremendous antioxidant properties. There occurs some oxidative stresses due to normal metabolism, antioxidants of natural origin serve for the prevention of the cells from those oxidation. Oxidative stress is basically the formation of free radicals in our body. These reactive oxygen are not good for cells and gathering of these may lead to inflammatory disease, cardiovascular disease and chronic disease cancer. Gallic acid or 3,4,5-trihydroxy benzoic acid is a naturally occurring compound having low molecular weight. Its presence is widespread in the plants like oak barks, grapes, different types of berries, tea, mango, gallnuts and in vegetables.

We have investigated that there exists a strong interaction between uracil and gallic acid in the ternary system of uracil and aqueous gallic acid solution based on some physicochemical methodologies and some important parameters have also been derived. [28] [29] [30]

Therefore the objectives, scope and applications of the research work in brief are

- The most important objective of the research work is to study certain non-bonding interactions of some significant molecules especially in diverse system and also to collect the appropriate information regarding the phenomenon for future upgradation.
- The solvation consequences of certain bioactive molecules in ternary system provide us valuable information about changes in their physical properties.
- The thermodynamic results obtained from our research works are no doubt of extreme importance.
- Selection of biologically active molecule and by studying its biological activity after inclusion opens up new scopes for numerous future researches. This also has vast application for the betterment of bioactive compounds in their activity.

- By the course of this research work we understand different hydrophilic and hydrophobic interactions with the help of some physicochemical methodologies.
- The application of different host-guest inclusion systems here is to enhance the bioavailability and to reduce the side effects or toxic effects of certain bioactive and industrially important molecules.

I.2. SELECTION OF BIOACTIVE MOLECULES, DYE MOLECULE, HOST MOLECULES, SOLVENTS USED IN THE RESEARCH WORK

The names of the bioactive molecules, dye molecule, host molecules and solvents used in the research work are listed below.

Dye molecule:

- Indigosulfonic Acid Dipotassium Salt (ISD)

Bioactive Molecules :

- DL-Aminoglutethimide
- Amiloride hydrochloride
- Alibendol
- Uracil
- Gallic acid

Host Molecules:

- α – Cyclodextrin
- β -Cyclodextrin

Solvents:

- Water
- Dimethyl sulfoxide
- Acetonitrile
- Ethanol

I.3. METHODS OF INVESTIGATION

The following methods of investigation have been used in our research work.

- NMR spectroscopy (2D NOESY,ROESY and ^{1}H NMR)
- UV-Vis spectroscopy
- Powder X-Ray Diffraction
- Fluorescence spectroscopy
- FTIR spectroscopy
- Isothermal Titration Calorimetric Study
- Mass spectroscopy
- Scanning Electron Microscopy
- Density study
- Refractive index study
- Viscosity study
- Cell viability study
- Antimicrobial study

The partial molar volume, viscosity B co-efficient and other thermodynamic parameters give us important information to explain solute-solute, ion-ion and ion-solvent interactions. The nature and extent of ion-solvent interaction can also be predicted from the sign and magnitude of the partial molar volume.

CHAPTER II

REVIEW OF THE EARLIER WORKS AND THEORY OF INVESTIGATION

II.1. Review of the Earlier Works

II.1.1. An overview of host guest chemistry

Host-guest chemistry usually involves compatible binding between two or more molecules and ions. The molecules involved in host-guest complex are held together in terms of non-covalent bonds. It encompasses molecular recognition; thus by appropriate choice of binding sites a host-guest complex is formed. An Inclusion complex is a distinct system. In 3D structures of large molecules non-covalent bonding cannot be maintained that is why large molecules bind specifically but transiently in many biological processes. The Non-covalent interactions are basically electrostatic or dispersive forces. Different types of non-bonding interactions are there but hydrogen bonds, ionic bonding, van der Waals forces, hydrophobic interactions are very common.[1, 2]

Cyclodextrins are cyclical cavity polymers consist of minimum 6-D-(+)-glycopyranose units connected by α-(1,4) linkages. Three types of common cyclodextrin molecules α, β and $_{\gamma}$ have various applications in food industry, pharmaceutical chemistry and in other consumer products. The universal production of cyclodextrins has crossed 10,000 tons per year. Due to suitable cavity diameter CDs can access the technique of different host guest complexes. They possess a hydrophobic central cavity which can accommodate variety of organic guest molecules and can be able to form host-guest inclusion complexes or supramolecular organizations. CDs are water soluble and also biodegradable which make them very special for executing and implementing in various applications. As the guest molecule enters the cavity of CD molecule, there occur some changes in the physical properties of the guest which may be used in different areas. To increase the bioavailability of any drug, CDs have no alternation.

Among the cyclodextrins, β-CD is the prominent one because of having modest cavity dimension, low production price and easy availability. The inclusion complexes of the bioactive molecules with CDs includes numerous pharmacological benefits e.g.

increase the stability, solubility, bioavailability and diminish the toxic effects of the drug.[3] [4] [5]

II.1.2. Inclusion Complex formation

The process of inclusion seems to happen between a host and a guest molecule via some non-bonding interactions or simply there occurs no formation of bonds. The cyclic host molecules are preferred for this like calixarenes, cyclodextrins etc. [6]

The hydrophobic cavity of CDs enables maximum organic moiety to enter and to fit perfectly. It does not include bond breaking or bond making. The non-bonding interactions are the responsible for the complex formation.

Expulsion of water molecule by the entering guest molecule may be the driving force in this process. The thermodynamic of the process rely on it.

Through the process of inclusion it is possible to protect the drug from environmental and enzymatic degradation, oxidation etc.

The overall inclusion phenomenon is dynamic itself as it includes very weak non-covalent forces. The strength of association depends on how perfectly the guest fitted into the void. ICs can be formed in solution phase or in crystalline phase. Choice of solvent is based on the solubility of the guest molecule but most of the time water is considered as the solvent media. Certain non-aqueous/organic solvents are also used for the purpose of inclusion.

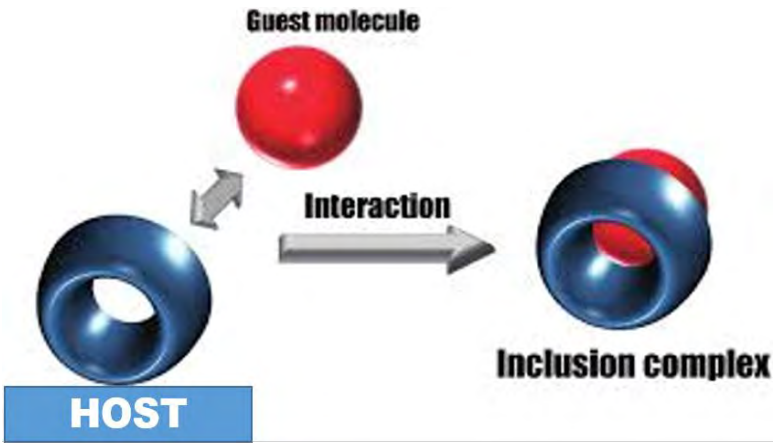

Scheme.II.1: Schematic diagram of host-guest inclusion complexation.

II.1.3. The stoichiometry of inclusion

The most common stoichiometry for the host guest inclusion is 1:1(H:G). Other stoichiometries are very few in literature.

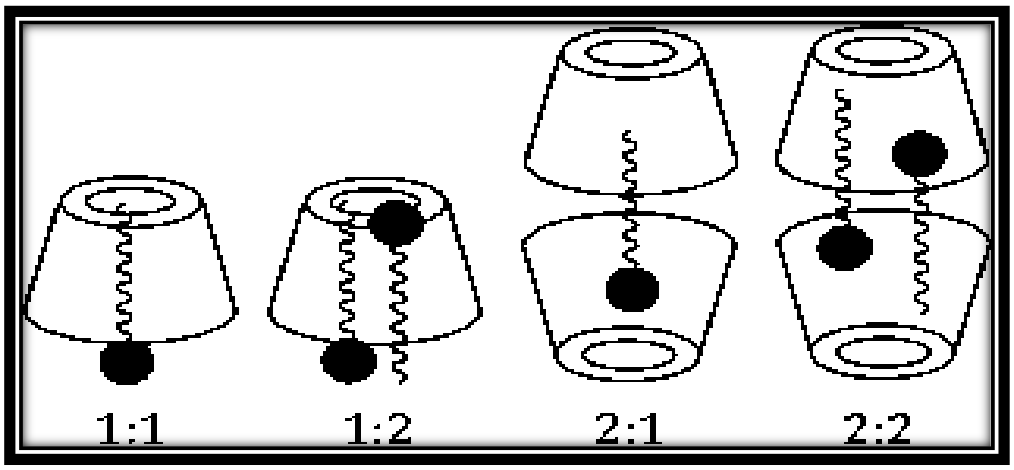

Fig.II.1. The different types of stoichiometries in Host-guest inclusion complex

Job's method is applied to determine the stoichiometry of the host-guest complex from the UV-Vis spectroscopic study. It is a process by which the total concentration of both the host and guest is kept fixed (while mixing different volumes of solutions of each in appropriate solvent) and the concentration of guest varies in a set of set of solutions. ΔA*R Vs R is plotted in the Job plot; Where ΔA stands for change in absorbance of the guest in presence of host and R=[G]/[G]+[CD]. If R value exhibits a maximum deviation at 0.5 then it is a 1:1 stoichiometry.

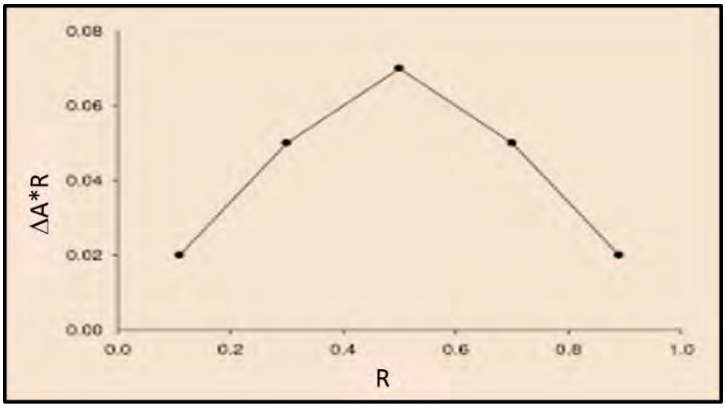

Fig.II.2: Representation of Job plot for 1:1(H:G)

II.1.4. Determination of both the stoichiometry and the association constant

With the help of Job's plot we can predict the extent of interaction and also the stoichiometry between the host and guest molecules. Data obtained from experimental findings are fitted in linear or non-linear models according to Benesi-Hildebrand double reciprocal equation. The equation is shown below.

$$\frac{1}{\Delta A} = \frac{1}{\Delta\varepsilon[G]ka} * \frac{1}{[H]} + \frac{1}{\Delta\varepsilon[G]} \qquad \textbf{(II.1)}$$

(ΔA is as stated above, Δε is the molar extinction co-efficient and [H] and [G] are the concentration terms of host and guest molecules.)

II.2. Theory of Investigations

II.2.1. Hydrophobic Interactions:

Hydrophobic effect is the affinity of nonpolar molecules to get aggregated in aqueous solution by excluding water molecules. Hydrophobicity means the fear of water and includes the isolation of water and nonpolar molecules, which enhance hydrogen bonding interaction in water molecules and decrease the area of contact of nonpolar and water molecules. According to thermodynamics, hydrophobic effect is nothing but the change in free energy of water surrounding a solute. Positive change in free energy of the surrounding solvent describes hydrophobicity, while a negative change in free energy denotes hydrophilicity.

Hydrophobic effects encompass important application in biological fields such as protein folding, formation of vesicles, membrane protein insertion into the nonpolar lipid and in separation of mixtures of polar and nonpolar solvents.

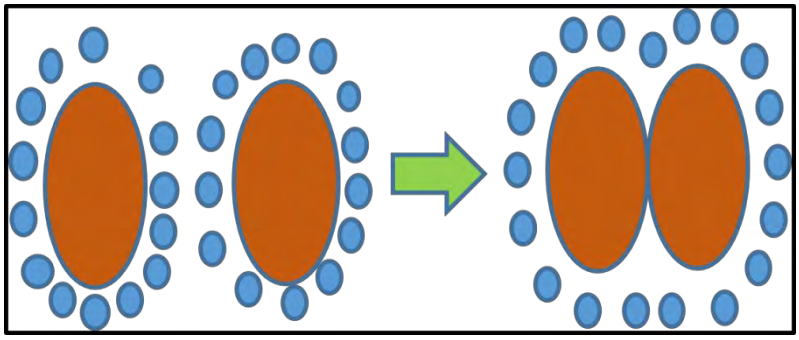

Fig.II.3: Hydrophobic interaction brings the interacting molecules closer.

II.2.2. van der Waals Forces:

Van der Waals forces of interactions are feeble forces in practice and particularly of 0.5-1kcal/mol. Forces produced are non-ionic and non-directional. It is a propensity of the electronegative atoms present in neutral molecules to divert the electron cloud of comparatively less electronegative adjacent atoms by means of covalent bonds.

Thus it introduced a partial positive and partial negative charge in the same molecule i.e. dispersion of charge occurs.

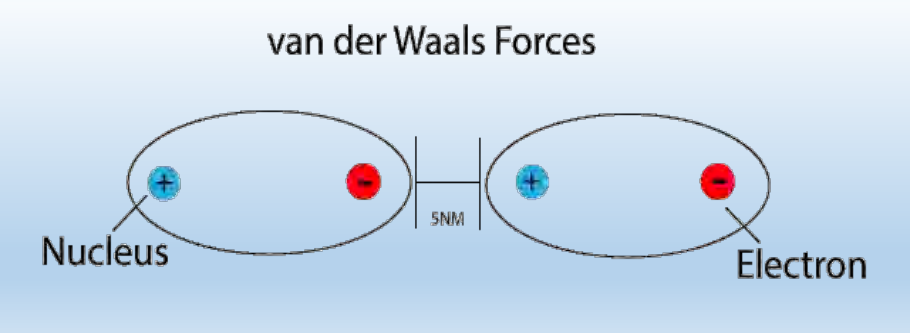

Fig.II.4: van der Waals forces of attraction between molecules

The forces also seems to occur between opposite charges of two interacting molecules placed close enough to each other in an arrangement that the positive end of one meets the negative end of the other. According to the mechanisms of charge dispersion, the forces are categorised.

Molecules that are capable of partial charge distribution because of having strong electronegative atoms can generate a permanent dipole in it which in turn can induce dipolar nature in other molecule. Thus there occurs interaction like ionic fashion but of very weak strength. This type of force is Keesom force (dipole-dipole interaction).

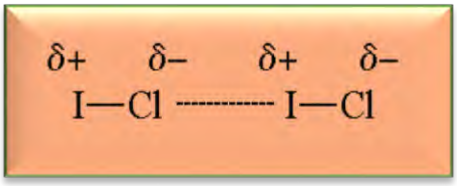

Fig.II.5. Dipole-dipole attraction

On the other hand if permanent dipole deforming the electron cloud of neighbouring molecule, it is termed as Debye force (dipole-induced dipole interaction).

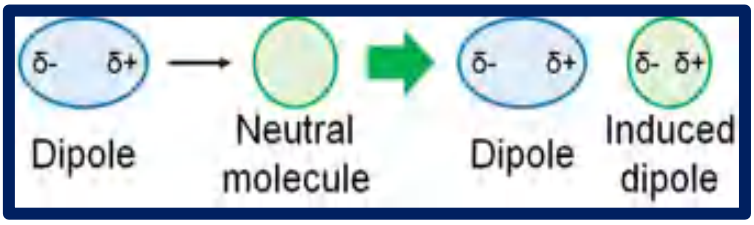

Fig.II.6. Dipole-induced dipole attraction

The force that operates due to partial charge distribution between two neighbouring neutral entities is the London force i.e. (induced dipole-induced dipole interaction).

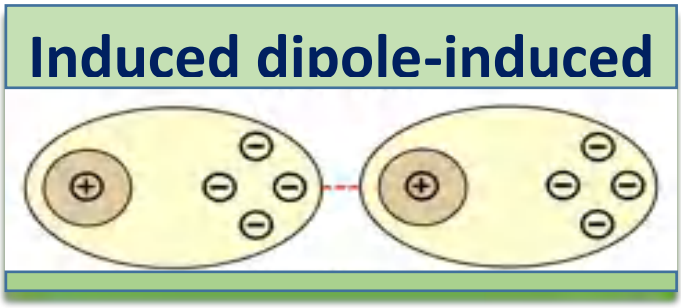

Fig.II.7. Induced dipole-induced dipole interaction

II.2.3. Hydrogen bonds:

The electrostatic force between a hydrogen atom which is covalently bonded to an electronegative atom or group and an electronegative atom with lone pair generates hydrogen bonding. Electronegative atoms actively participate here like fluorine, oxygen, nitrogen.

Hydrogen bonds are basically stronger forces than van der Waals forces ranging between 1-40kcal/mol but weaker than ionic or covalent bonds. Two types of hydrogen bonds are (a) intramolecular and (b) intermolecular .The strength and energy of hydrogen bonds depend on the nature of the involved donor acceptor atoms, geometry and the environment.

When hydrogen bond is formed involving a hydrogen atom and an electronegative atom from other part of the same molecule, it is intramolecular hydrogen bonding. On the other hand when an electronegative atom of one molecule attracts the hydrogen atom of other molecule, it is called intermolecular hydrogen bond. Hydrogen bonds have

significant contribution in the physical properties of different substances even in the structures (both secondary and tertiary) of nucleic acid and proteins. It also helps in generating various polymeric structures.

Hydrogen bonding markedly effects on the stability and boiling point of several compounds such as water. The high boiling point of water is owing to intermolecular hydrogen bonding.[7] [8, 9]

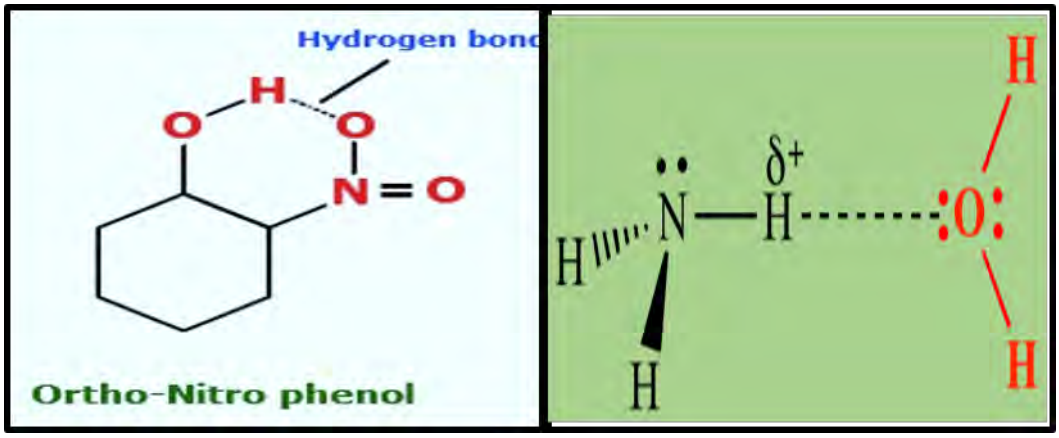

Fig.II.8: Intra and intermolecular Hydrogen bonding.

II.2.4. Electrostatic Forces:

Electrostatic force is the force between two charged particles by the action of attraction or repulsion can be measured by Coulomb's law. The force is proportional to the product of the charges of the two particles and inversely proportional to the square of the distance between the centres of the two charged particles.

II.2.5. Ion-Dipolar Attractions:

It is a kind of electrostatic force between the fully charged ion and a permanent dipole of a neutral polar molecule. The alignment of both the entities is such that the negative dipole of the neutral molecule is in close proximity to the positively charged ion and vice versa for the attraction to be maximum . These types of forces are much stronger than hydrogen bonding and dipole-dipole attractions as a fully charged ion is taking part.

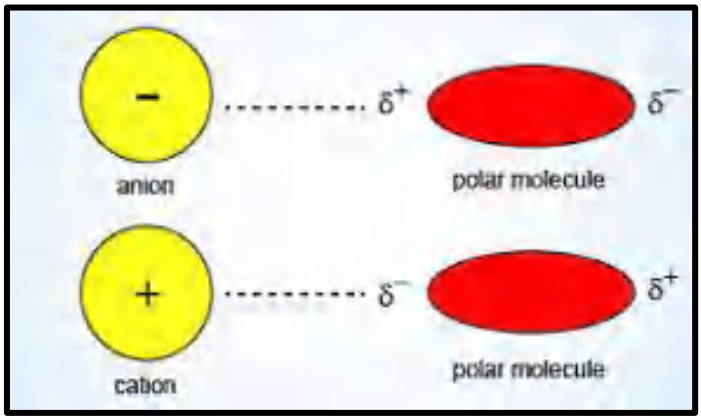

Fig.II.9: Ion-dipolar attraction between an ion and a dipole of a polar molecule.

The strength of the ion-dipole attraction generally depends on the charge of the ion and on the partial charge on the dipole of the molecule.

II.2.6. Solute-Solvent Interactions:

The intermolecular forces act between the solute and solvent molecules are the main cause of solubility and the solute-solvent interaction must be stronger than the solute-solute and solvent-solvent interaction. This is the reason why NaCl dissolves in water. As soon as NaCl get into the solution water molecules surrounds the ions Na^+ and Cl^- separately thus the bond between Na and Cl becomes weak; this occurs because of the salvation process. The dissolution power also depends on the nature of the solute particles whether they like the solvent or not. Solution chemistry covers many thermodynamic parameters and new implications based on these parameters.

II.2.7. NMR Spectroscopy:

Nuclear magnetic resonance is a very powerful technique for determining the structure of different molecules. It has vast application in the field of chemistry, material and engineering sciences.

NMR is a technique of exposing atomic nuclei to a strong magnetic field and by the effect of this field protons precess at different frequencies. The precessing protons are then irradiated by steadily changing frequencies and the frequency at which absorption occurs is observed. When the energy of radiation matches the energy of the proton for flipping, absorption occurs and signal is observed. The obtained spectrum is called Nuclear Magnetic Resonance spectrum.

All the protons do not absorb the same applied field. Absorption depends on the magnetic field felt by a specific proton. Different set of protons in different environment have different effective field strengths. Different protons will have to have different applied field strength for producing same effective field strength at a supplied radio-frequency which will cause absorption to occur. By measuring the applied field strength, absorption peaks are plotted for the set of protons.

Position of the signals

To find out the nature of the protons (aliphatic, aromatic, allylic, vinylic)of the variety of compounds the positioning of the signals are very important. Moreover the electronic environment is responsible for the absorption of protons.

The molecule under investigation when placed in a magnetic field, the electrons in it generates a secondary magnetic field opposite to the applied field. Induced field opposes the applied field, proton is said to be shielded and vice versa. Shielding causes upfield absorption while deshielding downfield. These shifts by shielding or deshielding of protons in the position of nmr absorption are chemical shifts. It is denoted by δ in ppm.

An NMR technique for the identification of carbon atoms analogous to hydrogen is also applied for structure determination of basically organic and organometallic compounds. It follows the rule as that of proton NMR.

Nuclear Overhauser Effect

It is a process of transferring nuclear spin polarisation from one (spin-active) to other nuclei through cross relaxation. It explains the interaction of two protons or nuclei in space when they are close enough. Here, the number of intervening bonds have no effects. By interpreting the 1H two dimensional NOESY spectrum it is possible to predict the geometry, structures and stereochemistry of different molecules including biomolecules. [10, 11]

2D ROESY

The 2D ROESY NMR spectrum is a two dimensional rotating frame overhauser enhancement spectroscopy having the same principle as NOESY. When protons are in

close vicinity in space, through space interactions generates cross peaks in the two dimensional XY plane. It is one of the suitable techniques for structure elucidation in solution phase but it requires spin lock while mixing the solutions.

II.2.8. FTIR Spectroscopy:

It is a method of obtaining the infrared spectrum of solid, liquid and gas. It accumulates high resolution spectral data ranging between 400-4000 cm^{-1} .

It causes an excitation of a molecule from lower to higher vibrational level associated with a number of closely placed rotational lines. Not all bonds in molecules can absorb infrared energy but only those which can generate a change in dipole moment can absorb in infra red region and the molecules are called infra red active. Vibrational transitions not associated with change in dipole moment of molecule are infrared inactive. N-H, C=O, O-H bonds are associated with change in dipole moment, strongly absorb in infrared. A molecule will exhibit a number of signals or peaks in IR region as absorption in IR region is quantised.

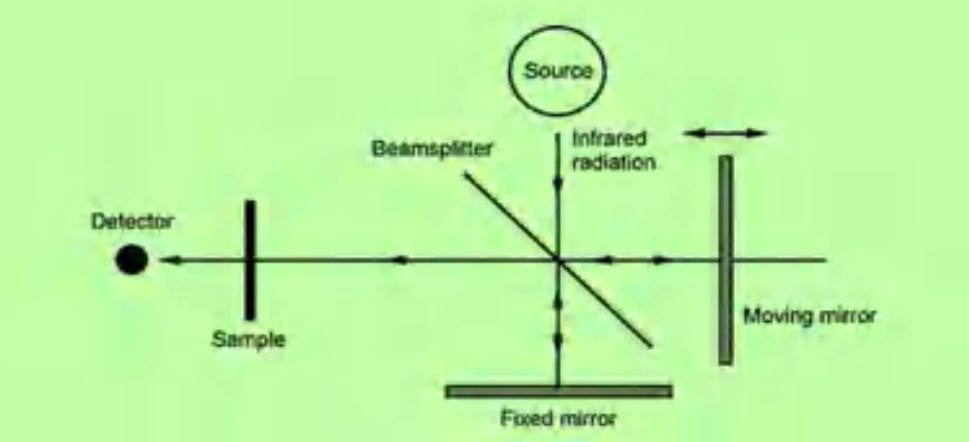

Fig.II.10: Principle of FTIR spectroscopy

There are classes of vibrations accompanied by IR spectra e.g. stretching, bending. Stretching vibration can also be classified into different categories. Hook's law is applied to measure the vibrational stretching frequencies.

$$\bar{\upsilon} = \frac{1}{2\pi c}\sqrt{(\frac{k}{\mu})} \qquad \textbf{(II.2)}$$

Where μ is the reduced mass which is equal to $m_1m_2/(m_1+m_2)$ and k is the force constant of the bond.

Generally by preparing KBr palette of the samples under observation we recorded the spectra. Sample should be taken in very small amount compared to dry KBr.

II.2.9. Isothermal Titration Calorimetric Study

Isothermal calorimetric study is a quantitative technique to determine the stoichiometry and some thermodynamic parameters involved in complexation. Very often it is used to find out the binding site of host molecules or different macromolecules. Thermodynamic measurements like change in enthalpy, binding constant, change in enthalpy, change in Gibb's free energy, entropy etc of two or more than two interacting molecules can be determined. The thermogram curve will be a sigmoidal curve for the stoichiometry.

The calorimeter is composed of two indistinguishable cells in an adiabatic jacket; one is sample cell and another is reference cell. Sample cell contains the host or the macromolecule and reference cell contains buffer or water.

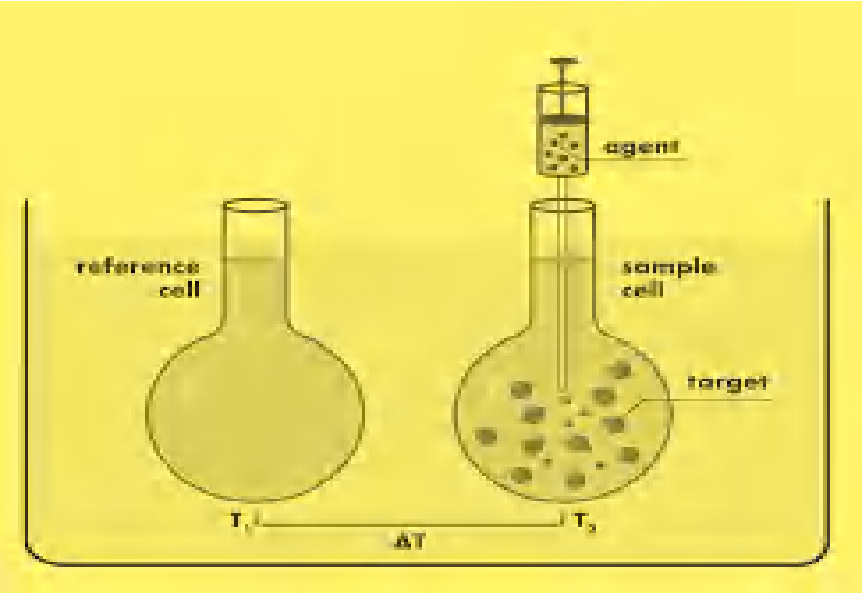

Fig.II.11: Pictorial representation of ITC experiment

Now, a minimum aliquots of ligand or guest molecule is injected in each injected. Heat may evolve or absorbed upon addition. The raw data of heat evolved versus time generate a number of spikes and every spike denotes single injection of guest or ligand.

II.2.10. UV-Visible Spectroscopy:

This spectroscopy is basically an electronic spectroscopy which includes the jumping of electrons from ground energy level to higher energy level. Molecules that have bonding and non-bonding electrons absorb UV or visible light for the excitation of the electrons to promote them to higher energy anti bonding orbitals. If the electrons are easily excited it concludes that they can absorb longer wavelength of light.

The transition of electrons follows some selection rules. The allowed transitions are n- π *, π -π * and σ-σ*. They can be arranged as follows σ-σ*> n- σ*> π -π *> n- π *.

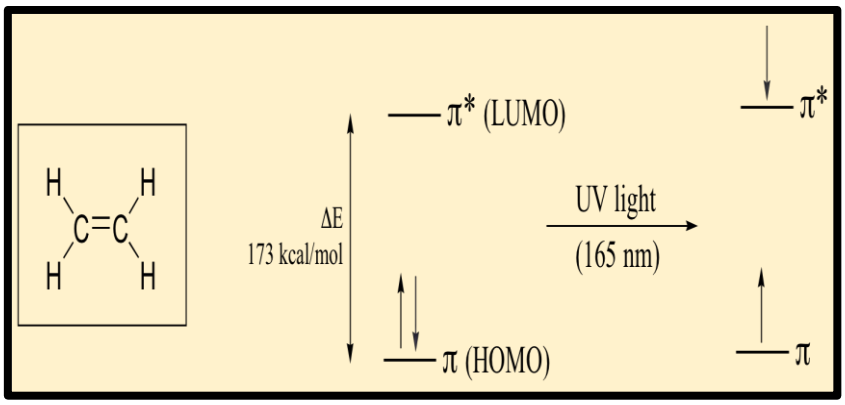

Fig.II.12: Excitation of electrons in ethylene.

The theory of UV-Vis spectroscopy is based on the Lambert's-Beer's law, Which is

$$\log(I_0/I) = \varepsilon cl = A \qquad \textbf{(II.3)}$$

Where I_0 is the intensity of the incident light; I is the intensity of the transmitted light; c is the concentration of solution; l is the path length of the sample and ε is the molar absorptivity.

With the help of the Benesi-Hildebrand equation, the compiled data obtained from UV-Visible spectroscopy are plotted in order to get association constant of different host-guest systems. The stoichiometry of inclusion is also interpreted by the help of this technique.

II.2.11. Fluorescence Spectroscopy

In fluorescence spectroscopy, at first excitation of molecule occurs via photon absorption from ground electronic energy level to any of the vibrational energy level of higher electronic energy level. When it collides with other molecules its energy drops down and it returns to the ground electronic state by obviously emitting photon. The emitting photons have different energies and frequencies. Jablonski diagram depicts the process. Now, analysis of the emitted light of different frequencies together with the relative intensities it is possible to predict the structure of different vibrational energy levels. Fluorescence intensity is proportional to the concentration of the fluorophore when the concentration is low.

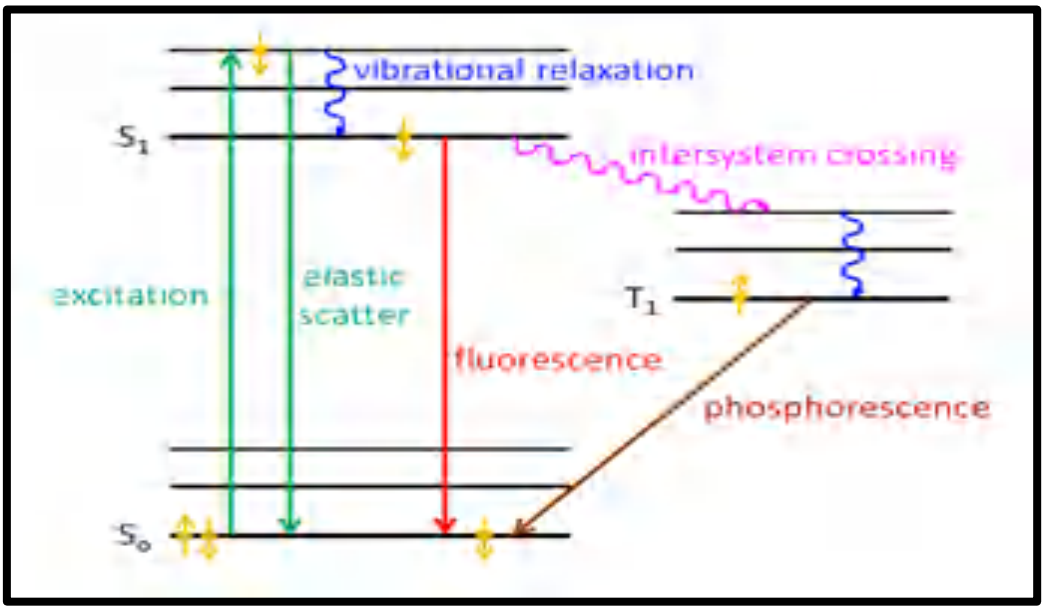

Fig.II.13: The Jablonski diagram of fluorescence

Fluorescence spectroscopy also helps in determining the association constant of the host-guest complex as we have done here.

II.2.12. Scanning Electron Microscopy:

This technique is basically used to explain the surface morphology of different species. The scanning electron microscope a beam of electrons is applied. The interaction of electrons with the atoms generates various signals which give us information about the topography of the surface and composition of the sample.

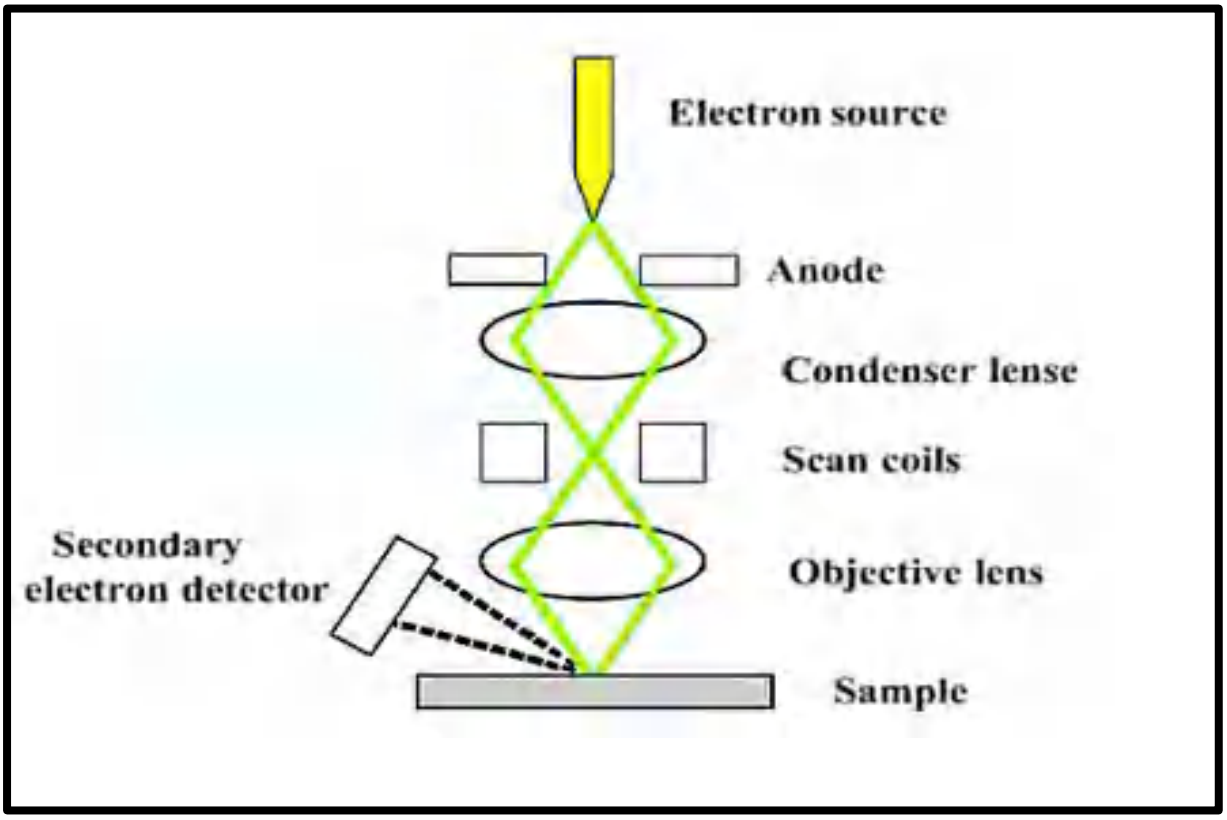

Fig:II.14: Working principle of SEM

SEM micrographs have a three dimensional appearance which helps to understand the morphology of a surface clearly. The samples should be dried completely as the sample chamber is in high vacuum state.

II.2.13. Powder X-Ray Diffraction (PXRD):

The X-ray diffraction stands on the principles of Bragg's law .When X-rays collide the surface of a crystalline substance , they get diffracted by the atoms of the crystals. The parts which do not scattered pass through the next layer of atoms and scattered and so on. By the process, we get a diffraction pattern. For the X-rays to be diffracted, the substance must be crystalline and the spacing between the layers of atoms should be close to the wavelength of radiation. X-ray diffraction study deals with constructive interference i.e. beams (monochromatic X-rays) that are diffracted by the two different layers are in phase. Constructive interference is the cause of appearance of peaks.

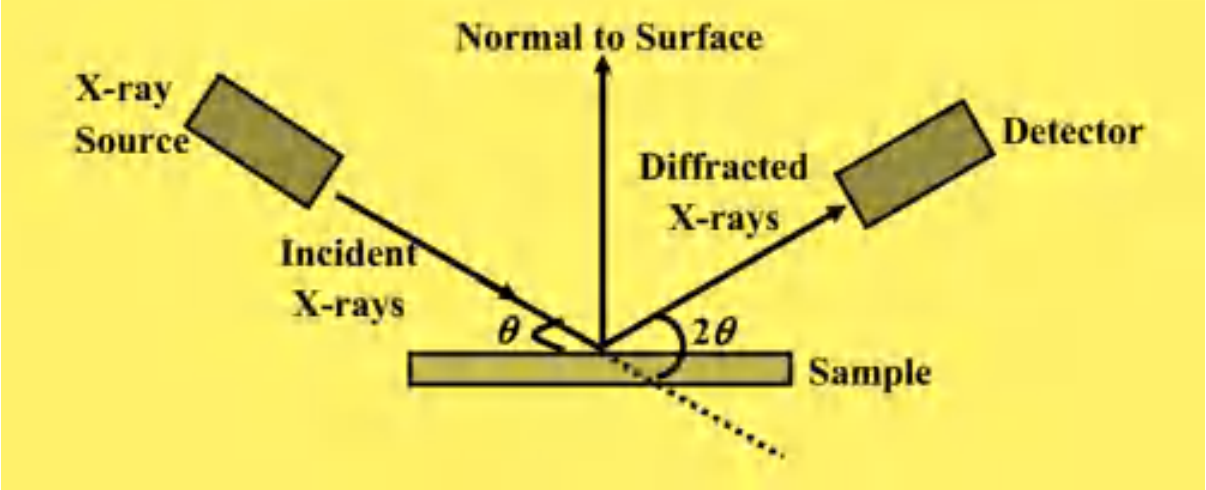

Fig.II.15: Pictorial representation of the diffraction of X-ray

The Bragg's equation is, $\mathbf{Sin\Theta = \frac{n\lambda}{2d}}$ **(II.4)**

Where, **Θ** is the incident angle,

λ is wavelength,

d is the interplanar distance,

n is integer.

II.2.14. Mass spectrometry:

Mass spectrometry is the most precise method to determine the elemental composition and the molecular mass of a compound. With a beam of energized electrons, molecules are bombarded. As a result, they get ionised and broken down into different fragments including some positive ions. Each type of ion possesses a specific mass to charge ratio (m/e). As the charge is unity for most ions, the m/e ratio is nothing but the molecular mass of the ion. Elimination of one electron from the parent molecule gives the parent ion.

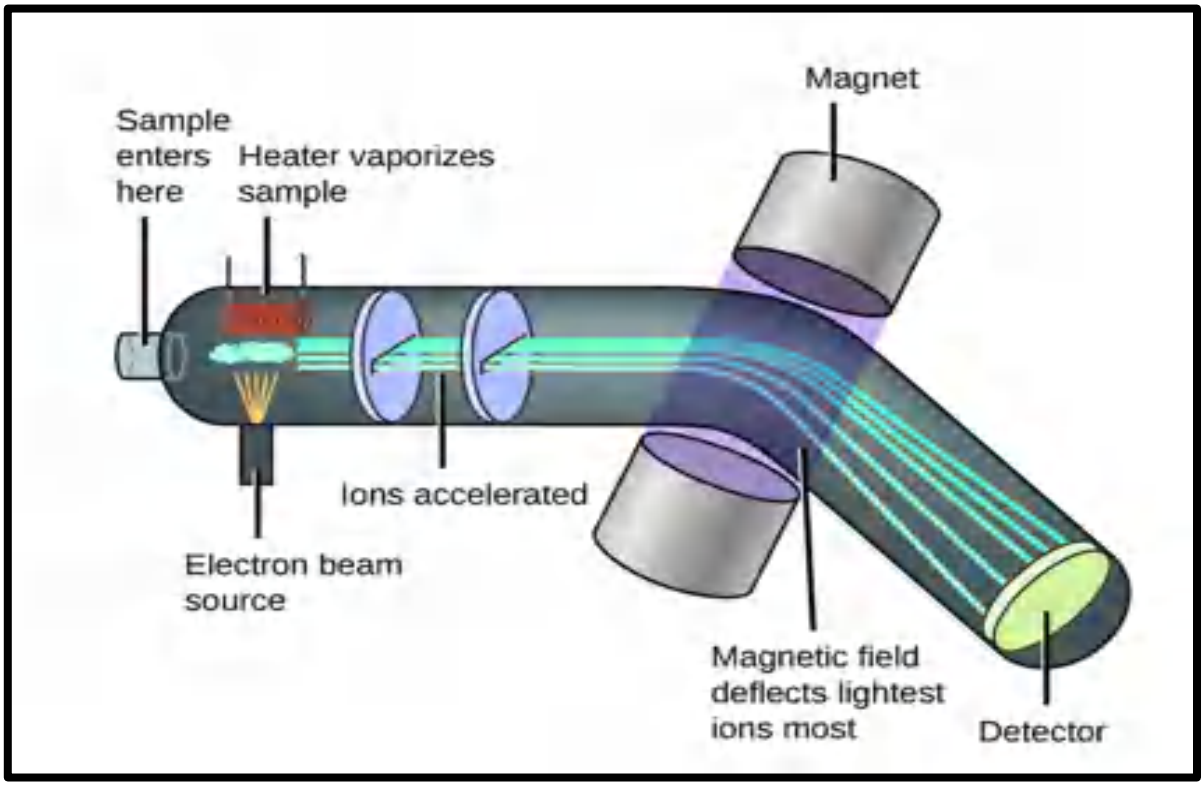

Fig.II.16: The working principle of mass spectrometry

In mass spectrometry the intensity of each signal designates the relative abundance of the respective ion generating the peak. The parent ion peak should not be bewildered with the base peak. The base peak has 100% abundance whereas the parent ion peak has very small abundance.

This spectrometry is tremendously useful for establishing or confirming structure of new compounds, to recognise two compounds, to find out the molecular formula of a compound, to verify the presence of certain structural units in a molecule and to reveal the exact molecular mass of a compound.

II.2.15. Techniques used to investigate the physicochemical parameters in solution

Solution chemistry reveals the chemistry between solute-solute, solute-solvent and solvent-solvent interactions generally in aqueous solution. The interactions that are taking place in solution are normally non-covalent bonds and based on attraction-repulsion process. Now by measuring different parameters of solution, we can have surprising results about different type of interactions between the involved species.

II.2.15.1. Density

Density measurements have a very important function in different type of interactions beween solute and solvent in solution as it is a physical property of substance of mass to volume; where other physical quantities also show vital role.

Apparent molar volume

The volumetric behaviour of electrolytes and non-electrolytes in solution supply useful information about the interactions between the molecules of solute-solvent and solute-solute. The structural properties of water are greatly affected by the interaction of solute, especially with ions with non-polar groups. Thus, for elucidating the structural interactions occurring in solution, the apparent and partial molar volumes and expansibilities of solute are the important tools. The apparent molar volume of the solute is its geometric volume including the changes in volume (extra volume) in addition of solvent. [12]

The apparent molar volumes (ϕ_v), of the solutes can be calculated by using the following relation.

$$\phi_v = \frac{M}{\rho} - \frac{1000(\rho - \rho_0)}{m\rho\rho_0} \qquad \textbf{(II.5)}$$

Where, M signify the molar mass of the solute; m is the molality of the solution; ρ and ρ_0 denote the densities of the solution and solvent respectively.

At infinite dilution apparent molar volume is called as the limiting molar apparent volume (ϕ_v^0). Linear plots of best fitted data of ϕ_v against the square root of molar concentrations ($\sqrt{m}$) give the values of limiting molar apparent volume (ϕ_v^0) and experimental slopes (S_v^*) by the use of Masson equation.

$$\varphi_v = \varphi_v^0 + S_v^* \sqrt{m} \qquad \textbf{(II.6)}$$

S_v^* is the experimental slope and signify the solute-solute interaction in solution. The limiting molar apparent volume ϕ_v^0 explains the solute-solvent interaction occuring

in solution. The large positive values of ϕ_v^0 indicates the presence of strong solute-solvent interaction. By correlating the values of limiting apparent molar volume (ϕ_v^0) and experimental slopes (S_v^*), the predominance of the interactions over each other can be presumed.

The negative values of the experimental slope S_v^* in our research work suggest less solute-solute interaction i.e.(uracil-uracil) and as the values of (ϕ_v^0) are large positive ,solute(uracil)-cosolute(aqueous gallic acid) interactions overcome the solute(uracil)-solute(uracil) interaction.

The physical significance of structure making- breaking interaction

The structure making and breaking tendency of any solute in the territory of solvent in solution can be expressed by Hepler's equation which supplies useful information regarding the interaction of solute-solvent.

As temperature imparts a significant role in the formation or deformation of any structure, correlating with this the limiting apparent molar volume (temperature dependence) will be in the form of the following equation.

$$\phi_v^0 = a_o + a_1 T + a_2 T^2 \qquad \textbf{(II.7)}$$

Where, α_0, α_1, α_2 are the empirical parameters and T is the temperature in Kelvin .

The limiting apparent molar expansibilities (ϕ_E^0) can be attained by differentiating the equation **(II.7)** with respect to temperature.

$$\phi_E^0 = (\delta\phi_v^0 / \delta T)_P = a_1 + 2a_2 T \qquad \textbf{(II.8)}$$

The value of limiting apparent molar expansibility changes with change in temperature, it's positive value tells us about the absence of caging.

In the chemistry of solution there are two types of solutes one is structure maker and another is structure breaker; whether a particular solute is structure maker or

structure breaker can be determined with the help of Hepler's constant $(\delta\phi_E^0/\delta T)_P$. Equation **(II.8)** can be arranged as the following.

$$(\delta\phi_E^0/\delta T)_P = (\delta^2\phi_v^0/\delta T^2)_P = 2a_2 \qquad \textbf{(II.9)}$$

The sign of $(\delta\phi_E^0/\delta T)_P$ decides solute's structure making and breaking capacity in solution. If the values are positive or small negative that means there occurs a structure making interaction otherwise the reverse will occur.

II.2.15.2. Viscosity

Among the various physical properties of liquids, viscosity is very common and delivers a bunch of data regarding the interactions happening in the solution between solute and solvent or ion-solvent. In simple words, viscosity is resistance to flow. In liquids, the molecular motion is controlled by the neighbouring molecules and as a result transport of momentum takes place not by the motion of the actual molecules but due to the intermolecular forces and it forms the base of all procedures for the prediction of the variations in viscosity of liquid mixtures.

An aqueous solution of electrolyte may possess large or less viscosity in comparison to water depending on the concentration range and solute.

The friction force that is needed to maintain a velocity difference of unity between the two parallel layers of liquid/fluid, which are at unit distance apart is termed as the co-efficient of viscosity or viscosity, denoted by the symbol η.

The temperature and concentration dependence of the viscosity co-efficient of aqueous electrolytic solution have been studied earlier and it gives useful evidences about the limit of ionic hydration inside the hydration co-spheres. Jones and Dole introduced an empirical equation by combining the relative viscosities of electrolytes with molarity

$$\eta/\eta_0 = \eta_r = 1 + A\sqrt{C} + Bc \qquad \text{(II.10)}$$

or

$$(\eta_r-1)/\sqrt{C} = A+B\sqrt{C} \quad \text{(II.11)}$$

Where η and η_0 are the co-effiecients of viscosity of solution and solvent respectively. A and B are the constants depending on the ion-ion and solute-solvent interactions. A can be theoretically measured. The constant A generally refers to long range interionic forces and always a positive value while B is associated with the ion's size. It is an changeable additive parameter and is related to the ion's partial molar entropy. [13]

Plots of $(\eta_r-1)/\sqrt{C}$ vs $\sqrt{C}$ are seen to be linear and by least square method the experimental values of A and B co-efficients can be evaluated.

By using Falkenhagen-Vernon equation the A coefficient can be measured theoretically.

$$A_{Theo} = \frac{0.2577\Lambda_o}{\eta_o(\varepsilon T)^{0.5}\lambda_+^o\lambda_-^o}\left[1-0.6863\left(\frac{\lambda_+^o\lambda_-^o}{\Lambda_o}\right)^2\right] \quad \text{(II.12)}$$

Symbols have their usual significance.

The viscosity B coefficient helps in classifying ions as water structure making and structure breaking. The temperature variation of viscosity B coefficient supplies information for such classification. Also the hydration number of molecules or ions can be determined from the viscosity B coefficient.

If , $dB_{ion}/dT>0$;it signifies ion is structure breaking.

If, $dB_{ion}/dT<0$; it signifies the ion is structure making

The negative or small positive values of dB_{ion}/dT denote structure making and large positive values denote structure breaking.

II.2.15.3 Refractive Index

Refractive index describes the propagating phenomenon of light i.e. how the path of the light gets deviated by entering into a medium. Refractive index is a physical property of solution. It varies with the change in pressure, temperature and wavelength.

The concentration of a binary solution can also be determined by the refractive index study. So it has a wide variety of application in industrial field as well as research related scopes.[14]

The refractive index (n_D) can be expressed as ,

$$n_D = c_0/c \tag{II.13}$$

= speed of light in vacuum / speed of light in material

If the refractive index value for a substance is an arbitrary value Q then it denotes that light passes through the medium Q times than travels in vacuum. If the value increases the speed of light in that material decreases.

According to Snell's law of refraction,

$$n_B/n_A = \text{Sin}\Theta_A/\text{Sin}\Theta_B = V_A/V_B \tag{II.14}$$

n_B and n_A are the refractive indices of the two medium and Θ_A and Θ_B are the incident angle and refracted angle of the light passing through one media to another. V_A and V_B are the speeds of light in the mediums.

The refractive index of a transparent substance is dependent on its density and so far it was not revealed until Lorentz described it. The Lorentz-Lorentz relation for molar refraction is given as follows,

$$R_M = \frac{(n_D^2-1)}{(n_D^2+2)}\frac{M}{\rho} \tag{II.15}$$

Where, R_M is the molar refraction; n_D is the refractive index; ρ is the density of the solution and M is the molar mass.

The limiting molar refraction has the formula of

$$R_M = R_M^0 + R_S\sqrt{m} \tag{II.16}$$

Where 'm' is the solution's molality and R_M^0 is the limiting molar refraction. R_M^0 can be considered as a measure of solute-solvent interaction in solution.

CHAPTER III

EXPERIMENTAL SECTION

III.1. NAME, STRUCTURE, PHYSICAL AND CHEMICAL PROPERTIES, PURIFICATION AND APPLICATIONS OF THE CHEMICALS USED IN THE RESEARCH WORK

III.1.1. Solvents

Here are the detailed discussions of some aqueous and non-aqueous solvents used in our research work.

Water:

Water is the indivisible part of every living organism. The existence of life relies on it. It is basically a tasteless, colourless, odourless inorganic compound having the chemical formula H_2O. Mostly it appears as liquid but can exist in three forms depending on atmospheric pressure and temperature; solid, liquid and gas. Its use is universal as a solvent.

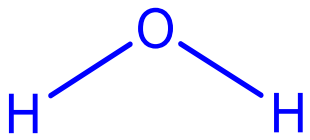

Source: Distilled water; distilled by fractional distillation method in laboratory.

Purification: First water was deionised and then distilled using alkaline $KMnO_4$ solution to exclude the organic materials.

Water	
Appearance	Liquid
Molar mass	18.015 g/mol
CAS number	7732-18-5
Melting point	273.15 K
Boiling point	373.15 K
Density	0.9970474 g/mL at 25^0C

Viscosity	0.890 cP
Refractive index	1.333 at 20^0C
Chemical formula	H_2O

Application: Water is very essential for every life. In industries, large quantities of water are used in the form of liquid water, ice and steam. By dissolving various substances in water , the physical and often chemical properties of those substances and their nature of interaction can be studied. Water is easily available than other solvents so it can be smartly used in plenty of projects either research based or industrial purposes. Every biochemical reaction that occurs in plants and other living bodies need water. The property of water to form emulsion is used in different processes. Its capacity of forming hydrogen bond makes other solutes dissolve in water.

Ethanol: Ethanol is an organic compound. It is volatile, flammable, colourless liquid and has a wine like pungent smell. [1, 2]

Ethanol	
Appearance	Liquid
Molar mass	46.07 g/mol
CAS number	64-17-5
Melting point	-114.1 ^{0}C
Boiling point	78.37 ^{0}C
Density	789 kg/m^3
Viscosity	1.2 mPa.s at 20^0C
Refractive index	1.3611
Chemical formula	C_2H_5OH

Source: purchased from Sigma Aldrich

Purification: Used as purchased.

Application: Ethanol is also considered as a universal solvent and it allows a plenty of polar-nonpolar, hydrophobic-hydrophilic compounds to dissolve in it due to its structural effect. Further its low boiling point helps in separating it from other media. Thus it can be used as an extracting agent. It is an essential agent for paints, vernishes

and cosmetics. It possesses antimicrobial property and used in different antimicrobial preservatives. [3]

Acetonitrile: It is an aprotic polar solvent basically a by product in the manufacture of acrylonitrile synthesis. It is the building block of many organic compounds.

Acetonitrile	
Appearance	Liquid
Molar mass	41.053 g/mol
CAS number	75-05-8
Melting point	227K-229 K
Boiling point	354.4 K-355.2 K
Density	0.786 g/cm^3
Acidity (pk_a)	25
Refractive index	1.344
Chemical formula	CH_3CN

Source: Purchased from Sigma Aldrich

Purification: Used as purchased

Application: The use of acetonitrile is generally as solvent of modest polarity. It can dissolve many non-polar and ionic compounds and acts as the mobile phase in HPLC. High dielectric constant makes it useful in batteries and also in cyclic voltametry. For the purification of butadienes in refineries acetonitrile has outstanding industrial value.

Dimethyl sulfoxide: DMSO is a very popular aprotic polar solvent like acetonitrile. It has no colour and scores of compounds including polar , non-polar dissolve in it. DMSO is miscible in water and in other organic solvents.

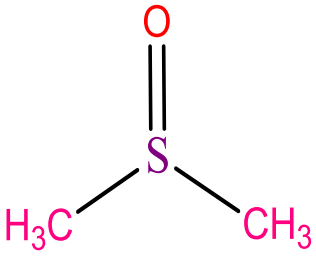

DMSO	
Appearance	Colourless liquid
Molar mass	78.13 g/mol
CAS number	67-68-5
Melting point	19 ^{0}C(292 K)
Boiling point	189 ^{0}C(462 K)
Density	1.1004 g/cm^3
Viscosity	1.996 cP at 20 ^{0}C
Refractive index	1.479
Chemical formula	C_2H_6OS

Source: Sigma Aldrich, Germany

Purification: Used as purchased. (99.0% purity)

Application: It is an organosulfur compound and used in various applications. For the purpose of mild oxidation in organic syntheses, in some sulfonium based oxidation reactions, DMSO is used as an oxidant. [4]

DMSO is sometimes used as solvent in salt involving reactions and because of its less acidity it can bear with strong bases and thus use in the studies of carbanions. In biochemistry and cell biology its use is as an extracting agent. The deuterated d_6-DMSO is extensively functional as solvent in NMR spectroscopy. In the study of in vitro drug discovery or designing DMSO is broadly used to dissolve compounds under test. The in-vivo experiments are also done with DMSO as vehicle.[5] [6, 7] [8, 9]

III.1.2. The biologically significant molecules

There are a number of bioactive molecules used in the research work and a detailed information about them is as follows.

Uracil: RNA has four nucleobases, one of which is uracil. It is linked to adenine by two hydrogen bonds. Uracil is absent in DNA or it is said that it is in demethylated form which is thymine. It is a pyrimidine derivative of natural occurrence. Uracil shows tautomeric shifts, amide form to imide form. But the amide or lactum tautomer is the popular one. [10]

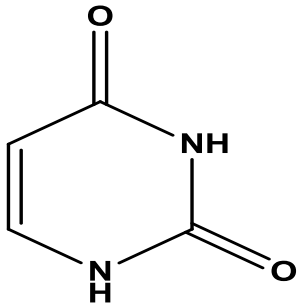

Uracil	
CAS Number	66-22-8
Molar mass	112.08676 g/mol
Appearance	solid
Melting point	335 ^{0}C (608 K)
Solubility	Soluble in water
Chemical formula	$C_4H_4N_2O_2$

Source: Sigma Aldrich, Germany

Purification: Used as purchased. Mass fraction purity is ≥ 0.99

Application: Uracil is biologically very significant molecule. In drug delivery and pharmaceuticals it is used extensively. Uracil plays vital role binding through ribose and phosphate in the synthesis of many enzymes which accelerate the function of the cell. It helps to detoxify many drugs and engages in the polysaccharide's biosynthesis. Uracil is the basic building unit of many anticancer drugs[11].

Gallic Acid: Gallic acid is a polyphenolic compound. It is trihydroxy benzoic acid. It is present in different berries, oak barks, tea leaves etc.

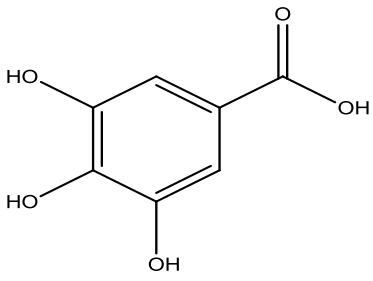

GALLIC ACID

Gallic acid	
CAS Number	149-91-7
Molar mass	170.12 g/mol
Appearance	White, yellowish white
Melting point	1.694 g/cm^3
Solubility in water	1.19 g/100mL at 20 ^{0}C(anhydrous) 1.5 g/100mL at 20 ^{0}C(monohydrate)
Chemical formula	$C_7H_6O_5$

Source: Sigma Aldrich

Purification: Used as purchased. Mass fraction purity≥ 0.99

Application: Gallic acid and its derivatives are extremely valuable for their properties such as antifungal, antibacterial, anti-inflammatory, anticancer. Gallic acid esters are industrially important components for pharmaceuticals and food industries. [12]

DL-Aminogluthimide: Aminoglutethimide is a medication in cushing's syndrome, breast cancer and prostate cancer. It had been used as anticonvulsant in early 1960 's but for its proficiency of inhibiting the production of certain hormones it is used in the treatment of hormone dependent breast carcinoma generally assisted by estrogen hormone.

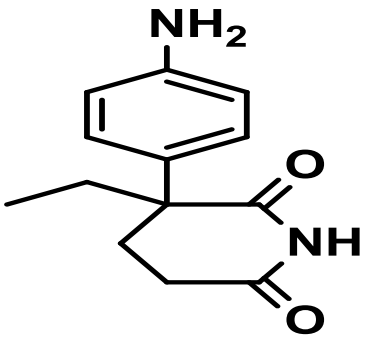

DL-Aminoglutethimide	
CAS Number	125-84-8
Molar mass	232.28 g/mol
Appearance	White powder

Melting point	152-154 ^{0}C
Solubility	Slightly soluble in H_2O; 0.2 mg/mL, soluble in acetonitrile
Chemical formula	$C_{13}H_{16}N_2O_2$

Source: TCI chemicals.

Purification: Used as purchased. The purity is >98%

Application: Generally **DL-AGT** is used in advanced breast and prostate cancers as a medicine. It is an anticonvulsant also. It is an aromatase inhibitory drug. For the treatment of metastatic breast cancer which are basically hormone assisted. The antitumor efficacy of the drug by suppressing the level of estrogen is due to its potency of inhibiting the conversion of cholesterols into steroid hormones.

Amiloride hydrochloride: Amiloride is taken as a medication of cardiac failure, high blood pressure and in liver cirrhosis. It works in our body by retaining potassium but excluding excess sodium with excess fluid .

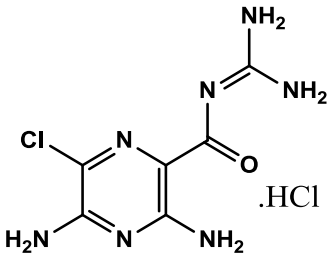

Amiloride hydrochloride	
CAS Number	2016-88-8
Molar mass	266.09 g/mol
Appearance	Yellowish white powder
Melting point	293 ^{0}C-294^{0}C
Solubility	<0.1g/100 mL in H2O at 19.5 ^{0}C
Chemical formula	$C_6H_8ClN_7O.ClH$

Source: Sigma Aldrich, Germany

Purification: Used as purchased

Application: It has natriuretic and diuretic effects though the effect is moderate i.e. by expulsion of excess sodium it can reduce the blood pressure. For the treatment of hypokalemia it has significant outcome. It can be taken along with other diuretic medicines.[13, 14]

Alibendol: Alibendol is 2-hydroxy-*N*-(2-hydroxyethyl)-3-methoxy-5-(2-propenyl)benzamide**.** Its use is as an antispasmodic medication. The use of alibendol is mostly as a constituent of some choleretic, cholekinetic drugs.

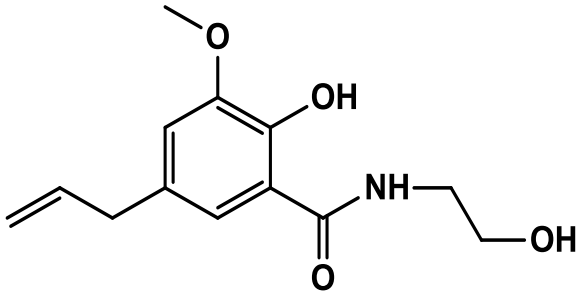

Alibendol	
CAS Number	26750-81-2
Molar mass	251.28 g/mol
Appearance	White solid
Melting point	97 ^{0}C-99 ^{0}C
Solubility	Ethanol, DMSO
Chemical formula	$C_{13}H_{17}NO_4$

Source: TCI chemicals.

Purification: Used as purchased. Its purity is >98%

Application: It is the antispasmodic drug. It gives relief from muscle spasms in stomach, intestine and other type of muscle contractions occur due to various reasons. Sometimes it is functional in choleretic and cholekinetic diseases. Loads of choleretic drugs have this compound as the main constituent. [15, 16]

III.1.3. Dye molecule (Industrially significant)

We have chosen the dye the following dye molecule for our research work.

Indigosulfonic acid dipotassium salt: It is a derivative of indigo dye which is of natural occurrence. The intra-molecular hydrogen bond is possible in the structure of ISD and due to this, it has high melting point. It has similar structure that of indigo carmine but has potassium in place of sodium.

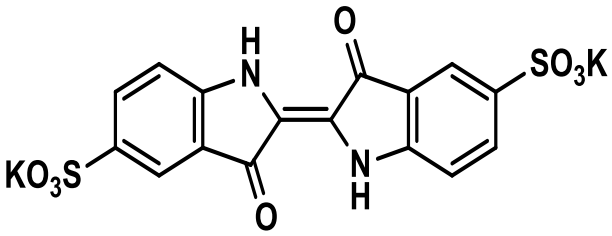

Indigosulfonic acid dipotassium salt	
CAS Number	13725-33-2
Molar mass	498.57 g/mol
Appearance	Blue solid
Melting point	>300 ^{0}C
Solubility	Partly in water,ethanol
Chemical formula	$C_{16}H_8K_2N_2O_8S_2$

Source: TCI chemicals.

Purification: Used as purchased. Purity is >90%

Application: It has applications in colouring products, textiles and other industrial and research based uses are there. It does not have much mentioning in literature. Due to its dark blue colour it is used as a colouring agent for different purposes.

III.1.4. Cyclodextrins

The use of cyclodextrin molecules, have taken a huge part of our research work. The cyclodextrin molecules that have been taken for our convenience are α and β cyclodextrins. Their descriptions are given here as follows.

α –Cyclodextrin: It is a cyclic amylose formed by the enzymatic degradation of raw vegetable materials or starch. There are six glucose subunits are joined by glycosidic α -1,4 bonds in this molecule. It is natural in origin. The glucose units are chiral and chair conformation makes the molecule rigid and also makes it truncated cone shaped with a void inside. Here the position of the secondary hydroxyl groups on the wider rim and primary hydroxyl groups are on the narrower rim.[17]

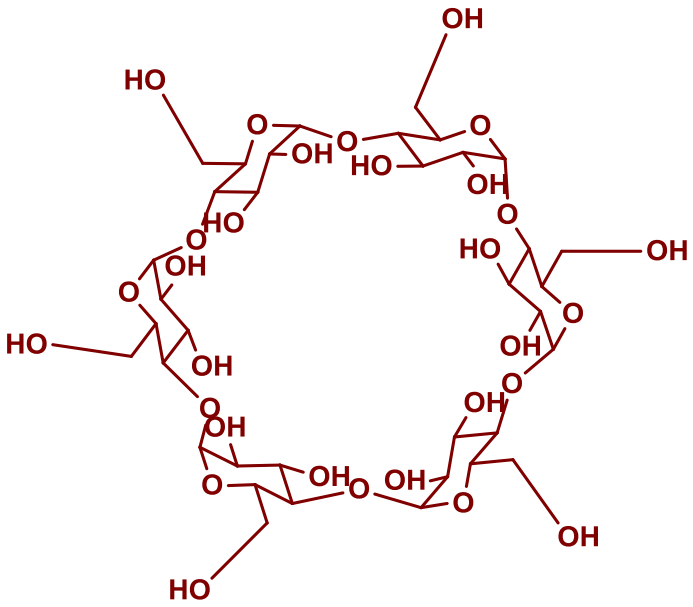

α -Cyclodextrin	
CAS Number	10016-20-3
Molar mass	972.84 g/mol
Appearance	White solid
Melting point	>278 ^{0}C
Solubility	H_2O:50mg/mL
Chemical formula	$C_{36}H_{60}O_{30}$
Internal diameter (A^0)	4.7-5.2
Number of glucose unit	6

Source: Sigma Aldrich.

Purification: Used as purchased. Purity ≥98%

Application: α –CD has numerous applications in pharmaceuticals, foods, cosmetics, textiles etc. It has a specific inner hydrophobic cavity which can accommodate

small molecules and can form inclusion complexes with them by some non-bonding interactions. It has profound application in drug delivery and also in drug designs.

β-Cyclodextrin: It has the same property like α – cyclodextrin. It has seven α-(D)-glucopyranose units connected to α-1,4 bonds. It is a amorphous white solid.

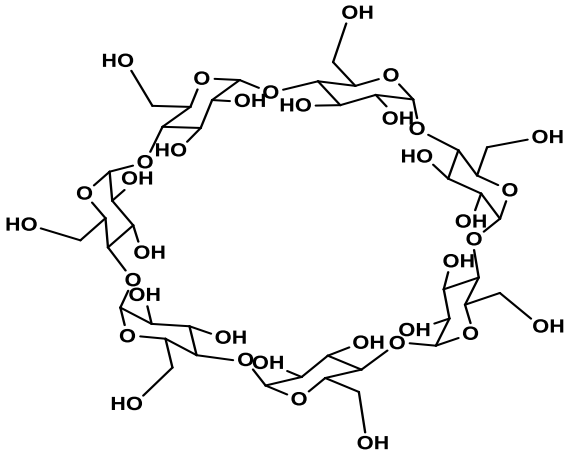

β -Cyclodextrin	
CAS Number	7585-39-9
Molar mass	1134.98 g/mol
Appearance	White solid
Melting point	290-300 ^{0}C
Solubility	18.5g/L
Chemical formula	$C_{42}H_{70}O_{35}$
Internal diameter(A^0)	6.4-7.5
Number of glucose unit	7

Source: Sigma Aldrich.

Purification: Used as purchased. Purity is ≥97%

Application: Application of β-CD is marvellous. The low production cost among the cyclodextrins makes it available for various applications. β –CD has the suitable cavity size to incorporate a number of valuable molecules of interest. Different guest molecules which are of biological importance are fitted in the cavity of β –CD to change their physical and chemical properties so as to make the compound more prospective in its activity. Low toxicity makes it an ideal component for the drug delivery and design.

III.2. EXPERIMENTAL PROCEDURES

III.2.1. Preparation of Inclusion Complexes:

At first, 20 mL 1.0 (mM) solutions of α and β-CD were prepared separately with triply distilled, deionized and degassed water which, allowed to stir for several hours on a magnetic stirrer. Then,20 mL 1.0 (mM) (prepared in purely distilled water or in 20% ethanol-water or 15% acetonitrile-water mixtures) solutions of guest molecules were added drop wise to the previously prepared aqueous solution of α-CD or β-CD making the ultimate equimolar mixture and were continued to stir for 48-72 hours at 55-60°C. The suspensions obtained after cooling the mixture to 5 °C were filtered to obtain white crystalline powder, which were then dried in air and preserved in vacuum desiccators.

III.2.2. Solution preparation

A stock solution for each component was equipped (digital electronic analytical balance, Mettler Toledo, AG 285, Switzerland) by mass, and the functioning solutions were obtained by mass dilution. The doubt of molarity of dissimilar salt solutions was evaluated to be ± 0.0003 mol·dm^{-3}.

Solvent mixtures are prepared from pure components which were taken independently in glass stoppered bottles and thermostated at the required temperature for adequate time. When the thermal equilibrium was ensured, the requisite volumes of each component were transferred in a dissimilar bottle which was already cleaned and dried methodically. Translation of essential mass of the relevant solvents to volume was skilled by using experimental densities of the solvents at experimental temperature. It was then Stoppard and the mixed contents were shaken well before use. While preparing different solvent mixtures care was taken to ensure that the same process was adopted right through the whole work. The physical properties of diverse pure and mixed solvents have been offered in the relevant chapters.

III.2.3. Preparation of multicomponent liquid mixtures:

The double and polycomponent liquid mixtures can be equipped by any one of the procedures discussed below:

(i) Mole fraction

(ii) Mass fraction

(iii) Volume fraction

(i) Mole fraction: The mole fraction (x_i) of the polycomponent liquid mixtures can be equipped using the following relation:

$$x_i = \frac{(w_i / M_i)}{\sum_{i=1}^{n}(w_i / M_i)}$$

Where, w_i, and M_i are mass and molecular mass of i^{th} component, correspondingly. The values of i depends on the number of components implicated in the development of a mixture.

(ii) Mass fraction: The mole fraction (w_i) of the polycomponent liquid mixtures can be equipped using the following relation:

$$w_i = \frac{(x_i / M_i)}{\sum_{i=1}^{n}(x_i M_i)}$$

(iii) Volume fraction: The volume fraction (ϕ_i) of the poly component liquid mixtures can be equipped by following employing three methods:

(a) Using volume: The volume fraction (ϕ_i) of the polycomponent liquid mixtures can be prepared by following relation

$$\phi_i = \frac{V_i}{\sum_{i=1}^{n} V_i}$$

Where, V_i, is the volume of pure liquid i.

(b) Using molar volume: The volume fraction (ϕ_i^l) of the polycomponent liquid mixtures can be equipped by following relation

$$\phi_i^l = \frac{x_i V_{mi}}{\sum_{i=1}^{n}(x_i V_{mi})}$$

Where, V_{mi} is the molar volume of pure liquid i.

(c) Using excess volume: The volume fraction (ϕ_i^{ex}) of the polycomponent liquid mixtures can be equipped by following relation

$$\phi_i^{ex} = \frac{x_i V_i}{\sum_{i=1}^{n} (x_i V_i) + V^E}$$

Where, V^E is the excess volume of the liquid mixture.

III.3. DETAILS OF THE INSTRUMENTS INVOLVED IN THE RESEARCH WORK:

III.3.1.Measurement of mass:

To measure mass has been carried out in a digital electronic analytical balance, Mettler Toledo, AG 285, Switzerland.

It can measure mass with excessive precision and accuracy. The weighing pot is of elevated accuracy and precision (0.0001g) is kept inside a glass enclosed space with sliding doors to save from harm from dust and air currents.

III.3.2. Thermostat:

Using Brookfield TC-550 thermostatic water bath temperature of the solutions under experiment were controlled . It has an accuracy of ± 0.01 K of the desired temperature.

III.3.3. Water distiller:

The glass distillation unit of the water distiller was of Bionics Scientific Technologies (P).Ltd. It produces contaminants free water.

It converts the water into vapour by heating it. During heating the contaminants like bacteria, some heavy metals, salts cannot get into vapour phase with water so they are left as residues in the heating/boiling chamber. The evaporated water is then condensed and the liquid form of water is collected in a container. This is how a very pure, mineral free , water is produced by the water distiller in laboratory. It is the cheapest way to get distilled water rather than buying.

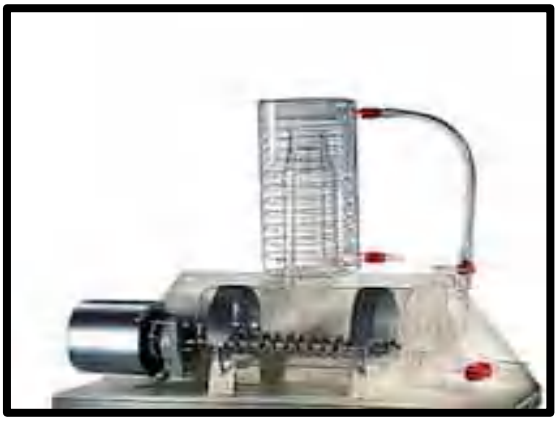

III.3.4. Magnetic stirrer:

In order to get homogeneous solutions and to promote heat and mass exchange in the mixture we used the Magnetic stirrer cum hot plate from IKA. Preparation of different required solutions and also to get solid inclusion complexes at a fixed temperature the magnetic stirrer was used.

III.3.5. Density Measurement:

The density measurementsof the solutions were measured by vibrating-tube density meter ,Anton Paar, DMA 4500M(temperature range 298.15 to 318.15 K). Calibration of the instrument was done with doubly distilled water and dry air. The uncertainty in measurement was ±0.00001 g cm^{-3}.

Here the mechanical oscillation of the U-tube at a frequency is converted into an AC voltage of the equivalent frequency associated to the density of the sample.

The related equation is , $\rho = A.\tau^2 - B$

Where,τ is the period; A and B are the instrument constants of each of the oscillator and ρ is the density of the sample.

III.3.6. Measurement of Viscosity

Brookfield DV-III Ultra Programmable Rheometer with fitted spindle size-42 was engaged to calculate the viscosities of the solutions. With the help of the following equation the viscosities were determined.

$$\eta = (100/RPM) \times TK \times torque \times SMC$$

Where RPM is the speed, TK (0.09373) is the torque constant and SMC (0.327) is the spindle multiplier constant.

The calibration of the instrument was achieved with supplied standard viscosity samples, water and aqueous solutions.

III.3.7. Refractive Index Measurement:

Refractive indices of the sample solutions were measured by the instrumentDigital Refractometer, Mettler Toledo 30GS of accuracy ±0.0005. It can be calibrated by different solutions by measuring their refractive indices e.g. distilled water, CCl_4, toluene and cyclohexane at a specific temperature.Very small quantity of the sample was poured in sample holder pan of the machine reading was taken.

Resolution	0.0001
Accuracy	± 0.0005
Measurement range	1.32-1.65
Temperature range	$10\text{-}40^0$

III.3.8. FT-IR Spectra Measurement:

The Perkin-Elmer FTIR spectrometer (shimadzu, Japan) has been used for all the IR data (in the scanning range of 4000−400 cm^{-1}).

In the KBr disk method the sample concentration should be very low 0.2-1 % and the disk has to be thicker than a film of liquid. Much grinding of KBr not needed because finely divided mixture of KBr absorbs more moisture.

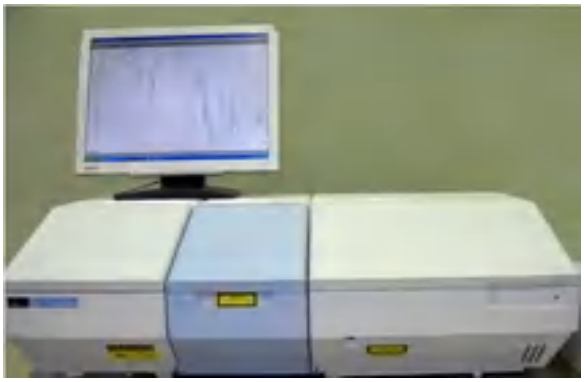

III.3.9. Isothermal titration calorimetry:

The various thermodynamic parameters regarding the inclusion process were collected from the Microcal VP-ITC (microcal now Malvern instrument). By this instrument direct quantitative measurement of the thermodynamic parameters can be obtained.

Only liquid, non-acidic samples are allowed into this machine. For each sample there should be a minimum requirement of 2 mL of reference and sample fluid. A spinning syringe is used to mix the reactants and for injecting the ligand or the sample of interest. The operator inputs all the experimental parameters and computer runs the experiment.Then the computer do the experiment. The sensitivity is 0.1 μcal. Its normal operating range is 2 ^{0}C to 80 ^{0}C. Two coin shaped cells have been enclosed guarded by the adiabatic jacket.

III.3.10. Measurement of UV-Visible Spectra

Using JASCO V-530 and Agilent 8453 UV-Visible Spectrophotometer, UV–visible spectral data were collected. The accuracy in wavelength is ±0.5 nm. The temperature , we have used in the range of 293.15K to 313.15K controlled by a digital thermostat attached to it.

Optical Specifications	
Slit width	1nm
Typical time scan	1.5 s (full range)
Wavelength range	190-1100 nm

It is a double beam spectrophotometer. First the baseline correction is done with the solvent/reference. Then the samples are taken in a cuvette for the experiment and spectra are recorded.

III.3.11. NMR Spectroscopic Measurement:

The NMR spectra were recorded in a Bruker Avance instrument at 298.15 K. The solutions were prepared in d_6-DMSO and D_2O as per requirements of the sample. Both

the 2D ROESY and NOESY as well as ^{1}H NMR spectra were recorded at 400 MHz. The δ values (chemical shifts) are represented in ppm (parts per million, D_2O; δ 4.79ppm).

III.3.12. Fluorescence Spectra Measurement

The Quantamaster-40 spectrofluorometer was used to record fluorescence spectral data at ambient temperature. Fluorescence is the emission of radiation when a molecule returns from higher electronic to ground level.

Resolution	0.06nm
Wavelength accuracy	± 0.5nm
Light source	High power continuous xenon arc lamp
Focal length	200nm
System control	spectroscopy software (computer controlled)
Emission range	185-680 nm

III.3.13. Powder X-Ray Diffraction (PXRD)

Powdered X-Ray Diffraction (PXRD) data of the test samples were recorded by D8 Bruker Advance (Cu-Kα radiation).

It can be applied for various findings like structure determination, identifying texture, phase analysis and many more. It includes primary and diffracted beam monochromator and equipped with many other drives electronically. It is basically computer controlled.

The ray produced by the x-ray tube is diffracted by the sample; detector records it. The sample rotates at a fixed angular velocity so that the glancing angle of the primary beam changes and the detector rotates round the sample at a double angular velocity.

III.3.14. Scanning Electron Microscopy (SEM)

To get the idea about the surface morphology of the samples under test the Scanning Electron Microscope (SEM), JEOL JSM IT 100 was used. The resolutions were maintained requirement wise to acquire clear and vivid micro images.

Double adhesive carbon-coated tape (tiny piece) is used for the sample preparation. The samples are sprinkled over it and excess amount of sample is removed. Samples for this experiment should be extremely dry because of high vacuum condition inside the sample chamber.

III.3.15. High Resolution Mass Spectrometry:

The mass spectrometric measurements were done by a quadruple time-of-flight (Q-TQF) high resolution instrument (with positive mode electrospray ionization) taking the solution of the ICs in methanol. This technique is a source of information both qualitative and quantitative.

First the samples are exposed to the ionisation source to get ionised. After that the ions move to the mass analyser and get separated according to their mass to charge ratio at different parts of the detector. As soon as the ions come in get in touch with detector, signals produced. Computer records the signals.

CHAPTER IV

ASSORTED INTERACTIONS PREVALENT IN URACIL AND AQUEOUS GALLIC ACID SOLUTION EXPLORED BY PHYSICOCHEMICAL CONTRIVANCE

Abstract

The solute-cosolute interaction of uracil by gallic acid has been studied through physicochemical investigation in aqueous environment. Here, we have carried out the density (ρ) and viscosity (η) measurements of uracil in w_1= 0.001, 0.002 and 0.003 mass fraction of aqueous gallic acid binary mixtures at T= 298.15K, 303.15K and 308.15K at pressure 1.013 bar. Some important parameters have been derived from the above physicochemical method, namely, limiting apparent molar volume (φ_V^0) and viscosity B-coefficients using extended Masson equation and Jones-Dole equation respectively. The refractive index (n_D) has been done on the same system at T=298.15K. Lorentz-Lorenz equation has used to evaluate molar refractive index (R_M) and limiting molar index (R_M^0). The NMR study used to measure the plausible selective site of solute-cosolute interaction.

Keywords: Solute-cosolute interactions, apparent molar volume, viscosity B-coefficient, molar refraction, NMR-study.

1. Introduction

Gallic acid is a secondary polyphenolic functionality metabolitenatural antioxidant. It is a water soluble organic compound present in grapes and in the leaves of many plants. Gallic acid esters are usedto in vitro potent antioxidant, such as tannins, catechin gallates and aliphatic gallates.However, gallic acid itself also acts as in vitro anticarcinogenic and antiangiogenic activity. Apart from its phytochemical role, gallic acid is also used in ink dyes, and the manufacture of paper, pharmaceutical industry, starting material for the synthesis of psychedelic alkaloid mescaline [1–5].

Uracil is a common naturally occurring pyrimidine group only found in RNA, its base pairs with adenine and is replaced by thymine in DNA. Uracil is planar and unsaturated with the molecular formula $C_4H_4N_2O_2$ and has the ability to absorb light. Uracil can

binds with base pairs depending on arrangement, in RNA it binds to adenine via two hydrogen bonds. Uracil is use in the body is to help carry out the synthesis of many enzymes necessary for cell function through bonding with ribose and phosphates [6–8].

To the best of our knowledge, the studies in the present ternary solution systems have not been reported earlier. Therefore, in present study we have endeavoured to make certain nature of interaction of solute itself (uracil) and with co-solute (gallic acid) in w_1=0.001, 0.002 and 0.003 mass fraction of aqueous medium at different temperatures (298.15-308.15)K with 5 interval to explain various noncovalent interactions prevailing in the ternary systems under investigation.

2. Experimental section

2.1 Source and purity of materials

Uracil and Gallic acid were purchased from Sigma-Aldrich. The mass fractions purity of both was ≥0.99. The reagents were always placed in the desiccators over P_2O_5 to keep them in dry atmosphere. These chemicals were used as received without further purification. The provenance and purity of the chemical used has been depicted in table1.

2.2 Apparatus and procedure

Solubility of the Uracil and Gallic acid in water (deionised, doubly distilled water) and the Uracil and Gallic acid has been checked precisely, prior to start of the experimental work and observe that Uracilis soluble in all proportion of aqueous Gallic acid solution. The mother solutions of Uracil were prepared by mass (Mettler Toledo AG-285 with uncertainty 0.0003g) and then the working solutions (six sets) were prepared by mass dilution. The conversion of molarity into molality [9] has been done using experimental density values of respective solutions.

The densities (ρ) of the solutions were measured by means of vibrating u-tube Anton Paar digital density meter (DMA 4500M) with a precision of ±0.00005 g.cm^{-3}maintained at ±0.01 K of the desired temperature. It was calibrated by passing deionised, triply distilled water and dry air [10].

The viscosities (η) were measured using a Brookfield DV-III Ultra Programmable Rheometer with fitted spindle size-42. The detail description has already been described earlier [11].

Refractive index (n_D) was measured with the help of a Digital Refractometer Mettler Toledo. The light source was LED, λ=589.3nm. The refractometer was calibrated twice using distilled water and calibration was checked after every few measurements [12]. The uncertainty of refractive index measurement was ±0.0002 units.

^{1}H-NMR spectra were recorded at 400 MHz Bruker instrument using D_2O as reference solvent at 298.15K.

3. Result and Discussion:

The physical parameters of binary mixtures in different mass fractions (w_1=0.001, 0.002, 0.003) of aqueous gallic acid (GA)solutions at three different temperatures (298.15K, 303.15K, 308.15K) and at 1.013 bar have been reported in table 2. The experimental measured values of density, viscosity of uracil (UA) as a function of concentration (molality), in different mass fractions of aqueous gallic acid (GA) mixture at three above mentioned temperatures have been listed in table 3.

3.1 Apparent molar volume:

Volumetric properties, like, apparent molar volume (φ_V) and limiting apparent molar volume (φ_V^0) consider important tools for understanding of interactions taking place in solution systems. The apparent molar volume can be regarded to be the sum of the geometric volume of the central solute molecule and changes in the solvent volume due to its interaction with the solute around the peripheral or co-sphere. Therefore, the apparent molar volumes (φ_V) have been determined from the solutions densities using the suitable equation [14] and the values are given in table 4.

$$\varphi_V = M/\rho - 1000\,(\rho - \rho_0)/m\rho\rho_0 \qquad (1)$$

where M is the molar mass of the solute, m is the molality of the solution, ρ and $\rho_0$are the density of the solution and aqueous gallic acid mixture respectively.

The values of (φ_V) are positive and large for all the systems, signifying strong solute-cosolute interactions. The apparent molar volumes (φ_V) are found to decrease with increasing concentration (molality, m) of uracil in same mass fraction of aqueous gallicacid at same temperature. It is also found that apparent molar volumes (φ_V) increase with both increasing temperature as well as mass fraction of aqueous gallic acid solution and varied with $\sqrt{m}$ and could be least-squares fitted to the extended Masson equation [13]from where limiting molar volume, φ_V^0(infinite dilution partial molar volume) have been estimated and the values have been represented in table 5.

$$\varphi_V = \varphi_V^0 + S_V^* \sqrt{m} \quad (2)$$

Here $\varphi_V^0$is the apparent molar volume at infinite dilution, S_V^* is the experimental slope. At infinite dilution solute molecule is surrounded only by the solvent molecules and remains infinite distant from each other. As a consequence, that $\varphi_V^0$is unaltered by itself interaction of uracil molecules and it is a measure only of the solute-cosolute (uracil-gallic acid) interaction.

An inspection of table 5 shows that $\varphi_V^0$are large and positive for all uracil at all the studied temperatures, suggesting the presence of strong solute-cosolute interaction. Comparing φ_V^0 with S_V^*values show that the magnitude of φ_V^0 is greater than S_V^*, suggesting that solute-cosolute interactions predominates over itself interaction of solute molecules in all solutions at all studied temperatures. Moreover, S_V^* values are negative at all studied temperatures indicates force of itself interaction of uracil molecules is very poor.

The variation of φ_V^0 with temperature are fitted to a polynomial of the following

$$\varphi_V^0 = a_0 + a_1 T + a_2 T^2 \quad (3)$$

Where T is the temperature in K and a_0, a_1 and $a_2$are the empirical coefficients depending on the solute, mass fraction of cosolute gallic acid. Values of coefficients of the above equation for the in aqueous gallic acid mixtures are reported in table 6.

The limiting apparent molar expansibilities, φ_E^0, can be evaluated by the following equation,

$$\varphi_E^0 = (\delta\varphi_V^0/\delta T)_P = a_1 + 2a_2T \quad (4)$$

The limiting apparent molar expansibilities, φ_E^0, change in magnitude with the change of temperature. The values of φ_E^0 for different solutions of studied gallic acid at (T=298.15, 303.15 and 308.15) K are reported in table 7.

All the values of φ_E^0 shown in the table 7 are positive for uracil in aqueous gallic acid and studied temperature. This fact helps to explain the absence of caging or packing effect for the gallic acid in solution [14].

The long-range structure-making and breaking capacity of the solute in mixed system can be determined by examining the sign of $(\delta\varphi_E^0/\delta T)_P$ developed by Hepler [15].

$$(\delta\varphi_E^0/\delta T)_P = (\delta^2\varphi_V^0/\delta T^2)_P = 2a_2 \quad (5)$$

The positive sign or small negative of $(\delta\varphi_E^0/\delta T)_P$ signifies the molecule is a structure-maker; otherwise, it is a structure-breaker [16]. The perusal of table 6 shows that, $(\delta\varphi_E^0/\delta T)_P$ values of citric acid are all positive under investigation. It shows the more symmetric rearrangement of the interacting molecules (uracil and gallic acid) with the formation of H-bonding, van der waal forces, dipole-dipole interactions etc. This symmetric arrangement is signifies the molecules of uracil and gallic acid is definitely interacting with structure–making tendency in all of the studied solution systems. The table 6 also showing the positively magnitude of $(\delta\varphi_E^0/\delta T)_P$ values in of uracil is depicting this structure–making tendency.

3.2 Viscosity:

The experimental viscosity data for studied systems are listed in table 3. The relative viscosity (η_r) has been calculated using extended Jones-Dole equation [17] for non electrolytes.

$$(\eta/\eta_0 - 1)/\sqrt{m} = (\eta_r - 1)/\sqrt{m} = A + B \cdot \sqrt{m} \quad (6)$$

Where $\eta_r = \eta/\eta_0$ is the relative viscosity, η and η_0 are the viscosities of ternary solutions (uracil+gallic acid) and solvent (aqueous mixture of gallic acid) respectively and m is the molality of uracil in ternary solutions. Where A is known as Falkenhagen coefficient [18]as it is determined by the ionic attraction theory of Falkenhagen-Vernon and B is

empirical constants known as viscosity *B*- coefficients, which are specifying to the interaction of solute itself and/or with cosolute molecules respectively. The values of *A*- and *B*-coefficients are estimated by least-square polynomial method by plotting $(\eta_r - 1)/\sqrt{m}$ against $\sqrt{m}$ with second order and reported in table 4. It is observed from table 4 the values of the *A*-coefficient are found to decrease with increase in temperature. This fact indicates the presence of very weak solute-solute interaction and also in excellent agreement with those obtained from S_V^* values.

The valuable information about the solvation of the solvated solutes and their effects on the structure of the cosolute gallic acid in the local vicinity of the solute (uracil) molecules in solutions has been obtained from viscosity *B*-coefficient [19]. It is found from table 4; the values of *B*-coefficient are positive and much higher than *A*-coefficient which signifies solute-cosolute interaction is dominant over solute-solute and cosolute-cosolute interaction. It is also observed that the positive magnitude of viscosity *B*-coefficient increases with increasing temperature and also increases with an increase in mass fraction of aqueous gallic acid mixture which suggests that solute-cosolute interaction is strengthened with rise in temperature as well as mass fraction of aqueous uric acid mixture. These results are in good agreement with those obtained from limiting apparent molar volume φ_V^0 values.

It is observed from table 4 that the values of the *B*-coefficient of citric acid increases with temperature, i.e., the *dB/dT* values are positive. From table 8, the small positive *dB/dT* values for the citric acid behaves behave almost as structure-maker.

Furthermore, it is attractive to observe that there is linear correlation between viscosity *B*-coefficients of the studied citric acid with the limiting apparent molar volumes (φ_V^0) in different mass fraction of aqueous uric acid solutions. From the above fact it means

$$B = A_1 + A_2 \varphi_V^0 \qquad (13)$$

The coefficients A_1 and A_2 are listed in table 8. As both viscosities *B*-coefficient and limiting apparent molar volumes define the solute-solvent interaction in solution. The linear variation of viscosity *B*-coefficient and limiting apparent molar volume (φ_V^0) reflects the positive slope (or A_2).

It is evident from this study, that there is a strong interaction between uracil and gallic acid and it becomes stronger with rise in temperature. As molecules of uracil are engaged with the gallic acid molecules, the interaction among the gallic acid molecules becomes less effective. We have obtained the derived parameters like, limiting apparent molar volume (φ_V^0), viscosity *B*-coefficient by interpolation and presented in table 5. The positive and significant magnitude of φ_V^0 and *B*-coefficient from table 5 clearly indicates that the limiting apparent molar volume (φ_V^0), viscosity *B*-coefficient is increases with increasing mass fraction of uracil, which indicates the positive effect of interaction of uracil with gallic acid.

3.3 Refractive Index:

The measurement of refractive index is also a suitable method for investigating the molecular interaction existing in solution. The molar refraction (R_M) can be evaluated from the Lorentz-Lorenz relation [20]. The refractive index of a substance is defined as the ratio c_o/c, where c and c_o is the velocity of light in the medium and in vacuum respectively. Stated more simply that the refractive index of a compound describes its ability to refract light as it passes from one medium to another and thus, the higher the refractive index of a compound, the more the light is refracted [21]. As stated by Deetlefs et al.[22] the refractive index of a substance is higher when its molecules are more tightly packed or in general when the compound is denser. Hence, a perusal of table 9 we found that the refractive index and the molar refraction are higher for the studied uracil and in all the mass fraction of aqueous gallic acid, indicating to the fact that the molecules are more tightly packed in the solution.

The Limiting molar refraction (R_M^0) estimated from the following equation (14)and presented in table 9.

$$R_M = R_M^0 + R_S\sqrt{m} \qquad (14)$$

Accordingly, we found that the higher values of refractive index and R_M^0which representing the fact that the molecules of uracil and are more tightly packed and greater solute-solvent interaction with gallic acid molecules than solute solvent interaction. This is also in good agreement with the results obtained from apparent molar volume and viscosity *B*-coefficients discussed above.

3.4 NMR Study: The site selective solute and cosolute interaction have been observed in ^{1}HNMR study. Gallic acid(GA) shows nmr peak at δ: 6.67 for phenolic OH group. Uracil(UA) shows nmr peak at δ: 7.44 and δ: 5.71 for C(5) and C(6) protons. NMR spectra suggest that Interaction occurs through C(5) and C(6) protons of uracil with phenolic OH group of gallic acid. This is shown in Figure1and Scheme1. Due to this weak interaction theC(5) and C(6) proton signal in uracil and gallic acid mixture (GU) shifts towards upfield and recorded at δ: 7.24 and δ: 5.57. This is obvious for the specific solute and cosolute interaction. This supports all the above physicochemical experiments along with spectroscopic data [23].

4. Conclusion:

It is evident from this study, that there is a strong interaction between uracil and gallic acid and it becomes stronger with rise in temperature. As molecules of uracil and gallic acid are engaged each other, solute-cosolute interaction is much greater than the solute-solute and solvent-solvent interactions.

Acknowledgement

The authors are thankful to the Departmental Special Assistance Scheme under the University Grants Commission, New Delhi (no. 540/6/DRS/2007, SAP-1), India for financial support and instrumental facilities in order to continue this research work.

One of the authors, Prof. M. N. Roy, is thankful to University Grant Commission, New Delhi, Government of India for being awarded onetime grant under Basic Scientific Research via the grant-in-Aid no. F.4-10/2010 (BSR) regarding his active service for augmenting of research facilities to facilitate further research work.

TABLES

Table 1: Source and purity of the chemicals

Chemical name	Source	mass fraction purity	Purification Method
uracil	SD Fine-Chem Ltd.	≥0.99	Used as procured
Gallic acid	SD Fine-Chem Ltd.	≥0.99	Used as procured

Table 2: Experimental values of density (ρ), viscosity (η) and refractive index (n_D) at 298.15 K and at pressure 1.013 bar of different mass fraction (w_1) of aq. gallic acid mixtures*

Aq. Gallic acid Mixture (w_1)	Temperature (K)	$\rho \times 10^{-3}$ /kg·m^{-3}	η /mP·s	n_D
0.001	298.15	0.99689	0.91	1.3319
	303.15	0.99547	0.83	
	308.15	0.99395	0.74	
0.002	298.15	0.99698	0.91	1.3324
	303.15	0.99556	0.84	
	308.15	0.99396	0.76	
0.003	298.15	0.99702	0.92	1.3329
	303.15	0.99564	0.85	
	308.15	0.99403	0.77	

Standard uncertainties u are: u (ρ) =0.002 kg·m^{-3}, u (η) =0.02 mP·s, u (n_D) =0.0002and u (T) =0.01K, (0.68 level of confidence)

Table 3: Experimental values of density (ρ) and viscosity (η), Uracil in different mass fractions of aqueous Gallic acidmixture (w_1) at three different temperatures and at pressure 1.013 bar*

[a]m /mol·kg^{-1}	$\rho\times10^{-3}$ /kg·m^{-3}	η /mP·s	[a]m /mol·kg^{-1}	$\rho\times10^{-3}$ /kg·m^{-3}	η /mP·s	[a]m /mol·kg^{-1}	$\rho\times10^{-3}$ /kg·m^{-3}	η /mP·s
	w_1=0.001			w_1=0.002			w_1=0.003	
	T = 298.15 K			T = 298.15 K			T = 298.15 K	
0.0100	0.99722	0.92	0.0100	0.99726	0.93	0.0100	0.99731	0.93
0.0252	0.99790	0.93	0.0252	0.99795	0.94	0.0252	0.99799	0.94
0.0404	0.99897	0.94	0.0404	0.99897	0.95	0.0404	0.99896	0.96
0.0556	1.00022	0.94	0.0556	1.00027	0.96	0.0556	1.00018	0.97
0.0709	1.00150	0.95	0.0709	1.00159	0.97	0.0709	1.00157	0.98
0.0863	1.00304	0.96	0.0863	1.00317	0.98	0.0863	1.00316	0.99
	T = 303.15 K			T = 303.15 K			T = 303.15 K	
0.0101	0.99518	0.84	0.0101	0.99588	0.85	0.0101	0.99593	0.86
0.0252	0.99652	0.85	0.0252	0.99651	0.86	0.0252	0.99655	0.87
0.0404	0.99759	0.86	0.0404	0.99756	0.87	0.0404	0.99755	0.88
0.0557	0.99834	0.87	0.0557	0.99877	0.88	0.0557	0.99874	0.89
0.0710	1.00014	0.87	0.0710	1.00025	0.89	0.0710	1.00014	0.90
0.0864	1.00158	0.88	0.0864	1.00174	0.89	0.0864	1.00173	0.91
	T = 308.15 K			T = 308.15 K			T = 308.15 K	
0.0101	0.99425	0.75	0.0101	0.99429	0.77	0.0101	0.99432	0.78
0.0253	0.99491	0.75	0.0253	0.99491	0.77	0.0253	0.99487	0.79
0.0405	0.99588	0.76	0.0405	0.99593	0.78	0.0405	0.99583	0.80
0.0558	0.99716	0.77	0.0558	0.99713	0.79	0.0558	0.99699	0.80
0.0712	0.99846	0.77	0.0712	0.99852	0.80	0.0712	0.99845	0.81
0.0866	0.99998	0.78	0.0866	0.99991	0.81	0.0866	0.99989	0.82

*Standard uncertainties u are: u (ρ) =0.00002 kg·m^{-3}, u (η) =0.02 mP·s and u (T) =0.01K (0.68 level of confidence)

[a]molality has been expressed per kg (gallic acid + water) solvent mixture

Table 4: Apparent molar volume (φ_V) and $(\eta_r\text{-}1)/\sqrt{m}$ of uracil in different mass fraction (w_1) of aqueous gallic acid mixtures at three different temperatures*

[a]molality /mol·kg^{-1}	$\varphi_V\times10^6$ /m^{3}mol^{-1}	$(\eta_r\text{-}1)/\sqrt{m}$ /kg$^{1/2}$mol$^{-1/2}$	[a]molality /mol·kg^{-1}	$\varphi_V\times10^6$ /m^{3}mol^{-1}	$(\eta_r\text{-}1)/\sqrt{m}$ /kg$^{1/2}$mol$^{-1/2}$	[a]molality /mol·kg^{-1}	$\varphi_V\times10^6$ /m^{3}mol^{-1}	$(\eta_r\text{-}1)/\sqrt{m}$ /kg$^{1/2}$mol$^{-1/2}$
w_1=0.001			w_1=0.002			w_1=0.003		
T = 298.15 K			T = 298.15 K			T = 298.15 K		
0.0100	183.25	0.11	0.0100	188. 17	0.12	0.0100	192.70	0.13
0.0252	168.21	0.13	0.0252	169.85	0.15	0.0252	170.21	0.15
0.0404	151.19	0.15	0.0404	158.12	0.17	0.0404	165.86	0.19
0.0556	144.82	0.16	0.0556	145.69	0.20	0.0556	157.17	0.21
0.0709	138.51	0.20	0.0709	139.15	0.21	0.0709	149.59	0.23
0.0863	131.83	0.21	0.0863	133.16	0.22	0.0863	138.35	0.24
T = 303.15 K			T = 303.15 K			T = 303.15 K		
0.0101	187.89	0.05	0.0101	192.91	0.08	0.0101	196.99	0.09
0.0252	171.41	0.10	0.0252	173.71	0.10	0.0252	183.21	0.12
0.0404	160.61	0.11	0.0404	163.63	0.11	0.0404	168.68	0.15
0.0557	150.36	0.13	0.0557	153.91	0.12	0.0557	158.72	0.17
0.0710	140.08	0.14	0.0710	143.53	0.15	0.0710	148.12	0.21
0.0864	135.53	0.15	0.0864	138.57	0.20	0.0864	142.12	0.22
T = 308.15 K			T = 308.15 K			T = 308.15 K		
0.0101	194.23	0.07	0.0101	196.23	0.06	0.0101	200.38	0.08
0.0253	175.13	0.10	0.0253	181.21	0.10	0.0253	183.13	0.11
0.0405	162.41	0.13	0.0405	167.89	0.13	0.0405	171.39	0.16
0.0558	150.26	0.15	0.0558	157.25	0.16	0.0558	160.38	0.18
0.0712	142.46	0.17	0.0712	148.88	0.18	0.0712	150.75	0.21
0.0866	138.96	0.18	0.0866	141.80	0.20	0.0866	143.11	0.22

*Standard uncertainties u are: u (T) =0.01K, the accuracy of φ_V is 1.86×10^{-6} m^3 mol^{-1} and $(\eta_r\text{-}1)/\sqrt{m}$ is 0.004 kg$^{1/2}$mol$^{-1/2}$ (0.68 level of confidence)

[a]molality has been expressed per kg of (gallic acid + water) solvent mixture

Table 5: Limiting apparent molar volume (φ_V^0), experimental slope (S_V^*), viscosity *A*- and *B*-coefficient of uracil in different mass fraction (w_1) of aqueous gallicic acid mixtures at three different temperatures*

Mass fraction (w_1)	T /K	$\varphi_V^0 \times 10^6$ /m^3 mol^{-1}	$S_V^* \times 10^6$ /m^{3}mol$^{-3/2}$ kg$^{1/2}$	*B* /kg mol^{-1}	*A* /kg$^{1/2}$ mol$^{-1/2}$
0.001	298.15	220.18	-417.12	0.41	0.02
	303.15	225.45	-451.27	0.49	0.01
	308.15	231.28	-493.79	0.67	0.05
0.002	298.15	225.98	-499.65	0.53	0.04
	303.15	230.63	-477.45	0.66	0.02
	308.15	236.16	-463.92	0.78	0.01
0.003	298.15	230.72	-448.89	0.65	0.03
	303.15	235.51	-453.56	0.77	0.01
	308.15	241.12	-442.87	0.93	0.04

*Standard uncertainties values of *u* are: *u* (*T*) =0.01K

Table 6: Values of various coefficients and standard deviation of equation-3 for uracil acid in different aqueous gallic acid solutions*

Aq. Gallic acid Mixture (w_1)	$a_0 \times 10^6$ /m^3 mol^{-1}	$a_1 \times 10^6$ / m^3 mol^{-1}K^{-1}	$a_2 \times 10^6$ / m^3 mol^{-1}K^{-2}	$(\delta\varphi_E^0/\delta T)_P \times 10^6$ / m^3 mol^{-1} K^{-2}
0.001	2014.72	-15.21	0.01	0.03
0.002	2141.61	-14.24	0.02	0.06
0.003	2212.43	-13.28	0.02	0.05
Average standard deviation	3.1	0.011	0.0002	0.0001

Table 7: Limiting apparent molar expansibilities (φ_E^0) for uracil in different mass fraction of aqueous gallic acid (w_1) at different temperature

Aq. gallic acid Mixture (w_1)	$\varphi_E^0 \times 10^6$/ m^3 mol^{-1} K^{-1}		
T/ K	298.15	303.15	308.15
0.001	1.012	1.142	1.253
0.002	3.729	3.928	4.227
0.003	-1.533	-1.344	-1.133
Average standard deviation	0.003	0.003	0.002

Table 8: Values of dB/dT, A_1 , A_2coefficients for the uracil in different mass fraction of aqueous gallic acid (w_1) at studied temperatures*

Aq. Gallic acid Mixture (w_1)	dB/dT	A_1	A_2
0.001	0.031	-6.746	0.021
0.002	0.026	-7.766	0.022
0.003	0.035	-8.295	0.034
Average standard deviation	0.001	0.005	0.003

*Standard uncertainties values of u are: u (T) =0.01K

Table 9: Refractive index (n_D), molar refraction (R_M) and limiting molar refraction (R_M^0) uracil in different mass fraction of aqueous gallic acid solutions at 298.15 K and at pressure 1.013 bar *

[a]molality /mol·kg^{-1}	n_D	$R_M\times10^6$ / m^3 mol^{-1}	$R_M^0\times10^6$ / m^3 mol^{-1}
w_1=0.001			
0.0100	1.3320	44.23	
0.0252	1.3323	44.23	
0.0404	1.3328	44.23	44.24±0.03
0.0556	1.3333	44.25	
0.0709	1.3338	44.25	
0.0863	1.3345	44.26	
w_1=0.002			
0.0100	1.3325	44.27	
0.0252	1.3327	44.27	
0.0404	1.3333	44.28	44.28±0.03
0.0556	1.3338	44.28	
0.0709	1.3343	44.31	
0.0863	1.3349	44.31	
w_1=0.003			
0.0100	1.3333	44.36	
0.0252	1.3336	44.37	
0.0404	1.3343	44.42	43.42±0.02
0.0556	1.3350	44.43	
0.0709	1.3356	44.45	
0.0863	1.3363	44.46	

*Standard uncertainties u are: $u(n_D)$ =0.02 and $u(T)$ =0.01K (0.68 level of confidence)

[a]molality has been expressed per kilogram of (gallic acid + water) solvent mixture

FIGURES

Fig 1: Plot of ^{1}HNMRspectra of gallic acid (GA), uracil (UA) and uracil+ gallic acid (GU) at 298.15K in D2O.

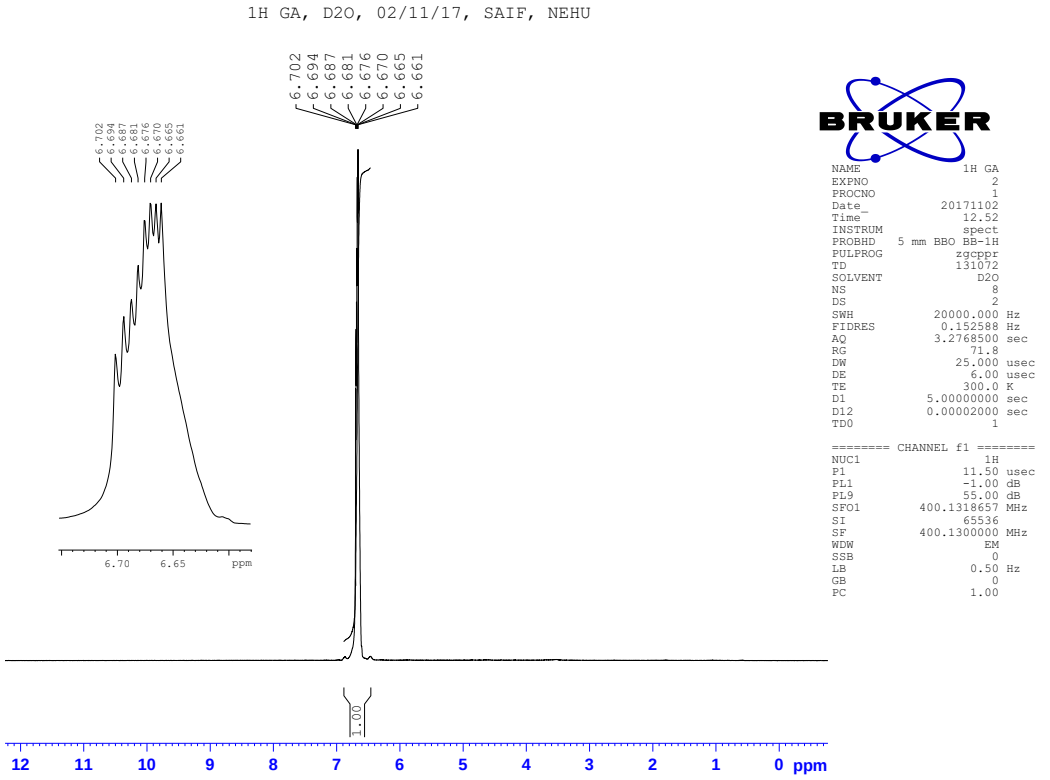

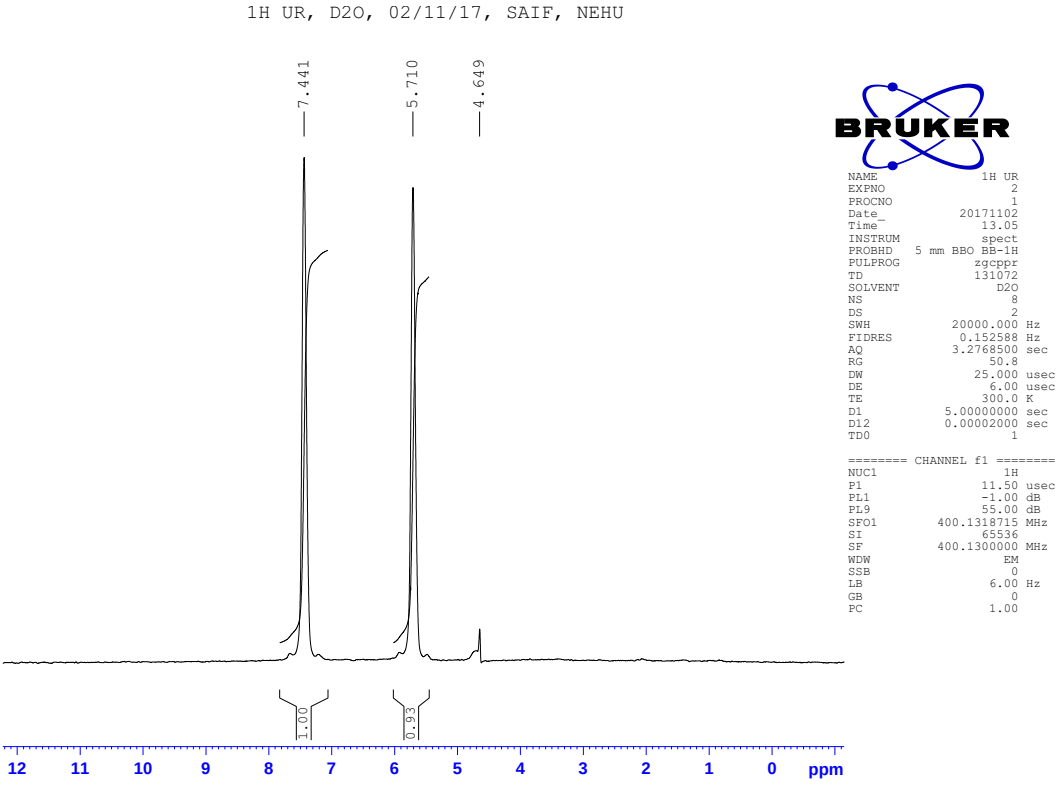

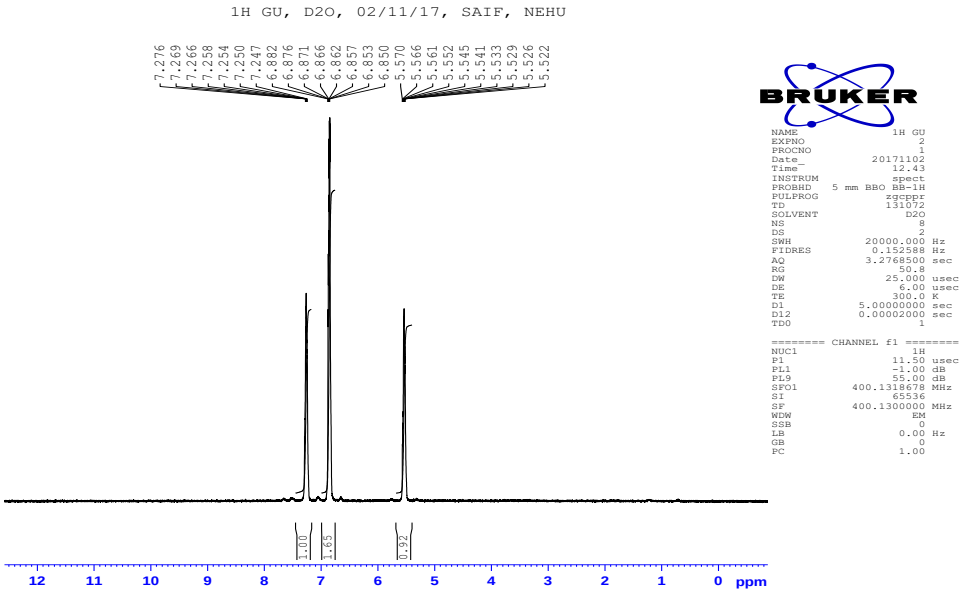

SCHEMES

Scheme1. Plausible solute-cosolute interaction C5and C6 proton of uracil with phenolic OH group of gallic acid.

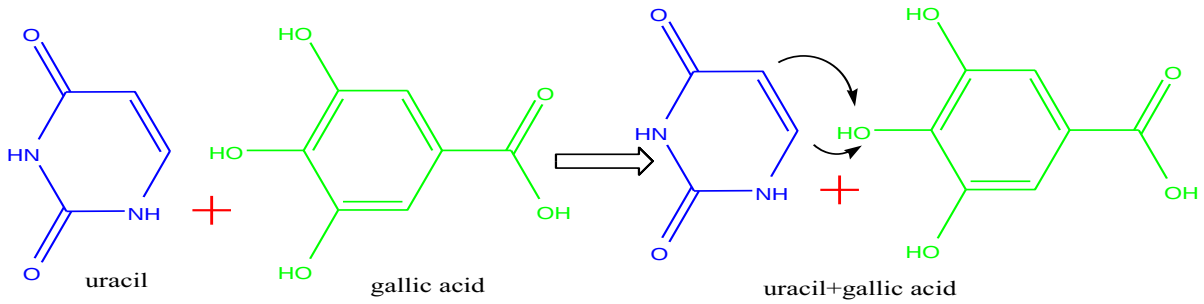

CHAPTER V

EXPLORING ENCAPSULATION OF AN ANTISPASMODIC DRUG ALIBENDOL WITH β-CYCLODEXTRIN MOLECULE BY SPECTROSCOPIC METHODOLOGIES

Abstract: The encapsulation of Alibendol (AB), the biologically potent muscle relaxant, within the cavity of β-cyclodextrin(β-CD) was studied in assistance of some spectroscopic techniques such as Uv-Vis spectroscopy, ^{1}HNMR spectroscopy, 2D ROESY, FT-IR spectroscopy. The study confirmed 1:1 stoichiometry of the host-guest inclusion complex. All the experiments showed a good correlation to establish a feasible inclusion through wider rim of the cyclodextrin molecule. The thermodynamic parameters explained the process of inclusion as exergonic and spontaneous.

Keywords: Alibendol, β–CD, 2D ROESY, 1:1

1. Introduction:

The muscle relaxant is a medication that reduces the contraction of muscles by disturbing skeletal muscle functioning. It may be used to reduce the indications which include hyperreflexia, muscle spasms, and pain. The muscle relaxants are categorized as spasmolytics and neuromuscular blockers. The latter category acts by entering at the neuromuscular end and does not affect the central nervous system. They can cause short-term paralysis during surgery. Spasmolytics are muscle relaxants, that basically focus on to reduce spasms and musculoskeletal pain. Sometimes spasmolytics and the neuromuscular blockers are conjointly spelled as muscle relaxants but mainly spasmolytics are the muscle relaxants.

The natives of South America who lived in the Amazon bed in the early century, used specially designed arrows that have poison on the tip and can cause skeletal muscle paralysis which bring about death. The research had done a lot of scientific studies thereafter and this leads to the discovery of many muscle relaxants/antispasmodic drugs that relax the muscle spasms [1, 2]. Antispasmodics are the spasmolytics that are given when there occurs smooth muscle spasms. They are immensely effective in the

gastrointestinal tract to diminish the aching in the intestine, stomach, and in urinary bladder. [3]

Alibendol, or 5-allyl-2-hydroxy-N-(2-hydroxyethyl)-3-methoxybenzamide, is an antispasmodic drug that reduces the muscle spasms. Different antispasmodic drugs including choleretic, cholekinetic contains this compound as an active ingredient.

For the treatment of dyspepsia causes from biliary insufficiency, alimentary intolerance, and constipation of hepatic origin, the use of this drug is commendable. [4]

A number of applications of cyclodextrins has been included in the literature till now . The fundamentals of interaction of cyclodextrins with other molecules, initiated by Schardinger and viliers 100 years back. CDs are the macrocyclic oligosaccharides and of natural occurrence. Three types of CDs α, β and γ having 6,7, 8 glucopyranose units (joined by α-1,4 lingkages) respectively, particularly generated from the enzymatic degradation of starch . The hydrophobic toroid shaped cavity of the CD can put specific molecule inside it, which possesses definite shape and can create some non-covalent interactions with CD to produce the inclusion complex .Outer surface is hydrophilic for the CD, which makes it water soluble. With this benefit, CDs are employed for drug carriers and new drug designs chiefly for the drugs, which have low solubility, bioavailability and have toxicity ,which causes side effects. [5]

In this work, we have designed an inclusion complex of alibendol and β –CD to overcome the above mentioned limitations of the drug (alibendol).The encapsulation of the above molecules was characterised by different techniques.

2. Experimental section

2.1. Source and purity of samples:

The drug (Alibendol) selected for experiment and β-CD were purchased from TCI Chemicals and Sigma-Aldrich, Germany respectively and used as purchased. The mass fraction purity of AB (Alibendol) and β-cyclodextrin were ≥0.98, 0.97 respectively.

2.2. Apparatus and procedure

Solubility of β-CD and the drug have been verified in triply distilled, deionized and degassed water. It was detected that the drug AB is poorly soluble in water. All the stock solutions of the drug were prepared by mass (Mettler Toledo AG-285 with uncertainty 0.0001 g) and the working solutions were prepared by mass dilution at 298.15 K. [6]. Necessary precautions were made to reduce the evaporation during mixing.

^{1}H NMR spectra were recorded in d_6- DMSO at 400 MHz using Bruker AVANCE 400 MHz instrument at 298.15K. Signals were quoted as values in ppm.

UV–visible spectra were recorded by Agilent 8453 Uv-visible spectrophotometer attached with a thermostat to control the temperature.

FTIR spectra were recorded by Perkin Elmer FT-IR Spectrometer applying KBr Disk technique with scanning range 400 to 4000 cm^{-1}.

2.3. Preparation of Solid Inclusion Complex of AB with β -CD:

For the formation of inclusion complex, β-CD of 1.134 g was mixed with 30 mL triply distilled and degassed water in a round bottom flask and stirred continuously over magnetic stirrer for few hours. Then 0.258g of AB was taken into a beaker along with 10 mL ethanol-water mixture (20%) and stirred over magnetic stirrer until a homogeneous mixture (completely dissolved) is formed. Here, 1:1 M ratio of β-CD and AB has been used. Guest mixture was then added into β-CD solution and stirred for 48 h without a break. The reaction mixture was then put in refrigerator for 52 h without any disturbance. After 2 days, a white solid was observed. The residue was filtered and washed for several times with distilled water. Finally, the dry white powder was acquired after drying in oven at 50°C for about 24 h. The resultant solid was the inclusion complex between AB and β-CD [7]. It was further analysed by FT-IR, NMR methods.

3. Result and discussion:

3.1. UV–visible spectroscopy

3.1. A. Job plot for determination of stoichiometry:

The stoichiometry of the IC has been discerned utilising continuous variation Job's method [8] in the solution medium by plotting ΔA × R against R (where ΔA is the difference in absorbance of AB without and with CD and R is [AB]/([AB]+[CD]) and the spectral data have been listed in Table 1. Sets of solution were made from AB and β-CD by changing the mole fraction of guest from 1-0 or vice versa in 20% ethanol-water mixture. The value of R at the maxima on curve provides the stoichiometry ratio of IC (IC-$_{1:2}$, R = 0.33; IC-$_{1:1,}$ R = 0.5; IC-$_{2:1,}$ R = 0.66) [9]. It has been found that the resultant curve shows the maximum at R = 0.5 suggesting that the complex has a stoichiometry of 1:1 (Fig. 1).

3.1.B. Association Constant: Interaction of AB With β-CD in liquid environment.

The UV absorption spectra of AB in [20%EtOH-H_2O (v/v)] β-CD medium have been analysed. The spectral data of AB in various concentration of β-CD at different temperatures have been registered in TableS1, S2 and S3. The strong absorption peaks of AB appears at 212 nm and with addition of β-CD blue shift occurs. No significant isosbestic point is spotted in the spectra. The absorbance intensities of AB gradually increase with increasing the concentration of β-CD. This fact confirms the encapsulation of guest molecule into the β-CD cavity due to the presence of hydrophobic and van der Waals interaction between the guest monomer and β-CD molecules [7, 10, 11]. Thus, such non-covalent interactions act as the main driving forces to incorporate the guest molecule into the CD cavity to form 1:1 IC throughout the complexation process by promoting the dissolution of the guest molecule (AB).

From the Job plot, it is confirmed that AB and β-CD form 1:1 IC. Hence, the IC formed between AB and CD can be represented as,

CD + AB⇄CD⋯AB

For a 1:1 complexation process the association constant (k_a) has been estimated by using the double reciprocal plots on the basis of Benesi-Hildebrand equation [12]. The absorption values are used in the following Benesi-Hildebrand Eq. (1) [13].

$$\frac{1}{\Delta A} = \frac{1}{\Delta\varepsilon[AB]ka}\frac{1}{[CD]} + \frac{1}{\Delta\varepsilon[AB]} \quad (1)$$

Fig.2 depicts the plots of 1 / ΔA against 1 / [CD] at temperatures 293.15K, 303.15K and 313.15 K. A good linear correlation was observed at all the three temperatures, showing that the IC is of 1:1 stoichiometry. The values of k_a were evaluated by using the Eq. (1) from the intercept/slope of the plots (Fig.2). The values are presented in Table 2. It has been found that the association constants have high positive values that designate that the interaction of the guest and host are strong to form inclusion complex.

3.1.C. Thermodynamic parameters show Spontaneity of formation of Inclusion Complex

The free energy change (ΔG) is a very vital thermodynamic parameter that has been estimated by using the Eq. (3) [14, 15]. From the plot of Association constants (k_a) against 1/T, enthalpy and entropy values have been obtained with the help of van't Hoff equation Eq. (2).

$$2.303 log k_a = -\frac{\Delta H^0}{RT} + \frac{\Delta S^0}{R} \quad (2)$$

It is found that the entropy is small negative. This fact supports the association of the host and guest. The enthalpy has also been found to be negative, which again is a strong evidence of interaction of the host and guest whereas the negative value of free energy change supports the spontaneity of the formation of the IC and support the fact that the complexation is an exergonic process.

$$\Delta G = \Delta H - T\Delta S \quad (3)$$

3.2. ^{1}H NMR: Supports inclusion:

The formation of IC can be explained on the light of the ^{1}H NMR spectroscopy study [16]. This method is based on the changes of chemical shifts of protons due to encapsulation of guest molecule into the β-Cyclodextrin [17]. In β-CD structure the H-3

(near wider opening side) and H-5 (close to narrow rim) are located inside of the β-Cyclodextrin cavity. The H-6 of methylene group (bearing the primary OH group) remains on the narrow opening side of β-Cyclodextrin and the rest of the other H atoms H-1, H-2, H-4 are situated on the outer surface of β-CD. The ^{1}H NMR spectra of β-CD, pure AB and the solid IC are represented in Fig. 4. It is clearly observed from Table 3 and Table 4 that for H3 and H5, a large up-field shift has been occurred. The considerable changes of chemical shifts (δ) suggested that the AB monomer entered into the nano hydrophobic hole of β-CD. The upfield shift of H-3 (δ = 0.050ppm) is much greater than the H-5 shifting (δ = 0.005ppm). On the other hand, minor chemical shifts are observed for 1'H, 2'H,3'H that are the part of the guest AB molecule, which further support the complexation process. A significant downfield shift for the protons 1'H, 2'H, 3'H of AB has been detected. In the IC these 'H's of AB are situated in hydrophobic hollow space of β-Cyclodextrin. The hydrophobic environment is responsible for the downfield shift of the protons of guest [18]. These all changes clearly indicate that well encapsulation of the guest AB into interior hydrophobic cavity of β-CD has been occurred and it enters through the wider ring opening side. The detailed variations of chemical shifts of the two binding partners before and after forming IC have already been mentioned in Table3 & 4.

3.3. 2D-ROESY Study to Confirm the Inclusion Phenomena:

The principle of 2D ROESY relies on the interaction of the protons which are present in the close proximity of 0.4 nm range to each other to produce NMR cross peaks [19] [20]. In our study, we have investigated the inclusion of the drug inside the nano-cavity of β-CD. The NMR study was carried out in d_6-DMSO. It is clear that the H-3 and H-5 protons of β- CD are present inside the cavity and hence if inclusion occurs, there should be the presence of such close proximity of 0.4 nm of the AB protons with H-3 and H-5 protons of CD which can produce rotating-frame nuclear overhauser effect to give cross peaks [21, 22]. In Fig.5 there are the presence of cross peaks due to the interaction of H-3 proton of β-CD and 2'H proton of AB and H-5 protons of β-CD with 3'H protons of AB. This clarifies the root of insertion of guest inside host through the wider rim. In the dynamic process of the inclusion the cross peaks are generated due to the insertion of the side chain of the guest but it is not possible of entering the second AB molecule as it

is sterically unfavourable. Hence, this incident signifies the inclusion phenomena of the said drug molecule into the CD cavity.

3.4: FTIR study:

Formation of the inclusion complex is enlightened with the help of FTIR spectroscopic study. Here, the deviation of peak shape, position and intensity of the FT-IR spectra of solid IC is used to confirm the inclusion [23]. The characteristic IR frequencies of AB, β-CD, and their solid IC are listed in Table5 along with the chemical bonds responsible for the corresponding stretching frequencies and the spectra are shown in Fig.6. In the IR spectra, Stretching of =C-H of the pure AB was observed at 3039cm^{-1} but the peak was not seen in the IR spectra of IC. The stretching of aromatic -C=C was found at 1606 cm^{-1} for the pure AB but the considerable shift of the spectra was observed in the inclusion complex at 1631cm^{-1} . On the other hand the peak due to O-H stretching of β-CD was observed at 3408 cm^{-1} which was shifted in the spectra of IC to 3385 cm^{-1}. The stretching frequency of the C-H from CH_2 was also found to be shifted from 2941 cm^{-1} to 2922cm^{-1}. This may be due to the interaction of the O-H groups with the polar part of the guest AB. Short band due to O-H bending at 1404 cm^{-1} was found absent. Band at 1465 cm^{-1} due to bending of $–CH_2-$ of AB was also found to be absent in IC. These are due to the interaction of the host and guest after formation of the IC. From the analysis of the 2D NMR spectra it is clear that the propenyl group of AB is inserted inside the CD molecule. Moreover the absence of O-H bending frequency, shifting of alkyl C-H stretching, shifting of C-N stretching conclude the outer sphere polar interaction of the host and guest. [24]

3.5. Effects of CD: interaction of AB with β-CD in liquid environment

Cyclodextrin has a unique structure to accommodate guest molecules of various dimensions. The cavity diameter of β-CD is 6.0-6.5 Å. Here, alibendol is a molecule of suitable size that can easily be incorporated by the host beta-cyclodextrin. The propenyl group of the alibendol at the C-5 position of the aromatic ring is hydrophobic in nature. This hydrophobic part of AB can easily enter inside the cyclodextrin cavity and participate in the hydrophobic interaction with the hydrophobic part of the CD molecule. The 2D NMR shows that 3'H interacts with the H-5 of cyclodextrin and 2'H

interacts with the H-3 of cyclodextrin. The C=O group at the C-1 position as well as the methoxy group at the C-3 position of the aromatic ring interact with the O-H Proton of cyclodextrin and thus a stable inclusion complex is formed. During the inclusion complexation, the guest enters through the wider rim of the CD molecule.

According to Shikari and his co-workers the water molecules which are polar in nature bound by the polar-apolar interaction inside the hydrophobic cavity of cyclodextrin molecule, which is in fact not so strong and as a consequence the relatively more stable inclusion complex is formed due to stronger apolar-apolar interaction removing the water molecule from the cavity [25] [26]. As a result a more stable lower energy state of the system is obtained where the ring strain of cyclodextrin moiety is reduced.

4. Conclusion: The incorporation of the antispasmodic AB within β-CD and their interactions have been studied by Uv-vis, ^{1}HNMR, 2D ROESY and FTIR spectroscopy. The 1:1 complexation was attributed by job's plot. The values of thermodynamic parameters also suggest the same. The generation of cross peaks in the 2D ROESY spectra is a confirmation that the inclusion complex has been formed between the drug and cyclodextrin. This work mainly focused on the establishment of the phenomenon of inclusion so that certain properties of the drug can be changed for betterment of its activity. The sound IC can be treated as a modified version of the drug which may lead to increase of water solubility of the drug and decrease its side effects (toxicity) or also may contribute in control drug delivery in near future with retention of its therapeutic activity.

Conflict of interest: There is no conflict of interest.

Acknowledgement: Authors are thankful to Dept. of Chemistry, University of North Bengal for laboratory and instrumental conveniences. Prof. M.N. Roy is obliged to University Grants Commission, New Delhi for awarding one time grant.

TABLES

Table: 1: Data of Job's plot of (AB+β-CD) system obtained from Uv-visible spectroscopy.

Guest conc. [D] (µm)	β-CD (µm)	R= [D]/ ([D]+[β-CD])	A @λmax 212 nm	ΔA (2.02707-A)	ΔAx[AB]/ ([AB]+[β-CD])
100	0	1	2.02707	0	0
90	10	0.9	1.91375	0.11332	0.101988
80	20	0.8	1.69433	0.33274	0.266192
70	30	0.7	1.51287	0.5142	0.35994
60	40	0.6	1.27714	0.74993	0.449958
50	50	0.5	1.05889	0.96818	0.48409
40	60	0.4	0.8708	1.15627	0.462508
30	70	0.3	0.6174	1.40967	0.422901
20	80	0.2	0.38435	1.64272	0.328544
10	90	0.1	0.17471	1.85236	0.185236
0	100	0	0.07143	1.95564	0

Table.2: Values of Association constants (K_a) obtained by Benesi-Hildebrand method from UV-vis spectroscopy and corresponding free energy change (ΔG^0), enthalpy (ΔH^0), entropy (ΔS^0) of the AB.β-CD inclusion complex at 293.15K, 303.15K and 313.15K.

Complex	k_a ($10^3 M^{-1}$)			ΔG^0 (kJ mol^{-1})	ΔH^0 (kJ mol^{-1})	ΔS^0 (J mol^{-1}) K^{-1}
	293.15K	303.15K	313.15K			
AB - β-CD	6.78	4.42	1.26	-21.14	-63.86	-143.31

Table3. ^{1}H-NMR spectral data of Alibendol (AB), β-CD, AB.β-CD(IC).

Alibendol (400 MHz, Solvated DMSO) δ /ppm	2.507-2.516 (1H, S); 3.289-3.371 (2H, td, J=6.0, 6.8 Hz); 3.513-3.542 (2H, t, J= 6.0 Hz); 3.718-3.818 (5H, t, J=20.0Hz); 5.036-5.113 (2H m); 5.926-6.027 (1H, tt, J= 6.8Hz, 3.6Hz); 6.924-6.928 (1H, d, J= 1.6Hz); 7.27 (1H, d; δ8.75 J=2.0Hz).
β-CD (400 MHz, Solvated DMSO) δ /ppm	2.33–2.56 (6H, t, J = 9.2 Hz), h5=3.27–3.37 (6H, dd, J = 9.6, 3.2 Hz), h3=3.55–3.66 (18H, m), 4.44-4.47 (6H, t, J = 9.2 Hz), 5.67–5.74 (6H, d, J = 3.6 Hz).
Alibendol- β-CD IC (400 MHz, Solvated DMSO)δ /ppm	2.33–2.56 (6H, t, J = 9.2 Hz), 2.507-2.516 (1H, S);**h5**=3.26–3.37(6H, dd, J = 9.6, 3.2 Hz), 3.323-3.412(2H, td, J=6.0, 6.8 Hz); 3.513-3.542 (2H, t, J= 6.0 Hz); **h3**=3.51–3.60(18H, m),3.718-3.818 (5H, t, J=20.0Hz); 4.44-4.47 (6H, t, J = 9.2 Hz), 5.046-5.124(2H m);5.67–5.74 (6H, d, J = 3.6 Hz).5.947-6.044 (1H, tt, J= 6.8Hz, 3.6Hz); 6.924-6.928 (1H, d, J= 1.6Hz); 7.27 (1H, d; δ8.75 J=2.0Hz).

[a] mixed in 1:1 molar ratio, 400 MHz, Solvent: DMSO-d_6;

Table.4: The chemical shift values of the protons of β-CD, Alibendol in pure state and in complexed state and their deviations from pure to complex.

	σ(ppm)			
Protons	β -CD	IC	Alibendol	Δσ ($\sigma_{complex}$-σ_{Pure})
H-3	3.605	3.555		-0.050
H-5	3.320	3.315		-0.005
1'H		3.36	3.33	0.03
2'H		5.99	5.97	0.02
3'H		5.08	5.07	0.01

Table.5: Data obtained from FT-IR spectroscopic study of β-CD, AB& β-CD+AB IC

Group	Wave number (Cm^{-1})		
	β-CD	AB	β-CD+ AB
stretching of O-H	3408		3385
stretching of –C-H from $–CH_2$	2941		2922
bending of –C-H from $–CH_2$ and bending of O-H	1404		…….
bending of C-O-C	1160		1155
vibration involving α-1,4linkage	954		949
Alkyl -C-H Stretching		3306	…..
Stretching =C-H		3039	…..
Stretching aromatic -C=C		1606	1631
$-CH_2-$ bending (m)		1465	…..
C-N stretching		1264	1266

Table S1. Data of Benesi-Hildebrand double reciprocal plot of the system (Alibendol+β-CD) obtained from Uv-Vis spectroscopy at 293.15 K.

A0	A1	ΔA	1/ΔA	1/CD
0.61996	0.75569	0.13573	7.367568	50000
0.61996	0.81599	0.19603	5.10126	33333
0.61996	0.86508	0.24512	4.079634	25000
0.61996	0.91828	0.29832	3.352105	20000
0.61996	0.97096	0.351	2.849003	16667
0.61996	1.00208	0.38212	2.616979	14286

Table S2. Data of Benesi-Hildebrand double reciprocal plot of the system (Alibendol+β-CD) obtained from Uv-Vis spectroscopy at 303.15 K.

A0	A1	ΔA	1/ΔA	1/CD
0.69196	0.81161	0.11965	8.35771	50000
0.69196	0.85686	0.1649	6.064281	33333
0.69196	0.91998	0.22802	4.38558	25000
0.69196	0.94354	0.25158	3.974879	20000
0.69196	0.97856	0.2866	3.489184	16667
0.69196	1.02998	0.33802	2.958405	14286

Table S3. Data of Benesi-Hildebrand double reciprocal plot of the system (Alibendol+β-CD) obtained from Uv-Vis spectroscopy at 313.15 K.

A0	A1	ΔA	1/ΔA	1/CD
0.78975	0.93989	0.15014	6.66045	50000
0.78975	0.99162	0.20187	4.953683	33333
0.78975	1.09739	0.30764	3.250553	25000
0.78975	1.1664	0.37665	2.654985	20000
0.78975	1.1883	0.39855	2.509095	16667
0.78975	1.24439	0.45464	2.199542	14286

Table S4. The van't Hoff equation data for the calculation of thermodynamic parameters (ΔH^0, ΔS^0, ΔG^0) of the inclusion complex (AB+β-CD).

k_a of the complex * 10^3	ka of beta complex	T	1/T	log(k_a)
6.78	6780	293.15	0.003411	3.83123
4.42	4420	303.15	0.003299	3.64542
1.26	1260	313.15	0.003193	3.10037

FIGURES

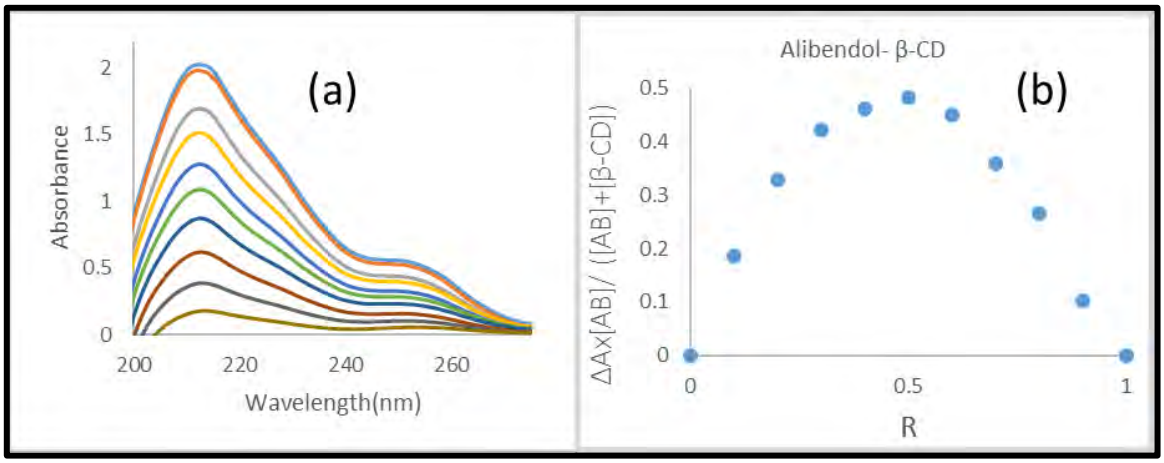

Fig.1. (a) Spectra of Job's plot of AB.β-CD at λ_{max}=212 nm, (b) Job plot of 1:1 stoichiometry where R=0.5; R= [Drug]/([Drug]+[CD])

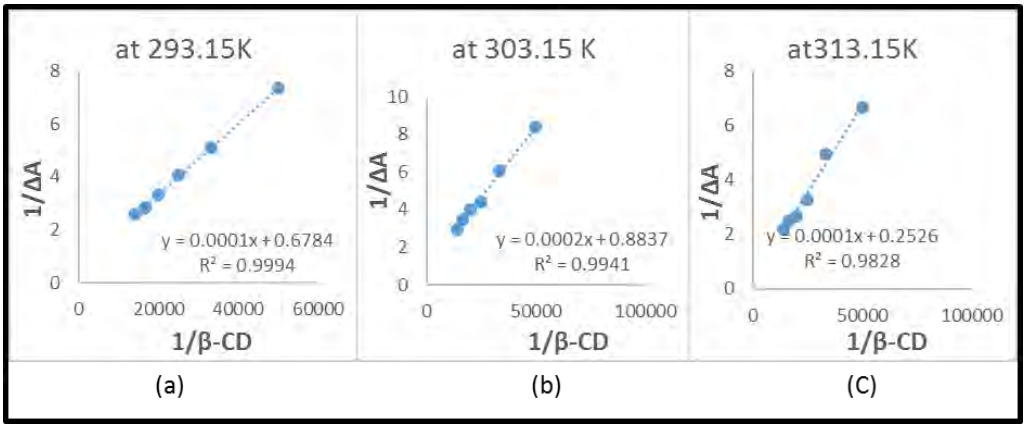

Fig. 2: Benesi-Hieldebrand double reciprocal plots of 1/ΔA against 1/β- [CD] at (a)293.15K, (b)303.15K and (c) 313.15 K.

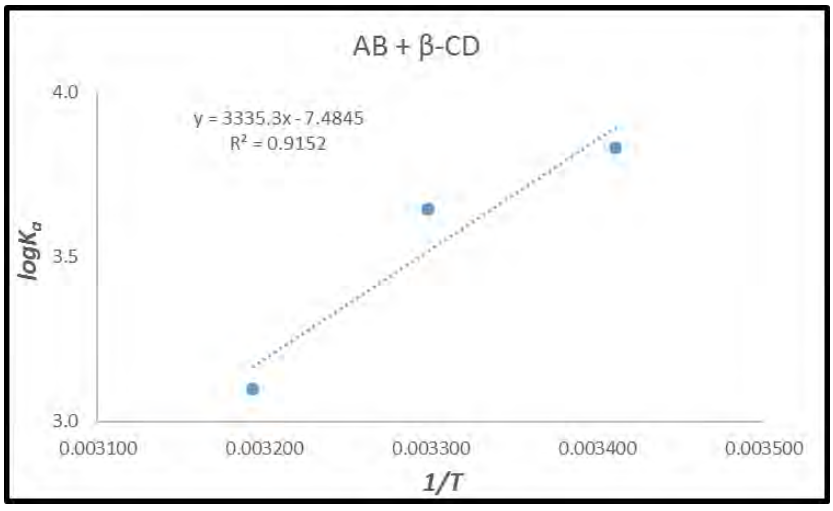

Fig. 3: Plot of $\log k_a$ Vs 1/T for the determination of thermodynamic parameters.

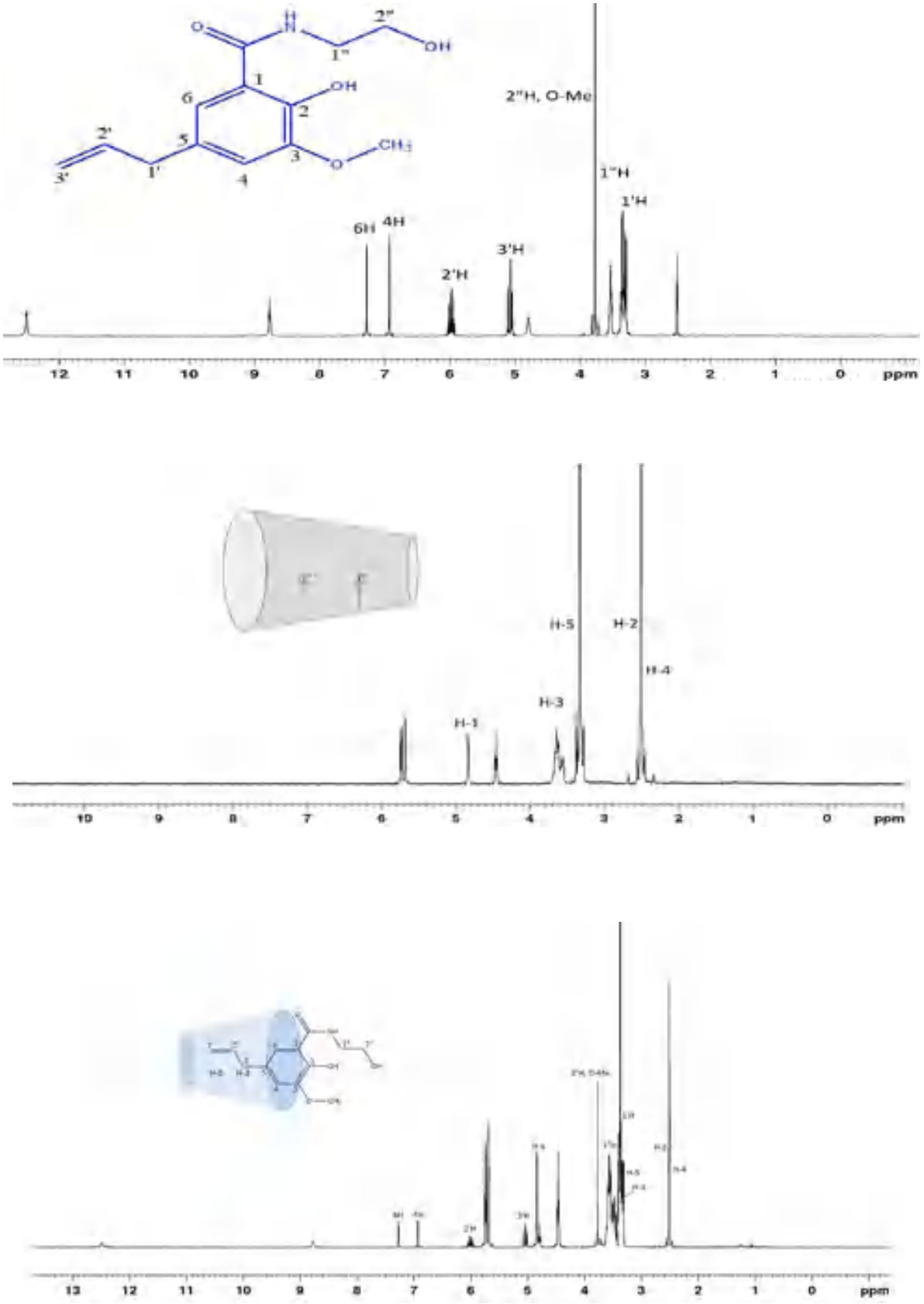

Fig.4.[1]H NMR spectra of pure Alibendol (top), pure β–CD (middle), AB - β–CD IC (bottom). (In d_6-DMSO, 400 MHz)

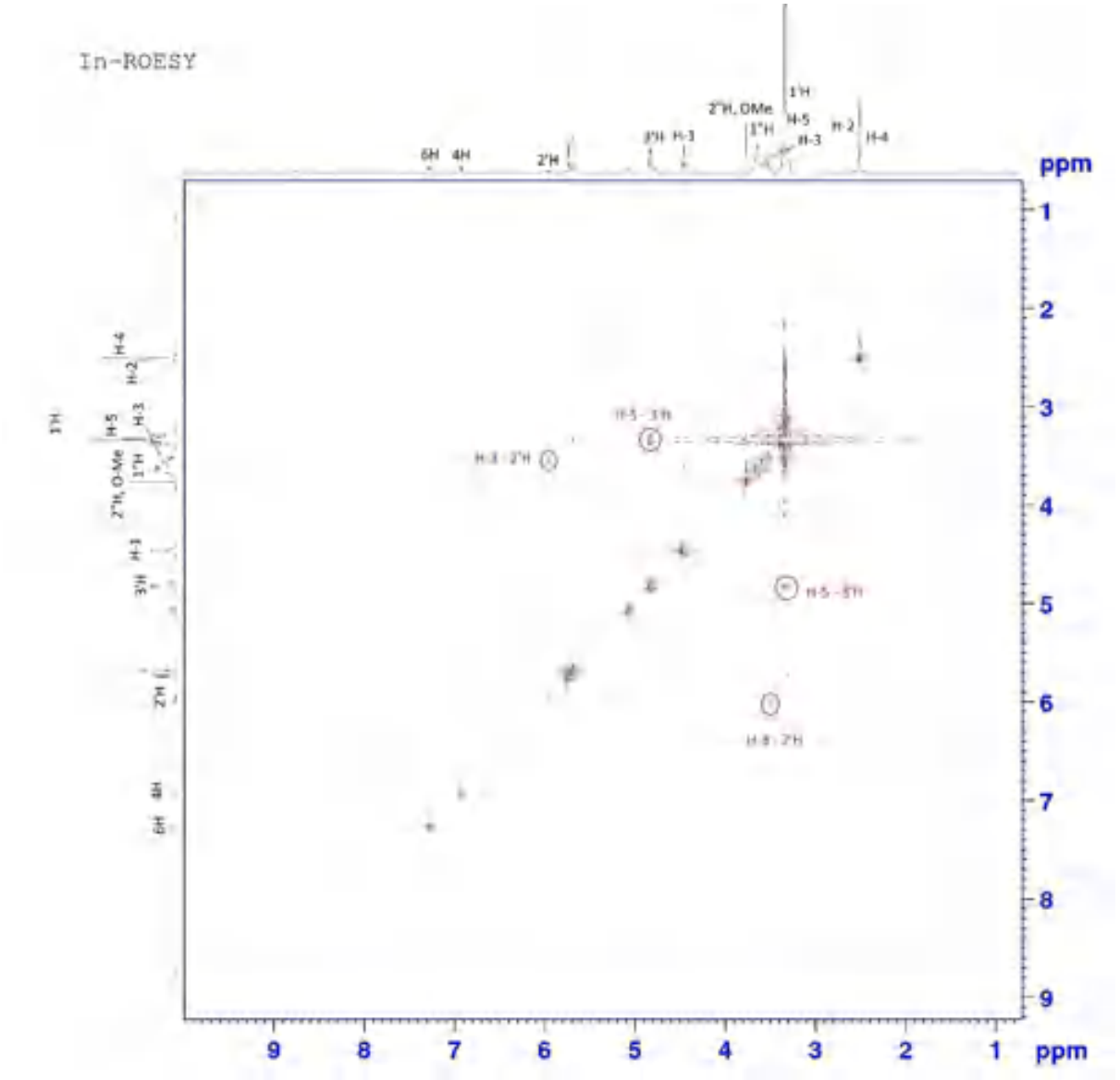

Fig 5: 2D ROESY spectra of the solid IC of AB -β-CD in d_6-DMSO. (Cross correlations are indicated by red circles)

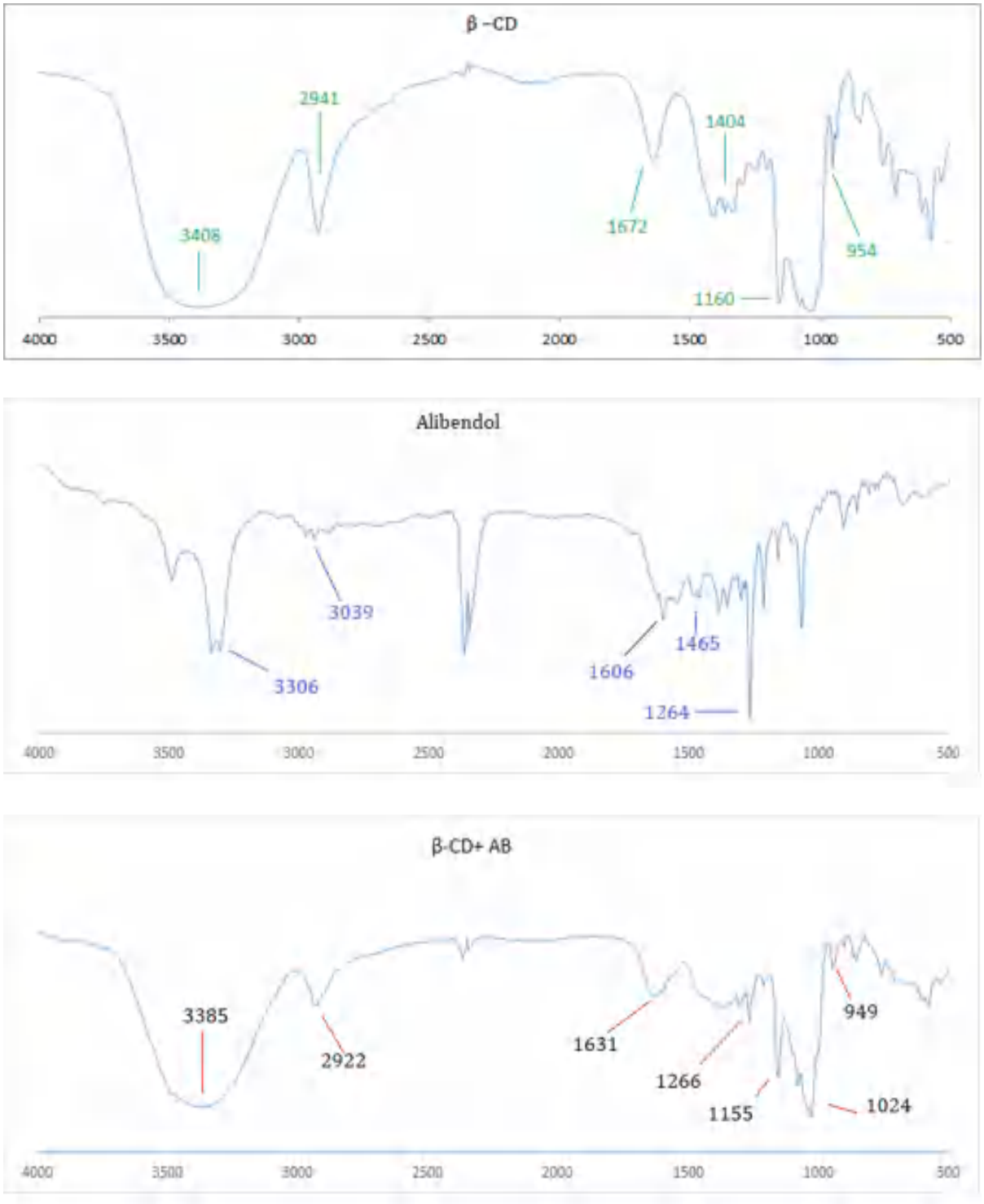

Fig.6.FT-IR Spectra of (top) pure β –CD (middle) pure Alibendol and (bottom) AB . β–CD inclusion complex.

SCHEMES

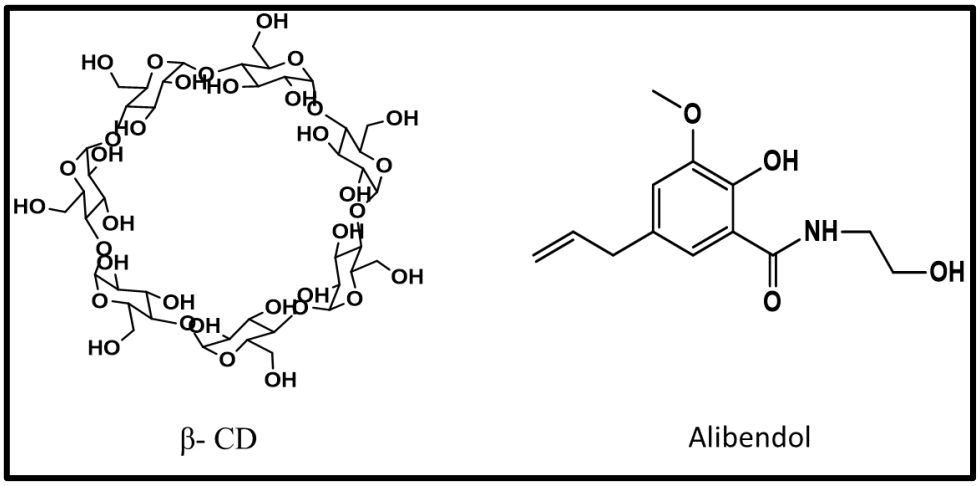

Scheme 1. Structures of the molecules

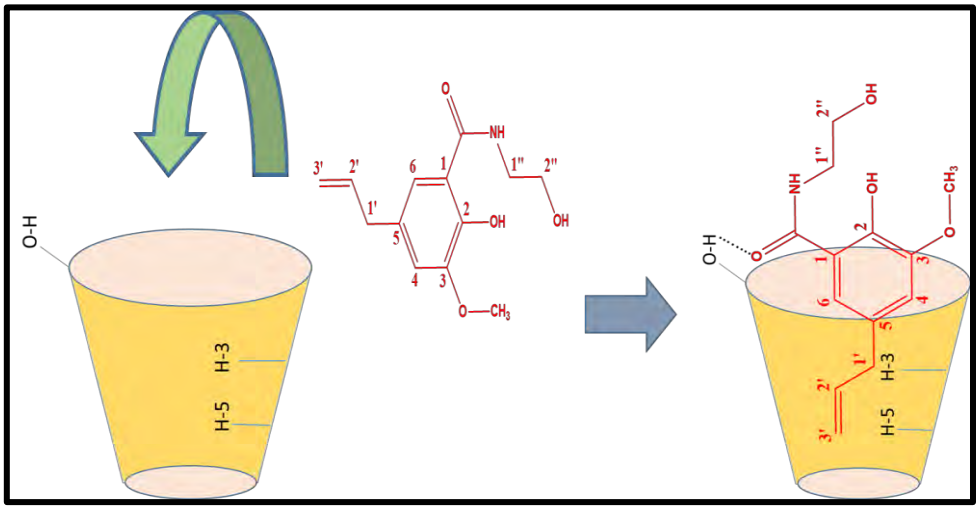

Scheme 2. Probable mechanism of inclusion.

CHAPTER VI

EXTENSIVE STUDY OF INCLUSION COMPLEXATION OF POTASSIUM SPARING DIURETIC AMILORIDE HYDROCHLORIDE WITH CYCLODEXTRIN MOLECULES BY MEANS OF ANTIMICROBIAL ASSAY

Abstract: Solubility development of supramolecular host-guest interaction between Amiloride hydrochloride with α and β-cyclodextrins were studied throughout this article. 1:1 host to guest stoichiometry of the inclusion complexation in the solution phase were confirmed by the Job's plot and further confirmation about the stoichiometry was also obtained from the mass spectra of the inclusion complexes. Association constants and thermodynamic parameter (ΔG) of the inclusion complexes were obtained using UV-vis spectroscopy. The mechanism of inclusion complexation was explored by 1H NMR spectroscopy. Furthermore, Density functional theory was employed to evaluate optimized geometries, adsorption energies, Non Covalent Interaction (NCI), electrostatic potential energy maps (ESP). The antimicrobial assay has also been done for the inclusion complexes.

Keywords: Cyclodextrins, Amiloride hydrochloride, Inclusion Complex, Binding constant, Antimicrobial activity, DFT.

Introduction:

Drugs play a significant role wherever they are used. In recent days drugs incorporated in cyclodextrins are of great concern because of its control release whenever it is within the cyclodextrin. A list of reports and other pharmacological applications are already there in the literature for the drug Amiloride hydrochloride **(Scheme 1)**. It is a guanidine diuretic and have moderate natriuretic and diuretic effects which means it has the capacity to excrete sodium through urine but sparing potassium, that is why it is also famous as 'potassium sparing diuretic'. No enzymatic basis was established for this action till now.

As the drug expels excess sodium from blood, automatically it reduces the blood pressure or any type of fluid withholding due to cardiac infarction. Amiloride also have some slight

non-postrual hypotensive effects. Chemically it is defined as 3,5-diamino-N-(diaminoethylene)-6-chloropyrazinecarboxamide, a synthetic pyrazine derivative.[1] It consists of a substituted pyrazine ring with an acylguanidine group attached to ring position 2, amino group attached at ring positions 3 and 5 , and a Cl group at position 6. Due to the presence of the guanidine moiety AMH is a weak base having pk_a of 8.7 in aqueous solution but it is weakly soluble in water. Protonation of Amiloride occurs in the guanidine group, not in the amino group. In recent days drug delivery through buccal route is an additional way due to the advantage of larger surface area and great accessibility[2].

Because of having very low permeability and unpleasant taste buccoadhesive film is the smartest way to consume the drug AMH. Generally AMH is being consumed in the form of nano liposomal dry powder inhaler and liposomal formulation in spite of these privileges the drug seems to have major limitations e.g. the formulation may easily wash off from nose which requires a constant dose administration moreover the formulation is not stable enough to retain its composition in the body[2].

AMH also have side effects on the central nervous, gastrointestinal endocrine, musculoskeletal, dermatological and haematological systems and some common side effects are nausea, vomiting, diarrhoea and headache.

The rate of dissolution and poor aqueous solubility are the two important factors of a drug that affect its process of development, way of administration, its formulation and its mode of therapeutic application. It seems to be very difficult for poorly water-soluble drugs to administer through various routes.

There are several techniques to increase the solubility, dissolution property and bioavailability of the concerned drug but these techniques have some disadvantages too. Complexation through cyclodextrins can be used as a substitute and the process has already gained attention of many researchers and scientists in recent days.

As AMH is poorly water soluble, the major problem with this drug is its administration. Even though buccal route is the smartest way for administration of this drug but it has certain drawbacks which makes the drug fail to show its activity. Its controlled release to

the target site might be achieved by the formation of inclusion complex with cyclodextrins.

Generally cyclodextrins are of three types α, β and γ cyclodextrins **(Scheme 1).** They are naturally occurring oligosaccharides with 6, 7 and 8 glucopyranose units with hydrophobic interior cavity and hydrophilic outer surface. Among the three cyclodextrins β-cyclodextrin is the most preferable one for complexation because of its perfect size and diameter**[3].** We have chosen α and β- CD for our work. The main advantage of cyclodextrins is their water solubility, which permits non-covalent interactions (hydrogen bonding, van Der Waals forces of interactions etc.) with the drug or the guest concerned. After insertion of the guest molecule into cyclodextrin (either fully or partially) their physicochemical and biological properties are changed which leads to increase their bioavailability, solubility and applicability. Moreover, cyclodextrins are nontoxic and can cause complexation with very less toxicity.

Now in this study, incorporation of AMH into cyclodextrins has been done and it was observed that the complexes have enhanced antimicrobial activity than the pure drug.

2. EXPERIMENTAL SECTION

2.1. Materials

Amiloride hydrochloride, α and β-cyclodextrin, purity ≥98.0% and ≥97.0% were purchased from Sigma-Aldrich and were kept in a refrigerator as received to maintain the quality of the sample.

2.2. Apparatus

The Agilent 8453 UV-Visible Spectrophotometer was performed to record UV-vis spectra with an uncertainty of wavelength accuracy of ±0.5 nm. An automated digital thermostat, Julabo was used to control the cell temperature during experiments.

The data of HRMS spectra (of the solid ICs) were collected from a high-resolution quadrupole time-of-flight (Q-TOF) instrument having the feature of positive-mode electrospray ionization where the methanol solution of the solid ICs were used.

1H NMR spectra were recorded in d_6-DMSO solvent at 400 MHz in Bruker Avance instrument. The chemical shifts data, δ values are presented in parts per million.

2.3. Procedure

2.3.1. Preparation Inclusion complexes: Aqueous solution of AMH and CDs were prepared with triply distilled water. A digital analytical balance METTLER TOLEDO AG-285 was used weigh with an uncertainty of ±0.1 mg and loss of materials were avoided taking sufficient precautions. The equimolar aqueous solution of AMH and CDs were prepared separately. The solutions containing aqueous CDs in a beaker were placed on a hot top of a magnetic stirrer for stirring and the aqueous AMH solution was added dropwise to it. The solution containing CDs and AMH was allowed to stir for 10 hours maintaining temperature at 40-45°C. At last, the solution was suspended at 5 °C and was filtered to obtain white crystalline powder, which were then dried in air and preserved in vacuum desiccators.

2.3.2. Computational Details: All density functional theory (DFT) calculations are carried out using the Gaussian 16 program[4]. Geometry optimizations at ground state of the AMH, α-CD, β CD and inclusion complexes were carried out at M06-2X/6-31+G(d) level of theory. Different studies revealed that compared to other hybrid functionals, the M06-2X functional delivers reliable and precisely non-covalently bonded interaction energies (hydrogen bonding, π–π stacking)[5]. During optimization solvent effects (water) were introduced by applying the Polarizable Continuum Model (PCM)[6] using the integral equation formalism variant. Vibration frequency calculations (no imaginary frequency) were obtained at the same level of theory to verify whether the optimized geometry resides to the minima on the potential energy surfaces. To interpret weak interactions like H-bonding, van der Waals interactions, steric interactions Non-Covalent Interaction (NCI) index plots of the reduced density gradient (RDG or s) were obtained using the Multiwfn 3.7 suite[7] at their corresponding ground state geometries. Finally, utilizing the following formula, adsorption energies or binding energies (ΔE_{ads}) of the composite systems were calculated:

$$\Delta E_{ads} = E_{AMH\text{-}CD} - E_{AMH-\ ECD}$$

Where E_{AMH-CD}, E_{AMH}, E_{CD} are the total energy of the geometry optimized complexes, AMH and the CD molecules, respectively.

2.3.3. Antimicrobial activity: Disk diffusion method was followed for viewing the antibacterial activity of synthesized test samples [Drug, IC-1, IC-2, DMSO corresponds to A(ii), B(iii), C(iv) and D(i) respectively] under study. Against three strains of gram positive bacteria (Bacillus subtilis ATCC 11774, Bacillus megaterium ATCC 14581 and Staphylococcus aureus ATCC 11632) and two strains of gram negative bacteria (Salmonella typhimurium ATCC25241and Escherichia coli ATCC 11229) antibacterial activity was assessed with seven different concentrations of each of the test samples (25, 50, 100, 200, 300, 400, 500 µg/ml). The microbes were cultured for 6 hrs on nutrient broth before their application to obtain rapidly growing healthy feasible cells. Nutrient agar plate was prepared by uniform mixing of 100 µl test organism with 15 ml sterilized nutrient agar through the process of solidification by cooling under laminar airflow. After 30 min of mixing paper disk soaked with appropriate concentration of test solution was placed in the nutrient agar plate. The zone of inhibition was calculated in the scale bar of millimeter calibration after 24 h of incubation at 37 °C.

3. Result and discussion

3.1 Job plot: the host – guest stoichiometry in inclusion complex:

As the molecular recognition of a guest molecule into the cavity of host molecule depends on the size of the guest molecule and the cavity volume of the host molecule, it is vital to determine the host to guest ratio in the inclusion complex i.e. the stoichiometry of the inclusion complex. Here, we employed the great Job's method[8], using UV-vis spectroscopic data to determine the stoichiometry of the host-guest inclusion complexes. A set of solutions of mole fraction ranging from 0 to 1 were prepared by mixing aqueous AMH and CDs and recorded the spectra at 298.15 K of temperature. The absorbance at λmax = 364 nm were considered for the calculation **(Figure 1).** The value of R, at the maxima of ΔA×R vs R plot, signifies the stoichiometry of inclusion complexes. Where, ΔA represents the differences in absorbance between pure AMH and each of the solutions of the set **(Table S1, S2 and Figure 1).** R indicates [CDs]/[AMH]+[CDs] and its value of R =

0.33, 0.5, 0.66 corresponding to the maxima recommends the 1:2, 1:1 and 2:1 host to guest stoichiometry in the inclusion complexes[9]. In case of our present work we found the maxima at R = 0.5 indicating 1:1 host to guest stoichiometry in the inclusion complexes[10] **(Scheme 2)**.

3.2 HRMS: The confirmation about the stoichiometry of the Inclusion complexes:

The molecular ion peak with an appreciable intensity at the m/z ratio corresponding to the molar mass of a host molecule added to the same of the guest molecule in the HRMS spectra is actually a great evidence for saying about the host-guest stoichiometry of the inclusion complex. The HRMS spectra of the prepared inclusion complexes were recorded after dissolving these in methanol. The spectra, shown in the **Figure 2 and 3**, have the molecular ion peaks at the m/z 1202.9025 and 1365.0427 correspond to the $[AMH+\alpha\text{-}CD+H]^+$ and $[AMH+\beta\text{-}CD+H]^+$ respectively, signify the formation of [AMH + α-CD] and [AMH + β-CD] inclusion complexes of 1:1 host to guest stoichiometry must have an appreciable stability of the molecular assembly formed[11],[12] (Scheme 2).

3.3 1H NMR spectral analysis:

The mechanism of inclusion complexation i.e. the identification of part of the guest molecule most probably the hydrophobic part that undergoes insertion into the hydrophobic cavity of cyclodextrin and the extent to which it get inserted into the hydrophobic cavity of cyclodextrin is yet to be explored. Here, 1H NMR spectra analysis appeared as the great technique to explore the same with a pronounced fulfilment.

Because of the truncated structure of cyclodextrins, H3 and H5 protons are oriented inside the cavity whereas H1, H2 and H4 protons are exposed to the outer side of CDs[13] (Figure.4). That's why, H3 and H5 protons of CDs would experience an interaction with the guest molecule undergoing insertion into the cavity of CDs and register a chemical shift in 1H NMR spectrum due to their mutual shielding through space[14]. Here the encapsulated aromatic moiety of the AMH, having ring current exerts diamagnetic shielding to the H3 and H5 protons of the CDs[15] **(Figure 4)**.

Here, the experiment goes through our expectation and it reflected in the same when we analyse the 1H NMR spectra of pure α-CD, β-CD, AMH as well as the inclusion complexes

are shown in **Figure 5 and 6**. The considerable upfield shift of the H3, H5 protons of CDs in the 1H NMR spectra confirms the formation of inclusion complexes.[16]

3.4 Ultraviolet Spectroscopy: The stability of the Inclusion Complexes:

The binding energy of the inclusion complexes formed in solution phase, saying about the stability of the inclusion complexes was calculated by employing well-known Benesi-Hildebrand equation[17],[18] and using UV-vis spectroscopic data. In the aqueous solution of cyclodextrin, the hydrophobic cavity of cyclodextrin being less polar compared to aqueous environment must have lower molar extinction coefficients (Δε) than that of the aqueous environment. This is why, we expected the absorbance of the guest molecule must change while going from polar aqueous media to the apolar hydrophobic cavity of the CDs to form ICs[19],[20] and we observed the same trend in absorbance which are shown in **Figure 7**. The UV-vis spectroscopic data **(Figure S3 and S4)** were fed into the following Benesi-Hildebrand equation (1) and the calculated values are listed in the **Table 1**.

$$\frac{1}{\Delta A} = \frac{1}{\Delta\varepsilon[AMH]K_a}\frac{1}{[CD]^n} + \frac{1}{\Delta\varepsilon[AMH]} \qquad (1)$$

Where, ΔA is the difference in absorbances of AMH without CDs and with the CDs. [AMH] represents the concentration of AMH. The value of (n) says about the stoichiometry of the ICs. When the linearity of the double reciprocal plot fits by putting n=1 in the above equation then it suggests 1:1 stoichiometry of the ICs. But, when n=2 suggests the 2:1 inclusion complex of the Host to the Guest[21]. Here, we observed a linear relationship of the Benesi-Hildebrand double reciprocal plot, considering n=1, indicating the composition of complex was 1:1.

The binding constant (Ka) of the inclusion complexes were calculated from the obtainable values of intercepts and slopes of the Benesi-Hildebrand double reciprocal plot **(Figure 7)** and are listed in the **Table 1.**

The binding constants of the inclusion complexes so obtained were fed into equation (2) and the change in free energy of the inclusion process were listed in the **Table 1**.

$$\Delta G = -RTlnK_a \qquad (2)$$

3.5 Theoretical study of the interaction in the inclusion complexes:

Optimized geometries of the AMH+α-CD and AMH+β-CD inclusion complexes are shown in **Figure 8**. In the relaxed geometry of the AMH+β-CD composites AMH occupies in the centre of the cavity indicating complete encapsulation by β-CD. On the other hand in AMH+α-CD due to the smaller radius of α-CD AMH is partially encapsulated. The higher affinity of AMH of AMH by β-CD has been confirmed by the strong H-bonds ranging from 1.94 Å to 2.93 Å which is short compared to the H- bonds in AMH+α-CD. The stronger Hydrogen bonding between –NH2 groups of AMH and –OH group of β-CD in AMH+β-CD accounts the large adsorption energy of -5.52eV which is high compared to AMH+α-CD (E_{ads} =-4.51 eV) in aqueous medium.

To account different weak interactions operating between AMH and α-CD, β-CD we have analysed the RDG plots as shown in the **Figure 9**. A large scattered points in the region --0.03-0.04 of the RDG plot revealed that predominant H-bonding interaction is operating between AMH and β-CD units while due to the partial inclusion this interaction is weaker in AMH+α-CD.

3.6 Antimicrobial activity:

All the synthesized samples except the solvent **DMSO (i)** displayed potent antimicrobial activity against both gram positive and gram negative bacteria as apparent by measuring the diameter of zone of inhibition **(Figure 10 and Table S5)**. In comparison to all the studied samples, quantitative measurement of inhibition zone in millimeter scale indicates that at uppermost (100 µg/ml) and lower most concentration (25 µg/ml) best activity was displayed by test **sample (iii)** (combination of α-Cyclodextrin and Amiloride hydrochloride) against both gram positive and gram negative bacteria, Escherichia coli with inhibitory zone of 25.33 ± 1.528 mm and 14 ± 1.732 mm respectively. Beside this **sample (iii)** at any used concentration displayed prominent zone of inhibition against both gram positive and gram negative microbes[22] reported bacteriostatic activity of amiloride against different strains of bacteria at concentration range of 25 to 1,300 µg /ml. The concentration range of **sample (iii)** used for antimicrobial activity in the present study lies within the above mentioned range. **Amiloride HCl, Sample (ii)** was also reported to display antimicrobacterial activity when used in combination with rifampicin[23]. Cyclodextrin was reported to appropriately control the drug release rate

of its conjugated antimicrobial component and thereby display effective antimicrobial activity[24]. Conjugation of α-Cyclodextrin with Moringin displayed potent antimicrobial activity against Staphylococcus aureus[25]. Similarly the antibacterial activity of essential oils extracted from Prostanthera increases by two to four fold when encapsulated with α-cyclodextrin[26]. In the present study conjugation of amiloride hydrochloride with α-Cyclodextrin showed better antimicrobial activity than amiloride hydrochloride alone probably due to better drug release kinetics of α-Cyclodextrin. Beside this, current study reports better antimicrobial activity of amiloride hydrochloride when conjugated with α-Cyclodextrin [**sample (iii)]** than β-Cyclodextrin [**sample (iv)]**. This finding contradicts with the finding of which reported better activity of β-Cyclodextrin than α-Cyclodextrin against Staphylococcus aureus and Escherichia coli when Complexes with Trans-Cinnamaldehyde[27]. Such contradict observation was probably because different drugs behaves differently with Cyclodextrin. Probably amiloride HCl showed better complex formation kinetics with α-Cyclodextrin [**sample (iii)]** than β-Cyclodextrin [**sample (iv)]** and thereby displaying better synergistic antimicrobial activity when conjugated with α-Cyclodextrin [**sample (iii)]**. At minimum tested concentration (25 µg/ml) sample A and C was found to be more effective against gram positive bacteria than gram negative bacteria. While **sample (i)**, failed to displayed any bactericidal activity at any of the used concentrations. This observation was supported by the observation of **Carlos de Brito et al. (2017)** which stated that concentrations of DMSO do not interfere with the viability of the bacterial strains.

Among the tested gram positive bacteria, sample **Drug (ii), IC-1 (iii) and IC-2 (iv)** was found to be effective at any used concentration against Bacillus subtilis. While **sample (ii)** and **(iv)** was found to be effective against Bacillus megaterium and Staphylococcus aureus at concentration of 100µg/ml, below which no activity was noted. The probable reason for this type of activity may be that at low concentration thick peptidoglycan layer, consisting of linear polysaccharide chains cross linked by short peptides makes the membrane wall of gram positive bacteria a rigid and compact structure which creates difficulty for silver nanoparticles to penetrate the bacterial cell wall[28]. Against gram negative bacteria Salmonella typhimurium **Sample (ii)** showed bactericidal activity at maximum concentration of 100µg/ml while **sample (iii)** displayed the activity from the concentration range of 50µg/ml. On the other side against Escherichia coli **sample (ii)**

showed better activity than **sample (iv)**. All the three bactericidal samples (viz. ii, iii and iv) showed better antimicrobial activity against gram positive bacteria than gram negative bacteria this is probably because thin peptidoglycan layer in the cell wall of gram negative bacteria allows easy penetration of the test samples damaging cellular and metabolic processes causing bacterial death[29].

4. Conclusions:

All the experiments suggest the successful formation of inclusion complex with 1:1 stoichiometry. The association constants of the inclusion complexes of AMH formed with β-cyclodextrin were found greater than that of the inclusion complexes formed with the α-cyclodextrin and hence more stable, this is may be due to the better fitness of the guest molecule into the larger hydrophobic cavity of β-cyclodextrin compared to the α-cyclodextrin. Furthermore analysis of adsorption energies, ESP, HOMO , LUMO distributions revealed that compared to AMH/α-CD , AMH/β-CD is quite stable and possesses significant amount of donor (guest) – acceptor (host) charge transfer interactions. Asymmetry in ESP maps suggests enhanced solubility of AMH/β-CD over the AMH/α-CD inclusion complexes. The ready availability of the association constants enables us to calculate the thermodynamic parameter(ΔG) of the inclusion process which makes the thermodynamic ground of the approach and recognise it as a thermodynamically viable process. The antimicrobial activity of the drug was seemed to be enhancing after inclusion especially with α-CD, which is complementary with the findings from association constants, i.e. more association constant less free the drug. Thus, the hydrophobic-hydrophobic interaction would become the driving forces for the formation of inclusion complexes.

Conflicts of interest: There are no conflicts of interest.

Acknowledgements: Prof. M. N. Roy would like to acknowledge UGC, New Delhi, Government of India, for being awarded One Time Grant under Basic Scientific Research (BSR) for augmenting innovative research in the field of Chemical Sciences via the grant-in-Aid no. F.4-10/2010 (BSR).

TABLES

Table 1: Association Constants obtained from Benesi-Hildebrand method (K_a) and change in free energy (ΔG).

Inclusion complexes	Binding constants (K_a/M^{-1})×10^3	Free energy change (ΔG) (kJ/M^{-1})
AMH+α-CD	5.66	-21.93
AMH+β-CD	6.93	-21.42

Table S1. UV-Vis spectroscopic data for the generation of Job plots of aqueous AMH+*α*-CD system at 298.15 K[a].

AMH + α - CYCLODEXTRIN							
AMH (mL)	α-CD (mL)	AMH (μM)	α-CD (μM)	$\frac{[AMH]}{[AMH]+[\alpha-CD]}$	Absorbance (A)	ΔA	$\frac{\Delta A \times [AMH]}{[AMH]+[\alpha-CD]}$
0	3	0	100	0	1.5203	1.5115	0.0000
0.3	2.7	10	90	0.1	1.3759	1.3759	0.1376
0.6	2.4	20	80	0.2	1.2276	1.2276	0.2455
0.9	2.1	30	70	0.3	1.0793	1.0793	0.3238
1.2	1.8	40	60	0.4	0.9343	0.9343	0.3737
1.5	1.5	50	50	0.5	0.7695	0.7695	0.3847
1.8	1.2	60	40	0.6	0.6221	0.6221	0.3733
2.1	0.9	70	30	0.7	0.4792	0.4792	0.3354
2.4	0.6	80	20	0.8	0.2930	0.2930	0.2344
2.7	0.3	90	10	0.9	0.1816	0.1816	0.1635
3	0	100	0	1	0.0088	0.0088	0.0088

[a]Standard uncertainties in temperature *u* are: *u*(T) = ±0.01 K.

Table S2. UV-Vis spectroscopic data for the generation of Job plots of aqueous AMH+β-CD system at 298.15 K[a].

AMH + β - CYCLODEXTRIN							
AMH (mL)	**β-CD (mL)**	**AMH (µM)**	**β-CD (µM)**	$\frac{[AMH]}{[AMH]+[\beta-CD]}$	**Absorbance (A)**	**ΔA**	$\frac{\Delta A \times [AMH]}{[AMH]+[\beta-CD]}$
0	3	0	100	0	1.5818	1.5721	0.0000
0.3	2.7	10	90	0.1	1.4080	1.4080	0.1408
0.6	2.4	20	80	0.2	1.2566	1.2566	0.2513
0.9	2.1	30	70	0.3	1.1105	1.1105	0.3332
1.2	1.8	40	60	0.4	0.9532	0.9532	0.3813
1.5	1.5	50	50	0.5	0.7977	0.7977	0.3989
1.8	1.2	60	40	0.6	0.6441	0.6441	0.3864
2.1	0.9	70	30	0.7	0.4749	0.4749	0.3324
2.4	0.6	80	20	0.8	0.3221	0.3221	0.2577
2.7	0.3	90	10	0.9	0.1812	0.1812	0.1631
3	0	100	0	1	0.0097	0.0097	0.0097

Table S3. UV-vis spectroscopic data for the Benesi-Hildebrand double reciprocal plot of (AMH+α-CD) system at 298.15K

Temp (K[a])	**AMH (µM)**	**α-CD (µM)**	**Ao**	**A**	**ΔA**	**1/[α-CD] (M^{-1})**	**1/ΔA**	**Intercept**	**Slope**	**Ka ($M^{-1}\times10^3$)**
298.15	35	25	0.5620	0.6042	0.0422	0.0400	23.6831	2.9815	527.18	5.66
	35	30		0.6098	0.0479	0.0333	20.8973			
	35	35		0.6171	0.0551	0.0286	18.1501			
	35	40		0.6208	0.0588	0.0250	17.0107			
	35	45		0.6345	0.0726	0.0222	13.7822			

Table S4. UV-vis spectroscopic data for the Benesi-Hildebrand double reciprocal plot of (AMH+ β-CD) system at 298.15K

Temp (K^a)	AMH (μM)	β-CD (μM)	Ao	A	ΔA	1/[β - CD] (M^{-1})	1/ΔA	Intercept	Slope	Ka ($M^{-1}\times10^3$)
298.15	35	25	0.5620	0.6053	0.0433	0.0400	23.0818	3.4689	500.37	6.93
	35	30		0.6107	0.0488	0.0333	20.5115			
	35	35		0.6179	0.0559	0.0286	17.8903			
	35	40		0.6215	0.0595	0.0250	16.8106			
	35	45		0.6351	0.0732	0.0222	13.6691			

Table S5: Antimicrobial activity of drug, IC-1, IC-2 and solvent DMSO sample name against tested microorganisms. Results are expressed as Mean ± SD of triplicate determinations.

		Zone of Inhibition (mm)		
Microorganisms	**Sample ID**	**25 μg/ml**	**50 μg/ml**	**100 μg/ml**
B Subtilis	(ii)	8.33 ± 2.52	14.33 ± 0.577	18.33 ± 1.523
	(iii)	5.33 ± 0.577	12.33 ± 0.577	18.67 ± 1.155
	(iv)	5.66 ± 0.577	9.33 ± 0.577	16.67 ± 0.577
	(i)	0	0	0
B megaterium	(ii)	0	0	14.33 ± 1.153
	(iii)	7.33 ± 0.577	10.67 ± 1.15	20.33 ± 0.577
	(iv)	0	0	12.33 ± 0.577
	(i)	0	0	0
S aureus	(ii)	0	0	11.33 ± 1.15
	(iii)	6.66 ± 0.577	13.33 ± 1.15	21.67 ± 2.08
	(iv)	0	0	10.67 ± 0.577
	(i)	0	0	0
S typhimurium	(ii)	0	0	10.67 ± 0.577
	(iii)	8 ± 1.732	14.67 ± 2.082	21.67 ± 2.082
	(iv)	0	6.33 ± 0.577	7.33 ± 0.577
	(i)	0	0	0
E Coli	(ii)	6.66 ± 0.577	12.33 ± 1.155	18 ± 1
	(iii)	14 ± 1.732	20.67 ± 0.577	25.33 ± 1.528
	(iv)	0	16 ± 2	21.33 ± 0.577
	(i)	0	0	0

FIGURES

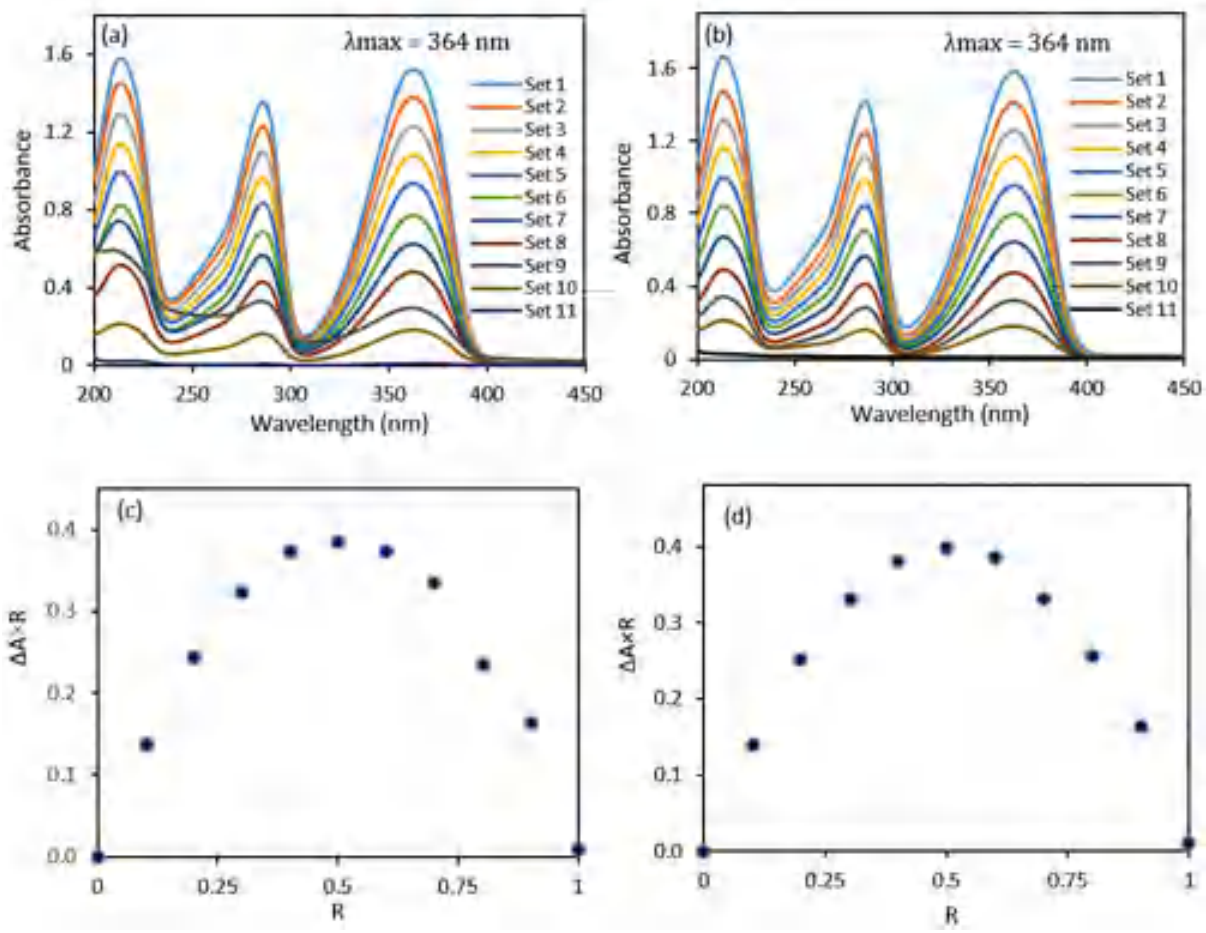

Figure 1 (a,b,c,d): UV-vis spectra for the generation of Job plots of (a) AMH+α-CD and (b) AMH+β-CD systems and Job Plots of (c) AMH+α-CD and (d) AMH+β-CD systems at = 364 nm.

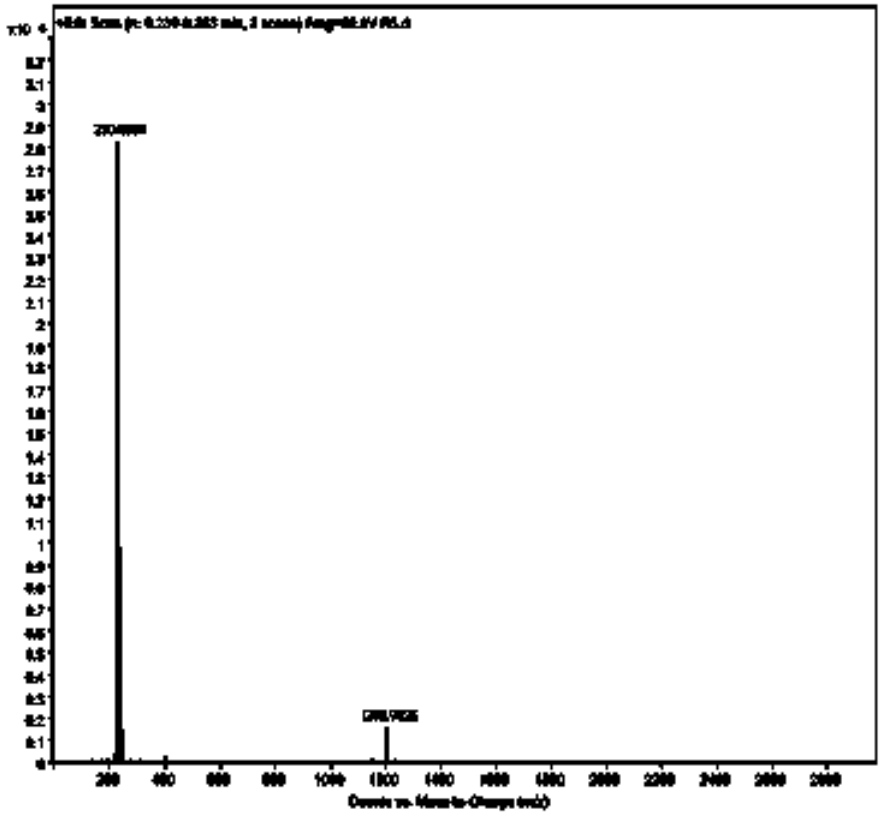

Figure 2: HRMS spectra of the AMH+α-CD Inclusion complex.

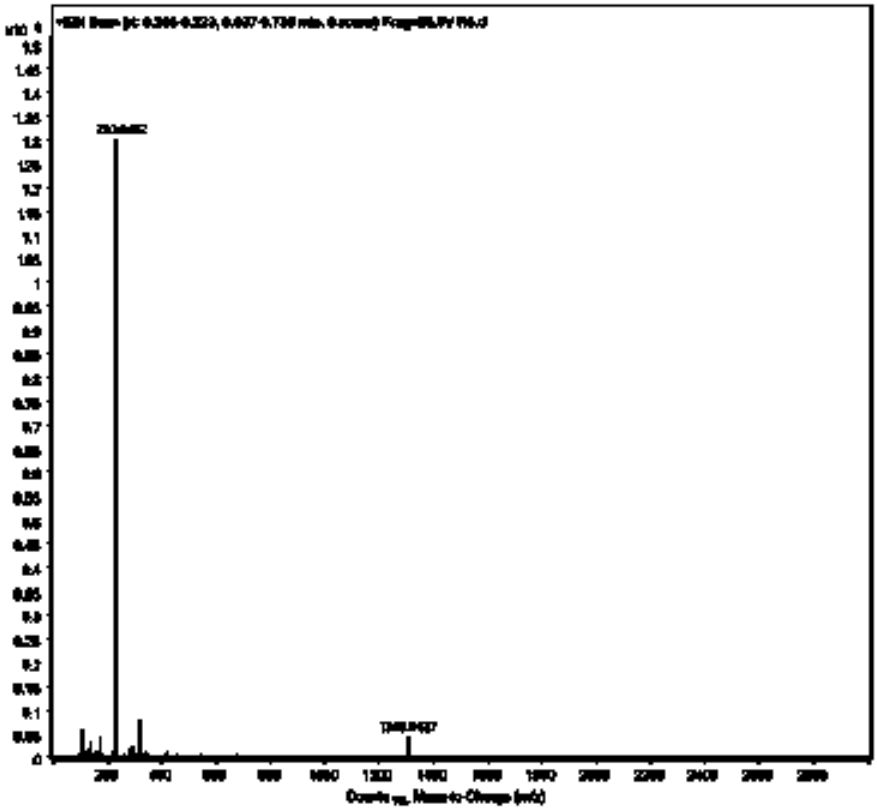

Figure 3: HRMS spectra of the AMH+β-CD Inclusion Complex.

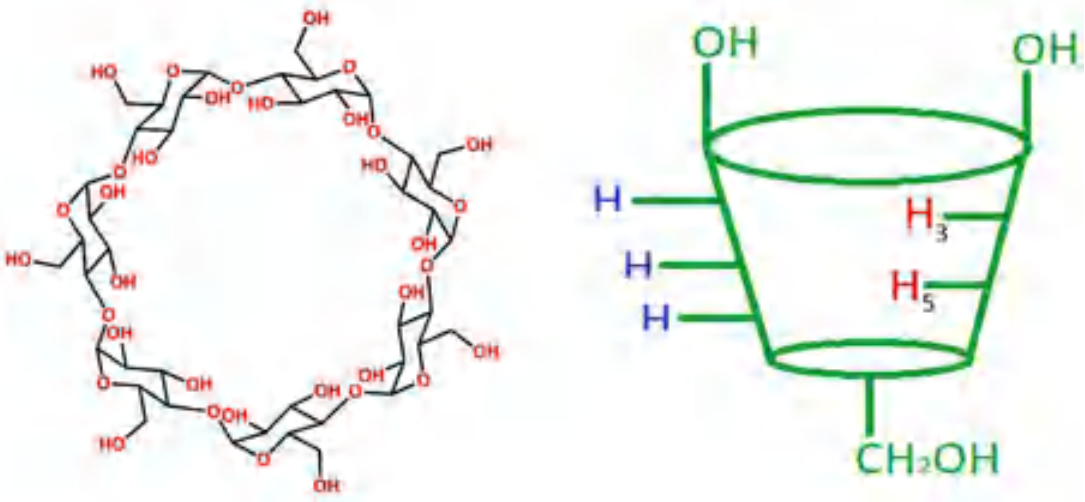

Figure 4: Truncated structure of Cyclodextrins showing H_3 and H_5 protons of Cyclodextrins.

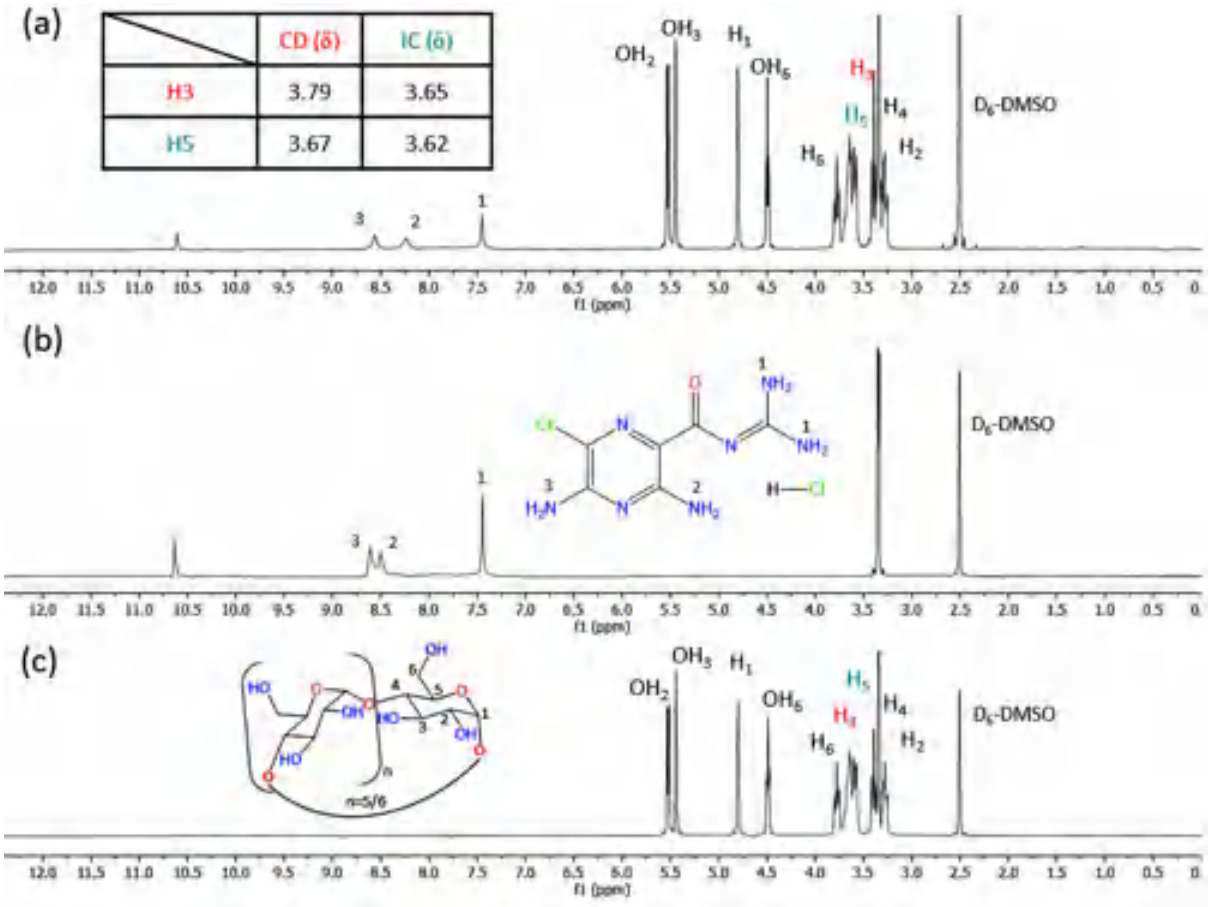

Figure 5(a,b,c): 1H NMR spectra of (a) AMH+α-CD Inclusion complex,(b) AMH and (c) α-CD

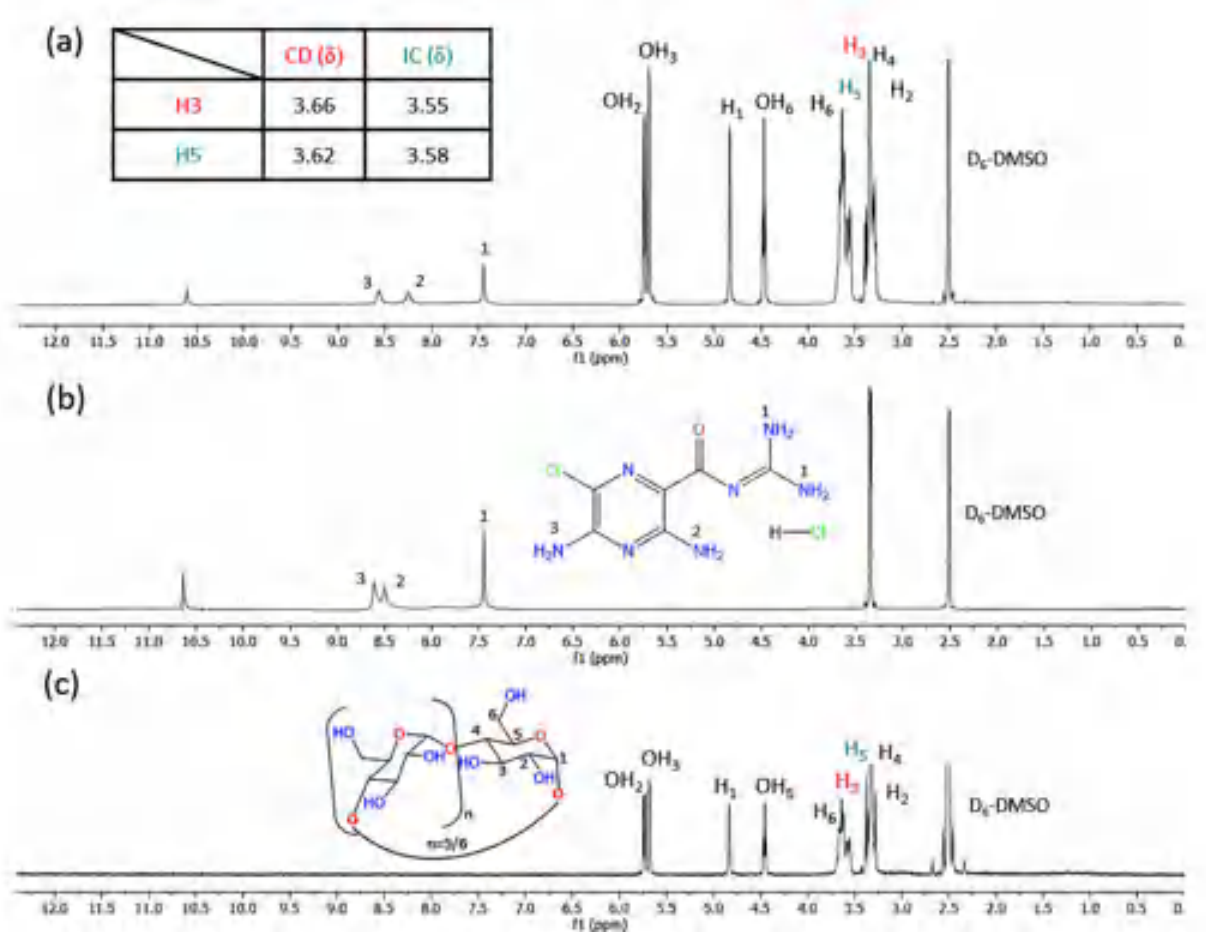

Figure 6(a,b,c): 1H NMR spectra of (a) AMH+β-CD Inclusion complex, (b) AMH and (c) β-CD.

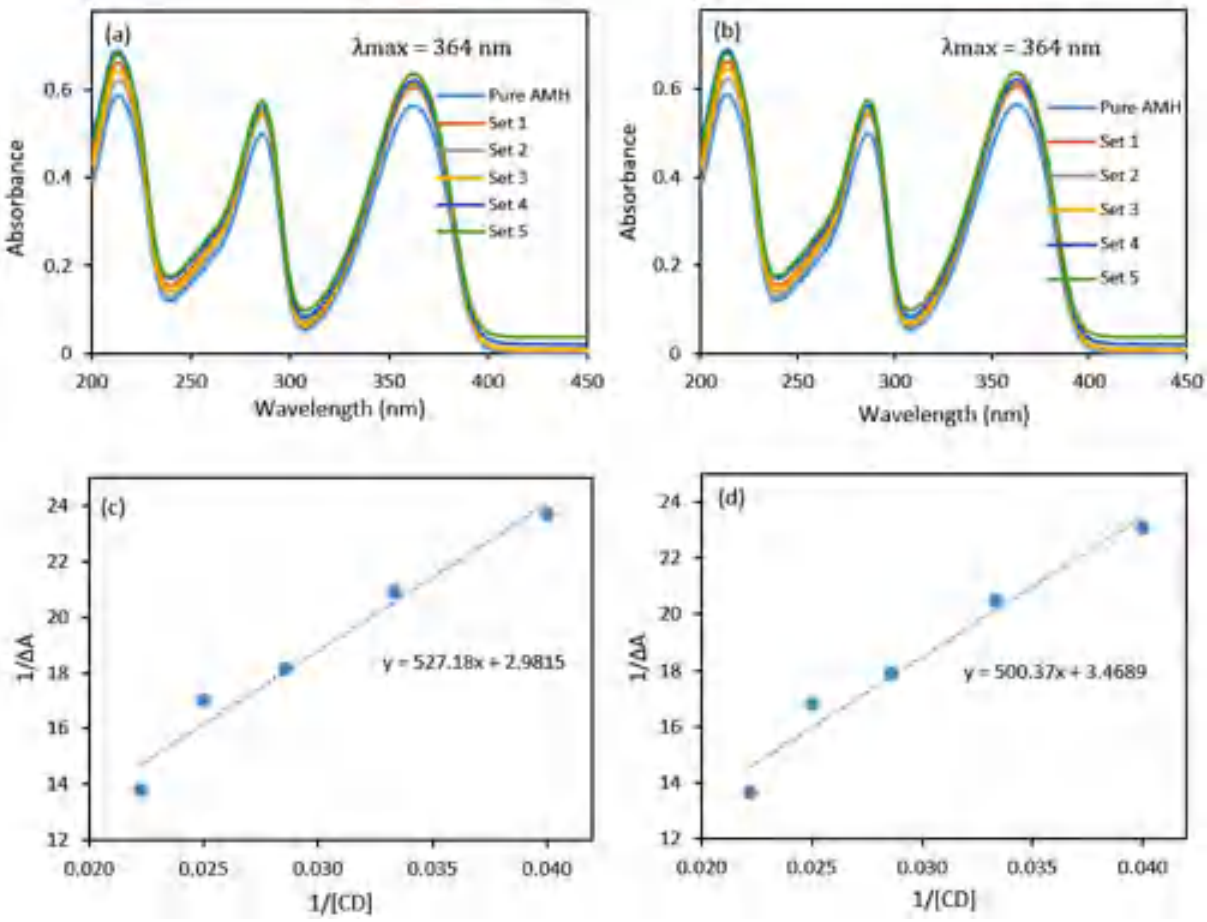

Figure 7(a,b,c,d): UV visible spectra (a) AMH+α-CD, (b) AMH+β-CD) systems for the generation of Benesi Hildebrand double reciprocal plots of (c) AMH+α-CD, (d) AMH+β-CD systems at 298.15K.

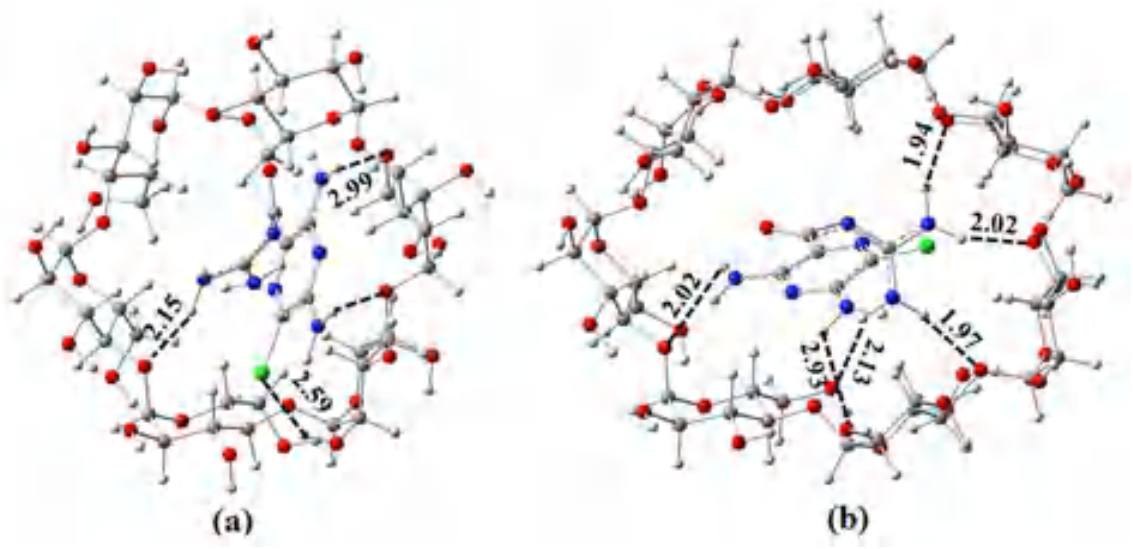

Figure 8: Optimized geometries for the (a) AMH+α-CD (b) AMH+β-CD composite at M06-2X/6-31+G(d) level of theory. Red, gray, white, blue color represent oxygen, carbon, hydrogen, nitrogen atoms respectively.

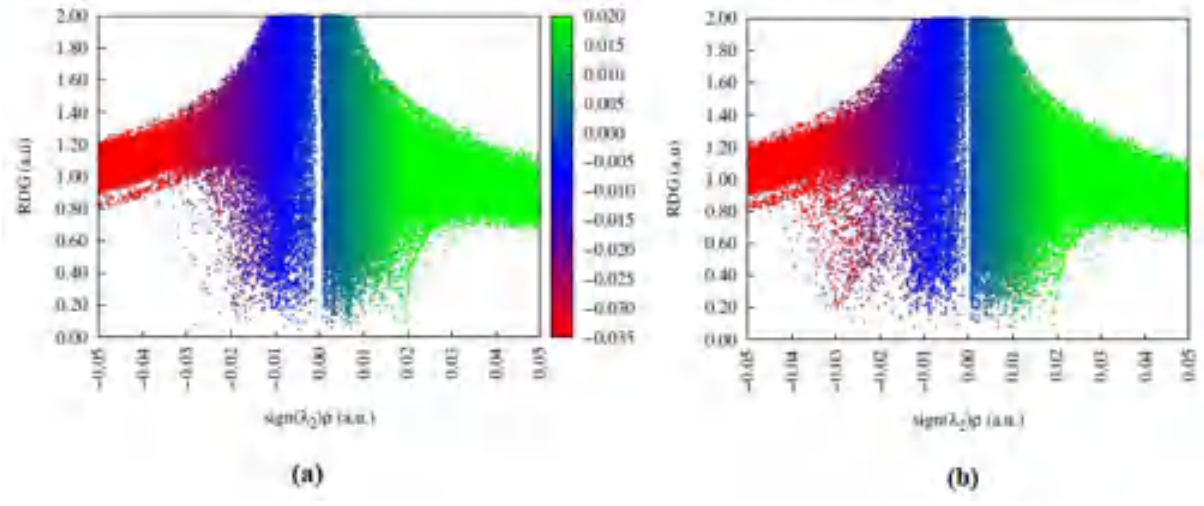

Figure 9: Plots of reduced density gradient (RDG) for (a) AMH+α-CD and (b) AMH+β-CD inclusion complexes.

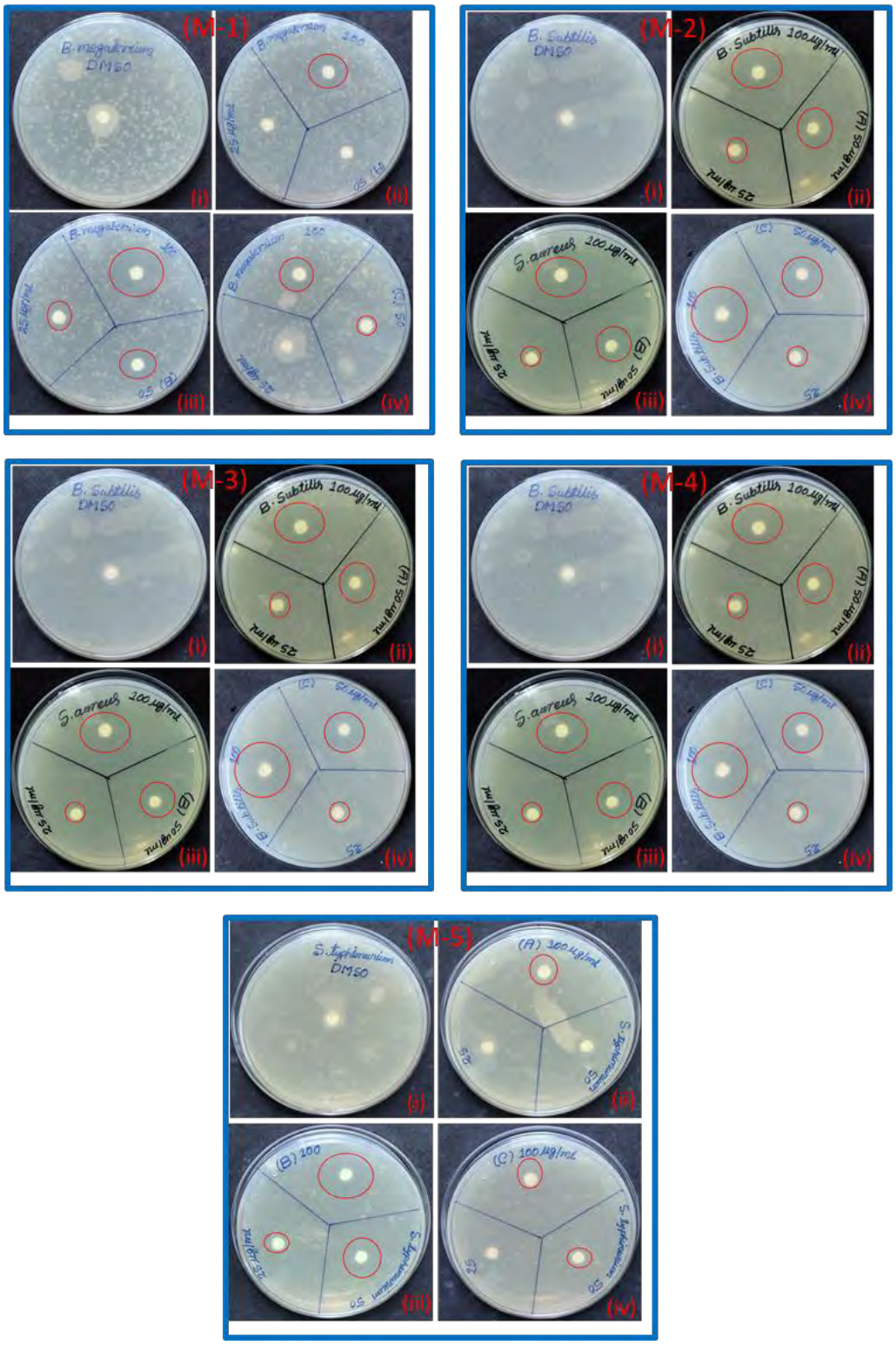

Figure 10(M-1, M-2, M-3, M-4, M-5): Antimicrobial activity of (i) DMSO, (ii) AMH, (iii) AMH+α-CD Inclusion complex, (iv) AMH+β-CD Inclusion complex against test organisms viz. **(M-1)** *B megaterium,* **(M-2)** *B Subtilis,* **(M-3)** *E Coli,* **(M-4)** *S aureus*, **(M-5)** *S typhimurium*. Antimicrobial potentiality was assessed at three different concentrations of each of the samples, viz. 100 µg/mL, 50 µg/mL and 25 µg/mL.

SCHEMES

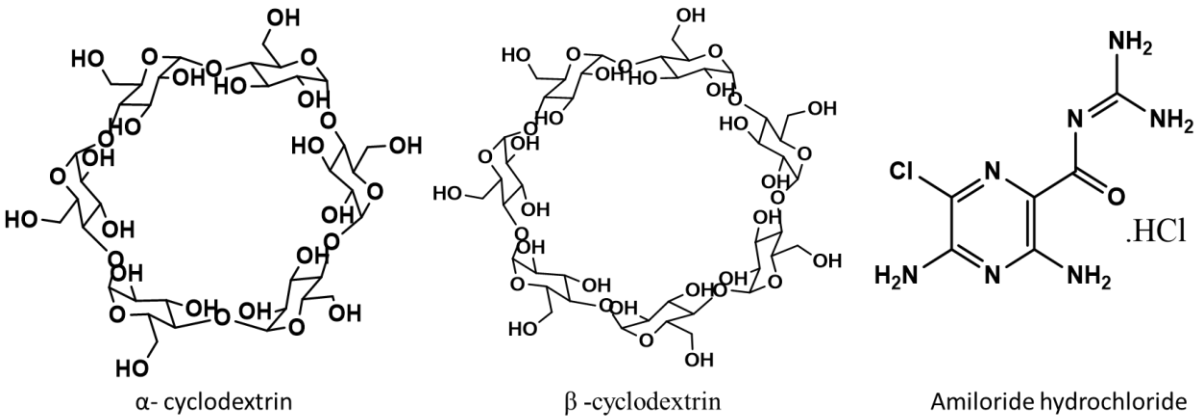

Scheme 1: Molecular structures of α–cyclodextrin, β-Cyclodextrin and Amiloride hydrochloride.

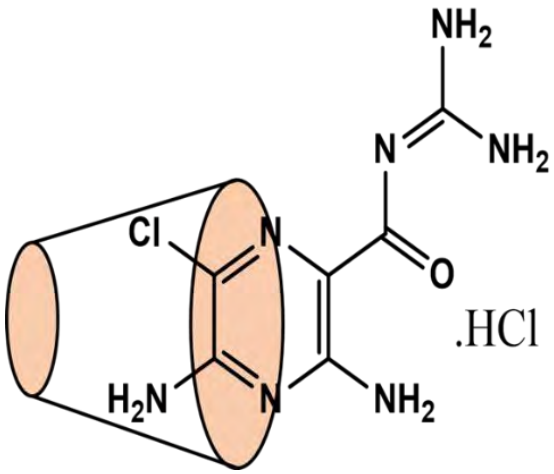

Scheme 2: Formation of Inclusion complex through the wider rim of the cyclodextrin.

CHAPTER VII

SYNTHESIS AND CHARACTERIZATION OF INCLUSION COMPLEX OF DL-AMINOGLUTETHIMIDE WITH β-CYCLODEXTRIN AND ITS INNOVATIVE APPLICATION IN BIOLOGICAL SYSTEM: COMPUTATIONAL AND EXPERIMENTAL INVESTIGATIONS

Abstract: Our present study intended to investigate the encapsulation of DL-AGT within the lipophilic cavity of β-CD molecule. The consequential inclusion system was characterized by UV-Visible spectroscopy, ^{1}HNMR study, PXRD study, SEM study, FT-IR study. Molecular docking was performed for the inclusion complex to discover the most proper orientation and it was seen that the drug DL-AGT fits into the cavity of β-CD in 1:1 ratio which was also confirmed from the Job's plot. Furthermore, a comparison was done on the basis of cell viability between the drug and its inclusion complex.

Keywords: DL-AGT, β-CD, Molecular docking, 1:1 ratio, Cell viability

1. Introduction:

The drug DL-Aminoglutethimide, (±)-3-(4-aminophenyl)-3-ethylpiperidine-2,6-dione (DL-AGT), used as an aromatase inhibitor for the treatment of advanced breast cancer and Cushing's syndrome was preferred as a suitable molecule for this work. According to Biopharmaceutics Classication System, it is a class ll drug with low water solubility but have good permeability[1]. DL-Aminoglutethimide, the drug that we have dealt with can cause aromatase inhibition. It was initially introduced as an anticonvulsant but due to its side effects of acting as a potent inhibitor of several enzymes on adrenal cortex, it is no longer been used. These drawbacks of this drug twisted into a clinical advantage in the treatment of cushing syndrome and advanced breast cancer. The growth of certain tumors rest on specific hormones and that makes the basis of endrocrine therapy of breast cancer. DL-AGT is found to be effective in hormone dependent breast carcinoma by suppressing the estrogen level in post menopausal women. It hinders the conversion of androgen to estrogen.[2] Moreover, this drug is very effective in painful bone metastates. However Aminoglutethimide has its side effects because of its toxicity[3] such as lethargy, depression and rash besides its benefits[4].

Nowadays, molecular encapsulation is an important aspect to increase the bioavailability of certain drugs to retain their therapeutic activity. Potent drug delivery systems including biocompatible polymers, nanoparticles have already been explored. Cyclodextrin based drug delivery systems are found to be most effective and reliable due to their non-toxicity and biodegradability[5, 6]. Cyclodextrins or cycloamyloses are truncated cone shaped cavity polymer having a minimum number of 6-D(+) glucopyranose units linked by α-1,4 bonds[7]. They can be natural or semi-synthetic (oligosaccharides)[8]. The α, β and γ cyclodextrins and their derivatives are immensely used in pharmaceutical science. For parental drug delivery, oral administration, cyclodextrins are extensively used. The applications of CDs are even more than the above as they are able to make inclusion complexes with some specific molecules which will be fitted in the cavity. So the size of the entering guest molecule is also an important parameter here[9]**.** The interaction between the host and the guest molecules are mainly non-covalent e.g. ion-dipole, hydrogen bonding and van der Waals types. The most widely accepted host for complex formation is β-CD for its suitable cavity diameter and low production cost[10, 11]. β-cyclodextrin consists of seven α-D-glucopyranose unit joined by α-1,4 linkage[12]. Cyclodextrins are able to modify the pharmacological properties of the encapsulated active substances like solubility, bioavailability, chemical stability, dispersibility and toxicity so by preparing the inclusion complexes with cyclodextrin molecules it can be possible to enhance or improve such properties of the active compounds[13-16].

In our present work, encapsulation of DL-Aminoglutethimide within the nano cavity of β– cyclodextrin was established by UV-Vis study, IR spectroscopic study, Powder X-Ray Diffraction study, ^{1}H NMR study, 2D ROESY study, Scanning Electron Microscopic study. Job plot implies the stoichiometry of the complex as 1:1, UV-visible study has given a proper explanation of the thermodynamic parameters of the inclusion process and association constant of the complex. Furthermore, the in vitro cell viability study between the drug and the inclusion complex showed that the Inclusion complex is less toxic on human normal kidney cell line than the drug. By the process of inclusion we are aiming towards the improvement of the properties of the drug (DL-AGT) i.e. to increase its solubility as it has low solubility, enhance specificity and reduce toxicity. Most notably, the stability constant for the complexation of DL-AGT and β-CD by UV-visible

spectroscopy was already there in the literature, though the whole project was on TM-β-CD and DL-AGT inclusion phenomenon [17].

2. Experimental Section:

2.1. Materials

The drug DL-AGT (purity>98%, Molecular weight= 232.28g/mol) was purchased from TCI chemicals India PVT. LTD, β-CD (purity≥97%; Molecular weight=1134.98 g/mol) was purchased from Sigma Aldrich Germany and all the reagents are used without further purification.

2.2. Methods

DL-Aminoglutemide and β-CD were weighed using Mettler Toledo AG-285 (uncertainty ±0.1mg) and their solutions were prepared in 15% acetonitrile solution (Acetonitrile-water mixture) at 298.15 K. Other solutions of required strengths were prepared by mass dilution.

Fourier transform infrared spectra (FTIR) were recorded on a PerkinElmer 8300 FT-IR spectrometer (PerkinElmer, Inc., Germany) using KBr disk procedure. Samples were prepared as thin KBr disks with minute amount of sample at room temperature. The range of scanning was kept at 4000−400 cm^{-1}. ^{1}H-NMR study was executed in DMSO-$d_6$medium using BRUKER AVANCE NEO 400 MHz (Bruker Inc., Germany) instrument where the solvent residual peak was taken as internal standard. UV-Visible Spectroscopy was performed in Agilent 8453 spectrophotometer (USA). PXRD data were obtained from Bruker D8 Advance (Germany), Cu Kα radiation source 45 kV, λ= 1.5406 A^0 with scanning range was from 5° to 80°.The scanning electron micrographs were determined by JEOL JSM-IT 100 scanning electron microscope model.

2.3. Molecular Docking: Molecular docking process was employed for the virtual screening of the small guest molecule (DL-AGT) and a host (β-CD) to find the geometry of the inclusion complex through PyRx software[18]. This software is written in the Python programming language with an intuitive user interface that run on all major operating

systems (Linux, Windows, and Mac OS)used to determine the binding parameters as well as binding geometry. It is a combination of several softwares such as AutoDockVina, AutoDock 4.2, Mayavi, Open Babel, etc. PyRx uses Vina and AutoDock 4.2 as docking softwares. The input files host, guest in the .pdb format were changed to .pdbqtfiles using inbuilt Autodock vina software. After preparing the files, they were exposed to docking by means of AutoDockVina. Before starting the docking calculation a grid box was prepared around the host molecule. This resulted in a binding site center of 8.3636, 24.4146, and 1.2278 for the X, Y, and Z axes, respectively.Grid box dimensions were set to be X, Y, and Z conformations equal to 25, 25, and 25, respectively. The grid space size was assigned perfectly, which allows selecting search space for the host to perform docking with the guest, normally, at the binding site. The interaction between DL-AGT and the respective β-CD was interpreted using the Lamarckian genetic algorithm (LGA). Once the calculations were ended, result of binding affinity ($KJ.mol^{-1}$) of the most stable conformation of the host with the guest was provided by the software in the table 4.

2.4. In-vitro cell viability study: The cell viability study of the drug and the synthesized complex was investigated by MTT assay. HEK-293 (Human normal kidney cell line) was cultured in 96 well micro titre plate at 37 ^{o}C, in presence of 5% carbon dioxide (CO_2) at a density of 5×10^3 cells/well in 100µl DMEM (Dulbecco's Modified Eagle Medium) Ham F-12 culture medium. After 24 hours of incubation, drugs (DL- AGT, β-CD.DL-AGT) were added in each well at different concentrations (50µM, 100µM, 150µM, 200µM, 250µM, 300µM, 350 µM,400µM,450µM,500µM) in triplicate. Then, the micro titre plate was incubated under the same experimental condition. Next day, after discarding the culture media from the treated plate 10µl (5mg/ml) of MTT powder [3-(4,5-dimethylthiazol-2-yl)-2,5-diphenyltetrazolium bromide] dissolved in 1X PBS was added in each well. Plate was again kept into incubator for 3 hours in the above mentioned condition. Finally, a formazan solubilizer i.e. Isopropanol was added to each well containing MTT solution and was shaken for about 10 minutes. At last, the absorbance was recorded by a micro titre plate reader (SPECTROstar^{Nano},Germany) at 620 nm[19]. The solutions of the concerned samples were prepared in DMSO.

2.5. Preparation method of inclusion complex:

By mixing β-CD and DL-ADT in the molar ratio of 1:1, the IC has been prepared. 1.0mmol of DL-AGT was dissolved in 25 mL of 15% acetonitrile and 1.0 mmol of β-CD in 25 mL of distilled water. Keeping the β-CD solution on a magnetic stirrer, the DL-AGT guest solution was added slowly and the mixture was allowed to stir for 36 hrs at constant temperature of 50^0C. The suspension thus obtained was filtered and dried in oven at 70^0C for 7 hrs. Ultimately the solid powder was procured and stored in a dessicator for future use.

3. Results and discussion:

3.1. Job plot: In order to determine the stoichiometry of the host-guest inclusion complex the continuous variation method or the Job's method is applied[20]. Here a set of solutions of the drug (DL-AGT) and β-CD was prepared by varying the mole fraction of DL-AGT from 0-1 and from the UV-Vis spectroscopy the absorbance of all the solutions are checked at the λ_{max} (238nm). By plotting ΔA*R against R, Job plot is generated, where ΔA is the difference in absorbance of the guest without and with β-CD and R= [DL-AGT]/[DL-AGT+β-CD]. The R_{max} value obtained from the Job plot is 0.5 (figure.1.a) which signifies a 1:1 complexation of the guest and host molecule[21].

3.2. Association constants and thermodynamic parameters: The association constants of DL-AGT and β-CD IC were calculated at three different temperatures by UV-Vis spectroscopy measuring the change in the molar extinction coefficient of the guest molecule when it enters into the hydrophobic cavity of β-CD from the hydrophilic environment. The absorbance changes of DL-AGT were studied by gradually increasing the concentration of β-CD. Benesi-Hildebrand equation is used for the determination of association constant[20].

$$\frac{1}{\Delta A} = \frac{1}{\Delta\varepsilon[AGT]}\frac{1}{Ka[CD]} + \frac{1}{\Delta\varepsilon[AGT]} \qquad \text{(Equation 1)}$$

Where [AGT] and [CD] are the concentrations of the guest molecule and the cyclodextrin molecule, Δε refers to the change in the molar extinction coefficient and ΔA is the change

in the absorbance of DL-AGT on addition of CD. From the double reciprocal plot of the Benesi-Hildebrand equation we have calculated the association constants at three different temperatures(293.15K,303.15K,313.15K) and the linearity of the plot suggests the 1:1 stoichiometry of the host and the guest molecule[22].

Furthermore, the important thermodynamic parameters are determined from the plot of logka Vs 1/T using equation 2.

$$2.303\log ka = -\frac{\Delta H^\circ}{RT} + \frac{\Delta S^\circ}{R} \qquad \text{(Equation 2)}$$

The spontaneity of the process i.e. the free energy change is measured by the following equation 3.

$$\Delta G^\circ = \Delta H^\circ - T\Delta S^\circ \qquad \text{(Equation 3)}$$

Where, the symbols have their usual significance. Now the values of thermodynamic parameters suggest that the process of inclusion is exothermic, spontaneous and entropy restricted. This restriction in entropy may be due to the molecular association between the guest and host molecules [23].

3.3. Solubility Study of DL-AGT.β-CD inclusion complex:

The ethanolic solubility between pure DL-AGT and DL-AGT.β-CD inclusion complex was evaluated using UV–visible spectroscopy. The UV–vis spectrum of DL-AGT.β-CD inclusion complex in different concentration using ethanolic solution was shown in Fig. 2. DL-AGT was sparingly soluble in water, therefore the experiment was modeled in ethanolic phase and the solubility of DL-AGT in ethanol was greatly enhanced when there occurs the formation of DL-AGT.β-CD inclusion complex. DL-AGT displayed absorption maximum peak (λ_{max}) at about 238 nm in the inclusion complex as shown in Fig. 2A and all the calculations were carried out using the λ_{max} value. The peak positions were independent of the concentrations of DL-AGT.β-CD but peak intensities were increasing upon increasing concentration. The plot of absorbance of DL-AGT.β-CD at 238 nm vs. the concentration of DL-AGT.β-CD, gives us a straight line as shown in Fig.2B. According to the Lambert–Beer law, the absorption coefficient of DL-AGT.β-CD in ethanolic solution was evaluated as 0.0907 L $g^{-1}cm^{-1}$. The UV spectra of DL-AGT.β-CD inclusion complex with saturated concentrations in ethanolic solution was shown in the Figure S5. The

absorbance value of saturated solution of DL-AGT.β-CD(inclusion complex) was found to be 1.59873 (Figure S5). The solubilities of pure DL-AGT and DL-AGT.β-CD in ethanol at 25°C were listed in the Table S5. So, it was cleared from the Table S5 that DL-AGT.β-CD inclusion complex has greater solubility with 17.62 $mg.mL^{-1}$ over pure DL-AGT with 7 $mg.mL^{-1}$. These results revealed that the water-soluble host β-CD played a crucial role to improve the solubility of DL-AGT remarkably by the formation of DL-AGT.β-CD inclusion complex. From the above we can also have a clear idea about the aqueous solubility of DL-AGT as there occurred an enhancement of solubility in ethanol after inclusion. [24] [25]

3.4. PXRD STUDY:

The diffractogram (Figure 3) of the DL-AGT.β-CD complex shows the disappearance of some of the pure DL-AGT spectral lines at the 2Θ values of 12.38, 15.09, 16.75, 17.95, 24.92 and the β-CD spectral lines at the 2Θ values of 4.63, 9.11 and 12.63 as shown in Table 2. Additionally, the appearance of new spectral lines of DL-AGT.β-CD complex at the 2Θ values of 17.85 and 18.50 are observed with less intense peaks. It is well known that the peak at 2θ = ∼20° in cyclodextrin based inclusion complexes is a feature of "channel-type" packaging in β-CD where only the head-to-head arrangement has been noticed. The disappearance of some peaks and the generation of new peaks with less intensity in the spectra of DL-AGT.β-CD inclusion complex suggest some sort of interactions between the guest and host molecules.

3.5. FT-IR Spectroscopy: The formation of inclusion complex can also be explained with the help of FT-IR spectroscopy. It is important to note that when the inclusion complex is formed, several characteristic peaks of the guest molecule might be shifted, reduced or disappeared. The stretching and bending vibrations of the three components viz, DL-AGT, β-CD and their IC are shown in Figure4.

In case of DL-AGT, the most important bands present in the IR spectrum are those related to the imide and amino functional groups. The N–H, C-H, C-O and C–N stretching modes give strong bands situated at 3500–3200, 2964, 1687 and 1202 cm^{-1}. The stretching at 3467 cm^{-1} and 3375 cm^{-1} may be due to the 1^0 and 2^0 amines respectively present in the drug molecule. The aromatic C=C stretching vibrations for DL-AGT were found at 1625, 1515, 1448 cm^{-1}. Bending vibrations of -NH and -NH2 appearing at 1625 display strong

bands in the IR spectrum. However, in β-CD, the O-H stretching vibration appeared at 3424 cm^{-1}. The C-H stretching frequency for β-CD appeared at 2921 cm^{-1}, and bending vibration of C-O-C in β-CD appeared at 1153 cm^{-1}. When, the inclusion complex is formed, a broad hump is observed at 3388 cm^{-1}. The characteristic peak for C=O was observed at 1687 cm^{-1} in case of DL-AGT which get slightly shifted at 1693 cm^{-1} in the IC. And the aromatic C=C stretching vibrations for DL-AGT in complex were shifted to 1632, 1515, 1454 cm^{-1} as well as the peak intensity got reduced to some extent. Thus from the above explanation and from Figure 4, it is noteworthy to say that most of the signals of β-CD and DL-AGT have been highly shifted with less peak intensity in the inclusion complex implying some non-bonding interactions of the guest and host in the inclusion complex.

3.6.1.^{1}HNMR study: For the prediction of the structure of the inclusion complex, ^{1}HNMR spectroscopy is a very convenient method. It delivers detailed information about the position of the H nuclei present in the structure of the concerned molecule/complex. As the host-guest inclusion process is based on weak non-bonding interactions, the changes occur in the chemical shifts values after inclusion are comparatively small than in other cases[26].

In β-CD, H3,H5 protons are located inside the cavity (H3 close to the wider rim and H5 close to the narrower rim) and H6 outside the cavity, near to the narrower rim[27]. When the guest molecule enters the cavity of β-CD, the protons inside the cavity (H3, H5) would definitely show some changes in chemical shift than that before[28]. It is observed that after inclusion H3 and H5 protons of β-CD were shifted to upfield but to a smaller extent.The ^{1}H-NMR spectra of DL-AGT, β-CD and inclusion complex were shown in Figure 5. Numerous peaks were found in the spectrum of DL-AGT as well as in β-CD which are shown in Table 3. Chemical shift changes were calculated from the inclusion complex with respect to both β-CD as well as DL-AGT as $\Delta\sigma = (\sigma_{complex} - \sigma_{DL\text{-}AGT/\beta\text{-}CD})$. In case of β-CD, the upfield shift is more for H3 **(-0.04** ppm) than for H5 (-**0.02** ppm). The result indicates that the inclusion occurred through the wider rim and as the H3 proton shifted to more upfield than the H5 proton .The signals relating to the aromatic protons (**H6', H7'**) of AGT almost remains constant in the spectrum of inclusion complex. However, all the protons related to the piperidine-2,6-dione moiety (**H2', H3', H4' H5')** are upfield shifted as shown in the table 3. Therefore, it can be concluded that only the non-aromatic part were incorporated in the cavity of β-CD after complexation.

It is also evident from the MD studies that the aromatic part of DL-AGT gets stabilised at the narrower end of the beta CD cavity. May be this is the reason of non-shifting of the aromatic protons of DL-AGT.

3.6.2 2D-ROESY NMR Study:

Two-dimensional (2D) NMR spectroscopy provides important information about the spatial arrangement between host and guest atoms by observation of intermolecular dipolar cross-correlations. If two protons are closely located in space i.e., closer than 0.4 nm can produce a nuclear Overhauser effect (NOE) cross-correlation in two-dimensional rotating frame nuclear Overhauser enhancement correlation (2D-ROESY) spectroscopy and therefore Cross-peaks in ROESY spectra will be obtained. The ROESY spectrum of the DL-AGT. β-CD complex (Figure 5b) showed appreciable correlations of H-3' and H-5' protons of DL-AGT with H-3 and H-5 protons of β-CD. These results indicate that the piperidine-2,6-dione moiety of DL-AGT are in close proximity with the H-3 protons of β-CD.These results further confirmed that the DL-AGT.β-CD inclusion complex was successfully formed in the solution phase.

3.7. Molecular Docking study: Molecular docking gives us an effective information about bond simulation between molecules[29].

In order to comprehend the orientation, conformation and interaction of drug/guest molecule within the cavity of β-CD, molecular modelling is a constructive computational technique[30].

Here, docking has been used to predict the possible bound conformation of β-CD.DL-AGT inclusion complex and to estimate the binding affinity[29]. The drug, within the binding cavity of β-CD was docked and the most probable binding conformation was obtained[6]. Results showed that the interaction between DL-AGT and β-CD is 1:1. The drug fitted comfortably within the pocket as shown in the Figure6. The binding affinity for DL-AGT and β-CD was found to be -23.012KJ/mol, which is in good agreement with the experimental findings from UV-Vis spectroscopy. The results also indicated that in the complex only the piperidine-2,6-dione moiety of AGT interacted with the H-3 protons of

CD cavity. The findings of this theoretical study are consistent with the results of FTIR, and NMR experiments.

3.8. SEM study: Scanning Electron Microscopy is one of the best techniques in describing the surface morphology of different chemical entities in solid state. The surface morphologies of host, guest and their inclusion complex have been shown in Figure7. Although both DL-AGT and β-CD are found in crystal form in different sizes. However, DL-AGT appears as irregular-shaped crystal particles with large dimensions(Figure 7A) whereas β-CD appeared as polyhedral crystal like structure(Figure 7B).When, complexation occurs, it is evident that the DL-AGT.β-CD IC (Figure 7C) exhibited a different surface morphology a thread like structure. This distinct surface morphology may be due to the formation of the inclusion complex[23]. The totally dissimilar surface morphology of the inclusion complex may assist the other experimental observations.

3.9. In vitro cell viability study: The synthesized inclusion complex of the drug DL-AGT and β-CD and the drug itself were evaluated for the cell viability study. The cells were exposed to varying concentrations of the drug and inclusion complex and the results of the cell viability obtained in the study have been depicted graphically Fig 8. After the drug treatment, the cell viability was found to be concentration dependent. In case of the drug, as concentration increases, the cell viability of normal kidney cells decreases. But, the cells are more viable in presence of the inclusion complex when compared with the drug. This might be because of the higher toxicity of the drug (DL-AGT) at higher concentration (as the amount of drug increases), normal cells lose their reproducibility and eventually die. But when compared with the inclusion complex the cell viability is more than the original drug as we move lower to higher concentration. So, it is worth mentioning that the complex is less toxic in nature than the drug itself and so the cells are able to grow and reproduce properly. This finding clearly indicates the fact that the inclusion complex is less toxic as it causes less anti-proliferative activity of cell when compared to the drug. This behaviour of the inclusion complex might be due to the controlled release of the drug from the cavity of β-CD[14].

4. Conclusion: In our present study we have synthesized an attainable inclusion complex of an aromatase inhibitory drug DL-AGT and a host β-CD. The process of inclusion was confirmed by ^{1}HNMR, PXRD, FTIR, SEM and the UV-Vis study. From the Job's plot(UV-Visible study) and from the shifting of the H3 and H5 protons of β-CD in the ^{1}HNMR spectra of the IC, it is confirmed that the inclusion occurred in a 1:1 stoichiometric ratio. Moreover, the solubility of the IC in ethanol is greater than the pure drug was also determined. The above experimental observations were further affirmed by molecular docking study, which helps to predict the most stable conformation of the inclusion complex. Lastly the cell viability study between the drug and its IC with β-CD implies that by increasing concentration, the inclusion complex shows less toxicity than the drug itself. So, this is an important finding about the inclusion complex of the drug with β-CD, which may improve the therapeutic activity of the drug towards its application it is meant for and also can change the path of science to a new direction.

Declaration of Competing Interest: No conflict of interest is there.

Acknowledgement: Authors express their gratitude to UGC-SAP, Department of Chemistry, University of North Bengal. Authors are highly indebted to the Department of Biotechnology, University of North Bengal for the Cell viability study.

TABLES

Table 1. Association constants (Ka), Gibb's free energy (ΔG^0), enthalpy (ΔH^0) and entropy (ΔS^0) of AGT-β-CD systems from UV-Vis spectroscopy

Complex	$k_a(10^3 M^{-1})$			ΔG^0KJ mol^{-1})	ΔH^0 ($kJmol^{-1}$)	ΔS^0 $Jmol^{-1}$) K^{-1}
	293.15K	303.15K	313.15k			
DL-AGT.β-CI	3.55	2.54	1.59	-19.81	-30.59	-36.16

Table 2:2Θ values of β-CD, DL-AGT and DL-AGT.β-CD inclusion complex from PXRD study.

Components	2Θ
β-CD	4.63, 9.11 , 12.63
DL-AGT	12.38 , 15.09 ,16.75 ,17.95 ,24.92
DL-AGT.β-CD IC	17.85 ,18.50

Table 3: Chemical shifts and its deviations for the protons of β-CD, DL-AGT in free state and in inclusion complex

	Chemical shift σ(ppm)			
Protons	**β-CD**	**DL-AGT**	**DL-AGT.β-CD**	**Δσ ($\sigma_{complex}$-σ_{free})**
H3	3.70		3.66	-0.04
H5	3.58		3.56	-0.02
H2’		5.11	5.07	-0.04
H3’		2.08	2.05	-0.03
H4’		1.81	1.78	-0.03
H5’		0.75	0.73	-0.02
H6’		6.93	6.93	0.0
H7’		6.55	6.55	0.0
Ar-NH_2		10.73	10.73	0.0

*Negative values of Δσ indicate upfield shifts.

Table 4: Binding Affinity of DL-AGT and β-CD from molecular docking

Ligand with receptor	Binding affinity (ΔG^0 KJ/mol)
DL-AGT-β-CD [IC]	-23.012

Table S1: Job plot data of DL-AGT/β-CD system by UV-Visible spectroscopy (at 298.15K).

drug conc. [DL-AGT] (μM)	[β-CD] (μM)	[DL-AGT]/ ([DL-AGT]+ [β-CD])	Absorbance(A) @λ_{max} 238nm	ΔA (0.471953-A)	ΔAx[DL-AGT]/ ([DL-AGT]+[β-CD])
0	100	0	0	0.471953	0
10	90	0.1	0.022884	0.449069	0.044906911
20	80	0.2	0.046735	0.425218	0.085043638
30	70	0.3	0.08291	0.389043	0.116712882
40	60	0.4	0.136551	0.335402	0.134160648
50	50	0.5	0.192047	0.279906	0.139953044
60	40	0.6	0.252155	0.219798	0.13187864
70	30	0.7	0.301264	0.170689	0.119482332
80	20	0.8	0.36616	0.105793	0.08463407
90	10	0.9	0.425218	0.046735	0.042061406
100	0	1	0.471953	8.5E-08	8.5E-08

Table S2: Data of Benesi-Hildebrand double reciprocal plot for DL-AGT.β-CD system from UV-Visible spectroscopy at 293.15K.

A0	A1	ΔA	[β-CD]	1/[β-CD]	1/ΔA
0.350255	0.466103	0.115848	2.0E-05	50000	8.632015
0.350255	0.533593	0.183338	3.0E-05	33333	5.454396
0.350255	0.581200	0.230945	4.0E-05	25000	4.33004
0.350255	0.631231	0.280976	5.0E-05	20000	3.559025
0.350255	0.654953	0.304698	6.0E-05	16667	3.281938
0.350255	0.676511	0.326256	7.0E-05	14286	3.065082

Table S3: Data of Benesi-Hildebrand double reciprocal plot for DL-AGT.β-CD system from UV-Visible spectroscopy at 303.15K.

A0	A1	ΔA	[β-CD]	1/[β-CD]	1/ΔA
0.338275	0.449632	0.111357	2.0E-05	50000	8.980157
0.338275	0.513881	0.175606	3.0E-05	33333	5.694566
0.338275	0.567746	0.229471	4.0E-05	25000	4.357849
0.338275	0.603692	0.265417	5.0E-05	20000	3.767657
0.338275	0.643238	0.304963	6.0E-05	16667	3.27909
0.338275	0.668577	0.330302	7.0E-05	14286	3.027536

Table S4: Data of Benesi-Hildebrand double reciprocal plot for DL-AGT.β-CD system from UV-Visible spectroscopy at 313.15K

A0	A1	ΔA	[β-CD]	1/[β-CD]	1/ΔA
0.317453	0.402578	0.085125	2.0E-05	50000	11.74739
0.317453	0.441405	0.123952	3.0E-05	33333	8.067627
0.317453	0.474593	0.15714	4.0E-05	25000	6.363754
0.317453	0.514473	0.19702	5.0E-05	20000	5.075614
0.317453	0.571728	0.254275	6.0E-05	16667	3.932754
0.317453	0.595930	0.278477	7.0E-05	14286	3.590957

Table S5: Solubility of DL-AGT and DL-AGT.β-CD in ethanol at 25°C.

Sample	Solubility in ethanol ($mg.ml^{-1}$)
DL-AGT	7
DL-AGT.β-CD	17.62

FIGURES

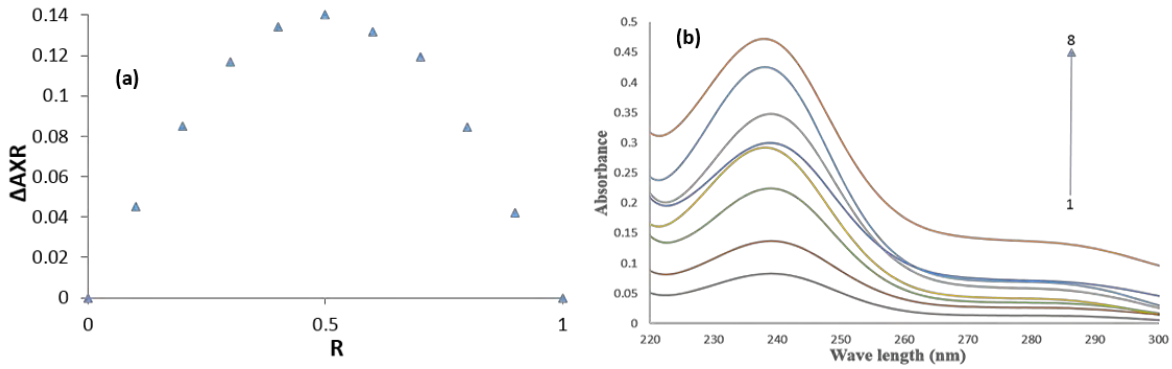

Figure 1: (a) Job plot for the stoichiometry 1:1 (Host:Guest) and (b) Spectra of Job's plot.

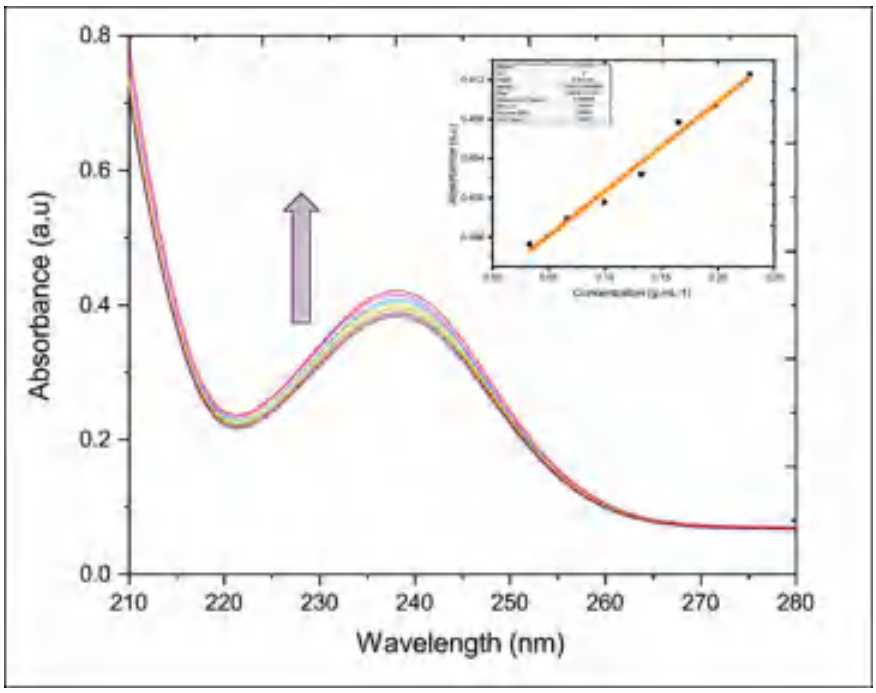

Figure 2: (A) UV spectra of DL-AGT.β-CD with different concentrations ($g.L^{-1}$) in ethanolic solution (at 298.15 K): (a) 0.033; (b) 0.066; (c) 0.099; (d) 0.132; (e) 0.165; (f) 0.198; (g) 0.228. (B) A plot of absorbance ratio of DL-AGT.β-CD at 238 nm vs. the concentration of DL-AGT.β-CD (inside the box)

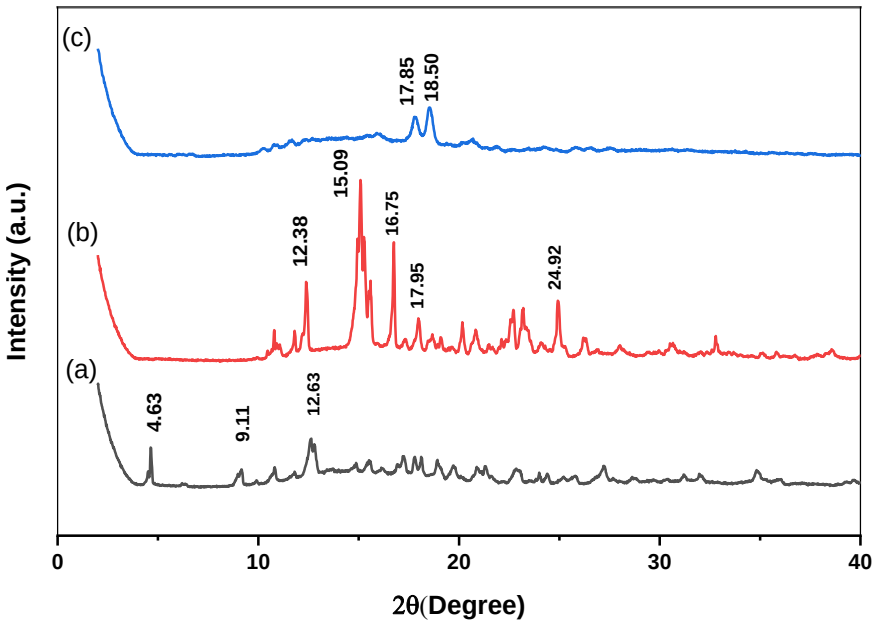

Figure 3: PXRD diffractogram of (a) β-CD, (b) DL-AGT and (c) DL-AGT.β-CD IC (inclusion complex)

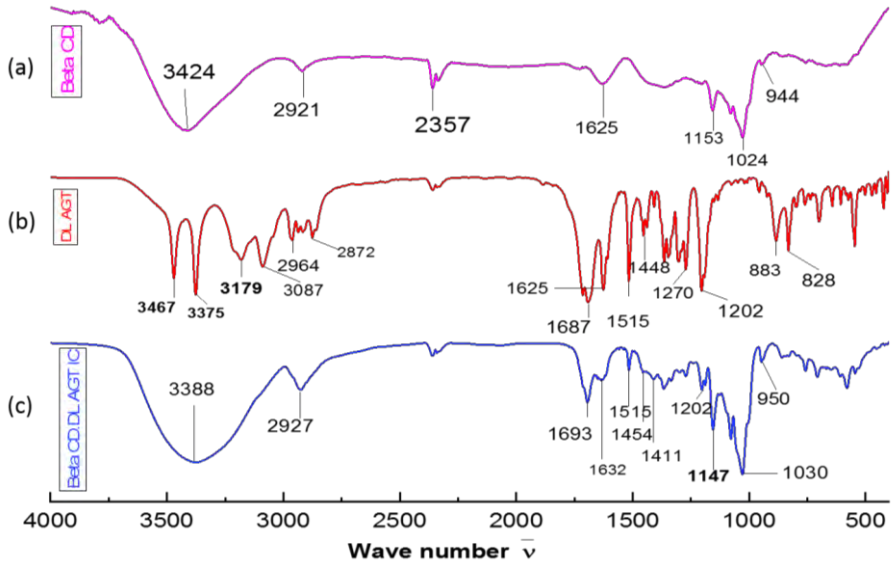

Figure 4: Infrared spectra of (a) β-CD, (b) DL-AGT and (c) β-CD.DL-AGT IC (Inclusion complex)

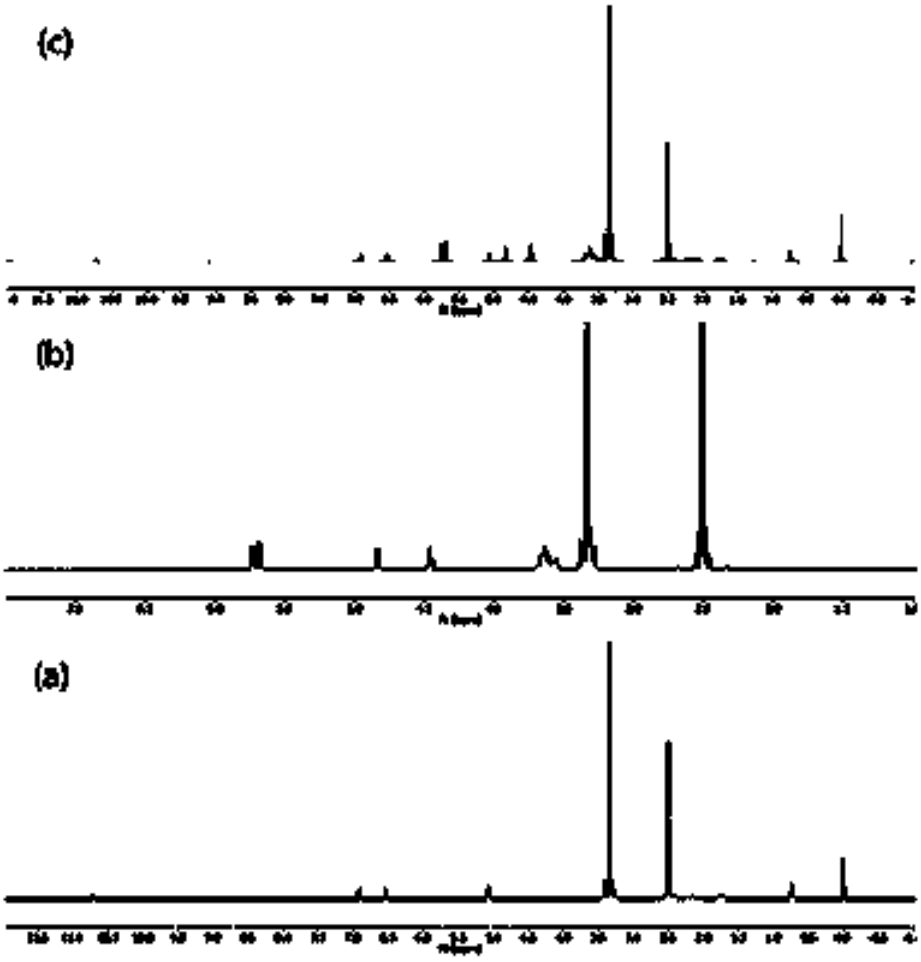

Figure 5a: ^{1}H NMR spectra of (a) DL-AGT (b) β-CD and (c) β-CD.DL-AGT IC

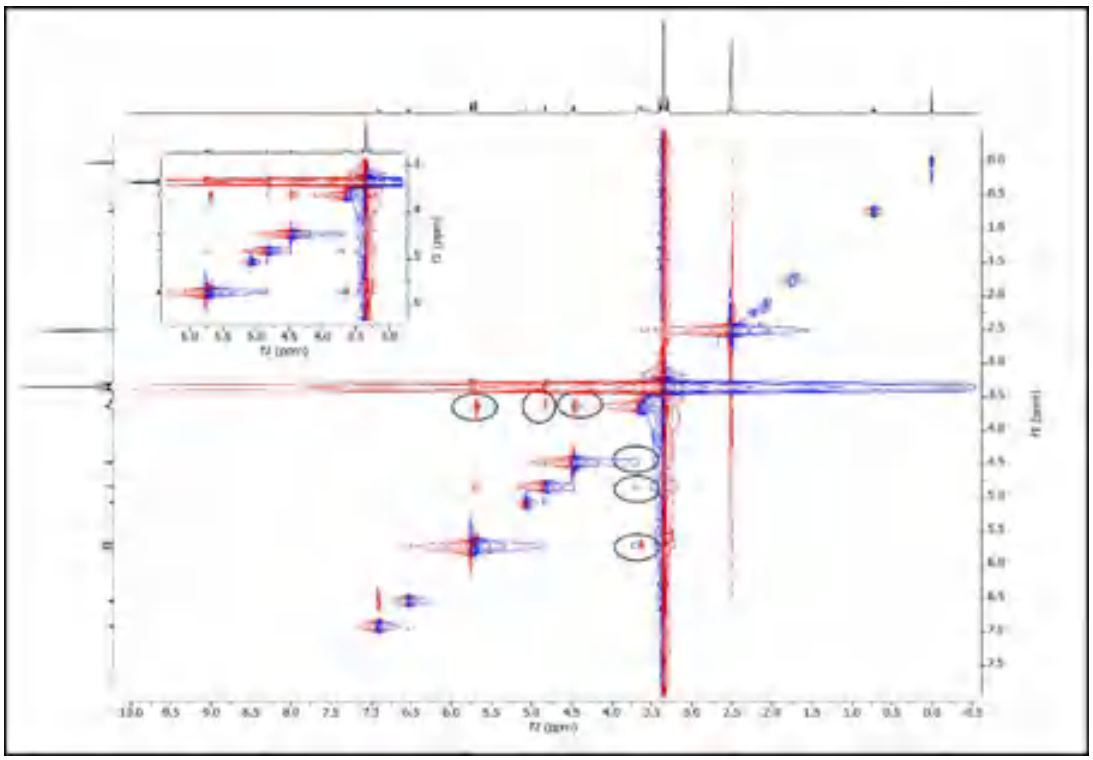

Figure 5b: ROESY spectrum of β-CD.DL-AGT IC in D_6-DMSO

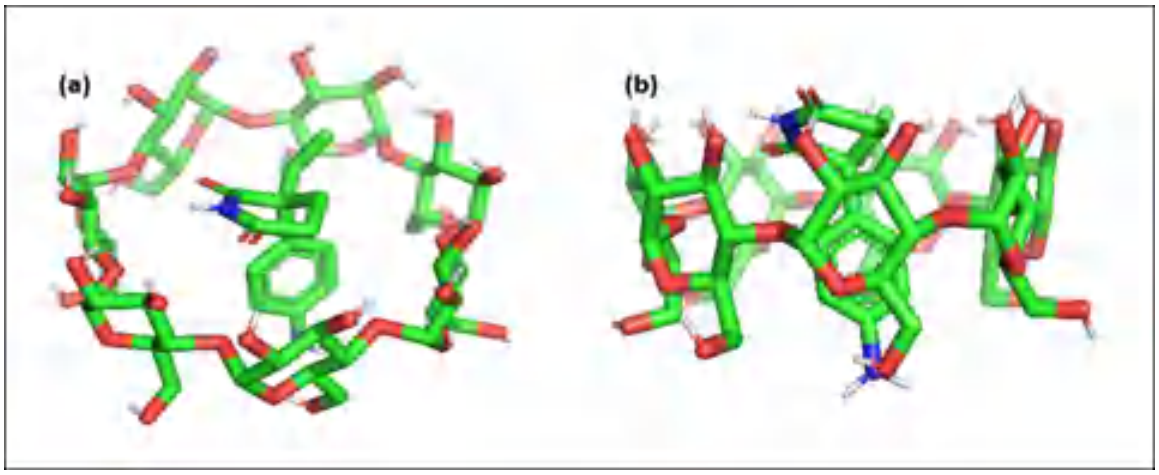

Figure.6: Mode of binding of the drug DL-AGT into β-CD [IC] (a) Top view (b) Side view

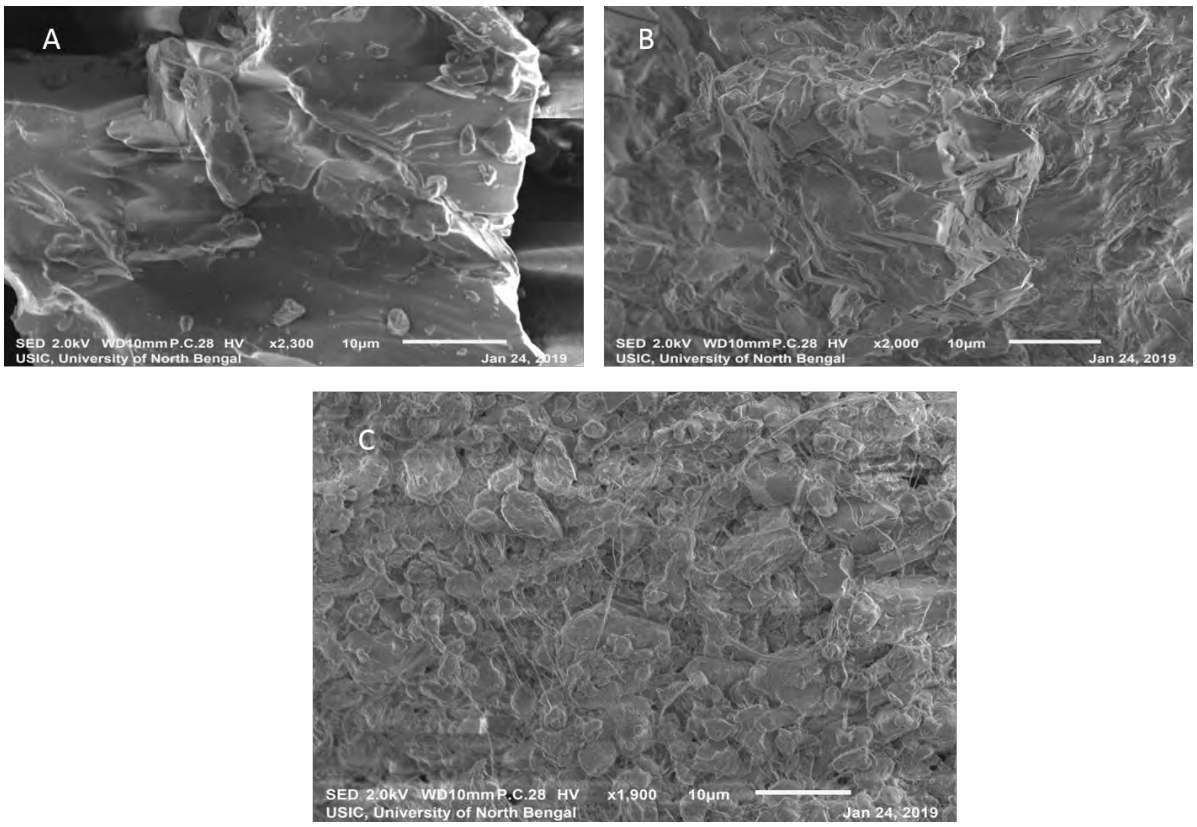

Figure7: SEM images of (A) DL-AGT (B) β-CD and (C) β-CD.DL-AGT IC.

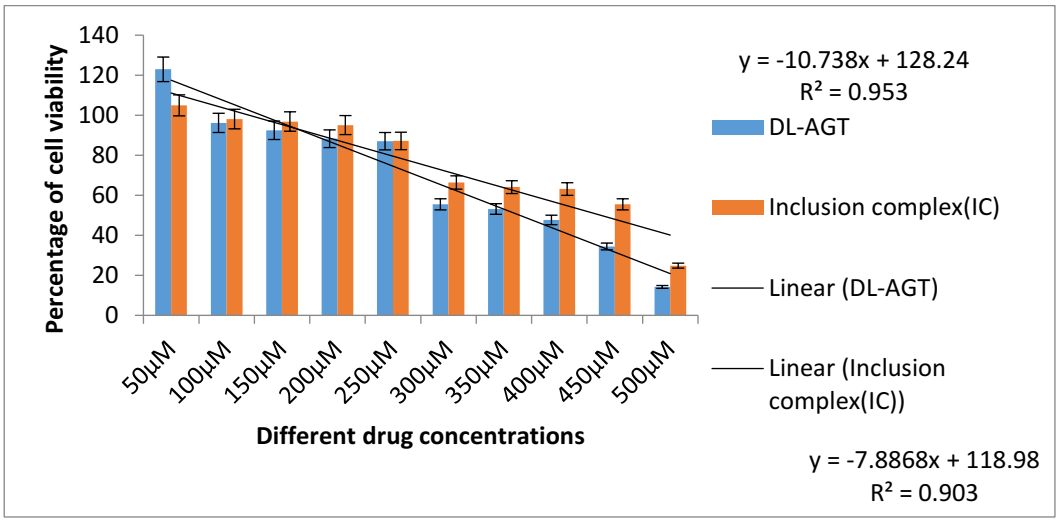

Figure8: In-vitro cell viability study of pure drug and its Inclusion complex

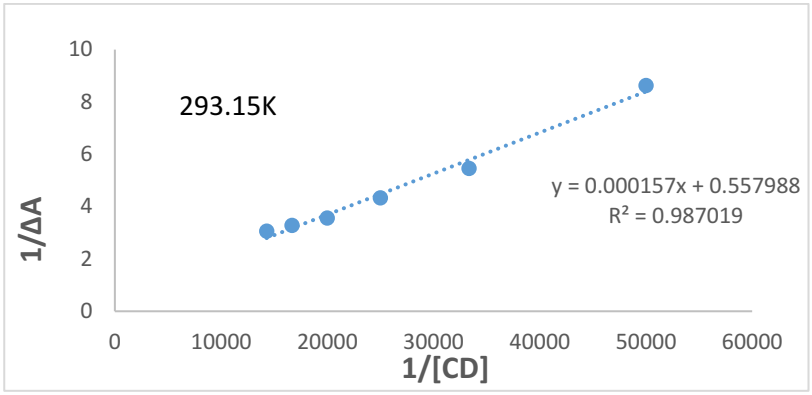

Figure S1: Benesi-Hildebrand double reciprocal plot at temperature 293.15K

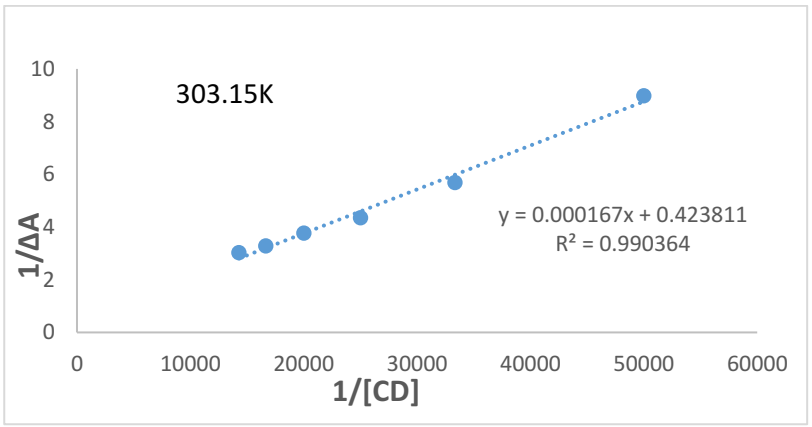

Figure S2: Benesi-Hildebrand double reciprocal plot at temperature 303.15K

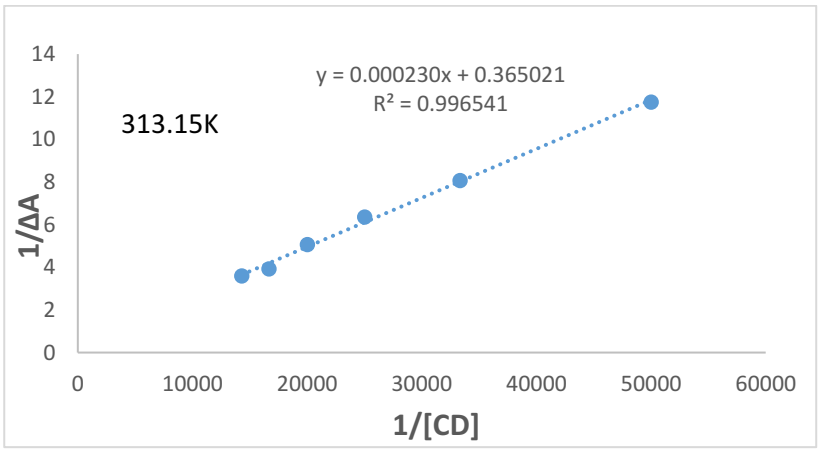

Figure S3: Benesi-Hildebrand double reciprocal plot at temperature 313.15K

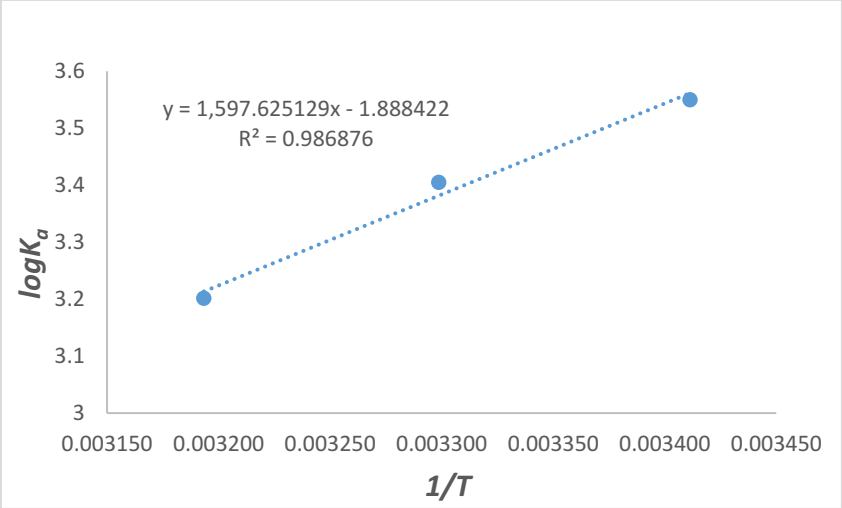

Figure S4: Plot of $\log k_a$ Vs 1/T (from where the thermodynamic parameters were determined)

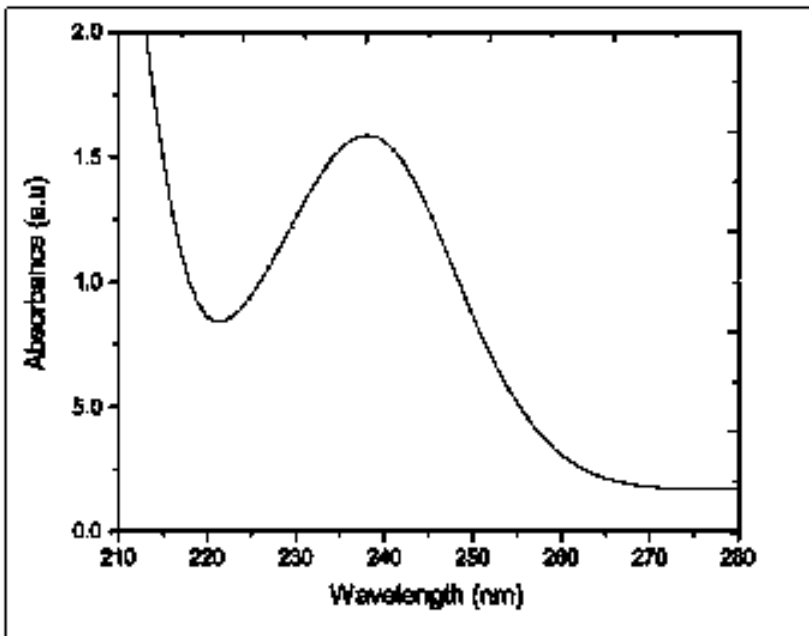

Figure S5: Absorption spectra of DL-AGT.β- CD inclusion complex with saturated concentration in ethanolic solution.

SCHEMES

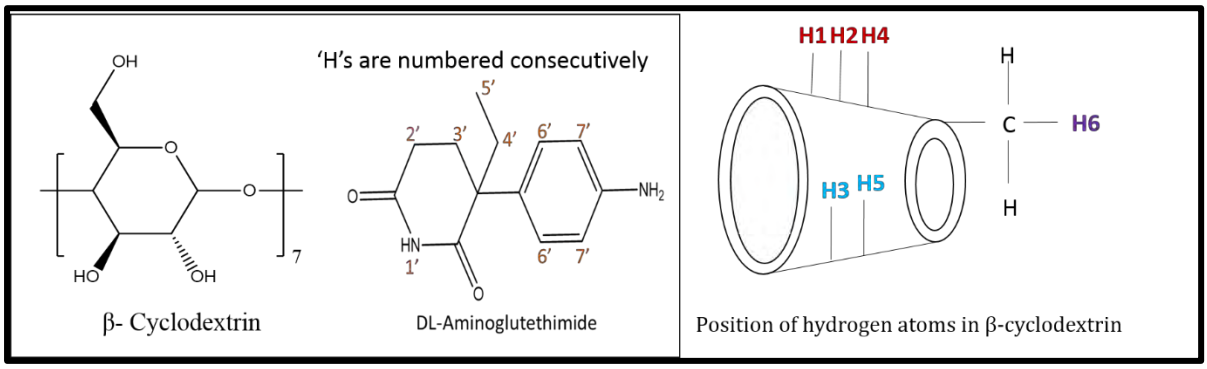

Scheme.1: Structures of the concerned molecules.

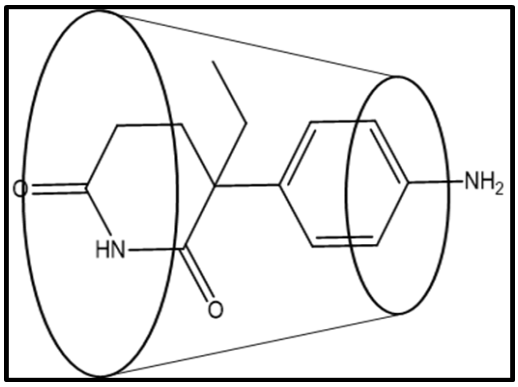

Scheme.2: The plausible mechanism of inclusion.

CHAPTER VIII

PROBING INCLUSION COMPLEX OF A DYE (ISD) WITH CYCLIC OLIGOSACCHARIDE FOR MINIMIZING HARMFUL EFFECTS

Abstract: Indigo is a colouring agent used widely in various fields. The synthetic indigo has many adverse effects when it is consumed with foods and beverages. Cyclodextrin (CD) is known to have special chemical characteristics and biological activities and has a suitable cavity that can include molecule of suitable diameter. In our present study, we have outlined different modes of characterization of the inclusion complex (IC) formation between poorly water soluble dye Indigosulfonic Acid Dipotassium Salt (ISD) and β-Cyclodextrin with the help of FTIR Spectroscopy, UV-Visible spectroscopy, fluorescence spectroscopy, ^{1}H NMR study, 2D NOESY, Isothermal Titration Calorimetric study and SEM analysis. ^{1}H-NMR study and other spectroscopic analysis clearly revealed the successful formation of the (IC) which is supported by cross-peaks formed in 2D-NOESY spectrum. Comparable association constants and thermodynamic parameters obtained from both UV-Visible study and ITC study confirmed the higher stability of the IC. The solubility of the IC was found higher than the pure ISD.

Keywords: Association constant, β-Cyclodextrin, Fluorescence study, Inclusion complex, Job plot.

1. INTRODUCTION

In the era of globalisation, host-guest inclusion chemistry based research has become a matter of utmost importance because of their substantial applications in the area of industrial and biomedical research [1].Now days, cyclodextrins (CDs) are being widely used for its excellent ability to form inclusion complexes with various biologically as well as industrially important compounds[2]. Such phenomenon which is known as inclusion brings about certain modifications in both physical and chemical properties of the complex formed [3]. Inclusion complexes (ICs) with CDs are being widely used as biomimetic systems and as unique media for various types of reactions [3-6]. The most common CDs belong to cyclic oligosaccharide category having distinctive truncated

cone-shaped structure with a hydrophobic cavity and hydrophilic rim. The hydrophilic wider rim contains primary and narrower rim contains secondary –OH groups. The specific structural features lead CD molecules to form inclusion complexes with a variety of hydrophobic and amphiphilic species in both the aqueous and mixed solvent medium [7]. Commonly there are three types of cyclodextrin molecules namely α-CD, β-CD and γ-CD basing on the number of glucopyranose units. α-CD, β-CD and γ-CD are made up of six and seven and eight glucopyranose units respectively with cavity diameter of 4.7Å and 6.0Å and 8.3 Å respectively. As the CD molecule has no free rotation about the glucopyranose linkage, the cyclodextrins are not perfectly cylindrical in shape rather toroidal or cone shaped[8-9].Thus, a hydrophobic cavity is formed within the molecule and the outer surface remains hydrophilic due to presence of –OH groups. The hydrophobic void of CD can trap the hydrophobic portion of the guest molecule to form a stable inclusion complex and the system is stabilised by different types of non-covalent interactions, such as van der Waals interactions, hydrogen bonding interactions etc.[10].

The ICs with cyclodextrin molecules have been reported to have diverse applications in scientific literature which comprises enhanced solubility, bioavailability, increased stability, masking of awkward taste and odour, decrease of volatility, probability of controlled drug delivery system and many more. However, ICs have special importance in the field of education and industry [11-14].ICs can be used to create stimuli responsive supramolecular substances. Here, various external stimuli for enzyme activation, photo sensing, thermal dependence, variations in pH/ redox environments, competitive binding are used to control the release of guest molecules from the Host-Guest complexes [15-18].Researchers paid importance on molecular sensing, release of anticancer drug and gene transfection in the past few years[19-22].

The host molecules are chosen for the formation of ICs because of their cyclic-constrained conformations, which is beneficial for the molecular selectivity [23]. Due to the amphiphilic nature CDs are able to form self-assemble in aqueous medium to form various well defined systems such as nano tubes, nano sheets and nano rods, micelle, vesicles which have been found applicable in various fields of drug delivery as well as cell imaging systems and nano devices [23-27]. Sophisticated probes are being designed

and applied for various systems such as molecular switches and machines, chemo sensors, transmembrane channels, molecular logic gates, and other interesting host-guest systems [28-30].

Dyes and their derivatives are used mostly as indicators but they also have vast applications in colouring foods, cosmetics, solvents, drugs, papers, waxes, plastics etc. Dyes as colouring agent are widely used to colour food and beverages as well as pharmaceutical products. This procedure is to enhance the attractiveness of products and also to help people to distinguish different pharmaceutical products. A number of dyes, especially organic colouring agents, sometimes show negative effect on the human body[31].Synthetic dyes are highly coloured, toxic, and carcinogenic in nature[32,33]. The colour of food and beverages are released inside our body when consumed. Indigo is known to be a natural dye extracted from plants Isatis Tinctoria and Indigofera Tinctoria. Because of having dark blue colour, they have wide spread applications in the textile industries and food technology. Due to the presence of intra and intermolecular H-bonding network the dye molecule becomes more stable which reflects in its high melting point 390-392^0 C[34].Indigosulfonic Acid Dipotassium Salt is known to be a derivative of naturally occurring dye Indigo. It has low solubility in water in pure form[35].ISD becomes harmful for our respiratory tract when it is swallowed. It also acts as a skin and eye irritant. Dye may be inserted inside of the β-CD molecule and therefore be used to increase the stability of the dye on surface as well as may get control released inside human body to reduce the severity of its adverse effect[36].Thus, inclusion of the colouring agent inside CD can be safe and significant as its release will be controlled and hence it will be less harmful [37]. In this work, we studied the inclusion of ISD inside the hydrophobic cavity of β-CD in both solution and the solid phase.

2. EXPERIMENTAL SECTION

2.1. Materials Used

2.1.1. Source and Purity Of Samples: Indigosulfonic Acid Dipotassium Salt was purchased from TCI chemicals (INDIA) Pvt. Ltd. having mass purity > 90.0% and alpha,

beta cyclodextrins have been purchased from Sigma Aldrich Germany having mass purity fraction ≥ 98% and used without further purification**(Table 1).**

2.2. Apparatus and Procedure: The mother solutions of ISD and β-CD were prepared by mass using Mettler Toledo AG-285(Uncertainty ±0.1 mg) at 298.15 K and other solutions of required strengths were prepared by mass dilution.

Fourier transform infrared spectra (FTIR) were recorded on a Perkin Elmer 8300 FT-IR spectrometer (Shimadzu, Japan) using KBr disk technique at a resolution 4 cm^{-1}. Samples were prepared as thin KBr disks with minute amount of sample at room temperature. The range of scanning was kept at 4000−400 cm^{-1}.

Isothermal titration calorimetry was used to determine the binding stoichiometry, association constant at 298.15 K using a MicroCal VP-ITC isothermal titration calorimeter (Microcal now Malvern instrument). At first, thermal equilibration was established at room temperature, followed by 120-s delay initially and then 28 subsequent injections of ISD into Beta CD solution. (The duration of each injection was 10s with a spacing time of 180s.) An enthalpy generation curve was produced in each injection (in micro calories per second versus time in minutes).The association affinity and thermodynamic properties of the binding phenomenon were determined by fitting the integrated heats of binding to the one-site binding model to give the association constant (K_a), stoichiometry (N^C), binding enthalpy (ΔH^0) and entropy (ΔS^0).^{1}H NMR and 2D NOESY were performed in D_2O medium using BRUKER AVANCE 400 MHz instrument.

UV-Visible Spectroscopy was performed in Agilent 8453 spectrophotometer (uncertainty ±2nm,1cm path quartz cell was used) and to control the temperature a digital thermostat was attached with the UV instrument. For fluorescence measurement, we used QuantaMaster 40 spectrofluorometer.The scanning electron micrographs were determined by JEOL JSM-IT 100 scanning electron microscope model.

2.3. Synthesis of the Inclusion Complex: The inclusion complex of ISD and β-CD was prepared by co-evaporation method. ISD (dye) and β-CD were accurately weighed according to their 1:1 molar ratio. Here, 0.2 mM of ISD was dissolved in 15 ml 20% ethanol-water solution. Then, it was added drop wise to 25 ml 0.4mM aqueous solution

of β-CD. The solution was stirred continuously with the help of a magnetic stirrer for 12 hours at 60^0C following the filtration of the mixture using filter paper and the precipitate obtained was washed with 50% ethanol. The crude residue was then air dried at room temperature for the next 6 hours and final dry inclusion compound was stored in a desiccator at room temperature.

3. RESULTS AND DISCUSSION

3.1. Job Plot for The Determination of Stoichiometry of the Host-Guest Inclusion Complex: UV-Vis spectroscopic study is used in the field of host-guest inclusion complexation to understand the subsistence of the IC as well as the stoichiometry. While entering from the highly polar bulk solution to the hydrophobic cavity, the guest molecule experiences a variation of the molar extinction coefficient (Δε)[38]and thus change in the absorption pattern took place. We found the absorption maxima for the guest molecule at 289 nm.**(Fig.1**. absorption pattern)[39].

The continuous variation method, in other words, Job's plot method was applied to determine the stoichiometric ratio of the host and guest molecule. The sample solutions of different concentration ratios of β-CD and Guest were prepared and mixed in such a way that the total volume of host and guest molecule remains constant. The changes in absorption spectra were recorded and shown in the **table 2.** We plotted ΔA×R against R [where ΔA is the difference in absorbance of ISD without and with CD i.e.(ISD+β-CD) and R = [ISD]/ ([ISD] + [β-CD])] to determine the stoichiometric ratio.We found the R_{max} value near 0.5[40]**(Fig. 2).** In general; R = 0.5 stands for 1:1 or 2:2 G:H (guest: host) complexes; R = 0.33 for 1:2 G:H complexes[41].Thus the value of R ,obtained experimentally, indicates successful inclusion of one guest molecule inside the hollow cavity of one molecule of β-CD promising the 1:1 host-guest inclusion.

3.2. Association constants and thermodynamic parameters: UV-Visible spectroscopy being the most consistent method to calculate the association constant (K_a) for the formation of IC [42].Incorporation of the guest (act as a chromophore) molecule inside the hydrophobic cavity of the CD molecule indulges some variations of the chemical environment [43, 40].

The guest molecule binds to the host molecule by means of hydrophobic interactions. We recorded the UV-Visible spectra of the complexes at different concentrations of the host molecule keeping the concentration of the guest molecule fixed **(Fig.1).**The changes in the values of absorbance (at λ_{max}= 289nm) were noted at three distinct temperatures. A graph of $1/\Delta A$ against 1/[CD] was plotted to calculate the association constant using Benesi–Hildebrand equation (See supporting information **Table 3, 4, 5 and Fig. 4)[**40,44] equation (1).

$$\frac{1}{\Delta A} = \frac{1}{\Delta\varepsilon[ISD]K_a} x \frac{1}{[CD]} + \frac{1}{\Delta\varepsilon[ISD]} \quad (1)$$

The higher positive values of K_a at three different temperatures signify the increasing feasibility of the process (**Table 6).**The values of the K_a were used to determine the change in the enthalpy (ΔH^0) and entropy (ΔS^0) of the inclusion process. We plotted log K_a against $1/T$ following van't Hoff equation (2) **(Fig. 5).** The values of ΔH^0 and ΔS^0 found are given in the table6 and from these values ΔG^0 was calculated[2,42].

$$2.303 \log K_f = -\frac{\Delta H^0}{RT} + \frac{\Delta S^0}{R} \quad (2)$$

In this experiment, the values of ΔH^0 and ΔS^0 were found to be negative. This signifies that the formation of the IC is an exothermic process and is entropy-restricted **(Table 6)[**2].This may be due to the molecular association of the CD and ISD molecules. As a result of association, the entropy is decreased, which is contrary for a process to be spontaneous. However, the restriction due to negative ΔS value is overcome by the highly negative value of ΔH making the entire inclusion process thermodynamically favourable.

The negative Gibb's free energy change (ΔG^0) of a process is the measure of the spontaneity of that process. Thus, ΔG^0 of the process of inclusion was calculated using the values of thermodynamic parameters ΔH^0 and $\Delta S^0$from the following equation (3) at 298.15K.

$$\Delta G^0 = \Delta H^0 - T\Delta S^0 \quad (3)$$

It is seen that the value of ΔG^0 is negative **(Table 6).** This, in fact, concludes that the formation of the ICs is feasible and the process is an exergonic one. This is due to the effective association of the guest ISD molecule inside the suitable cavity of CD molecule.

3.3. Fluorescence study: With the help of fluorescence study we can evaluate the binding constant by observing the reasonable change in the fluorescence emission spectrum due to some sort of interactions between β-CD and ISD.

The modified Stern-Volmer equation (equation 4) was employed to determine the extent of interaction (association constant K_a) between the host and guest molecule used in this experiment,

$$\frac{F_0}{\Delta F} = \frac{1}{F_q.K_a.[\mathrm{Q}]} + \frac{1}{F_q} \qquad (4)$$

Where, ΔF is the difference in fluorescence at a concentration [Q] in absence and presence of cyclodextrin. K_a, the quenching constant, is equivalent to the association constant. F_q is the fraction of fluorescence accessible to the quencher (here cyclodextrin). From the plot of $F_0/\Delta F$ vs 1/[Q] the binding constant was calculated[44-46].

The concentration of ISD was kept constant at 0.5μM while the concentrations of β-CD varied from 0.2 μM to 0.8 μM. **(Table7, Fig.6).** From fluorescence study, the association constant was found to be 9.51×10^3 at 298.15K, which is comparable to the association constant obtained from the UV-Visible spectroscopy at 293.15K**(Table7).**

3.4. Calorimetric characterization of complexation: In order to calculate the weak binding constants and the corresponding thermodynamic parameters for the host-guest inclusion complex with high accuracy, we have applied Isothermal titration calorimetry (ITC) method. This analytical method is used to determine binding constants ranging from 10^8 to 10^2 M^{-1} [47].It has become an effective method for directly determining the thermodynamic parameters instead of the previously used van't Hoff equation methodology, ITC method is more precise in terms of the determination of thermodynamic parameters [48]. The ITC diagrams of ISD binding to β-CD are given in **Fig. 7.**

From the plot of ITC, of ISD and Beta CD, the upper graph denotes heat release upon each injection of ISD to the sample cell i.e. in Beta CD[49]. The heat release is generally due to complexation of the guest molecule with the host until saturation is achieved that means guest molecules are getting associated to the specific number of the host molecules. It has been observed that the process of inclusion of ISD inside the β-CD is exothermic in nature and the magnitude of the heat evolved during the inclusion process decreases gradually with each injection until complete saturation is achieved.

The extent of the host-guest inclusion is supported by the structural orientation of cyclodextrin molecule which makes the non-polar part of the guest molecule to enter into the hollow cavity of CD molecule, thus the inclusion complex gets stability [42].Another driving force for inclusion process can be attributed to the fact of releasing the water molecules from the hydrophobic cavity into the bulk and hence the total entropy of the system gets increased[50]. The incorporation of the guest molecule takes place from the wider rim of the β-CD molecule, as evident from NOESY spectrum.

The heats of binding were plotted as a function of the molar ratio of [CD/ISD]. The binding parameters like the stoichiometry of binding (N^c), the equilibrium binding constant (K), enthalpy of complexation (ΔH^0) and standard changes in free energy (ΔG^0) and entropy (ΔS^0) were estimated from ITC data on the basis of fitting the data according to the independent binding model. The values of thermodynamic parameters, particularly ΔH^0 and ΔS^0**(Table 6),** shows that of the complexation deals with non-covalent forces in solvent medium, e.g. electrostatic, hydrophobic, van der Waals, and H-bonding interaction. The complexation process was found to be exothermic ($\Delta H^0<0$) and spontaneous ($\Delta G^0<0$) with positive entropic contribution. The negative value of ΔH^0 indicates heat evolution during the inclusion phenomenon while positive entropy changes (ΔS^0) usually arise from the translational and conformational freedoms of host and guest upon complexation.

Negative Gibbs energy indicates that inclusion process is a spontaneous one under experimental conditions; $-T\Delta S^0$, denotes that inclusion of ISD in the CDs is accompanied by displacement of water molecules from the CD cavity. On the other hand, comparatively it has been observed that smaller $-T\Delta S^0$ terms are associated with larger CD cavities [51].Every peak shown in the binding isotherm indicates a single injection of

the guest molecule into the host solution. The exothermicity of the calorimetry peaks **(Fig. 7)** arises because of the considerable interaction between ISD and β-CD molecule. The stoichiometry (N^c) of the inclusion phenomena using ITC analysis is determined from the value of number of binding sites. We obtained the value very close to 1 (Table 8), which clearly indicates 1:1 stoichiometry, which is in good agreement with the 1:1 stoichiometric ratio obtained from the Benesi-Hildebrand plot analysis of the UV-Visible spectroscopic data.

The principal forces involved are van der Waals and hydrophobic interactions. Hydrophobic interactions are entropy driven ($|H^0|<|T\Delta S^0|$), whereas van der Waals interactions are essentially enthalpy driven processes, [52, 53]. From the data obtained, it has been found that the binding of ISD with β-CDs are entropy driven as the enthalpy value of the interaction is smaller with respect to the entropy of the interaction ($|H^0|<|T\Delta S^0|$). This indicates hydrophobic interactions predominate over major van der Waal's interactions in this case.

3.5. FT-IR SPECTROSCOPY

During inclusion procedure, if the guest molecule gets inserted into the hollow cavity of CD molecule some changes in stretching frequencies of the concerned spectral bands will take place, in other words either the spectral bands will get shifted from their previous positions or two spectral bands get merged or widening of bands happen. From the FTIR spectral pattern, we found some bands were absent and some got shifted from its earlier positions in the inclusion complex **(Table 9, Fig.8).** In the IC the bands due to the O-H stretching, stretching of –C-H from $-CH_2$, bending of C-O-C of β-CD are found shifted from 3406.34 cm^{-1} to 3458.65 cm^{-1}, 2944.46 cm^{-1} to 2934.45cm^{-1}, 1163.56cm^{-1} to 1152.45cm^{-1}. On the other hand, band at 1631.15 cm^{-1} for the Stretching due to conjugated C=O was found shifted to 1661.53 cm^{-1} and stretching due to C-N was shifted from 1420.43 cm^{-1} to 1464.32 cm^{-1}. In pure CD bending of –C-H from $-CH_2$ and bending of O-H at 1403.38 cm^{-1} were found absent. In the guest molecule, stretching due to aliphatic N-H bond at 3446.17 cm^{-1}, out of plane C-H bending at 820.27cm^{-1} and broad band due to bending of N-H bond at 674.07 cm^{-1} were found absent in the FT-IR spectra of ISD-CD IC.

3.6.^{1}H NMR AND 2D NOESY spectral analysis of solid inclusion complex: The inclusion complex formation between β-CD and ISD can be established with thehelp of ^{1}H NMR study. The change in chemical shifts values of the protons of inclusion complex is of main interest here. The H3, H5 protons of β-CD situated in the interior hydrophobic cavity where H3 is at the wider rim and H5 is at the narrower rim. The chemical shift values obtained from the ^{1}H-NMR spectroscopic analysis were recorded **(table10 and Fig.9).**

From the data tabulated in the **table 10** it is seen that H3 proton experiences more interaction compared to H5 proton. The more up field shift of the H3 proton of β-CD in the inclusion complex than the H5 proton clearly suggest that insertion occurs through the wider rim **(Table 11).** The other protons are at the same position as in the pure β-CD. So, from the chemical shifts values of the interacting protons (mainly H3 and H5) we can come to the conclusion that the guest molecule is entering towards the hydrophobic cavity from the hydrophilic environment[54,55]. This, in fact, supports the association constant values obtained from UV-Vis, fluorescence and ITC studies.

In NOE spectroscopy the two protons at 0.4 nm apart in space can cause nuclear overhauser effect [36]. It is an imperative method to interpret the extent of interaction among the host (β-cyclodextrin) and guest (ISD) molecules when two protons are in close proximity (3-5Å).Then the appearance of an NOE cross peak can be detected among the relevant protons in the NOESY spectrum. The existence of the host-guest interaction in ISD-β-CD inclusion complex can be proved by Nuclear Overhauser Effect measurements (NOESY spectrum) in D_2O medium. The NOESY spectrum of the IC shows significant NOE cross-peaks between the H''3 and H''5 protons of cyclodextrin and the aromatic protons (H1, H2, H3, H4, H5, H6) of ISD molecule**(Fig.10).** These results obtained satisfactorily coincide with the tentative complex structure given in **fig.11,** indicating the partial inclusion of dye molecule into the cavity of Cyclodextrin. Such observation strongly supports the existence of the non-covalent type of interaction in the complexation of ISD by the β-CD molecule.

The NOE cross-peaks between aromatic protons of ISD (circled in the **Fig. 10)** and H"5, H"3 protons of CD was observed implying complete insertion of non-polar part of ISD into the β-CD cavity. The NOESY spectrum also specified the insertion of the non-polar

part of the ISD into the β-CD cavity by the interaction between H1, H2, H3 protons of the guest molecule and H"3, H"5 from the CD, which completely supports the shift of H"3 and H"5 protons in the 1H-NMR spectroscopic study.

3.7. Structural Effect of Cyclodextrin: The formation of host-guest IC is mainly focused on the structural combination of both the molecules. ICs are formed only when there is the stronger association between the guest and host molecules over other forces. The complexation strength depends on the factors such as the size of the guest molecule, the van der Waals interactions, the release of water molecules, hydrogen bonding, charge transfer interactions, hydrophobic interactions, the release of conformational strain etc. Here, the hydrophobic part of the dye molecule enters inside the hydrophobic cavity of the CD molecule during the formation of the inclusion complex and it is stated that no covalent bond forms or breaks in the system of IC[8, 56].

The interesting fact is that the cavity of the CD molecule is blocked by water molecules but this is unfavourable. When the hydrophobic part of the guest molecule enters inside the hollow cavity of CD, the water molecules are easily replaced. It is clear that the hydrophobic interaction predominates here. However, entropy of the system increases due to the elimination of the water molecules to the bulk as seen from the ITC experiment, which helps the process of formation of the ICs to be spontaneous. The size of the guest molecule or more specifically the hydrophobic part of the guest molecule, which enters into the CD cavity, is another determining factor for the formation of the IC. The hydrophobic part of ISD fits better inside β-CD by relieving the ring strain of the CD as well as lowering the energy of the system. Encapsulation of a single ISD molecule sterically blocks the side of the wider rim inhibiting other molecule to enter inside the cavity, which is reflected in the UV-Vis study of Job plot.

3.8. SEM Study: Scanning Electron Microscope study is a qualitative method to figure out the morphological changes of the starting compound and the inclusion complex attained by the complexation by host β-CD molecule.**Fig.12** shows the micro images of A, B and C. The surface morphology of the three components namely β-cyclodextrin (host), ISD (guest) and their inclusion complex were studied by scanning electron microscope. The surface morphology of β-CD appears as flat configuration having a regular arrangement of fine lines whereas pure ISD is found to have thread/flakes like

morphology. ISD.β-CD inclusion complex appears like irregular shaped crystals [the surface looks like crystals (though no real crystals are there) here only the surface morphology is considered], in which the original morphology of both of the starting compounds gets disappeared.Those changes on the surface structure of the isolated compounds indicate the establishment of interactions with a new phase formation.

CONCLUSION

In this study we have successfully characterised the inclusion of the dye molecule Indigosulfonic Acid Dipotassium Salt inside the naturally occurring oligosaccharide β-CD molecule. The IC was characterised using various thermodynamic as well as spectroscopic methods. The negative value of ΔG of the process, the high association constant from UV-Vis and ITC study of the inclusion show that the IC formed is more stable compared to the pure ISD. The higher stability may be the main reason for the controlled release of the ISD. The inclusion complex found to have higher solubility in water compared to the free ISD. Thus it may reduce the toxic effect generated from colouring foods and drugs. Moreover its controlled release inside the body may reduce the toxicity. As cyclodextrins have very low toxicity, it might be anticipated that the inclusion process makes the overall moiety (IC) of very low toxicity. This study may further open scopes for scientific and industrial research in future.

ACKNOWLEDGEMENTS

All the authors have extreme gratitude to the Special Assistance Scheme, Department of Chemistry, and NBU for instrumental and financial support. Prof. M.N. Roy is also grateful to the UGC-BSR (Basic Scientific Research) for the one-time grant award. Authors would also like to acknowledge USIC, NBU for doing SEM.

TABLES

Table 1: Details of Chemicals used

Name of chemicals	Molecular Weight (g/mol)	Source	CAS number	Purification method	Mass purity
β-Cyclodextrin	1134.98	Sigma Aldrich Germany	7585-39-9	Used as purchased	≥97%
Indigosulfonic Acid Dipotassium Salt	498.57	TCI Chemicals Pvt.Ltd. India	13725-33-2	Used as purchased	>90%
Distilled Water	18	Self-made	-	-	-

Table2: Data for Job Plot performed by UV-Vis spectroscopy for ISD-β-CD system at 298.15K[a]

Guestconc. [ISD] (μm)	β-CD (μm)	R= [ISD]/ ([ISD]+[β-CD])	A @λmax 289 nm	ΔA (0.39195-A)	ΔA X [ISD]/ ([ISD]+[β-CD])
100	0	1	0.39195	0	0
90	10	0.9	0.34407	0.04788	0.043092
80	20	0.8	0.30812	0.08383	0.067064
70	30	0.7	0.27243	0.11952	0.083664
60	40	0.6	0.23841	0.15354	0.092124
50	50	0.5	0.19298	0.19897	0.099485
40	60	0.4	0.1663	0.22565	0.09026
30	70	0.3	0.1345	0.25745	0.077235
20	80	0.2	0.09087	0.30108	0.060216
10	90	0.1	0.05604	0.33591	0.033591
0	100	0	0.01112	0.38083	0

[a]Standard uncertainties in temperature: ± 0.01K, Pressure:± 10kPa

Table 3: Data for the Benesi-Hildebrand double reciprocal plot performed by UV-VIS spectroscopic study for ISD-β-CD complex at 293.15 K

	[ISD] (μM)	[CD] (μM)	A_0	A_1	ΔA	1/ΔA	1/cd
ISD+β-CD	50	10	0.21546	0.22035	0.00489	204.499	100000.00
	50	20	0.21546	0.22473	0.00927	107.8749	50000.00
	50	30	0.21546	0.22804	0.01258	79.49126	33333.33
	50	40	0.21546	0.22924	0.01378	72.56894	25000.00
	50	50	0.21546	0.23439	0.01893	52.8262	20000.00
	50	60	0.21546	0.23559	0.02013	49.6771	16666.67
	50	70	0.21546	0.23681	0.02135	46.83841	14285.71
	50	80	0.21546	0.23951	0.02405	41.58004	12500.00
	50	90	0.21546	0.24102	0.02556	39.12363	11111.11
	50	100	0.21546	0.24447	0.02901	34.47087	10000.00

Table 4: Data for the Benesi-Hildebrand double reciprocal plot performed by UV-VIS spectroscopic study for ISD-β-CD systems at 303.15 K

	[Drug] (μM)	[CD] (μM)	A_0	A_1	ΔA	1/ΔA	1/[CD]
ISD-β-CD	50	10	0.20213	0.20707	0.00494	202.4291	100000
	50	20	0.20213	0.21126	0.00913	109.529	50000
	50	30	0.20213	0.21561	0.01348	74.18398	33333
	50	40	0.20213	0.21906	0.01693	59.06675	25000
	50	50	0.20213	0.22258	0.02045	48.89976	20000
	50	60	0.20213	0.22429	0.02216	45.12635	16667
	50	70	0.20213	0.22641	0.02428	41.18616	14286
	50	80	0.20213	0.22656	0.02443	40.93328	12500
	50	90	0.20213	0.22879	0.02666	37.50938	11111
	50	100	0.20213	0.23637	0.03424	29.20561	10000

Table 5: Data for the Benesi-Hildebrand double reciprocal plot performed by UV-VIS spectroscopic study for ISD-β-CD systems at 313.15 K

	[Drug] (μM)	[CD] (μM)	A_0	A_1	ΔA	1/ΔA	1/[CD]
ISD+β-CD	50	10	0.19368	0.19822	0.00454	220.26432	100000
	50	20	0.19368	0.20315	0.00947	105.59662	50000
	50	30	0.19368	0.20616	0.01248	80.128205	33333
	50	40	0.19368	0.20761	0.01393	71.787509	25000
	50	50	0.19368	0.21313	0.01945	51.413882	20000
	50	60	0.19368	0.21394	0.02026	49.358342	16667
	50	70	0.19368	0.21496	0.02128	46.992481	14286
	50	80	0.19368	0.21971	0.02603	38.417211	12500
	50	90	0.19368	0.22884	0.03516	28.441411	11111
	50	100	0.19368	0.23792	0.04424	22.603978	10000

Table 6: Association constants obtained by the Benesi–Hildebrand method (K_a) from UV-Visible study, Fluorescence study and ITC study along with corresponding thermodynamic parameters of Indigosulfonic Acid dipotassium Salt-β-cyclodextrin inclusion complexes at 293.15K[a], 303.15K[a] and 313.15K[a].

Method	K_a**(10³M⁻¹)**			ΔG^0 **(kJmol⁻¹)**	ΔH^0 **(kJ mol⁻¹)**	ΔS^0**(Jmol⁻¹) K⁻¹**
	293.15K	303.15K	313.15K			
UV-Vis Spectroscopy	9.82	7.13	5.07	-2.38	-5.23	-9.55
Fluorescence Spectroscopy	9.51	-	-	-	-	-
ITC study	8.70±1.98			-3.203	-1.60±0.23	5.38

Table 7: Data for calculation of Association Constant using fluorescence spectroscopic study

Fo	F	ΔF= Fo-F	1/[β-CD] /M-1	1/ΔF	Intercept	Slope	K_a /M^{-1}
987921.44	1028281.44	40360.00	50000.00	2.48E-05			
987921.44	1038976.82	51055.38	33333.33	1.96E-05			
987921.44	1052248.39	64326.95	25000.00	1.55E-05	3.8E-06	4E-10	9512.25
987921.44	1067024.89	79103.46	20000.00	1.26E-05			
987921.44	1080453.77	92532.33	16666.67	1.08E-05			
987921.44	1092249.02	104327.58	14285.71	9.59E-06			
987921.44	1101122.40	113200.96	12500.00	8.83E-06			

Table 8: Value indicating the Binding sites obtained from Isothermal Titration Calorimetric study.

Temperature(K)	Number of binding sites(N^C)
298.15	0.954±0.0693

Table 9: Data obtained from FT-IR spectroscopic study of β-CD, ISD and β-CD+ISD.

Groups	Wave number(Cm^{-1})		
	β-CD	ISD	ISD-β-CD
stretching of O-H	3406.34		3458.65
stretching of –C-H from $–CH_2$	2944.46		2934.45
bending of –C-H from $–CH_2$ and bending of O-H	1403.38		
bending of C-O-C	1163.56		1152.45
vibration involving α-1,4 linkage	958.23		957.34
Stretching due to Aliphatic N-H bond		3446.17	
Stretching due to conjugated C=O		1631.15	1661.53
Stretching due to C-N		1420.43	1464.32
Out of plane C-H bending		820.27	
Broad band due to bending of N-H bond		674.07	

Table 10: The chemical shift values of β-CD, pure ISD and ISD-β-CD IC obtained from ^1H- NMR spectroscopy.

β-CD(400 MHz, Solvated in D_2O) δ /ppm	3.48–3.53 (6H,t, J = 9.2 Hz), 3.56–3.59 (6H, dd, J = 9.6, 3.2 Hz), 3.73–3.78 (18H,m), 3.87–3.92 (6H, t, J = 9.2 Hz), 5.00–5.01 (6H, d, J = 3.6 Hz).
ISD	6.85-6.87(2H,d,J=6.8Hz),7.65-7.67(2H,d,J=7.6Hz),7.92(2H,s)
ISD-β-CD IC	3.42-3.48 (6H, t, J = 9.2 Hz), 3.51-3.57 (6H, dd, J =9.6, 3.2 Hz), 3.53-3.59 (18H, m), 3.63-3.67 (6H, t, J=9.2 Hz), 5.01-5.02 (6H, d, J = 3.6 Hz), 0.95(3H, s);6.87-6.90(2H,d,J=6.8Hz),7.69-7.72(2H,d,J=7.6Hz),7.98(2H, s).

Table 11: Change in chemical shifts (ppm) of the H3 and H5 protons of β-cyclodextrin molecule in host-guest complexes in D_2O.

Protons of CD	ISD+β-CD
H3	0.24
H5	0.19

FIGURES

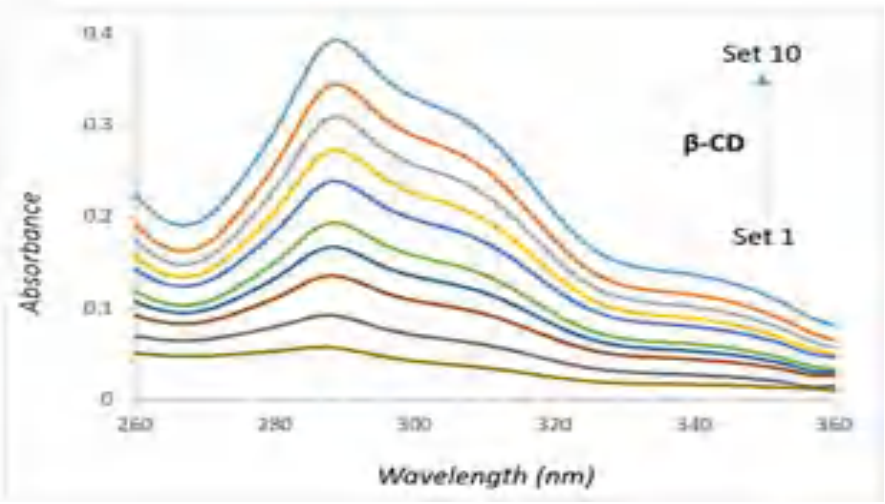

Fig.1: Absorption spectra of intensity against wavelength obtained from UV-Visible spectroscopy at varying concentration of β-Cyclodextrin keeping the guest concentration (Indigosulfonic acid dipotassium salt) constant. The different lines represent absorption pattern at a particular concentration of β-CD.

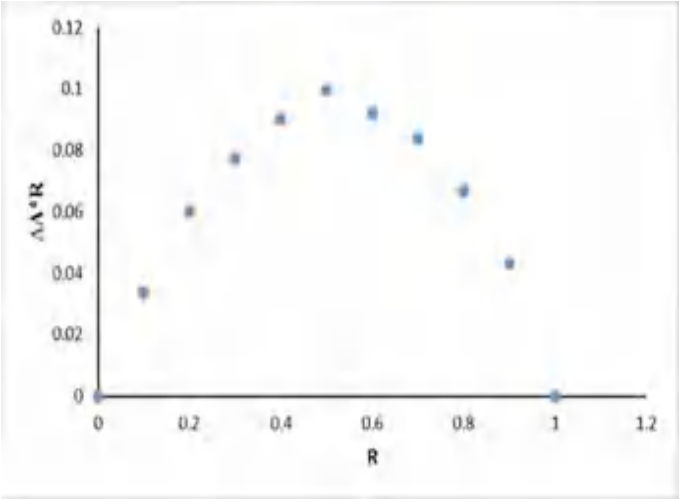

Fig.2: Job plot of β-Cyclodextrin (β-CD) and Indigosulfonic Acid dipotassium salt (ISD) system at λ_{max} (Indigosulfonic Acid Dipotassium Salt) = 289 nm

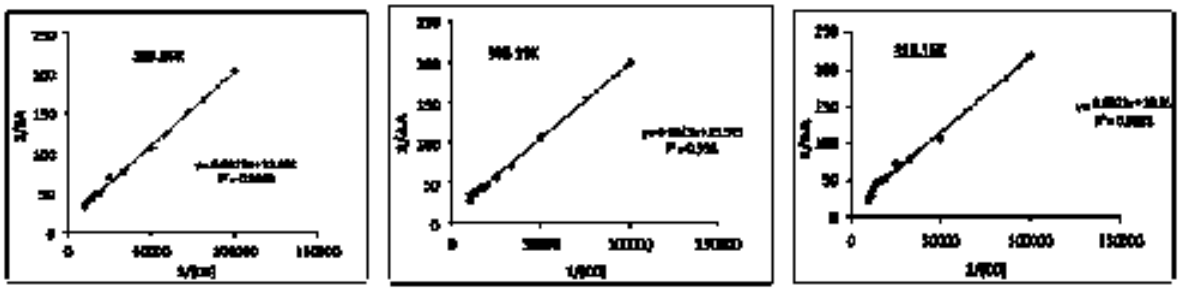

Fig.4: Benesi-Hildebrand double reciprocal plot for the effect of β-CD on the absorbance of ISD at three different temperatures 293.15 K, 303.15 K and 313.15 K.

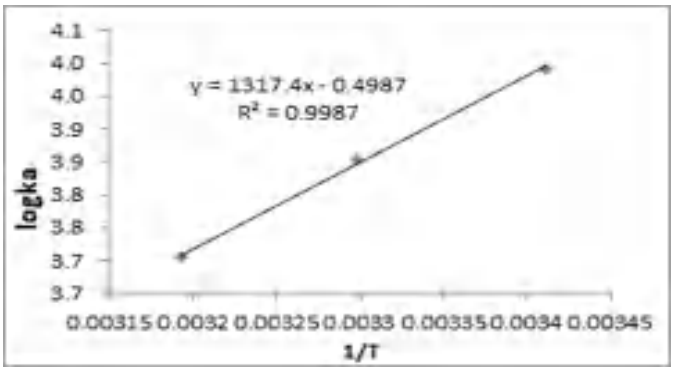

Fig.5 : Plot of logK_a vs 1/T for the interaction of β-CD with ISD.

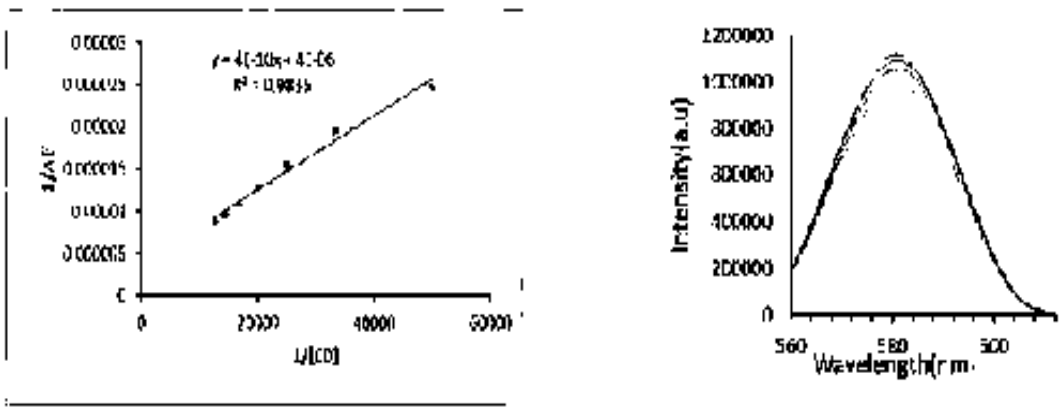

Fig.6: Plot of 1/ΔF (ΔF is the absorbance difference of guest in presence and absent of CD) Vs 1/[CD] ([CD] is the concentration of CD) from the Stern-Volmer equation and fluorescence spectra of Indigosulfonic Acid Dipotassium salt and β-Cyclodextrin at different molar concentration.

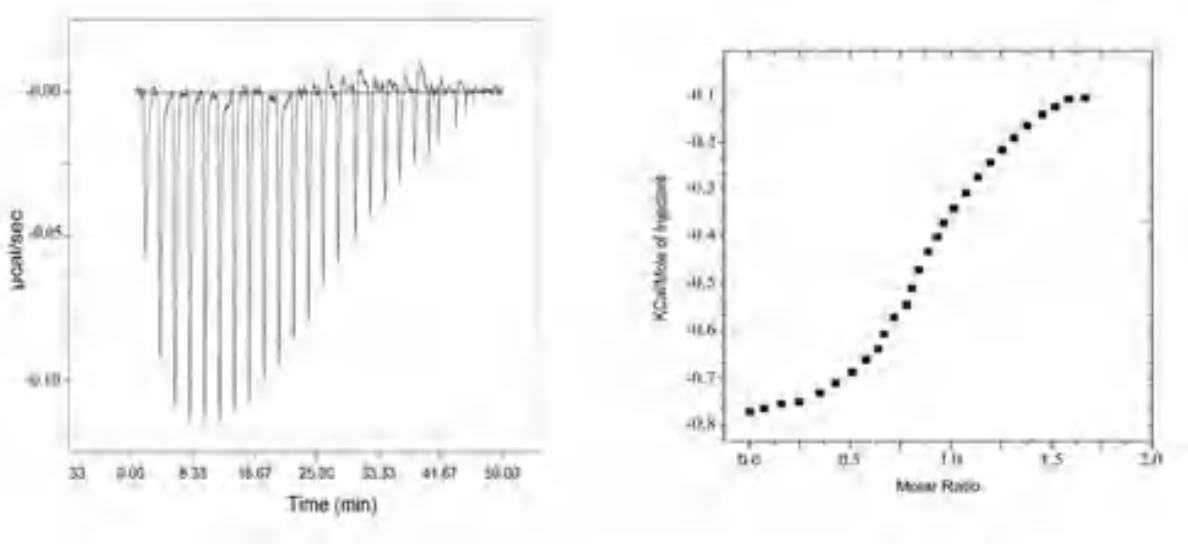

Fig.7: Representative ITC(Isothermal Titrtion Calorimetry) profiles for the titration of ISD(Indigosulfonic Acid Dipotassium salt) (500mM) with β-CD (50 mM) at 298.15 K. figure above represent the raw data for the continuous injection of β-CDs(β-Cyclodextrin) into the ISD(Indigosulfonic Acid dipotassium Salt), after correction of heat of dilution. Figure below is the binding isotherm fitted to the raw data and the bottom panels show the integrated heat data after correction of heat of dilution.

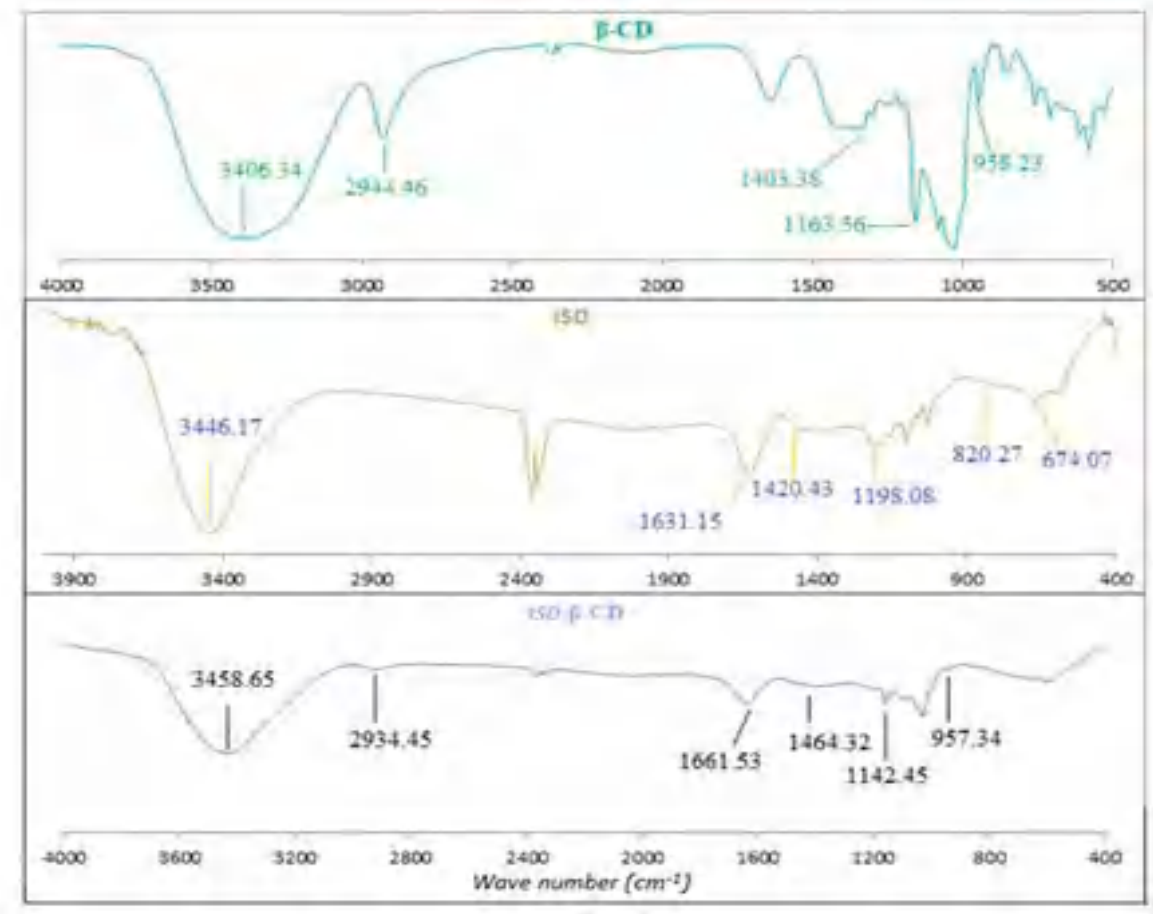

Fig.8: FT-IR spectra of β-Cyclodextrin, pure Indigosulfonic acid dipotassium salt and ISD-β-Cyclodextrin inclusion complex.

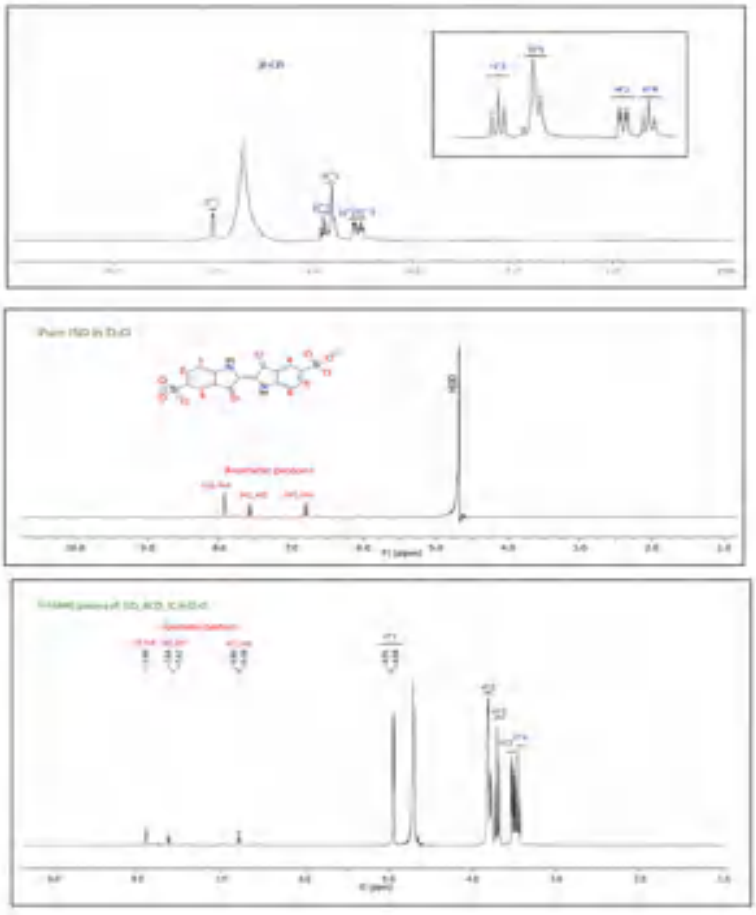

Fig.9: ^{1}H NMR spectra of β-Cyclodextrin, pure Indigosulfonic acid dipotassium salt and β-CD-ISD inclusion complex.

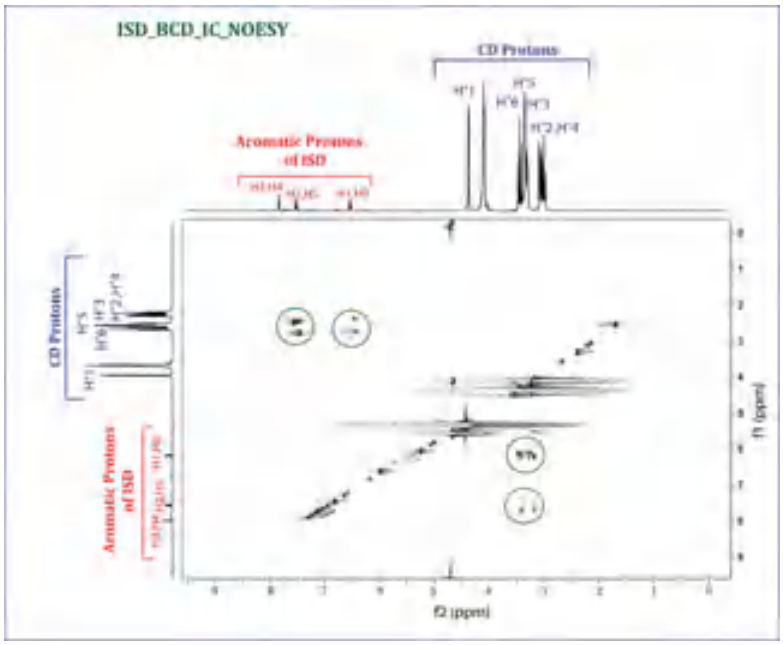

Fig.10:2D NOESY NMR spectra of ISD-β-Cyclodextrin inclusion complex.

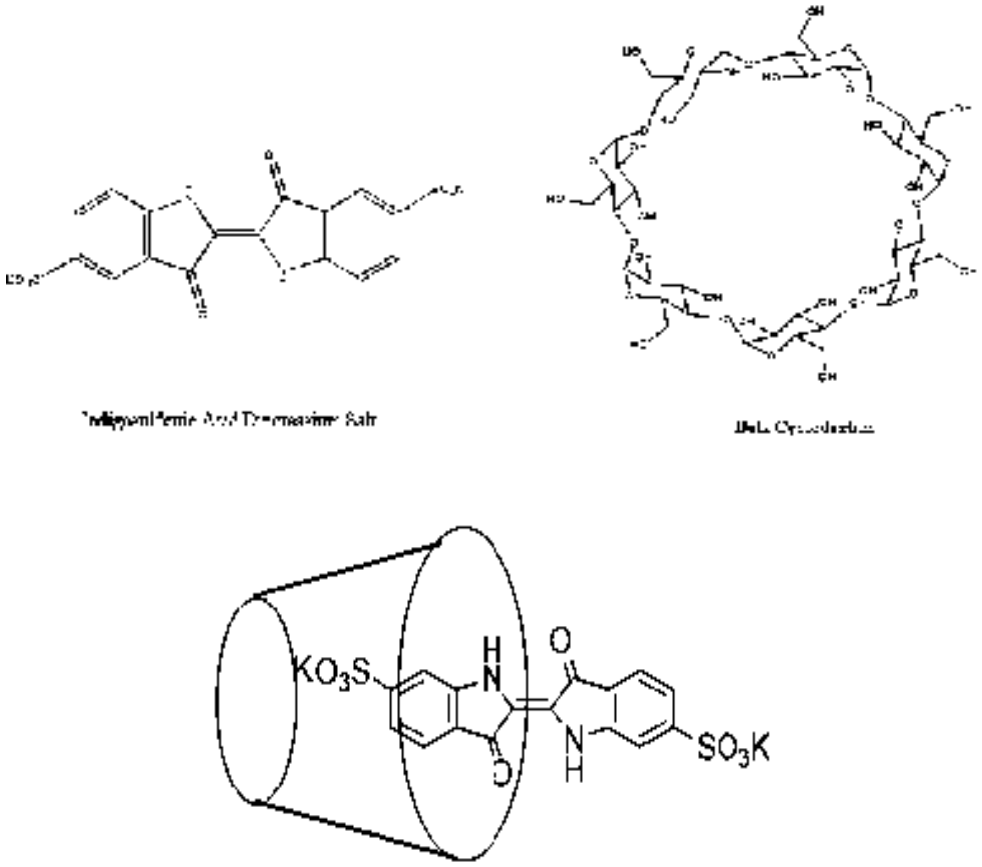

Inclusion Complexation through the wider rim

Fig 11: Structures of Indigosulfonic Acid Dipotassium Salt and β-Cyclodextrin and their schematic representation of inclusion.

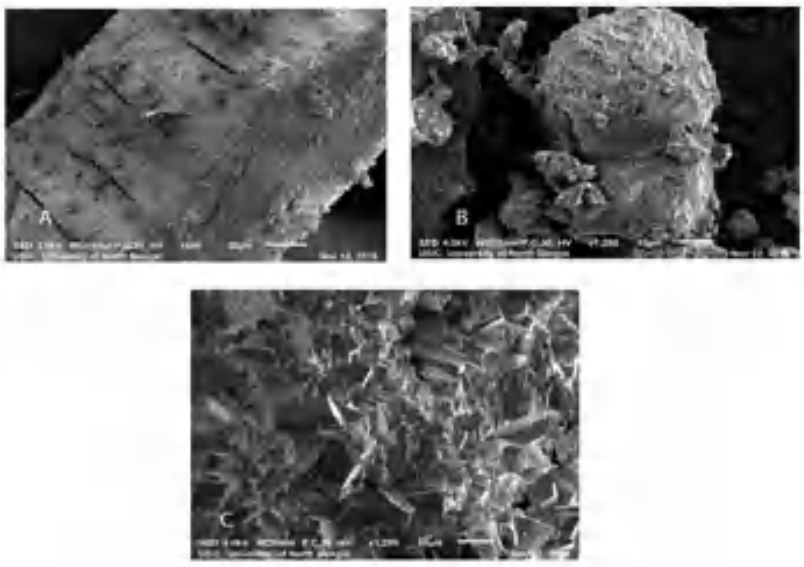

Fig.12: SEM images of (A) pure β-Cyclodextrin, (B) pure Indigosulfonic acid Dipotassium Salt and (C) ISD.β-CD inclusion complex.

CHAPTER IX

CONCLUDING REMARKS

The thesis includes the study of the host-guest inclusion system along with solution behaviour of certain bioactive molecules. The host-guest chemistry itself is a broad of research but here in this thesis we have much focused on the synthesis and characterization of the host-guest system. The guest molecules that have been taken for the host-guest systems are industrially and biologically significant, so as the title.

The above mentioned systems are characterised by different physicochemical and spectroscopic techniques e.g. Uv-visible, FTIR, ^{1}HNMR, 2D NOESY, 2D ROESY, fluorescence spectroscopy, SEM study, Powder X-ray diffraction study, Isothermal titration calorimetric study etc.

Further, ICs are exposed to cell viability study and antimicrobial assay for proper understanding of the properties of the complexed systems.

Apart from host-guest inclusion systems, we have also studied the behaviour of certain bioactive compounds in solution by investigating the physicochemical parameters – density, viscosity, refractive index etc.

The works, inventions that have been done throughout the course of research are customized as chapters herein.

Chapter IV: Two bioactive compounds that have profound importance in biological system, uracil and gallic acid were brought in contact with each other to elucidate their interaction phenomena in solution. The solute-cosolute interactions of uracil in aqueous gallic acid solution were studied with the help of viscosity, density, refractive index measurements at different temperatures. The study showed that the solute-cosolute interactions predominate over solute-solute and solvent-solvent, which suggest the existence of strong interaction between the molecules of uracil and gallic acid.

Chapter V: The incorporation of the antispasmodic AB(Alibendol) within β-CD and their interactions have been studied by Uv-vis, ^{1}HNMR, 2D ROESY and FTIR spectroscopy. The 1:1 complexation was verified by job's plot. The values of thermodynamic parameters

also suggest the same. The generation of cross peaks in the 2D ROESY spectra is a confirmation that the inclusion complex has been formed between the drug and cyclodextrin. This work mainly focused on the establishment of the phenomenon of inclusion so that certain properties of the drug can be changed for betterment of its activity. The sound IC can be treated as a modified version of the drug which may lead to increase of water solubility of the drug and decrease its side effects (toxicity) or also may contribute in control drug delivery in near future with retention of its therapeutic activity.

Chapter VI: Here in this work we studied the formation inclusion complex of Amiloride hydrochloride with α and β cyclodextrins by mass spectrometry, ^{1}H NMR and Uv-visible spectroscopy. The complex so formed was subjected to antimicrobial assay and the complex formed with α-CD comes out to possess greater antimicrobial activity than the drug ,which correlates with the association constants i.e. the binding with β-CD is more compact i.e. the drug is less free in the complex of β-CD.

Chapter VII: In this work, we have synthesized an attainable inclusion complex of an aromatase inhibitory drug DL-AGT and a host β-CD. The process of inclusion was confirmed by ^{1}HNMR, PXRD, FTIR, SEM and the UV-Vis study. From the Job's plot(UV-Visible study) and from the shifting of the H3 and H5 protons of β-CD in the ^{1}HNMR spectra of the IC, it is confirmed that the inclusion occurred in a 1:1 stoichiometric ratio. Moreover, the solubility of the IC in ethanol is greater than the pure drug was also determined. The above experimental observations were further affirmed by molecular docking study, which helps to predict the most stable conformation of the inclusion complex. Lastly the cell viability study between the drug and its IC with β-CD implies that by increasing concentration, the inclusion complex shows less toxicity than the drug itself. So, this is an important finding about the inclusion complex of the drug with β-CD, which may improve the therapeutic activity of the drug towards its application it is meant for and also can change the path of science to a new direction.

Chapter VIII: In this study we have successfully characterised the inclusion of the dye molecule Indigosulfonic Acid Dipotassium Salt inside the naturally occurring oligosaccharide β-CD molecule. The IC was characterised using various thermodynamic as well as spectroscopic methods. The negative value of ΔG of the process, the high

association constant from UV-Vis and ITC study of the inclusion show that the IC formed is more stable compared to the pure ISD. The higher stability may be the main reason for the controlled release of the ISD. The inclusion complex found to have higher solubility in water compared to the free ISD. Thus, it may reduce the toxic effect generated from colouring foods and drugs. Moreover, its controlled release inside the body may reduce the toxicity. As cyclodextrins have very low toxicity, it might be predicted that the inclusion process makes the overall moiety (IC) of very low toxicity. This study may further open scopes for scientific and industrial research in future.

BIBLIOGRAPHY

CHAPTER I

[1] N. Lin, A. Dufresne, Supramolecular hydrogels from in situ host–guest inclusion between chemically modified cellulose nanocrystals and cyclodextrin, Biomacromolecules 14(3) (2013) 871-880.

[2] T. Kida, T. Iwamoto, H. Asahara, T. Hinoue, M. Akashi, Chiral recognition and kinetic resolution of aromatic amines via supramolecular chiral nanocapsules in nonpolar solvents, Journal of the American Chemical Society 135(9) (2013) 3371-3374.

[3] Z.-Q. Shi, Y.-T. Cai, J. Deng, W.-F. Zhao, C.-S. Zhao, Host–guest self-assembly toward reversible thermoresponsive switching for bacteria killing and detachment, ACS applied materials & interfaces 8(36) (2016) 23523-23532.

[4] Y. Zhu, W. Liu, X. Zhang, J. He, J. Chen, Y. Wang, T. Cao, Directing silicon–graphene self-assembly as a core/shell anode for high-performance lithium-ion batteries, Langmuir 29(2) (2013) 744-749.

[5] H. Li, F. Li, B. Zhang, X. Zhou, F. Yu, L. Sun, Visible light-driven water oxidation promoted by host–guest interaction between photosensitizer and catalyst with a high quantum efficiency, Journal of the American Chemical Society 137(13) (2015) 4332-4335.

[6] T. Wimmer, Cyclodextrins, Ullmann's Encyclopedia of Industrial Chemistry (2000).

[7] T. Do Thi, K. Nauwelaerts, M. Froeyen, L. Baudemprez, M. Van Speybroeck, P. Augustijns, P. Annaert, J. Martens, J. Van Humbeeck, G. Van den Mooter, Comparison of the complexation between methylprednisolone and different cyclodextrins in solution by 1H-NMR and molecular modeling studies, Journal of pharmaceutical sciences 99(9) (2010) 3863-3873.

[8] S.R. Gandhi, J.D.S.S. Quintans, G.R. Gandhi, A.A.D.S. Araújo, L.J. Quintans Junior, The use of cyclodextrin inclusion complexes to improve anticancer drug profiles: a systematic review, Expert Opinion on Drug Delivery 17(8) (2020) 1069-1080.

[9] A.D. McNaught, A. Wilkinson, Compendium of chemical terminology, Blackwell Science Oxford1997.

[10] K. Liu, H. Liu, L. Li, W. Li, J. Liu, T. Tang, Adsorption of methyl violet from aqueous solution using β-cyclodextrin immobilised onto mesoporous silica, Supramolecular Chemistry (2021) 1-15.

[11] M. Šuleková, M. Smrčová, A. Hudák, M. Heželová, M. Fedorová, Organic colouring agents in the pharmaceutical industry, Folia Vet 61(3) (2017) 32-46.

[12] A. Dąbrowski, Adsorption—from theory to practice, Advances in colloid and interface science 93(1-3) (2001) 135-224.

[13] A. Reife, H.S. Freeman, Pollution Prevention in the Production of Dyes and Pigments, Textile Chemist & Colorist & American Dyestuff Reporter 32(1) (2000).

[14] M. Irimia-Vladu, E.D. Głowacki, P.A. Troshin, G. Schwabegger, L. Leonat, D.K. Susarova, O. Krystal, M. Ullah, Y. Kanbur, M.A. Bodea, Indigo-A natural pigment for high performance ambipolar organic field effect transistors and circuits, Advanced Materials 24(3) (2012) 375-380.

[15] J. Seixas de Melo, A. Moura, M. Melo, Photophysical and spectroscopic studies of indigo derivatives in their keto and leuco forms, The Journal of Physical Chemistry A 108(34) (2004) 6975-6981.

[16] S. Saha, A. Roy, M.N. Roy, Mechanistic Investigation of Inclusion Complexes of a Sulfa Drug with α-and β-Cyclodextrins, Industrial & Engineering Chemistry Research 56(41) (2017) 11672-11683.

[17] Y. Yang, Q. Hu, Q. Zhang, K. Jiang, W. Lin, Y. Yang, Y. Cui, G. Qian, A large capacity cationic metal–organic framework nanocarrier for physiological pH responsive drug delivery, Molecular Pharmaceutics 13(8) (2016) 2782-2786.

[18] P. Lønning, S. Kvinnsland, Mechanisms of action of aminoglutethimide as endocrine therapy of breast cancer, Drugs 35(6) (1988) 685-710.

[19] R.J. Santen, J.W. Thomas, E. Samojlik, A.E. Boucher, A. Lipton, H. Harvey, Adequacy of estrogen suppression with aminoglutethimide and hydrocortisone as treatment of human breast cancer: correlation of hormonal data with clinical responses, Cancer research 42(8 Supplement) (1982) 3397s-3401s.

[20] W. Miller, Aromatase inhibitors, Endocrine-Related Cancer 3(1) (1996) 65-79.

[21] P. Lønning, The potency and clinical efficacy of aromatase inhibitors across the breast cancer continuum, Annals of Oncology 22(3) (2011) 503-514.

[22] P. Kumar, G. Chhabra, K. Pathak, Development and Statistical Optimization of Buccoadhesive Films of Amiloride Hydrochloride: In-vitro and Ex-vivo Evaluation, Ind. J. Pharm. Edu. Res 46(2) (2012) 145-153.

[23] W.I. Baba, A.F. Lant, A.J. Smith, M.M. Townshend, G.M. Wilson, Pharmacological effects in animals and normal human subjects of the diuretic amiloride hydrochloride (MK-870, Clinical Pharmacology & Therapeutics 9(3) (1968) 318-327.

[24] D.J. Mazzo, Amiloride hydrochloride, Analytical profiles of drug substances, Elsevier1986, pp. 1-34.

[25] E.-J. Kim, J.-Y. Kim, H.-J. Rhee, A Synthesis of Alibendol, 2-Hydroxy-N-(2-hydroxyethyl)-3-methoxy-5-(2-propenyl) benzamide via m-CPBA Oxidation of o-Vanillin, Bulletin of the Korean Chemical Society 25(11) (2004) 1720-1722.

[26] J.K. Ryu, A sensitive, acetonitrile-free, HPLC method for determination of alibendol in dog plasma and its application to pharmacokinetic studies, Journal of Pharmaceutical Investigation 42(4) (2012) 185-190.

[27] A. Pałasz, D. Cież, In search of uracil derivatives as bioactive agents. Uracils and fused uracils: Synthesis, biological activity and applications, European journal of medicinal chemistry 97 (2015) 582-611.

[28] D. Kalita, R. Kar, J.G. Handique, A theoretical study on the antioxidant property of gallic acid and its derivatives, Journal of Theoretical and Computational Chemistry 11(02) (2012) 391-402.

[29] B. Badhani, N. Sharma, R. Kakkar, Gallic acid: a versatile antioxidant with promising therapeutic and industrial applications, Rsc Advances 5(35) (2015) 27540-27557.

[30] N. Kahkeshani, F. Farzaei, M. Fotouhi, S.S. Alavi, R. Bahramsoltani, R. Naseri, S. Momtaz, Z. Abbasabadi, R. Rahimi, M.H. Farzaei, Pharmacological effects of gallic acid in health and diseases: A mechanistic review, Iranian Journal of Basic Medical Sciences 22(3) (2019) 225.

CHAPTER II

[1] J.W. Steed, J.L. Atwood, Supramolecular chemistry, John Wiley & Sons2022.

[2] H. Lodish, A. Berk, C.A. Kaiser, C. Kaiser, M. Krieger, M.P. Scott, A. Bretscher, H. Ploegh, P. Matsudaira, Molecular cell biology, Macmillan2008.

[3] Y. Liu, G.-S. Chen, Y. Chen, J. Lin, Inclusion complexes of azadirachtin with native and methylated cyclodextrins: solubilization and binding ability, Bioorganic & medicinal chemistry 13(12) (2005) 4037-4042.

[4] U. Singh, K. Aithal, N. Udupa, Physicochemical and Biological Studies of Inclusion Complex of Methotrexate with β-Cyclodextrin, Pharmacy and Pharmacology Communications 3(12) (1997) 573-577.

[5] F. Du, T. Pan, X. Ji, J. Hu, T. Ren, Study on the preparation of geranyl acetone and β-cyclodextrin inclusion complex and its application in cigarette flavoring, Scientific reports 10(1) (2020) 1-10.

[6] Y.V. Lisnyak, A.V. Martynov, V.N. Baumer, O.V. Shishkin, A.V. Gubskaya, Crystal and molecular structure of β-cyclodextrin inclusion complex with succinic acid, Journal of inclusion phenomena and macrocyclic chemistry 58(3) (2007) 367-375.

[7] E. Arunan, G.R. Desiraju, R.A. Klein, J. Sadlej, S. Scheiner, I. Alkorta, D.C. Clary, R.H. Crabtree, J.J. Dannenberg, P. Hobza, Definition of the hydrogen bond (IUPAC Recommendations 2011), Pure and applied chemistry 83(8) (2011) 1637-1641.

[8] A.D. McNaught, A. Wilkinson, Compendium of chemical terminology, Blackwell Science Oxford1997.

[9] J.R. Sabin, Hydrogen bonds involving sulfur. I. Hydrogen sulfide dimer, Journal of the American Chemical Society 93(15) (1971) 3613-3620.

[10] R.E. Schirmer, J.H. Noggle, The nuclear Overhauser effect; chemical applications by Joseph N. Noggle and Roger E. Schirmer, Academic Press1971.

[11] D. Neuhaus, Nuclear overhauser effect, eMagRes (2007).

[12] C. Klofutar, J. Horvat, D. Rudan-Tasič, Apparent Molar Volume and Apparent Molar Expansibility of Sodium Saccharin, Potassium Acesulfame and Aspartame, Acta chimica slovenica 53(3) (2006).

[13] R.S. Patil, V.R. Shaikh, P.D. Patil, A.U. Borse, K.J. Patil, The viscosity B and D coefficient (Jones–Dole equation) studies in aqueous solutions of alkyltrimethylammonium bromides at 298.15 K, Journal of Molecular Liquids 200 (2014) 416-424.

[14] C.-Y. Tan, Y.-X. Huang, Dependence of refractive index on concentration and temperature in electrolyte solution, polar solution, nonpolar solution, and protein solution, Journal of Chemical & Engineering Data 60(10) (2015) 2827-2833.

CHAPTER III

[1] S. Kim, J. Chen, T. Cheng, A. Gindulyte, J. He, S. He, Q. Li, B.A. Shoemaker, P.A. Thiessen, B. Yu, PubChem in 2021: new data content and improved web interfaces, Nucleic acids research 49(D1) (2021) D1388-D1395.

[2] S. Thapa, A Comprehensive Review on COVID-19 Pandemic: Causes, Effects, and Concerns From Environmental Perspective, J Environ Sci 17(6) (2021) 196.

[3] G.V. Zuccotti, V. Fabiano, Safety issues with ethanol as an excipient in drugs intended for pediatric use, Expert opinion on drug safety 10(4) (2011) 499-502.

[4] T.T. Tidwell, Oxidation of alcohols by activated dimethyl sulfoxide and related reactions: an update, Synthesis 1990(10) (1990) 857-870.

[5] F. Maran, D. Celadon, M.G. Severin, E. Vianello, Electrochemical determination of the pKa of weak acids in N, N-dimethylformamide, Journal of the American Chemical Society 113(24) (1991) 9320-9329.

[6] T.T. Cushnie, B. Cushnie, J. Echeverría, W. Fowsantear, S. Thammawat, J.L. Dodgson, S. Law, S.M. Clow, Bioprospecting for antibacterial drugs: A multidisciplinary perspective on natural product source material, bioassay selection and avoidable pitfalls, Pharmaceutical Research 37(7) (2020) 1-24.

[7] P.E. Ilouga, D. Winkler, C. Kirchhoff, B. Schierholz, J. Wölcke, Investigation of 3 industry-wide applied storage conditions for compound libraries, Journal of biomolecular screening 12(1) (2007) 21-32.

[8] K.V. Balakin, N.P. Savchuk, I.V. Tetko, In silico approaches to prediction of aqueous and DMSO solubility of drug-like compounds: trends, problems and solutions, Current medicinal chemistry 13(2) (2006) 223-241.

[9] W.-J. Cai, J.-H. Huang, S.-Q. Zhang, B. Wu, P. Kapahi, X.-M. Zhang, Z.-Y. Shen, Icariin and its derivative icariside II extend healthspan via insulin/IGF-1 pathway in C. elegans, PloS one 6(12) (2011) e28835.

[10] H. Khajehsharifi, Z. Eskandari, N. Sareban, Using partial least squares and principal component regression in simultaneous spectrophotometric analysis of pyrimidine bases, Arabian Journal of Chemistry 10 (2017) S141-S147.

[11] R. Zhou, S. Li, T. Liu, Measurement and correlation of solubility of uracil in supercritical Carbon Dioxide, Journal of Chemical & Engineering Data 53(11) (2008) 2679-2682.

[12] A. Daneshfar, H.S. Ghaziaskar, N. Homayoun, Solubility of gallic acid in methanol, ethanol, water, and ethyl acetate, Journal of Chemical & Engineering Data 53(3) (2008) 776-778.

[13] W.I. Baba, A.F. Lant, A.J. Smith, M.M. Townshend, G.M. Wilson, Pharmacological effects in animals and normal human subjects of the diuretic amiloride hydrochloride (MK-870, Clinical Pharmacology & Therapeutics 9(3) (1968) 318-327.

[14] D.J. Mazzo, Amiloride hydrochloride, Analytical profiles of drug substances, Elsevier1986, pp. 1-34.

[15] L. Curtis, The Gale Encyclopedia of Surgery and Medical Tests, Reference Reviews (2010).

[16] R. Littrell, L. Hayes, V. Stillner, Carisoprodol (Soma): a new and cautious perspective on an old agent, Southern medical journal 86(7) (1993) 753-756.

[17] T. Do Thi, K. Nauwelaerts, M. Froeyen, L. Baudemprez, M. Van Speybroeck, P. Augustijns, P. Annaert, J. Martens, J. Van Humbeeck, G. Van den Mooter, Comparison of the complexation between methylprednisolone and different cyclodextrins in solution by 1H-NMR and molecular modeling studies, Journal of pharmaceutical sciences 99(9) (2010) 3863-3873.

CHAPTER IV

[1] R.N. Saladi, A.N. Persaud, The causes of skin cancer: a comprehensive review, Drugs Today (Barc.) 41 (2005) 37–53.

[2] A. Gescher, U. Pastorino, S.M. Plummer, M.M. Manson, Suppression of tumour development by substances derived from the diet – mechanisms and clinical implications, Br. J. Clin. Pharmacol. 45 (1998) 1–12.

[3] M.M. Manson, Cancer prevention – the potential for diet to modulate molecular signalling, Trends Mol. Med. 9 (2003) 11–18.

[4] T.C. Reddy, P. Aparoy, N.K. Babu, K.A. Kumar, S.K. Kalangi, P. Reddanna, Kinetics and docking studies of a COX-2 inhibitorisolated from Terminalia bellerica fruits, Protein Pept. Lett. 17 (2010) 1251–1257.

[5] T. Chandramohan Reddy, D. Bharat Reddy, A. Aparna, K.M. Arunasree, G. Gupta, C. Achari, G.V. Reddy, V. Lakshmipathi, A. Subramanyam, P. Reddanna, Anti-leukemic effects of gallic acid on human leukemia K562 cells: downregulation of COX-2, inhibition of BCR/ABL kinase and NF-kappaB inactivation, Toxicol. In Vitro 26 (2012) 396–405.

[6] D. Davidson and O. Baudisch, The preparation of uracil from urea, J. Am. Chem. Soc. 48(1926)2379-2383.

[7] P. Molnar, L. Marton, R. Izrael, H. L. Palinkas and B.G. Vertessy, Uracil moieties in Plasmodium falciparumgenomic DNA, FEBS Open Bio 8 (2018) 1763–1772.

[8] K. Séron, Marie-Odile Blondel, R. Haguenauer-Tsapis, and C. Volland*, Uracil-induced Down-regulation of the yeast uracil permease,J Bacteriol. 181(1999)1793–1800.

[9] D. P. Shoemaker and C. W. Garland, Experiments in Physical Chemistry, McGraw-Hill Publishers, New York, 1967, p 131-138.

[10] A. Bhattacharjee and M. N. Roy, Ion association and solvation behaviour of tetraalkyl ammonium iodides in binary mixture of dichloromethane + N, N-dimethyl formamide probed by conductometric study, Phys. Chem. Chem. Phys. 12 (2010) 1-9.

[11] D. Ekka and M. N. Roy, Quantitative and qualitative analysis of ionic salvation of individual ions of imidazolium based ionic liquids in significant solution systems by conductance and FT-IR spectroscopy, RSC Advances 4 (2014) 19831-19845.

[12] M. N. Roy, S. Saha, S. Barman, D. Ekka, Host–guest inclusion complexes of RNA nucleosides inside aqueous cyclodextrins explored by physicochemical and spectroscopic methods, RSC Adv., 2016,6, 8881–8891

[13] D. O. Masson, Ion-solvent interactions, Phil. Mag., 8 (1929) 218-235.

[14] F. J. Millero, The Partial Molal Volumes of Electrolytes in Aqueous Solution. In: Horne RA (ed) Water and Aqueous Solutions: Structure, Thermodynamics and Transport Process. Wiley Interscience, New York, 1972, 519-595.

[15] L. G. Hepler, Studies on viscosities and densities of R4NX in ME + water mixtures of different temperatures, Can. J. Chem. 47 (1969) 4613-4617.

[16] M. N. Roy, V. K. Dakua and B. Sinha, Partial molar volumes, viscosity B-coefficients and adiabatic compressibilities of sodium molybdate in aqueous 1,3-dioxalane mixture from 303.15 to 323.15 K, Int. J. Thermophys. 28 (2007) 1275-1284.

[17] G. Jones and D. Dole, The viscosity of aqueous solutions of strong electrolytes with special reference to barium chloride, J. Am. Chem. Soc. 51 (1929) 2950-2964.

[18] J. D. Pandey, K. Mishra, A. Shukla, V. Mishran and R. D. Rai, Apparent molal volume, apparent molal compressibility, verification of jones-dole equation and thermodynamic studies of aqueous urea and its derivative Thermochimica Acta, 117 (1987) 245-259.

[19] F. J. Millero,The molal volumes of electrolytes, Chem. Rev. 71 (1971) 147-176.

[20] V. Minkin, O. Osipov and Y. Zhdanov, Dipole Moments In Organic Chemistry, Plenum Press, New York, 1970.

[21] M. Born and E. Wolf, Principles of Optics: Electromagnetic Theory of Propagation, Interference and Diffraction of Light, Cambridge University Press, London, 7th Ed., 1999.

[22] M. Deetlefs, K. Seddon and M. Shara, Predicting physical properties of ionic liquid, Phys. Chem. Chem. Phys. 8 (2006) 642-649.

[23] S. Kamathama, N. Kumar, Padmaja Gudipalli, Isolation and characterization of gallic acid and methyl gallate from the seed coats of Givotia rottleriformis Griff. and their anti-proliferative effect on human epidermoid carcinoma A431 cells,Toxicology Reports 2 (2015) 520–529.

CHAPTER V

[1] J. Mahbuba, R.T. Al-Nafakh, The effect of Atracurium on the pulse rate during rapid tracheal intubation, Al-Qadisiyah Medical Journal 5(8) (2009) 121-127.

[2] W. Bowman, Neuromuscular block, British journal of pharmacology 147(S1) (2006) S277-S286.

[3] S.K. Hadley, S.M. Gaarder, Treatment of irritable bowel syndrome, American family physician 72(12) (2005) 2501-2506.

[4] E.-J. Kim, J.-Y. Kim, H.-J. Rhee, A Synthesis of Alibendol, 2-Hydroxy-N-(2-hydroxyethyl)-3-methoxy-5-(2-propenyl) benzamide via m-CPBA Oxidation of o-Vanillin, Bulletin of the Korean Chemical Society 25(11) (2004) 1720-1722.

[5] S.R. Gandhi, J.D.S.S. Quintans, G.R. Gandhi, A.A.D.S. Araújo, L.J. Quintans Junior, The use of cyclodextrin inclusion complexes to improve anticancer drug profiles: a systematic review, Expert Opinion on Drug Delivery 17(8) (2020) 1069-1080.

[6] K. Kim, Mechanically interlocked molecules incorporating cucurbituril and their supramolecular assemblies, Chemical Society Reviews 31(2) (2002) 96-107.

[7] K. Moon, A.E. Kaifer, Modes of binding interaction between viologen guests and the cucurbit [7] uril host, Organic letters 6(2) (2004) 185-188.

[8] V.V. Gobre, R.V. Pinjari, S.P. Gejji, Density functional investigations on the charge distribution, vibrational spectra, and NMR chemical shifts in cucurbit [n] uril (n= 5− 12) Hosts, The Journal of Physical Chemistry A 114(12) (2010) 4464-4470.

[9] S. Saha, T. Ray, S. Basak, M.N. Roy, NMR, surface tension and conductivity studies to determine the inclusion mechanism: thermodynamics of host–guest inclusion complexes of natural amino acids in aqueous cyclodextrins, New Journal of Chemistry 40(1) (2016) 651-661.

[10] X.-M. Li, F. Fan, J.-S. Lu, S.-F. Xue, Y.-Q. Zhang, Q.-J. Zhu, Z. Tao, G.A. Lawrance, G. Wei, Host–guest complexes of cucurbit [8] uril with some pentaerythritol derivative guests, New Journal of Chemistry 35(5) (2011) 1088-1095.

[11] Q. Zhou, H. Wang, T. Gao, Y. Yu, B. Ling, L. Mao, H. Zhang, X. Meng, X. Zhou, Supramolecular vesicle: triggered by formation of pseudorotaxane between cucurbit [6] uril and surfactant, Chemical Communications 47(40) (2011) 11315-11317.

[12] Y. Jang, R. Natarajan, Y.H. Ko, K. Kim, Cucurbit [7] uril: a high-affinity host for encapsulation of amino saccharides and supramolecular stabilization of their α-anomers in water, Angewandte Chemie International Edition 53(4) (2014) 1003-1007.

[13] B. Rajbanshi, A. Dutta, B. Mahato, D. Roy, D.K. Maiti, S. Bhattacharyya, M.N. Roy, Study to explore host guest inclusion complexes of vitamin B1 with CD molecules for enhancing stability and innovative application in biological system, Journal of Molecular Liquids 298 (2020) 111952.

[14] W.L. Mock, N.Y. Shih, Structure and selectivity in host-guest complexes of cucurbituril, The Journal of organic chemistry 51(23) (1986) 4440-4446.

[15] S. Li, H. Yin, G. Martinz, I.W. Wyman, D. Bardelang, D.H. Macartney, R. Wang, Supramolecular encapsulation of benzocaine and its metabolite para-aminobenzoic acid by cucurbit [7] uril, New Journal of Chemistry 40(4) (2016) 3484-3490.

[16] R. Ghosh, N. Roy, S. Saha, S. Das, B.K. Barman, D. Roy, V.K. Dakua, M.N.J.C.P.L. Roy, Synthesis and characterization of an industrially significant ionic liquid and its inclusion complex with β-cyclodextrin and its soluble derivative for their advanced applications, 769 (2021) 138401.

[17] F.-D. Zhu, Z.-H. Zhang, S.-M. Chi, S.-L. Chen, Y.-F. Wang, H.-Y. Zhu, Z. Lei, Y. Zhao, Experimental and molecular docking investigation of the inclusion complexes between 20(S)-protopanaxatriol and four modified β-cyclodextrins, Carbohydrate Research 500 (2021) 108256.

[18] N. Roy, B. Ghosh, D. Roy, B. Bhaumik, M.N. Roy, Exploring the Inclusion Complex of a Drug (Umbelliferone) with α-Cyclodextrin Optimized by Molecular Docking and Increasing Bioavailability with Minimizing the Doses in Human Body, ACS Omega 5(46) (2020) 30243-30251.

[19] I. Correia, N. Bezzenine, N. Ronzani, N. Platzer, J.C. Beloeil, B.T.J.J.o.P.O.C. Doan, Study of inclusion complexes of acridine with β-and (2, 6-di-O-methyl)-β-cyclodextrin by use of solubility diagrams and NMR spectroscopy, 15(9) (2002) 647-659.

[20] S. Saha, A. Roy, M.N.J.I. Roy, E.C. Research, Mechanistic Investigation of Inclusion Complexes of a Sulfa Drug with α-and β-Cyclodextrins, 56(41) (2017) 11672-11683.

[21] B. Yang, J. Lin, Y. Chen, Y.J.B. Liu, m. chemistry, Artemether/hydroxypropyl-β-cyclodextrin host–guest system: characterization, phase-solubility and inclusion mode, 17(17) (2009) 6311-6317.

[22] A.C. Servais, A. Rousseau, M. Fillet, K. Lomsadze, A. Salgado, J. Crommen, B.J.J.o.s.s. Chankvetadze, Capillary electrophoretic and nuclear magnetic resonance studies on the opposite affinity pattern of propranolol enantiomers towards various cyclodextrins, 33(11) (2010) 1617-1624.

[23] J.S. Negi, S. Singh, Spectroscopic investigation on the inclusion complex formation between amisulpride and γ-cyclodextrin, Carbohydrate Polymers 92(2) (2013) 1835-1843.

[24] B.K. Barman, S. Barman, M.N. Roy, Inclusion complexation between tetrabutylphosphonium methanesulfonate as guest and α- and β-cyclodextrin as hosts investigated by physicochemical methodology, Journal of Molecular Liquids 264 (2018) 80-87.

[25] H. Shekaari, F. Jebali, Volumetric and conductometric studies of some amino acids in aqueous ionic liquid, 1-hexyl-3-methylimidazolium chloride solutions at 298.15 K, Physics and Chemistry of Liquids 49(5) (2011) 572-587.

[26] S. Barman, B.K. Barman, M.N. Roy, Preparation, characterization and binding behaviors of host-guest inclusion complexes of metoclopramide hydrochloride with α- and β-cyclodextrin molecules, Journal of Molecular Structure 1155 (2018) 503-512.

CHAPTER VI

[1] H.A. Arida, I.A. Maghrabi, S.I. Zayed, Development of New Thin-Film Micro-sensor for Potentiometric Determination of Amiloride, Int. J. Electrochem. Sci 9 (2014) 2728-2736.

[2] D.J. Mazzo, Amiloride hydrochloride, Analytical profiles of drug substances, Elsevier1986, pp. 1-34.

[3] B. Gidwani, A. Vyas, A comprehensive review on cyclodextrin-based carriers for delivery of chemotherapeutic cytotoxic anticancer drugs, BioMed research international 2015 (2015).

[4] M.J. Frisch, G.W. Trucks, H.B. Schlegel, G.E. Scuseria, M.A. Robb, J.R. Cheeseman, G. Scalmani, V. Barone, G.A. Petersson, H. Nakatsuji, X. Li, M. Caricato, A.V. Marenich, J. Bloino, B.G. Janesko, R. Gomperts, B. Mennucci, H.P. Hratchian, J.V. Ortiz, A.F. Izmaylov, J.L. Sonnenberg, Williams, F. Ding, F. Lipparini, F. Egidi, J. Goings, B. Peng, A. Petrone, T. Henderson, D. Ranasinghe, V.G. Zakrzewski, J. Gao, N. Rega, G. Zheng, W. Liang, M. Hada, M. Ehara, K. Toyota, R. Fukuda, J. Hasegawa, M. Ishida, T. Nakajima, Y. Honda, O. Kitao, H. Nakai, T. Vreven, K. Throssell, J.A. Montgomery Jr., J.E. Peralta, F. Ogliaro, M.J. Bearpark, J.J. Heyd, E.N. Brothers, K.N. Kudin, V.N. Staroverov, T.A. Keith, R. Kobayashi, J. Normand, K. Raghavachari, A.P. Rendell, J.C. Burant, S.S. Iyengar, J. Tomasi, M. Cossi, J.M. Millam, M. Klene, C. Adamo, R. Cammi, J.W. Ochterski, R.L. Martin, K. Morokuma, O. Farkas, J.B. Foresman, D.J. Fox, Gaussian 16 Rev. C.01, Wallingford, CT, 2016.

[5] T. Ghosh, S. Mondal, R. Maiti, S.M. Nawaz, N.N. Ghosh, E. Dinda, A. Biswas, S.K. Maity, A. Mallik, D.K. Maiti, Complementary amide-based donor–acceptor with unique nano-scale aggregation, fluorescence, and band gap-lowering properties: a WORM memory device, Nanotechnology 32(2) (2020) 025208.

[6] M. Cossi, V. Barone, R. Cammi, J. Tomasi, Ab initio study of solvated molecules: a new implementation of the polarizable continuum model, Chemical Physics Letters 255(4) (1996) 327-335.

[7] T. Lu, F. Chen, Multiwfn: A multifunctional wavefunction analyzer, Journal of Computational Chemistry 33(5) (2012) 580-592.

[8] P. Job, Formation and stability of inorganic complexes in solution, 1928.

[9] J.S. Renny, L.L. Tomasevich, E.H. Tallmadge, D.B. Collum, Method of continuous variations: applications of job plots to the study of molecular associations in organometallic chemistry, Angew Chem Int Ed Engl 52(46) (2013) 11998-2013.

[10] J.V. Caso, L. Russo, M. Palmieri, G. Malgieri, S. Galdiero, A. Falanga, C. Isernia, R. Iacovino, Investigating the inclusion properties of aromatic amino acids complexing beta-cyclodextrins in model peptides, Amino Acids 47(10) (2015) 2215-27.

[11] J.Q. Zhang, K.M. Jiang, K. An, S.H. Ren, X.G. Xie, Y. Jin, J. Lin, Novel water-soluble fisetin/cyclodextrins inclusion complexes: Preparation, characterization, molecular docking and bioavailability, Carbohydr Res 418 (2015) 20-28.

[12] Y. Okada, K. Ueyama, J.-i. Nishikawa, M. Semma, A. Ichikawa, Effect of 6-O-α-maltosyl-β cyclodextrin and its cholesterol inclusion complex on cellular cholesterol levels and ABCA1 and ABCG1 expression in mouse mastocytoma P-815 cells, 2012.

[13] A. Fernandes, G. Ivanova, N.F. Brás, N. Mateus, M.J. Ramos, M. Rangel, V. de Freitas, Structural characterization of inclusion complexes between cyanidin-3-O-glucoside and β-cyclodextrin, Carbohydrate Polymers 102 (2014) 269-277.

[14] V. Sindelar, F.M. Cejas Ma Fau - Raymo, W. Raymo Fm Fau - Chen, S.E. Chen W Fau - Parker, A.E. Parker Se Fau - Kaifer, A.E. Kaifer, Supramolecular assembly of 2,7-dimethyldiazapyrenium and cucurbit[8]uril: a new fluorescent host for detection of catechol and dopamine, (0947-6539 (Print)).

[15] L.J. Yang, S.X. Ma, S.Y. Zhou, W. Chen, M.W. Yuan, Y.Q. Yin, X.D. Yang, Preparation and characterization of inclusion complexes of naringenin with beta-cyclodextrin or its derivative, Carbohydr Polym 98(1) (2013) 861-9.

[16] W.-W. Fan, Z.-F. Li, J.-B. Li, Y.-P. Yang, Y. Yuan, H.-Q. Tang, L.-X. Gao, Q.-H. Jin, Z.-W. Zhang, C.-L. Zhang, Synthesis, structure, terahertz spectroscopy and luminescent properties of copper (I) complexes with bis(diphenylphosphino)methane and N-donor ligands, Journal of Molecular Structure 1099 (2015) 351-358.

[17] B. Rajbanshi, S. Saha, K. Das, B.K. Barman, S. Sengupta, A. Bhattacharjee, M.N. Roy, Study to Probe Subsistence of Host-Guest Inclusion Complexes of α and β-Cyclodextrins with Biologically Potent Drugs for Safety Regulatory Dischargement, Scientific Reports 8(1) (2018) 13031.

[18] H.A. Benesi, J.H. Hildebrand, A Spectrophotometric Investigation of the Interaction of Iodine with Aromatic Hydrocarbons, Journal of the American Chemical Society 71(8) (1949) 2703-2707.

[19] F. Cramer, W. Saenger, H.C. Spatz, Inclusion Compounds. XIX.1a The Formation of Inclusion Compounds of α-Cyclodextrin in Aqueous Solutions. Thermodynamics and Kinetics, Journal of the American Chemical Society 89(1) (1967) 14-20.

[20] B. Rajbanshi, A. Dutta, B. Mahato, D. Roy, D.K. Maiti, S. Bhattacharyya, M.N. Roy, Study to explore host guest inclusion complexes of vitamin B1 with CD molecules for enhancing stability and innovative application in biological system, Journal of Molecular Liquids 298 (2020) 111952.

[21] K. Kano, R. Nishiyabu, T. Asada, Y. Kuroda, Static and Dynamic Behavior of 2:1 Inclusion Complexes of Cyclodextrins and Charged Porphyrins in Aqueous Organic Media, Journal of the American Chemical Society 124(33) (2002) 9937-9944.

[22] S. Giunta, C. Pieri, G. Groppa, Amiloride, a diuretic with in vitro antimicrobial activity, Pharmacological research communications 16(8) (1984) 821-9.

[23] S.C. Mitini-Nkhoma, N. Fernando, G.K.D. Ishaka, S.M. Handunnetti, S.L. Pathirana, Ion Transport Modulators as Antimycobacterial Agents, Tuberculosis Research and Treatment 2020 (2020) 3767915.

[24] Y. Inoue, R. Suzuki, I. Murata, H. Nomura, Y. Isshiki, I. Kanamoto, Evaluation of Antibacterial Activity Expression of the Hinokitiol/Cyclodextrin Complex Against Bacteria, ACS Omega 5(42) (2020) 27180-27187.

[25] L. Romeo, V. Lanza Cariccio, R. Iori, P. Rollin, P. Bramanti, E. Mazzon, The α-Cyclodextrin/Moringin Complex: A New Promising Antimicrobial Agent against Staphylococcus aureus, Molecules 23(9) (2018).

[26] N.J. Sadgrove, B.W. Greatrex, G.L. Jones, #±-Cyclodextrin encapsulation enhances antimicrobial activity of cineole-rich essential oils from Australian species of Prostanthera (Lamiaceae), 2015.

[27] J.-Y. Chun, Y.-J. Jo, P. Bjrapha, M.-J. Choi, S.-G. Min, Antimicrobial Effect of α- or β-Cyclodextrin Complexes with Trans-Cinnamaldehyde Against Staphylococcus aureus and Escherichia coli, Drying Technology 33(3) (2015) 377-383.

[28] S.M. Roopan, Rohit, G. Madhumitha, A.A. Rahuman, C. Kamaraj, A. Bharathi, T.V. Surendra, Low-cost and eco-friendly phyto-synthesis of silver nanoparticles using Cocos nucifera coir extract and its larvicidal activity, Industrial Crops and Products 43 (2013) 631-635.

[29] N.S. Flores-López, M. Cortez-Valadez, G.M. Moreno-Ibarra, E. Larios-Rodríguez, E.I. Torres-Flores, Y. Delgado-Beleño, C.E. Martinez-Nuñez, L.P. Ramírez-Rodríguez, H. Arizpe-Chávez, J. Castro-Rosas, R. Ramirez-Bon, M. Flores-Acosta, Silver nanoparticles and silver ions stabilized in NaCl nanocrystals, Physica E: Low-dimensional Systems and Nanostructures 84 (2016) 482-488.

CHAPTER VII

[1] R.-A. Mitran, S. Nastase, C. Matei, D. Berger, Tailoring the dissolution rate enhancement of aminoglutethimide by functionalization of MCM-41 silica: a hydrogen bonding propensity approach, RSC advances 5(4) (2015) 2592-2601.

[2] W. Miller, Aromatase inhibitors, Endocrine-Related Cancer 3(1) (1996) 65-79.

[3] P. Lønning, The potency and clinical efficacy of aromatase inhibitors across the breast cancer continuum, Annals of Oncology 22(3) (2011) 503-514.

[4] I.E. Smith, A.L. Harris, M. Morgan, J.-C. Gazet, J.A. McKinna, Tamoxifen versus aminoglutethimide versus combined tamoxifen and aminoglutethimide in the treatment of advanced breast carcinoma, Cancer research 42(8 Supplement) (1982) 3430s-3432s.

[5] Y. Yang, J. Gao, X. Ma, G. Huang, Inclusion complex of tamibarotene with hydroxypropyl-β-cyclodextrin: Preparation, characterization, in-vitro and in-vivo evaluation, asian journal of pharmaceutical sciences 12(2) (2017) 187-192.

[6] L. Tom, C.R. Nirmal, A. Dusthackeer, B. Magizhaveni, M. Kurup, Formulation and evaluation of β-cyclodextrin-mediated inclusion complexes of isoniazid scaffolds: molecular docking and in vitro assessment of antitubercular properties, New Journal of Chemistry 44(11) (2020) 4467-4477.

[7] S.R. Gandhi, J.D.S.S. Quintans, G.R. Gandhi, A.A.D.S. Araújo, L.J. Quintans Junior, The use of cyclodextrin inclusion complexes to improve anticancer drug profiles: a systematic review, Expert Opinion on Drug Delivery 17(8) (2020) 1069-1080.

[8] F. Giordano, C. Novak, J.R. Moyano, Thermal analysis of cyclodextrins and their inclusion compounds, Thermochimica Acta 380(2) (2001) 123-151.

[9] S. Haiahem, L. Nouar, I. Djilani, A. Bouhadiba, F. Madi, D.E. Khatmi, Host-guest inclusion complex between β-cyclodextrin and paeonol: A theoretical approach, Comptes Rendus Chimie 16(4) (2013) 372-379.

[10] U. Singh, K. Aithal, N. Udupa, Physicochemical and Biological Studies of Inclusion Complex of Methotrexate with β-Cyclodextrin, Pharmacy and Pharmacology Communications 3(12) (1997) 573-577.

[11] Y. Liu, G.-S. Chen, Y. Chen, J. Lin, Inclusion complexes of azadirachtin with native and methylated cyclodextrins: solubilization and binding ability, Bioorganic & medicinal chemistry 13(12) (2005) 4037-4042.

[12] F. D'Aria, C. Serri, M. Niccoli, L. Mayol, V. Quagliariello, R.V. Iaffaioli, M. Biondi, C. Giancola, Host–guest inclusion complex of quercetin and hydroxypropyl-β-cyclodextrin, Journal of Thermal Analysis and Calorimetry 130(1) (2017) 451-456.

[13] M. Butnariu, M. Peana, I. Sarac, S. Chirumbolo, H. Tzoupis, C.T. Chasapis, G. Bjørklund, Analytical and in silico study of the inclusion complexes between tropane alkaloids atropine and scopolamine with cyclodextrins, Chemical Papers (2021) 1-11.

[14] P. Bomzan, N. Roy, A. Sharma, V. Rai, S. Ghosh, A. Kumar, M.N. Roy, Molecular encapsulation study of indole-3-methanol in cyclodextrins: Effect on antimicrobial activity and cytotoxicity, Journal of Molecular Structure 1225 (2021) 129093.

[15] M. Paczkowska, M. Mizera, D. Szymanowska-Powałowska, K. Lewandowska, W. Błaszczak, J. Gościańska, R. Pietrzak, J. Cielecka-Piontek, β-Cyclodextrin complexation as an effective drug delivery system for meropenem, European Journal of Pharmaceutics and Biopharmaceutics 99 (2016) 24-34.

[16] K.M. Al Azzam, E. Muhammad, Host-guest inclusion complexes between mitiglinide and the naturally occurring cyclodextrins α, β, and γ: a theoretical approach, Advanced pharmaceutical bulletin 5(2) (2015) 289.

[17] M. Nowakowski, M. Dlugosz, J. Taraszewska, J. Wojcik, Complexation of aminoglutethimide with native and modified cyclodextrins, Journal of Physical Organic Chemistry 22(10) (2009) 948-953.

[18] S. Dallakyan, A.J. Olson, Small-molecule library screening by docking with PyRx, Chemical biology, Springer2015, pp. 243-250.

[19] F. Denizot, R. Lang, Rapid colorimetric assay for cell growth and survival: modifications to the tetrazolium dye procedure giving improved sensitivity and reliability, Journal of immunological methods 89(2) (1986) 271-277.

[20] S. Saha, A. Roy, M.N. Roy, Mechanistic Investigation of Inclusion Complexes of a Sulfa Drug with α-and β-Cyclodextrins, Industrial & Engineering Chemistry Research 56(41) (2017) 11672-11683.

[21] S. Saha, A. Roy, K. Roy, M.N. Roy, Study to explore the mechanism to form inclusion complexes of β-cyclodextrin with vitamin molecules, Scientific reports 6(1) (2016) 1-12.

[22] S. Barman, B.K. Barman, M.N. Roy, Preparation, characterization and binding behaviors of host-guest inclusion complexes of metoclopramide hydrochloride with α- and β-cyclodextrin molecules, Journal of Molecular Structure 1155 (2018) 503-512.

[23] B. Rajbanshi, A. Dutta, B. Mahato, D. Roy, D.K. Maiti, S. Bhattacharyya, M.N. Roy, Study to explore host guest inclusion complexes of vitamin B1 with CD molecules for enhancing stability and innovative application in biological system, Journal of Molecular Liquids 298 (2020) 111952.

[24] B. Ghosh, N. Roy, D. Roy, S. Mandal, S. Ali, P. Bomzan, K. Roy, M. Nath Roy, An extensive investigation on supramolecular assembly of a drug (MEP) with βCD for innovative applications, Journal of Molecular Liquids 344 (2021) 117977.

[25] W. Zhang, X. Gong, Y. Cai, C. Zhang, X. Yu, J. Fan, G. Diao, Investigation of water-soluble inclusion complex of hypericin with β-cyclodextrin polymer, Carbohydrate Polymers 95(1) (2013) 366-370.

[26] T.R. Usacheva, V.A. Volynkin, V.T. Panyushkin, D.A. Lindt, T.L. Pham, T.T.H. Nguyen, T.M.H. Le, D.A. Alister, D.N. Kabirov, N.N. Kuranova, Complexation of Cyclodextrins with Benzoic Acid in Water-Organic Solvents: A Solvation-Thermodynamic Approach, Molecules 26(15) (2021) 4408.

[27] T. Do Thi, K. Nauwelaerts, M. Froeyen, L. Baudemprez, M. Van Speybroeck, P. Augustijns, P. Annaert, J. Martens, J. Van Humbeeck, G. Van den Mooter, Comparison of the complexation between methylprednisolone and different cyclodextrins in solution by 1H-NMR and molecular modeling studies, Journal of pharmaceutical sciences 99(9) (2010) 3863-3873.

[28] X. Zhao, D. Xiao, J.P. Alonso, D.-Y. Wang, Inclusion complex between beta-cyclodextrin and phenylphosphonicdiamide as novel bio-based flame retardant to epoxy: Inclusion behavior, characterization and flammability, Materials & Design 114 (2017) 623-632.

[29] A.A. Rezende, R.S. Santos, L.N. Andrade, R.G. Amaral, M.M. Pereira, C. Bani, M. Chen, R. Priefer, C.F. da Silva, R.L. de Albuquerque Júnior, Anti-tumor efficiency of

perillylalcohol/β-cyclodextrin inclusion complexes in a sarcoma S180-induced mice model, Pharmaceutics 13(2) (2021) 245.

[30] F.M. Mady, U.F. Aly, Experimental, molecular docking investigations and bioavailability study on the inclusion complexes of finasteride and cyclodextrins, Drug design, development and therapy 11 (2017) 1681.

CHAPTER VIII

[1] J. Carrazana, B. Reija, P.R. Cabrer, W. Al-Soufi, M. Novo, J.V. Tato, Complexation of Methyl Orange with ß-cyclodextrin: Detailed Analysis and Application to Quantification of Polymer-bound Cyclodextrin, Supramolecular Chemistry 16(8) (2004) 549-559.

[2] S. Saha, T. Ray, S. Basak, M.N. Roy, NMR, surface tension and conductivity studies to determine the inclusion mechanism: thermodynamics of host–guest inclusion complexes of natural amino acids in aqueous cyclodextrins, New Journal of Chemistry 40(1) (2016) 651-661.

[3] M.L. Bender, M. Komiyama, Cyclodextrin chemistry, Springer Science & Business Media2012.

[4] J.H. Fendler, Membrane mimetic chemistry: characterizations and applications of micelles, microemulsions, monolayers, bilayers, vesicles, host-guest systems, and polyions, Wiley New York1982.

[5] J.L. Atwood, J.E.D. Davies, D.D. MacNicol, Inclusion compounds, Academic Press1984.

[6] K. Kalyanasundaram, Photochemistry in microheterogeneous systems, Elsevier2012.

[7] Y. Izadmanesh, J.B. Ghasemi, Thermodynamic study of β-cyclodextrin-dye inclusion complexes using gradient flow injection technique and molecular modeling, Spectrochimica Acta Part A: Molecular and Biomolecular Spectroscopy 165 (2016) 54-60.

[8] B.K. Barman, A. Dutta, M.N. Roy, Sustenance of Inclusion Complexes of Ionic Liquid with Cyclic Oligosaccharide Molecules in Liquid and Solid Phases by Diverse Approaches, ChemistrySelect 3(26) (2018) 7527-7534.

[9] S. Barman, B.K. Barman, M.N. Roy, Preparation, characterization and binding behaviors of host-guest inclusion complexes of metoclopramide hydrochloride with α- and β-cyclodextrin molecules, Journal of Molecular Structure 1155 (2018) 503-512.

[10] L. Liu, Q.-X. Guo, Use of quantum chemical methods to study cyclodextrin chemistry, Journal of inclusion phenomena and macrocyclic chemistry 50(1-2) (2004) 95-103.

[11] E. Kompantseva, M. Gavrilin, L. Ushakova, β-Cyclodextrin derivatives and their applications in pharmacology (a review), Pharmaceutical chemistry journal 30(4) (1996) 258-262.

[12] C. Yañez, M. Araya, S. Bollo, Complexation of herbicide bentazon with native and modified β-cyclodextrin, Journal of Inclusion Phenomena and Macrocyclic Chemistry 68(1-2) (2010) 237-241.

[13] P. Persico, C. Carfagna, Cosmeto-Textiles: State of the art and future perspectives, Advances in Science and Technology, Trans Tech Publ, 2013, pp. 39-46.

[14] T. Wang, M. Wang, C. Ding, J. Fu, Mono-benzimidazole functionalized β-cyclodextrins as supramolecular nanovalves for pH-triggered release of p-coumaric acid, Chemical Communications 50(83) (2014) 12469-12472.

[15] H. Zhou, T. Yamada, N. Kimizuka, Supramolecular thermo-electrochemical cells: enhanced thermoelectric performance by host–guest complexation and salt-induced crystallization, Journal of the American Chemical Society 138(33) (2016) 10502-10507.

[16] L. Stricker, E.-C. Fritz, M. Peterlechner, N.L. Doltsinis, B.J. Ravoo, Arylazopyrazoles as light-responsive molecular switches in cyclodextrin-based supramolecular systems, Journal of the American Chemical Society 138(13) (2016) 4547-4554.

[17] M. Xue, W. Wei, Y. Su, D. Johnson, J.R. Heath, Supramolecular probes for assessing glutamine uptake enable semi-quantitative metabolic models in single cells, Journal of the American Chemical Society 138(9) (2016) 3085-3093.

[18] P. Díez, A. Sánchez, M. Gamella, P. Martínez-Ruíz, E. Aznar, C. De La Torre, J.R. Murguía, R. Martínez-Máñez, R. Villalonga, J.M. Pingarrón, Toward the design of smart delivery systems controlled by integrated enzyme-based biocomputing ensembles, Journal of the American Chemical Society 136(25) (2014) 9116-9123.

[19] Y.L. Sun, Y.W. Yang, D.X. Chen, G. Wang, Y. Zhou, C.Y. Wang, J.F. Stoddart, Mechanized Silica Nanoparticles Based on Pillar [5] arenes for On-Command Cargo Release, Small 9(19) (2013) 3224-3229.

[20] Y. Zhou, L.L. Tan, Q.L. Li, X.L. Qiu, A.D. Qi, Y. Tao, Y.W. Yang, Acetylcholine-triggered cargo release from supramolecular nanovalves based on different macrocyclic receptors, Chemistry–A European Journal 20(11) (2014) 2998-3004.

[21] H. Li, D.-X. Chen, Y.-L. Sun, Y.B. Zheng, L.-L. Tan, P.S. Weiss, Y.-W. Yang, Viologen-mediated assembly of and sensing with carboxylatopillar [5] arene-modified gold nanoparticles, Journal of the American Chemical Society 135(4) (2013) 1570-1576.

[22] Z. Zhang, G. Wu, J. Gao, T. Song, Inclusion complex of a Bcl-2 inhibitor with cyclodextrin: characterization, cellular accumulation, and in vivo antitumor activity, Molecular Pharmaceutics 7(4) (2010) 1348-1354.

[23] G. Yu, K. Jie, F. Huang, Supramolecular amphiphiles based on host–guest molecular recognition motifs, Chemical reviews 115(15) (2015) 7240-7303.

[24] E. Iglesias, Inclusion complexation of novocaine by β-cyclodextrin in aqueous solutions, The Journal of organic chemistry 71(12) (2006) 4383-4392.

[25] J. Liu, W.E. Hennink, M.J. Van Steenbergen, R. Zhuo, X. Jiang, Versatile supramolecular gene vector based on host–guest interaction, Bioconjugate Chemistry 27(4) (2016) 1143-1152.

[26] Z. Aytac, Z.I. Yildiz, F. Kayaci-Senirmak, N.O. San Keskin, S.I. Kusku, E. Durgun, T. Tekinay, T. Uyar, Fast-dissolving, prolonged release, and antibacterial cyclodextrin/limonene-inclusion complex nanofibrous webs via polymer-free electrospinning, Journal of agricultural and food chemistry 64(39) (2016) 7325-7334.

[27] X. Chen, Z. Liu, S.G. Parker, X. Zhang, J.J. Gooding, Y. Ru, Y. Liu, Y. Zhou, Light-induced hydrogel based on tumor-targeting mesoporous silica nanoparticles as a theranostic platform for sustained cancer treatment, ACS applied materials & interfaces 8(25) (2016) 15857-15863.

[28] Z.-Q. Shi, Y.-T. Cai, J. Deng, W.-F. Zhao, C.-S. Zhao, Host–guest self-assembly toward reversible thermoresponsive switching for bacteria killing and detachment, ACS applied materials & interfaces 8(36) (2016) 23523-23532.

[29] H. Dong, Y. Wei, W. Zhang, C. Wei, C. Zhang, J. Yao, Y.S. Zhao, Broadband tunable microlasers based on controlled intramolecular charge-transfer process in organic supramolecular microcrystals, Journal of the American Chemical Society 138(4) (2016) 1118-1121.

[30] H. Li, F. Li, B. Zhang, X. Zhou, F. Yu, L. Sun, Visible light-driven water oxidation promoted by host–guest interaction between photosensitizer and catalyst with a high quantum efficiency, Journal of the American Chemical Society 137(13) (2015) 4332-4335.

[31] M. Šuleková, M. Smrčová, A. Hudák, M. Heželová, M. Fedorová, Organic colouring agents in the pharmaceutical industry, Folia Veterinaria 61(3) (2017) 32-46.

[32] A. Dąbrowski, Adsorption—from theory to practice, Advances in colloid and interface science 93(1-3) (2001) 135-224.

[33] A. Reife, Dyes, environmental chemistry, Kirk-Othmer Encyclopedia of Chemical Technology (2000).

[34] M. Irimia-Vladu, E.D. Głowacki, P.A. Troshin, G. Schwabegger, L. Leonat, D.K. Susarova, O. Krystal, M. Ullah, Y. Kanbur, M.A. Bodea, Indigo-A natural pigment for high performance ambipolar organic field effect transistors and circuits, Advanced Materials 24(3) (2012) 375-380.

[35] J. Seixas de Melo, A. Moura, M. Melo, Photophysical and spectroscopic studies of indigo derivatives in their keto and leuco forms, The Journal of Physical Chemistry A 108(34) (2004) 6975-6981.

[36] S. Saha, A. Roy, M.N. Roy, Mechanistic Investigation of Inclusion Complexes of a Sulfa Drug with α-and β-Cyclodextrins, Industrial & Engineering Chemistry Research 56(41) (2017) 11672-11683.

[37] Y. Yang, Q. Hu, Q. Zhang, K. Jiang, W. Lin, Y. Yang, Y. Cui, G. Qian, A large capacity cationic metal–organic framework nanocarrier for physiological pH responsive drug delivery, Molecular pharmaceutics 13(8) (2016) 2782-2786.

[38] F. Cramer, W. Saenger, H.-C. Spatz, Inclusion compounds. XIX. 1a The formation of inclusion compounds of α-cyclodextrin in aqueous solutions. Thermodynamics and kinetics, Journal of the American Chemical Society 89(1) (1967) 14-20.

[39] A. Roy, S. Saha, B. Datta, M.N. Roy, Insertion behavior of imidazolium and pyrrolidinium based ionic liquids into α and β-cyclodextrins: mechanism and factors leading to host–guest inclusion complexes, RSC Advances 6(102) (2016) 100016-100027.

[40] J.V. Caso, L. Russo, M. Palmieri, G. Malgieri, S. Galdiero, A. Falanga, C. Isernia, R. Iacovino, Investigating the inclusion properties of aromatic amino acids complexing beta-cyclodextrins in model peptides, Amino Acids 47(10) (2015) 2215-2227.

[41] J.S. Renny, L.L. Tomasevich, E.H. Tallmadge, D.B. Collum, Method of continuous variations: applications of job plots to the study of molecular associations in organometallic chemistry, Angewandte Chemie International Edition 52(46) (2013) 11998-12013.

[42] S. Saha, A. Roy, K. Roy, M.N. Roy, Study to explore the mechanism to form inclusion complexes of β-cyclodextrin with vitamin molecules, Scientific reports 6 (2016) 35764.

[43] M. Shah, V. Shah, A. Ghosh, Z. Zhang, T. Minko, Molecular inclusion complexes of β-cyclodextrin derivatives enhance aqueous solubility and cellular internalization of paclitaxel: Preformulation and in vitro assessments, Journal of pharmaceutics & pharmacology 2(2) (2015) 8.

[44] H.A. Benesi, J. Hildebrand, A spectrophotometric investigation of the interaction of iodine with aromatic hydrocarbons, Journal of the American Chemical Society 71(8) (1949) 2703-2707.

[45] N. Roy, R. Ghosh, K. Das, D. Roy, T. Ghosh, M.N. Roy, Study to synthesize and characterize host-guest encapsulation of antidiabetic drug (TgC) and hydroxy propyl-β-cyclodextrin augmenting the antidiabetic applicability in biological system, Journal of Molecular Structure 1179 (2019) 642-650.

[46] V.D. Suryawanshi, L.S. Walekar, A.H. Gore, P.V. Anbhule, G.B. Kolekar, Spectroscopic analysis on the binding interaction of biologically active pyrimidine derivative with bovine serum albumin, Journal of pharmaceutical analysis 6(1) (2016) 56-63.

[47] G. Wenz, C. Strassnig, C. Thiele, A. Engelke, B. Morgenstern, K. Hegetschweiler, Recognition of Ionic Guests by Ionic β-Cyclodextrin Derivatives, Chemistry–A European Journal 14(24) (2008) 7202-7211.

[48] G.A. Holdgate, W.H. Ward, Measurements of binding thermodynamics in drug discovery, Drug discovery today 10(22) (2005) 1543-1550.

[49] B. Roy, P. Guha, P. Nahak, G. Karmakar, S. Maiti, A.K. Mandal, A.G. Bykov, A.V. Akentiev, B.A. Noskov, K. Tsuchiya, Biophysical Correlates on the Composition, Functionality, and Structure of Dendrimer–Liposome Aggregates, ACS Omega 3(9) (2018) 12235-12245.

[50] H. Shekaari, F. Jebali, Volumetric and conductometric studies of some amino acids in aqueous ionic liquid, 1-hexyl-3-methylimidazolium chloride solutions at 298.15 K, Physics and Chemistry of Liquids 49(5) (2011) 572-587.

[51] N.A. Todorova, F.P. Schwarz, The role of water in the thermodynamics of drug binding to cyclodextrin, The Journal of Chemical Thermodynamics 39(7) (2007) 1038-1048.

[52] M. Rekharsky, Y. Inoue, Microcalorimetry in Cyclodextrins and Their Complexes: Chemistry, Analytical Methods, Applications, Wiley–VCH Verlag GmbH & Co. KGaA (2006) 215-222.

[53] A. Cooper, C.M. Johnson, J.H. Lakey, M. Nöllmann, Heat does not come in different colours: entropy–enthalpy compensation, free energy windows, quantum confinement, pressure perturbation calorimetry, solvation and the multiple causes of heat capacity effects in biomolecular interactions, Biophysical chemistry 93(2-3) (2001) 215-230.

[54] B.K. Barman, B. Rajbanshi, A. Yasmin, M.N. Roy, Exploring inclusion complexes of ionic liquids with α-and β-cyclodextrin by NMR, IR, mass, density, viscosity, surface tension and conductance study, Journal of Molecular Structure 1159 (2018) 205-215.

[55] M.N. Roy, A. Roy, S. Saha, Probing inclusion complexes of cyclodextrins with amino acids by physicochemical approach, Carbohydrate polymers 151 (2016) 458-466.

[56] D. Ekka, M.N. Roy, Molecular interactions of α-amino acids insight into aqueous β-cyclodextrin systems, Amino Acids 45(4) (2013) 755-777.

[57] V. Balzani and E Scandola Supramolecular Photochemistry, Ellis Horwood, New York, 1991, pp. 288-318.

[58] Synthesis of a New Indigo Vat Dye * 1Nwokonkwo D. C. and 2Okafor C. O. 1Department of Industrial Chemistry, Faculty of Sciences, Ebonyi State University Abakaliki, Nigeria. 2Department of Pure and Industrial Chemistry,University of Nigeria, Nsukka, Nigeria.

INDEX

I

J

M

N

P

R

S

T

U

V

W

https://doi.org/10.30799/jacs.217.20060102 J. Adv. Chem. Sci. – Volume 6 Issue 1 (2020) 667–670

Share Your Innovations through JACS Directory

Journal of Advanced Chemical Sciences

Visit Journal at http://www.jacsdirectory.com/jacs

ISSN: 2394-5311

Assorted Interactions Prevalent in Uracil and Aqueous Gallic Acid Solution Explored by Physicochemical Contrivance

Samapika Ray, Habibur Rahaman, Kanak Roy, Mahendra Nath Roy*

Department of Chemistry, University of North Bengal, Darjeeling – 734 013, West Bengal, India.

ARTICLEDETAILS

Article history:
Received 08 February 2020
Accepted 28 March 2020
Available online 11 May 2020

Keywords:
Solute-Cosolute Interactions
Apparent Molar Volume
Viscosity B-Coefficient

ABSTRACT

The solute-cosolute interaction of uracil by gallic acid has been studied through physicochemical investigation in aqueous environment. Here, we have carried out the density (ρ) and viscosity (η) measurements of uracil in w_1= 0.001, 0.002 and 0.003 mass fraction of aqueous gallic acid binary mixtures at T= 298.15 K, 303.15 K and 308.15 K at pressure 1.013 bar. Some important parameters have been derived from the above physicochemical method, namely, limiting apparent molar volume (φ_V^0) and viscosity B-coefficients using extended Masson equation and Jones-Dole equation respectively. The refractive index (n_D) has been done on the same system at T=298.15 K. Lorentz-Lorenz equation has used to evaluate molar refractive index (R_M) and limiting molar index (R_M^0). The NMR study used to measure the plausible selective site of solute-cosolute interaction.

1. Introduction

Gallic acid is a secondary polyphenolic functionality metabolite natural antioxidant. It is a water-soluble organic compound present in grapes and in the leaves of many plants. Gallic acid esters are used to in vitro potent antioxidant, such as tannins, catechin gallates and aliphatic gallates. However, gallic acid itself also acts as in vitro anticarcinogenic and antiangiogenic activity. Apart from its phytochemical role, gallic acid is also used in ink dyes, and the manufacture of paper, pharmaceutical industry, starting material for the synthesis of psychedelic alkaloid mescaline [1–5].

Uracil is a common naturally occurring pyrimidine group only found in RNA, its base pairs with adenine and is replaced by thymine in DNA. Uracil is planar and unsaturated with the molecular formula $C_4H_4N_2O_2$ and has the ability to absorb light. Uracil can bind with base pairs depending on arrangement, in RNA it binds to adenine via two hydrogen bonds. Uracil is use in the body is to help carry out the synthesis of many enzymes necessary for cell function through bonding with ribose and phosphates [6–8].

To the best of our knowledge, the studies in the present ternary solution systems have not been reported earlier. Therefore, in present study we have endeavored to make certain nature of interaction of solute itself (uracil) and with co-solute (gallic acid) in w_1=0.001, 0.002 and 0.003 mass fraction of aqueous medium at different temperatures 298.15 K - 308.15 K with 5 interval to explain various noncovalent interactions prevailing in the ternary systems under investigation.

2. Experimental Methods

2.1 Materials

Uracil and Gallic acid were purchased from Sigma-Aldrich. The mass fractions purity of both was ≥0.99. The reagents were always placed in the desiccators over P_2O_5 to keep them in dry atmosphere. These chemicals were used as received without further purification. The provenance and purity of the chemical used has been depicted in Table 1.

2.2 Procedure

Solubility of the uracil and gallic acid in water (deionised, doubly distilled water) and in uracil and gallic acid solutions have been checked precisely, prior to the experimental work and observe that uracil is soluble in all proportion of aqueous gallic acid solution. The mother solutions of uracil were prepared by mass (Mettler Toledo AG-285 with uncertainty 0.0003 g) and then the working solutions (six sets) were prepared by mass dilution. The conversion of molarity into molality [9] has been done using experimental density values of respective solutions.

Table 1 Source and purity of the chemicals

Chemical name	Source	Mass fraction purity	Purification method
Uracil	SD Fine-Chem Ltd.	≥0.99	Used as procured
Gallic acid	SD Fine-Chem Ltd.	≥0.99	Used as procured

The densities (ρ) of the solutions were measured by means of vibrating u-tube Anton Paar digital density meter (DMA 4500M) with a precision of ±0.00005 g.cm^{-3} maintained at ±0.01 K of the desired temperature. It was calibrated by passing deionised, triply distilled water and dry air [10].

The viscosities (η) were measured using a Brookfield DV-III Ultra Programmable Rheometer with fitted spindle size-42. The detail description has already been described in the previous work [11].

Refractive index (n_D) was measured with the help of a Digital Refractometer Mettler Toledo. The light source was LED, λ=589.3 nm. The refractometer was calibrated twice using distilled water and calibration was checked after every few measurements [12]. The uncertainty of refractive index measurement was ±0.0002 units.

^{1}H-NMR spectra were recorded at 400 MHz Bruker instrument using D_2O as reference solvent at 298.15 K.

3. Results and Discussion

The physical parameters of binary mixtures in different mass fractions (w_1=0.001, 0.002, 0.003) of aqueous gallic acid (GA) solutions at three different temperatures (298.15 K, 303.15 K, 308.15 K) and at 1.013 bar have been reported in Table 2. The experimental measured values of density, viscosity of uracil (UA) as a function of concentration (molality), in different mass fractions of aqueous gallic acid (GA) mixture at three above mentioned temperatures have been listed in Table 3.

3.1 Apparent Molar Volume

Volumetric properties, like, apparent molar volume (φ_V) and limiting apparent molar volume (φ_V^0) consider important tools for understanding of interactions taking place in solution systems. The apparent molar volume can be regarded to be the sum of the geometric volume of the

*Corresponding Author:mahendraroy2002@yahoo.co.in(Mahendra Nath Roy)

https://doi.org/10.30799/jacs.217.20060102

Cite this Article as: Samapika Ray, Habibur Rahaman, Kanak Roy, Mahendra Nath Roy, Assorted interactions prevalent in uracil and aqueous gallic acid solution explored by physicochemical contrivance, J. Adv. Chem. Sci. 6(1) (2020) 667–670.

central solute molecule and changes in the solvent volume due to its interaction with the solute around the peripheral or co-sphere. Therefore, the apparent molar volumes (φ_V) have been determined from the solutions densities using the suitable equation and the values are given in Table 4.

$$\varphi_V = M/\rho - 1000\,(\rho - \rho_0)/m\rho\rho_0 \quad (1)$$

where M is the molar mass of the solute, m is the molality of the solution, ρ and ρ_0 are the density of the solution and aqueous gallic acid mixture respectively.

Table 2 Experimental values of density (ρ), viscosity (η) and refractive index (n_D) at 298.15 K and at pressure 1.013 bar of different mass fraction (w_1) of aq. gallic acid mixtures*

Aq. Gallic acid Mixture (w_1)	Temp., K	$\rho\times10^{-3}$ kg·m^{-3}	η mP·s	n_D
0.001	298.15	0.99689	0.91	1.3319
	303.15	0.99547	0.83	
	308.15	0.99395	0.74	
0.002	298.15	0.99698	0.91	1.3324
	303.15	0.99556	0.84	
	308.15	0.99396	0.76	
0.003	298.15	0.99702	0.92	1.3329
	303.15	0.99564	0.85	
	308.15	0.99403	0.77	

**Standard uncertainties u are: u (ρ) =0.002 kg·m^{-3}, u (η) =0.02 mP·s, u (n_D) =0.0002 and u (T) =0.01K, (0.68 level of confidence)*

Table 3 Experimental values of density (ρ) and viscosity (η), Uracil in different mass fractions of aqueous Gallic acid mixture (w_1) at three different temperatures and at pressure 1.013 bar*

[a]m molkg^{-1}	$\rho\times10^{-3}$ kgm^{-3}	η mP.s	[a]m molkg^{-1}	$\rho\times10^{-3}$ kgm^{-3}	η mP.s	[a]m molkg^{-1}	$\rho\times10^{-3}$ kgm^{-3}	η mP.s
	w_1=0.001			w_1=0.002			w_1=0.003	
Temp.	298.15 K			298.15 K			298.15 K	
0.0100	0.99722	0.92	0.0100	0.99726	0.93	0.0100	0.99731	0.93
0.0252	0.99790	0.93	0.0252	0.99795	0.94	0.0252	0.99799	0.94
0.0404	0.99897	0.94	0.0404	0.99897	0.95	0.0404	0.99896	0.96
0.0556	1.00022	0.94	0.0556	1.00027	0.96	0.0556	1.00018	0.97
0.0709	1.00150	0.95	0.0709	1.00159	0.97	0.0709	1.00157	0.98
0.0863	1.00304	0.96	0.0863	1.00317	0.98	0.0863	1.00316	0.99
Temp.	298.15 K			298.15 K			298.15 K	
0.0101	0.99518	0.84	0.0101	0.99588	0.85	0.0101	0.99593	0.86
0.0252	0.99652	0.85	0.0252	0.99651	0.86	0.0252	0.99655	0.87
0.0404	0.99759	0.86	0.0404	0.99756	0.87	0.0404	0.99755	0.88
0.0557	0.99834	0.87	0.0557	0.99877	0.88	0.0557	0.99874	0.89
0.0710	1.00014	0.87	0.0710	1.00025	0.89	0.0710	1.00014	0.90
0.0864	1.00158	0.88	0.0864	1.00174	0.89	0.0864	1.00173	0.91
Temp.	298.15 K			298.15 K			298.15 K	
0.0101	0.99425	0.75	0.0101	0.99429	0.77	0.0101	0.99432	0.78
0.0253	0.99491	0.75	0.0253	0.99491	0.77	0.0253	0.99487	0.79
0.0405	0.99588	0.76	0.0405	0.99593	0.78	0.0405	0.99583	0.80
0.0558	0.99716	0.77	0.0558	0.99713	0.79	0.0558	0.99699	0.80
0.0712	0.99846	0.77	0.0712	0.99852	0.80	0.0712	0.99845	0.81
0.0866	0.99998	0.78	0.0866	0.99991	0.81	0.0866	0.99989	0.82

**Standard uncertainties u are: u (ρ) =0.00002 kgm^{-3}, u (η) =0.02 mPs and u (T) =0.01K (0.68 level of confidence)*
[a]molality has been expressed per kg (gallic acid + water) solvent mixture

Table 4 Apparent molar volume (φ_V) and $(\eta_r\text{-}1)/\sqrt{m}$ of uracil in different mass fraction (w_1) of aqueous gallic acid mixtures at three different temperatures*

[a]molality mol kg^{-1}	$\varphi_V\times10^6$ m^3 mol^{-1}	$(\eta_r\text{-}1)/\sqrt{m}$ Kg$^{0.5}$ mol$^{-0.5}$	[a]molality mol kg^{-1}	$\varphi_V\times10^6$ m^3 mol^{-1}	$(\eta_r\text{-}1)/\sqrt{m}$ Kg$^{0.5}$ mol$^{-0.5}$	[a]molality mol kg^{-1}	$\varphi_V\times10^6$ m^3 mol^{-1}	$(\eta_r\text{-}1)/\sqrt{m}$ Kg$^{0.5}$ mol$^{-0.5}$
w_1=0.001			w_1=0.002			w_1=0.003		
T = 298.15 K			T = 298.15 K			T = 298.15 K		
0.0100	183.2	0.11	0.0100	188. 2	0.12	0.0100	192.7	0.13
0.0252	168.2	0.13	0.0252	169.9	0.15	0.0252	170.2	0.15
0.0404	151.2	0.15	0.0404	158.1	0.17	0.0404	165.9	0.19
0.0556	144.8	0.16	0.0556	145.7	0.20	0.0556	157.2	0.21
0.0709	138.5	0.20	0.0709	139.2	0.21	0.0709	149.6	0.23
0.0863	131.8	0.21	0.0863	133.2	0.22	0.0863	138.4	0.24
T = 303.15 K			T = 303.15 K			T = 303.15 K		
0.0101	187.9	0.05	0.0101	192.9	0.08	0.0101	197.0	0.09
0.0252	171.4	0.10	0.0252	173.7	0.10	0.0252	183.2	0.12
0.0404	160.6	0.11	0.0404	163.6	0.11	0.0404	168.7	0.15
0.0557	150.4	0.13	0.0557	153.9	0.12	0.0557	158.7	0.17
0.0710	140.1	0.14	0.0710	143.5	0.15	0.0710	148.1	0.21
0.0864	135.5	0.15	0.0864	138.6	0.20	0.0864	142.1	0.22
T = 308.15 K			T = 308.15 K			T = 308.15 K		
0.0101	194.2	0.07	0.0101	196.2	0.06	0.0101	200.4	0.08
0.0253	175.1	0.10	0.0253	181.2	0.10	0.0253	183.1	0.11
0.0405	162.4	0.13	0.0405	167.9	0.13	0.0405	171.4	0.16
0.0558	150.3	0.15	0.0558	157.3	0.16	0.0558	160.4	0.18
0.0712	142.5	0.17	0.0712	148.9	0.18	0.0712	150.7	0.21
0.0866	138.9	0.18	0.0866	141.8	0.20	0.0866	143.1	0.22

**Standard uncertainties u are: u (T) =0.01 K, the accuracy of φ_V is 1.86×10^{-6} m^3 mol^{-1} and $(\eta_r\text{-}1)/\sqrt{m}$ is 0.004 kg$^{1/2}$mol$^{-1/2}$ (0.68 level of confidence)*
[a]molality has been expressed per kg of (gallic acid + water) solvent mixture

The values of (φ_V) are positive and large for all the systems, signifying strong solute-cosolute interactions. The apparent molar volumes (φ_V) are found to decrease with increasing concentration (molality, m) of uracil in same mass fraction of aqueous gallic acid at same temperature. It is also found that apparent molar volumes (φ_V) increase with both increasing temperature as well as mass fraction of aqueous gallic acid solution and varied with $\sqrt{m}$ and could be least-squares fitted to the extended Masson equation [13] from where limiting molar volume, φ_V^0 (infinite dilution partial molar volume) have been estimated and the values have been represented in Table 5.

$$\varphi_V = \varphi_V^0 + S_V^*\sqrt{m} \quad (2)$$

where φ_V^0 is the apparent molar volume at infinite dilution, S_V^* is the experimental slope. At infinite dilution solute molecule is surrounded only by the solvent molecules and remains infinite distant from each other. As a consequence, that φ_V^0 is unaltered by itself interaction of uracil molecules and it is a measure only of the solute-cosolute (uracil-gallic acid) interaction.

Table 5 Limiting apparent molar volume (φ_V^0), experimental slope (S_V^*), viscosity A- and B-coefficient of uracil in different mass fraction (w_1) of aqueous gallicic acid mixtures at three different temperatures*

Mass fraction (w_1)	T K	$\varphi_V^0\times10^6$ m^3 mol^{-1}	$S_V^*\times10^6$ m^3 mol$^{-3/2}$ kg$^{1/2}$	B kg mol^{-1}	A kg$^{1/2}$ mol$^{-1/2}$
	298.15	220.18	-417.12	0.41	0.02
0.001	303.15	225.45	-451.27	0.49	0.01
	308.15	231.28	-493.79	0.67	0.05
	298.15	225.98	-499.65	0.53	0.04
0.002	303.15	230.63	-477.45	0.66	0.02
	308.15	236.16	-463.92	0.78	0.01
	298.15	230.72	-448.89	0.65	0.03
0.003	303.15	235.51	-453.56	0.77	0.01
	308.15	241.12	-442.87	0.93	0.04

**Standard uncertainties values of u are: u (T) =0.01 K*

An inspection of Table 5 shows that φ_V^0 are large and positive for all uracil at all the studied temperatures, suggesting the presence of strong solute-cosolute interaction. Comparing φ_V^0 with S_V^* values show that the magnitude of φ_V^0 is greater than S_V^*, suggesting that solute-cosolute interactions predominates over itself interaction of solute molecules in all solutions at all studied temperatures. Moreover, S_V^* values are negative at all studied temperatures indicates force of itself interaction of uracil molecules is very poor.

The variation of φ_V^0 with temperature are fitted to the following polynomial,

$$\varphi_V^0 = a_0 + a_1 T + a_2 T^2 \quad (3)$$

where T is the temperature in K and a_0, a_1 and a_2 are the empirical coefficients depending on the solute, mass fraction of cosolute gallic acid. Values of coefficients of the above equation for the in aqueous gallic acid mixtures are reported in Table 6.

Table 6 Values of various coefficients and standard deviation of equation-3 for uracil acid in different aqueous gallic acid solutions*

Aq. Gallic acid Mixture (w_1)	$a_0\times10^6$ m^3 mol^{-1}	$a_1\times10^6$ m^3 mol^{-1}K^{-1}	$a_2\times10^6$ m^3 mol^{-1}K^{-2}	$(\delta\varphi_E^0/\delta T)_P\times10^6$ m^3 mol^{-1} K^{-2}
0.001	2014.72	-15.21	0.01	0.03
0.002	2141.61	-14.24	0.02	0.06
0.003	2212.43	-13.28	0.02	0.05
Average SD	3.1	0.011	0.0002	0.0001

The limiting apparent molar expansibilities, φ_E^0, can be evaluated by the following equation,

$$\varphi_E^0 = (\delta\varphi_V^0/\delta T)_P = a_1 + 2a_2T \quad (4)$$

https://doi.org/10.30799/jacs.217.20060102

Cite this Article as: Samapika Ray, Habibur Rahaman, Kanak Roy, Mahendra Nath Roy, Assorted interactions prevalent in uracil and aqueous gallic acid solution explored by physicochemical contrivance, J. Adv. Chem. Sci. 6(1) (2020) 667–670.

The limiting apparent molar expansibilities, φ_E^0, change in magnitude with the change of temperature. The values of φ_E^0 for different solutions of studied gallic acid at *T*=298.15, 303.15 and 308.15 K are shown in Table 7.

Table 7 Limiting apparent molar expansibilities (φ_E^0) for uracil in different mass fraction of aqueous gallic acid (w_1) at different temperature

Aq. gallic acid mixture (w_1)	$\varphi_E^0\times10^6$, m^3 mol^{-1}K^{-1}		
T/ K	298.15	303.15	308.15
0.001	1.012	1.142	1.253
0.002	3.729	3.928	4.227
0.003	-1.533	-1.344	-1.133
Average SD	0.003	0.003	0.002

All the values of φ_E^0 shown in the Table 7 are positive for uracil in aqueous gallic acid and studied temperature. This fact helps to explain the absence of caging or packing effect for the gallic acid in solution [14].

The long-range structure-making and breaking capacity of the solute in mixed system can be determined by examining the sign of $(\delta\varphi_E^0/\delta T)_P$ developed by Hepler [15].

$$(\delta\varphi_E^0/\delta T)_P = (\delta^2\varphi_V^0/\delta T^2)_P = 2a_2 \quad (5)$$

The positive sign or small negative of $(\delta\varphi_E^0/\delta T)_P$ signifies the molecule is a structure-maker; otherwise, it is a structure-breaker [16]. The perusal of Table 6 shows that, $(\delta\varphi_E^0/\delta T)_P$ values of citric acid are all positive under investigation. It shows the more symmetric rearrangement of the interacting molecules (uracil and gallic acid) with the formation of H-bonding, Van der Waals forces, dipole-dipole interactions etc. This symmetric arrangement is signifying the molecules of uracil and gallic acid is definitely interacting with structure–making tendency in all of the studied solution systems. The Table 6 also showing the positively magnitude of $(\delta\varphi_E^0/\delta T)_P$ values in of uracil is depicting this structure–making tendency.

3.2 Viscosity

The experimental viscosity data for studied systems are listed in Table 3. The relative viscosity (η_r) has been calculated using extended Jones-Dole equation [17] for non-electrolytes.

$$(\eta/\eta_0 - 1)/\sqrt{m} = (\eta_r - 1)/\sqrt{m} = A + B\cdot\sqrt{m} \quad (6)$$

where $\eta_r = \eta/\eta_0$ is the relative viscosity, η and η_0 are the viscosities of ternary solutions (uracil+gallic acid) and solvent (aqueous mixture of gallic acid) respectively and *m* is the molality of uracil in ternary solutions. Where *A* is known as Falkenhagen coefficient [18] as it is determined by the ionic attraction theory of Falkenhagen-Vernon and *B* is empirical constants known as viscosity *B*- coefficients, which are specifying to the interaction of solute itself and/or with cosolute molecules respectively. The values of *A*- and *B*-coefficients are estimated by least-square polynomial method by plotting $(\eta_r - 1)/\sqrt{m}$ against $\sqrt{m}$ with second order and reported in Table 4.

It is observed from Table 4 the values of the *A*-coefficient are found to decrease with increase in temperature. This fact indicates the presence of very weak solute-solute interaction and also in excellent agreement with those obtained from S_V^* values.

The valuable information about the solvation of the solvated solutes and their effects on the structure of the cosolute gallic acid in the local vicinity of the solute (uracil) molecules in solutions has been obtained from viscosity *B*-coefficient [19]. It is found from Table 4; the values of *B*-coefficient are positive and much higher than *A*-coefficient which signifies solute-cosolute interaction is dominant over solute-solute and cosolute-cosolute interaction. It is also observed that the positive magnitude of viscosity *B*-coefficient increases with increasing temperature and also increases with an increase in mass fraction of aqueous gallic acid mixture which suggests that solute-cosolute interaction is strengthened with rise in temperature as well as mass fraction of aqueous uric acid mixture. These results are in good agreement with those obtained from limiting apparent molar volume φ_V^0 values.

It is observed from Table 4 that the values of the *B*-coefficient of citric acid increases with temperature, i.e., the *dB/dT* values are positive. From Table 8, the small positive *dB/dT* values for the citric acid behaves behave almost as structure-maker.

Furthermore, it is attractive to observe that there is linear correlation between viscosity *B*-coefficients of the studied citric acid with the limiting apparent molar volumes (φ_V^0) in different mass fraction of aqueous uric acid solutions. From the above fact it means

$$B = A_1 + A_2\,\varphi_V^0 \quad (13)$$

The coefficients A_1 and A_2 are listed in Table 8. As both viscosities *B*-coefficient and limiting apparent molar volumes define the solute-solvent interaction in solution. The linear variation of viscosity *B*-coefficient and limiting apparent molar volume (φ_V^0) reflects the positive slope (or A_2).

Table 8 Values of dB/dT, A_1, A_2 coefficients for the uracil in different mass fraction of aqueous gallic acid (w_1) at studied temperatures*

Aq. Gallic acid Mixture (w_1)	*dB/dT*	A_1	A_2
0.001	0.031	-6.746	0.021
0.002	0.026	-7.766	0.022
0.003	0.035	-8.295	0.034
Average standard deviation	0.001	0.005	0.003

** Standard uncertainties values of u are: u (T) =0.01 K*

It is evident from this study, that there is a strong interaction between uracil and gallic acid and it becomes stronger with rise in temperature. As molecules of uracil are engaged with the gallic acid molecules, the interaction among the gallic acid molecules becomes less effective. We have obtained the derived parameters like, limiting apparent molar volume (φ_V^0), viscosity *B*-coefficient by interpolation and presented in Table 5. The positive and significant magnitude of φ_V^0 and *B*-coefficient from Table 5 clearly indicates that the limiting apparent molar volume (φ_V^0), viscosity *B*-coefficient is increases with increasing mass fraction of uracil, which indicates the positive effect of interaction of uracil with gallic acid.

3.3 Refractive Index

The measurement of refractive index is also a suitable method for investigating the molecular interaction existing in solution. The molar refraction (R_M) can be evaluated from the Lorentz-Lorenz relation [20]. The refractive index of a substance is defined as the ratio c_o/c, where *c* and c_o is the velocity of light in the medium and in vacuum respectively. Stated more simply that the refractive index of a compound describes its ability to refract light as it passes from one medium to another and thus, the higher the refractive index of a compound, the more the light is refracted [21].

As stated by Deetlefs et al. [22] the refractive index of a substance is higher when its molecules are more tightly packed or in general when the compound is denser. Hence, a perusal of Table 9 it has found as the refractive index and the molar refraction are higher for the studied uracil and in all the mass fraction of aqueous gallic acid, indicating to the fact that the molecules are more tightly packed in the solution.

Table 9 Refractive index (n_D), molar refraction (R_M) and limiting molar refraction (R_M^0) uracil in different mass fraction of aqueous gallic acid solutions at 298.15 K and at pressure 1.013 bar *

[a]molality mol·kg^{-1}	n_D	$R_M\times10^6$ m^3 mol^{-1}	$R_M^0\times10^6$ m^3 mol^{-1}
w_1=0.001			
0.0100	1.3320	44.23	
0.0252	1.3323	44.23	
0.0404	1.3328	44.23	44.24±0.03
0.0556	1.3333	44.25	
0.0709	1.3338	44.25	
0.0863	1.3345	44.26	
w_1=0.002			
0.0100	1.3325	44.27	
0.0252	1.3327	44.27	
0.0404	1.3333	44.28	44.28±0.03
0.0556	1.3338	44.28	
0.0709	1.3343	44.31	
0.0863	1.3349	44.31	
w_1=0.003			
0.0100	1.3333	44.36	
0.0252	1.3336	44.37	
0.0404	1.3343	44.42	43.42±0.02
0.0556	1.3350	44.43	
0.0709	1.3356	44.45	
0.0863	1.3363	44.46	

**Standard uncertainties u are: u(n_D) =0.02 and u(T) =0.01K (0.68 level of confidence)*
[a]molality has been expressed per kilogram of (gallic acid + water) solvent mixture

The limiting molar refraction (R_M^0) estimated from the following Eq. (14) and presented in Table 9.

$$R_M = R_M^0 + R_S\sqrt{m} \quad (14)$$

https://doi.org/10.30799/jacs.217.20060102

Accordingly, it has been found that the higher values of refractive index and R_M^0 which representing the fact that the molecules of uracil and are more tightly packed and greater solute-solvent interaction with gallic acid molecules than solute solvent interaction. This is also in good agreement with the results obtained from apparent molar volume and viscosity *B*-coefficients discussed above.

3.4 NMR Study

The site selective solute and cosolute interaction have been observed in ^{1}H NMR study. Gallic acid (GA) shows NMR peak at δ: 6.67 for phenolic OH group. Uracil (UA) shows NMR peak at δ: 7.44 and δ: 5.71 for C(5) and C(6) protons. NMR spectra suggest that interaction occurs through C(5) and C(6) protons of uracil with phenolic OH group of gallic acid. This is shown in Fig. 1and Scheme 1. Due to this weak interaction the C(5) and C(6) proton signal in uracil and gallic acid mixture (GU) shifts towards upfield and recorded at δ: 7.24 and δ: 5.57. This is obvious for the specific solute and cosolute interaction. This supports all the above physicochemical experiments along with spectroscopic data [23].

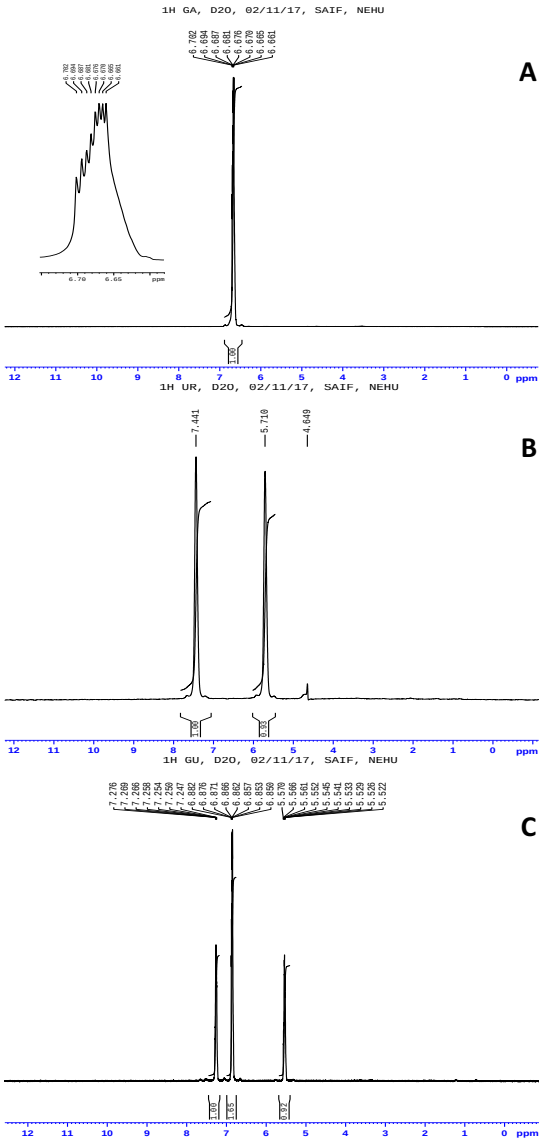

Fig. 1 Plot of ^{1}HNMR spectra of a) gallic acid (GA), b) uracil (UA) and c) uracil+ gallic acid (GU) at 298.15 K in D_2O

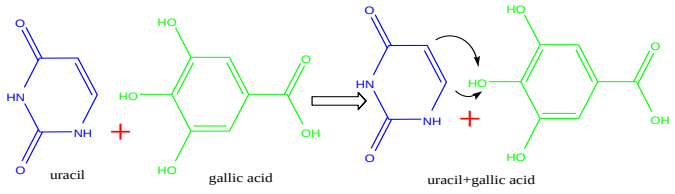

Scheme 1 Plausible solute-cosolute interaction C5 and C6 proton of uracil with phenolic OH group of gallic acid

4. Conclusion

It is evident from this study that there is a strong interaction between uracil and gallic acid and it becomes stronger with rise in temperature. As molecules of uracil and gallic acid are engaged each other, solute-cosolute interaction is much greater than the solute-solute and solvent-solvent interactions.

Acknowledgement

The authors are thankful to the Departmental Special Assistance Scheme under the University Grants Commission, New Delhi (no. 540/6/DRS/2007, SAP-1), India for financial support and instrumental facilities in order to continue this research work.

One of the authors, Prof. M.N. Roy, is thankful to University Grant Commission, New Delhi, Government of India for being awarded onetime grant under Basic Scientific Research via the grant-in-Aid no. F.4-10/2010 (BSR) regarding his active service for augmenting of research facilities to facilitate further research work.

References

[1] R.N. Saladi, A.N. Persaud, The causes of skin cancer: a comprehensive review, Drugs Today (Barc.) 41 (2005) 37–53.
[2] A. Gescher, U. Pastorino, S.M. Plummer, M.M. Manson, Suppression of tumour development by substances derived from the diet – mechanisms and clinical implications, Br. J. Clin. Pharmacol. 45 (1998) 1–12.
[3] M.M. Manson, Cancer prevention – the potential for diet to modulate molecular signalling, Trends Mol. Med. 9 (2003) 11–18.
[4] T.C. Reddy, P. Aparoy, N.K. Babu, K.A. Kumar, S.K. Kalangi, P. Reddanna, Kinetics and docking studies of a COX-2 inhibitorisolated from *Terminalia bellerica* fruits, Protein Pept. Lett. 17 (2010) 1251–1257.
[5] T. Chandramohan Reddy, D. Bharat Reddy, A. Aparna, K.M. Arunasree, G. Gupta, et al., Anti-leukemic effects of gallic acid on human leukemia K562 cells: downregulation of COX-2, inhibition of BCR/ABL kinase and NF-kappaB inactivation, Toxicol. In Vitro 26 (2012) 396–405.
[6] D. Davidson, O. Baudisch, The preparation of uracil from urea, J. Am. Chem. Soc. 48 (1926) 2379-2383.
[7] P. Molnar, L. Marton, R. Izrael, H.L. Palinkas, B.G. Vertessy, Uracil moieties in *Plasmodium falciparum* genomic DNA, FEBS Open Bio 8 (2018) 1763–1772.
[8] K. Séron, Marie-Odile Blondel, R. Haguenauer-Tsapis, C. Volland, Uracil-induced Down-regulation of the yeast uracil permease, J. Bacteriol. 181 (1999) 1793–1800.
[9] D.P. Shoemaker,C.W. Garland, Experiments in physical chemistry, McGraw-Hill Publishers, New York, 1967, pp.131-138.
[10] A. Bhattacharjee, M.N. Roy, Ion association and solvation behaviour of tetraalkyl ammonium iodides in binary mixture of dichloromethane+N,N-dimethyl formamide probed by conductometric study, Phys. Chem. Chem. Phys. 12 (2010) 1-9.
[11] D. Ekka, M.N. Roy, Quantitative and qualitative analysis of ionic salvation of individual ions of imidazolium based ionic liquids in significant solution systems by conductance and FT-IR spectroscopy, RSC Adv. 4 (2014) 19831-19845.
[12] M.N. Roy, S. Saha, S. Barman, D. Ekka, Host–guest inclusion complexes of RNA nucleosides inside aqueous cyclodextrins explored by physicochemical and spectroscopic methods, RSC Adv. 6 (2016) 8881–8891.
[13] D.O. Masson, Ion-solvent interactions, Phil. Mag. 8 (1929) 218-235.
[14] F.J. Millero, The partial molal volumes of electrolytes in aqueous solution. In: R.A. Horne (Ed.), Water and aqueous solutions: Structure, thermodynamics and transport process, Wiley Interscience, New York, 1972, pp.519-595.
[15] L.G. Hepler, Studies on viscosities and densities of R_4NX in ME + water mixtures of different temperatures, Can. J. Chem. 47 (1969) 4613-4617.
[16] M.N. Roy, V.K. Dakua, B. Sinha, Partial molar volumes, viscosity B-coefficients and adiabatic compressibilities of sodium molybdate in aqueous 1,3-dioxalane mixture from 303.15 to 323.15 K, Int. J. Thermophys. 28 (2007) 1275-1284.
[17] G. Jones, D. Dole, The viscosity of aqueous solutions of strong electrolytes with special reference to barium chloride, J. Am. Chem. Soc. 51 (1929) 2950-2964.
[18] J.D. Pandey, K. Mishra, A. Shukla, V. Mishran, R.D. Rai, Apparent molal volume, apparent molal compressibility, verification of jones-dole equation and thermodynamic studies of aqueous urea and its derivative, Thermochim. Acta 117 (1987) 245-259.
[19] F.J. Millero, The molal volumes of electrolytes, Chem. Rev. 71 (1971) 147-176.
[20] V. Minkin, O. Osipov, Y. Zhdanov, Dipole moments in organic chemistry, Plenum Press, New York, 1970.
[21] M. Born, E. Wolf, Principles of optics: Electromagnetic theory of propagation, interference and diffraction of light, 7th Edn., Cambridge University Press, London, 1999.
[22] M. Deetlefs, K. Seddon, M. Shara, Predicting physical properties of ionic liquid, Phys. Chem. Chem. Phys. 8 (2006) 642-649.
[23] S. Kamathama, N. Kumar, Padmaja Gudipalli, Isolation and characterization of gallic acid and methyl gallate from the seed coats of *Givotia rottleriformis* Griff. and their anti-proliferative effect on human epidermoid carcinoma A431 cells, Toxicol. Rep. 2 (2015) 520–529.

https://doi.org/10.30799/jacs.217.20060102

Cite this Article as: Samapika Ray, Habibur Rahaman, Kanak Roy, Mahendra Nath Roy, Assorted interactions prevalent in uracil and aqueous gallic acid solution explored by physicochemical contrivance, J. Adv. Chem. Sci. 6(1) (2020) 667–670.

JCBPS; Section A; February 2021 –April 2021, Vol. 11, No. 2; 304-323, E- ISSN: 2249 –1929
[DOI: 10.24214/jcbps.A.11.2.30403.]

Journal of Chemical, Biological and Physical Sciences

An International Peer Review E-3 Journal of Sciences

*Available online at*www.jcbsc.org

Section A: Chemical Sciences

CODEN (USA): JCBPAT Research Article

Probing Inclusion Complex of a Dye (ISD) with Cyclic Oligosaccharide for Minimizing Harmful Effects

Samapika Ray[1], Ananya Yasmin[2], Biraj Kumar Barman[3], Kanak Roy[4], Tanusree Ray[5]and MahendraNath Roy[1]*

[1]Department of Chemistry, University of North Bengal, Darjeeling-734013, India.

[2]Kalipada Ghosh Tarai Mahavidyalaya, Bagdogra, Darjeeling, India.

[3]Parimal Mitra Smriti Mahavidyalaya, Malbazar, Jalpaiguri, India.

[4]Alipurduar University, Alipurduar, India.[5]Siliguri College, Darjeeling, India.

Received: 17 February 2021; **Revised: 10** March 2021; **Accepted:** 08 April 2021

Abstract: Indigo is a colouring agent used widely in various fields. The synthetic indigo has many adverse effects when it is consumed with foods and beverages. Cyclodextrin (CD) is known to have special chemical characteristics and biological activities and has a suitable cavity that can include molecule of suitable diameter. In our present study, we have outlined different modes of characterization of the inclusion complex (IC) formation between poorly water soluble dye Indigosulfonic Acid Dipotassium Salt (ISD) and β-Cyclodextrin with the help of FTIR Spectroscopy, UV-Visible spectroscopy, fluorescence spectroscopy, ^{1}H NMR study, 2D NOESY, Isothermal Titration Calorimetric study and SEM analysis. ^{1}H-NMR study and other spectroscopic analysis clearly revealed the successful formation of the (IC) which is supported by cross-peaks formed in 2D-NOESY spectrum. Comparable association constants and thermodynamic parameters obtained from both UV-Visible study and ITC study confirmed the higher stability of the IC. The solubility of the IC was found higher than the pure ISD.

Keywords: Association constant, β-Cyclodextrin, Fluorescence study, Inclusion complex, Job plot.

1. INTRODUCTION

In the era of globalisation, host-guest inclusion chemistry based research has become a matter of utmost importance because of their substantial applications in the area of industrial and biomedical research [1].Now days, cyclodextrins (CDs) are being widely used for its excellent ability to form inclusion complexes with various biologically as well as industrially important compounds[2]. Such phenomenon which is known as inclusion brings about certain modifications in both physical and chemical properties of the complex formed [3]. Inclusion complexes (ICs) with CDs are being widely used as biomimetic systems and as unique media for various types of reactions [3-6]. The most common CDs belong to cyclic oligosaccharide category having distinctive truncated cone-shaped structure with a hydrophobic cavity and hydrophilic rim. The hydrophilic wider rim contains primary and narrower rim contains secondary –OH groups. The specific structural features lead CD molecules to form inclusion complexes with a variety of hydrophobic and amphiphilic species in both the aqueous and mixed solvent medium [7]. Commonly there are three types of cyclodextrin molecules namely α-CD, β-CD and γ-CD basing on the number of glucopyranose units. α-CD, β-CD and γ-CD are made up of six and seven and eight glucopyranose units respectively with cavity diameter of 4.7Å and 6.0Å and 8.3 Å respectively. As the CD molecule has no free rotation about the glucopyranose linkage, the cyclodextrins are not perfectly cylindrical in shape rather toroidal or cone shaped [8-9].Thus, a hydrophobic cavity is formed within the molecule and the outer surface remains hydrophilic due to presence of –OH groups. The hydrophobic void of CD can trap the hydrophobic portion of the guest molecule to form a stable inclusion complex and the system is stabilised by different types of non-covalent interactions, such as van der Waals interactions, hydrogen bonding interactions etc.[10].

The ICs with cyclodextrin molecules have been reported to have diverse applications in scientific literature which comprises enhanced solubility, bioavailability, increased stability, masking of awkward taste and odour, decrease of volatility, probability of controlled drug delivery system and many more. However, ICs have special importance in the field of education and industry [11-14].ICs can be used to create stimuli responsive supramolecular substances. Here, various external stimuli for enzyme activation, photo sensing, thermal dependence, variations in pH/ redox environments, competitive binding are used to control the release of guest molecules from the Host-Guest complexes [15-18].Researchers paid importance on molecular sensing, release of anticancer drug and gene transfection in the past few years[19-22].

The host molecules are chosen for the formation of ICs because of their cyclic-constrained conformations, which is beneficial for the molecular selectivity [23]. Due to the amphiphilic nature CDs are able to form self-assemble in aqueous medium to form various well defined systems such as nano tubes, nano sheets and nano rods, micelle, vesicles which have been found applicable in various fields of drug delivery as well as cell imaging systems and nano devices [23-27]. Sophisticated probes are being designed and applied for various systems such as molecular switches and machines, chemo sensors, transmembrane channels, molecular logic gates, and other interesting host-guest systems [28-30].

Dyes and their derivatives are used mostly as indicators but they also have vast applications in colouring foods, cosmetics, solvents, drugs, papers, waxes, plastics etc. Dyes as colouring agent are widely used to colour food and beverages as well as pharmaceutical products. This procedure is to enhance the attractiveness of products and also to help people to distinguish different pharmaceutical products. A number of dyes, especially organic colouring agents, sometimes show negative effect on the human body[31].Synthetic dyes are highly coloured, toxic, and carcinogenic in nature[32,33]. The colour of food and beverages are released inside our body when consumed. Indigo is known to be a natural dye extracted from plants Isatis Tinctoria and Indigofera Tinctoria. Because of having dark

blue colour, they have wide spread applications in the textile industries and food technology. Due to the presence of intra and intermolecular H-bonding network the dye molecule becomes more stable which reflects in its high melting point 390-392^0 C[34].Indigosulfonic Acid Dipotassium Salt is known to be a derivative of naturally occurring dye Indigo. It has low solubility in water in pure form [35].ISD becomes harmful for our respiratory tract when it is swallowed. It also acts as a skin and eye irritant. Dye may be inserted inside of the β-CD molecule and therefore be used to increase the stability of the dye on surface as well as may get control released inside human body to reduce the severity of its adverse effect [36].Thus, inclusion of the colouring agent inside CD can be safe and significant as its release will be controlled and hence it will be less harmful [37]. In this work, we studied the inclusion of ISD inside the hydrophobic cavity of β-CD in both solution and the solid phase.

2. EXPERIMENTAL SECTION

2.1. Materials Used

2.1.1. Source and Purity Of Samples: Indigosulfonic Acid Dipotassium Salt was purchased from TCI chemicals (INDIA) Pvt. Ltd. having mass purity > 90.0% and alpha, beta cyclodextrins have been purchased from Sigma Aldrich Germany having mass purity fraction ≥ 98% and used without further purification**(Table 1).**

Table 1: Details of Chemicals used

Name of chemicals	Molecular Weight (g/mol)	Source	CAS number	Purification method	Mass purity
β-Cyclodextrin	1134.98	Sigma Aldrich Germany	7585-39-9	Used as purchased	≥97%
Indigosulfonic Acid Dipotassium Salt	498.57	TCI Chemicals Pvt.Ltd. India	13725-33-2	Used as purchased	>90%
Distilled Water	18	Self-made	-	-	-

2.2. Apparatus and Procedure: The mother solutions of ISD and β-CD were prepared by mass using Mettler Toledo AG-285(Uncertainty ±0.1 mg) at 298.15 K and other solutions of required strengths were prepared by mass dilution.

Fourier transform infrared spectra (FTIR) were recorded on a Perkin Elmer 8300 FT-IR spectrometer (Shimadzu, Japan) using KBr disk technique at a resolution 4 cm^{-1}. Samples were prepared as thin KBr disks with minute amount of sample at room temperature. The range of scanning was kept at 4000−400 cm^{-1}.

Isothermal titration calorimetry was used to determine the binding stoichiometry, association constant at 298.15 K using a MicroCal VP-ITC isothermal titration calorimeter (Microcal now Malvern instrument). At first, thermal equilibration was established at room temperature, followed by 120-s delay initially and then 28 subsequent injections of ISD into Beta CD solution. (The duration of each injection was 10s with a spacing time of 180s.) An enthalpy generation curve was produced in each injection (in micro calories per second versus time in minutes).The association affinity and thermodynamic properties of the binding phenomenon were determined by fitting the integrated heats

of binding to the one-site binding model to give the association constant (K_a), stoichiometry (N^C), binding enthalpy (ΔH^0) and entropy (ΔS^0).^{1}H NMR and 2D NOESY were performed in D_2O medium using BRUKER AVANCE 400 MHz instrument.

UV-Visible Spectroscopy was performed in Agilent 8453 spectrophotometer (uncertainty ±2nm, 1cm path quartz cell was used) and to control the temperature a digital thermostat was attached with the UV instrument. For fluorescence measurement, we used Quanta Master 40 spectrofluorometer.The scanning electron micrographs were determined by JEOL JSM-IT 100 scanning electron microscope model.

2.3. Synthesis of the Inclusion Complex: The inclusion complex of ISD and β-CD was prepared by co-evaporation method. ISD (dye) and β-CD were accurately weighed according to their 1:1 molar ratio. Here, 0.2 mM of ISD was dissolved in 15 ml 20% ethanol-water solution. Then, it was added drop wise to 25 ml 0.4mM aqueous solution of β-CD. The solution was stirred continuously with the help of a magnetic stirrer for 12 hours at 60^{0}C following the filtration of the mixture using filter paper and the precipitate obtained was washed with 50% ethanol. The crude residue was then air dried at room temperature for the next 6 hours and final dry inclusion compound was stored in a desiccator at room temperature.

3. RESULTS AND DISCUSSION

3.1. Job Plot for The Determination of Stoichiometry of the Host-Guest Inclusion Complex: UV-Vis spectroscopic study is used in the field of host-guest inclusion complexation to understand the subsistence of the IC as well as the stoichiometry. While entering from the highly polar bulk solution to the hydrophobic cavity, the guest molecule experiences a variation of the molar extinction coefficient ($\Delta\varepsilon$)[38]and thus change in the absorption pattern took place. We found the absorption maxima for the guest molecule at 289 nm.**(Fig.1**. absorption pattern)[39].

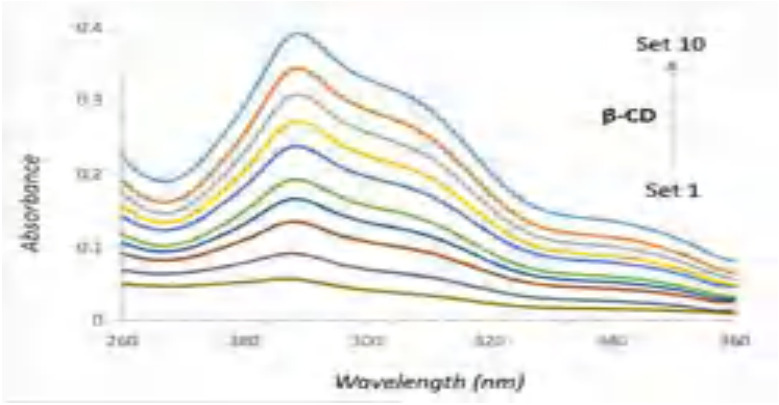

Fig.1: Absorption spectra of intensity against wavelength obtained from UV-Visible spectroscopy at varying concentration of β-Cyclodextrin keeping the guest concentration (Indigo sulfonic acid dipotassium salt) constant. The different lines represent absorption pattern at a particular concentration of β-CD.

The continuous variation method, in other words, Job's plot method was applied to determine the stoichiometric ratio of the host and guest molecule. The sample solutions of different concentration ratios of β-CD and Guest were prepared and mixed in such a way that the total volume of host and

guest molecule remains constant. The changes in absorption spectra were recorded and shown in the **table 2.** We plotted ΔA×R against R [where ΔA is the difference in absorbance of ISD without and with CD i.e.(ISD+β-CD) and R = [ISD]/ ([ISD] + [β-CD])] to determine the stoichiometric ratio.We found the R_{max} value near 0.5[40]**(Fig. 2).** In general; R = 0.5 stands for 1:1 or 2:2 G:H (guest: host) complexes; R = 0.33 for 1:2 G:H complexes[41].Thus the value of R ,obtained experimentally, indicates successful inclusion of one guest molecule inside the hollow cavity of one molecule of β-CD promising the 1:1 host-guest inclusion.

Table2: Data for Job Plot performed by UV-Vis spectroscopy for ISD-β-CD system at 298.15K[a]

Guestconc. [ISD] (μm)	β-CD (μm)	R= [ISD]/ ([ISD]+[β-CD])	A @λmax 289 nm	ΔA (0.39195-A)	ΔA X [ISD]/ ([ISD]+[β-CD])
100	0	1	0.39195	0	0
90	10	0.9	0.34407	0.04788	0.043092
80	20	0.8	0.30812	0.08383	0.067064
70	30	0.7	0.27243	0.11952	0.083664
60	40	0.6	0.23841	0.15354	0.092124
50	50	0.5	0.19298	0.19897	0.099485
40	60	0.4	0.1663	0.22565	0.09026
30	70	0.3	0.1345	0.25745	0.077235
20	80	0.2	0.09087	0.30108	0.060216
10	90	0.1	0.05604	0.33591	0.033591
0	100	0	0.01112	0.38083	0

[a]Standard uncertainties in temperature: ± 0.01K, Pressure:± 10kPa

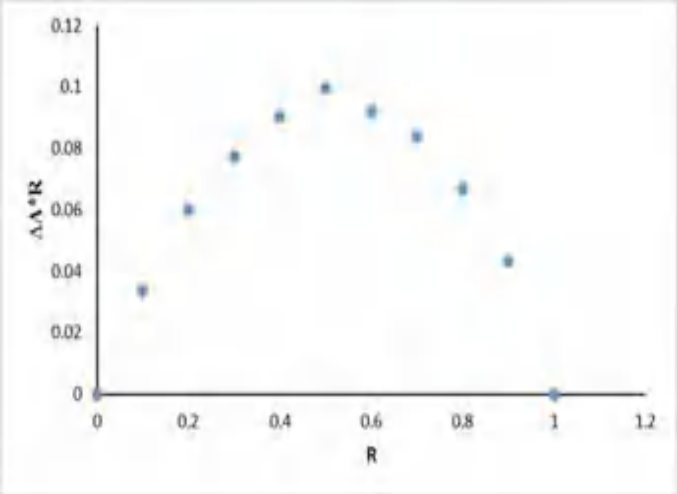

Fig.2: Job plot of β-Cyclodextrin (β-CD) and Indigosulfonic Acid dipotassium salt (ISD) system at λ_{max} (Indigosulfonic Acid Dipotassium Salt) = 289 nm

3.2. Association constants and thermodynamic parameters: UV-Visible spectroscopy being the most consistent method to calculate the association constant (K_a) for the formation of IC [42].Incorporation of the guest (act as a chromophore) molecule inside the hydrophobic cavity of the CD molecule indulges some variations of the chemical environment [43, 40].

The guest molecule binds to the host molecule by means of hydrophobic interactions. We recorded the UV-Visible spectra of the complexes at different concentrations of the host molecule keeping the concentration of the guest molecule fixed **(Fig.1).**The changes in the values of absorbance (at λ_{max}= 289nm) were noted at three distinct temperatures. A graph of $1/\Delta A$ against 1/[CD] was plotted to calculate the association constant using Benesi–Hildebrand equation (See supporting information **Table 3, 4, 5 and Fig. 4)[**40,44] equation (1).

$$\frac{1}{\Delta A} = \frac{1}{\Delta\varepsilon[ISD]K_a} x \frac{1}{[CD]} + \frac{1}{\Delta\varepsilon[ISD]} \quad (1)$$

The higher positive values of K_a at three different temperatures signify the increasing feasibility of the process (**Table 6).**The values of the K_a were used to determine the change in the enthalpy (ΔH^0) and entropy (ΔS^0) of the inclusion process. We plotted log K_a against *1/T* following van't Hoff equation (2) **(Fig. 5).** The values of ΔH^0 and ΔS^0 found are given in the table6 and from these values ΔG^0 was calculated[2,42].

$$2.303 \log K_f = -\frac{\Delta H^0}{RT} + \frac{\Delta S^0}{R} \quad (2)$$

In this experiment, the values of ΔH^0 and ΔS^0 were found to be negative. This signifies that the formation of the IC is an exothermic process and is entropy-restricted **(Table 6)**[2].This may be due to the molecular association of the CD and ISD molecules. As a result of association, the entropy is decreased, which is contrary for a process to be spontaneous. However, the restriction due to negative ΔS value is overcome by the highly negative value of ΔH making the entire inclusion process thermodynamically favourable.

The negative Gibb's free energy change (ΔG^0) of a process is the measure of the spontaneity of that process. Thus, ΔG^0 of the process of inclusion was calculated using the values of thermodynamic parameters ΔH^0 and $\Delta S^0$from the following equation (3) at 298.15K.

$$\Delta G^0 = \Delta H^0 - T\Delta S^0 \quad (3)$$

It is seen that the value of ΔG^0 is negative **(Table 6).** This, in fact, concludes that the formation of the ICs is feasible and the process is an exergonic one. This is due to the effective association of the guest ISD molecule inside the suitable cavity of CD molecule.

Table 3: Data for the Benesi-Hildebrand double reciprocal plot performed by UV-VIS spectroscopic study for ISD-β-CD complex at 293.15 K

	[ISD] (μM)	[CD] (μM)	A_0	A_1	ΔA	1/ΔA	1/cd
ISD+β-CD	50	10	0.21546	0.22035	0.00489	204.499	100000.00
	50	20	0.21546	0.22473	0.00927	107.8749	50000.00
	50	30	0.21546	0.22804	0.01258	79.49126	33333.33
	50	40	0.21546	0.22924	0.01378	72.56894	25000.00

50	50	0.21546	0.23439	0.01893	52.8262	20000.00
50	60	0.21546	0.23559	0.02013	49.6771	16666.67
50	70	0.21546	0.23681	0.02135	46.83841	14285.71
50	80	0.21546	0.23951	0.02405	41.58004	12500.00
50	90	0.21546	0.24102	0.02556	39.12363	11111.11
50	100	0.21546	0.24447	0.02901	34.47087	10000.00

Table 4: Data for the Benesi-Hildebrand double reciprocal plot performed by UV-VIS spectroscopic study for ISD-β-CD systems at 303.15 K

	[Drug] (μM)	[CD] (μM)	A_0	A_1	ΔA	1/ΔA	1/[CD]
ISD-β-CD	50	10	0.20213	0.20707	0.00494	202.4291	100000
	50	20	0.20213	0.21126	0.00913	109.529	50000
	50	30	0.20213	0.21561	0.01348	74.18398	33333
	50	40	0.20213	0.21906	0.01693	59.06675	25000
	50	50	0.20213	0.22258	0.02045	48.89976	20000
	50	60	0.20213	0.22429	0.02216	45.12635	16667
	50	70	0.20213	0.22641	0.02428	41.18616	14286
	50	80	0.20213	0.22656	0.02443	40.93328	12500
	50	90	0.20213	0.22879	0.02666	37.50938	11111
	50	100	0.20213	0.23637	0.03424	29.20561	10000

Table 5: Data for the Benesi-Hildebrand double reciprocal plot performed by UV-VIS spectroscopic study for ISD-β-CD systems at 313.15 K

	[Drug] (μM)	[CD] (μM)	A_0	A_1	ΔA	1/ΔA	1/[CD]
ISD+β-CD	50	10	0.19368	0.19822	0.00454	220.26432	100000
	50	20	0.19368	0.20315	0.00947	105.59662	50000
	50	30	0.19368	0.20616	0.01248	80.128205	33333
	50	40	0.19368	0.20761	0.01393	71.787509	25000
	50	50	0.19368	0.21313	0.01945	51.413882	20000
	50	60	0.19368	0.21394	0.02026	49.358342	16667
	50	70	0.19368	0.21496	0.02128	46.992481	14286
	50	80	0.19368	0.21971	0.02603	38.417211	12500
	50	90	0.19368	0.22884	0.03516	28.441411	11111
	50	100	0.19368	0.23792	0.04424	22.603978	10000

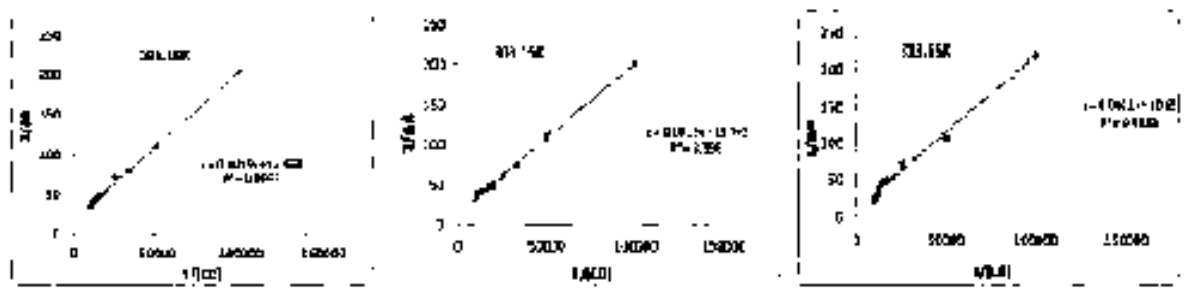

Fig.4: Benesi-Hildebrand double reciprocal plot for the effect of β-CD on the absorbance of ISD at three different temperatures 293.15 K, 303.15 K and 313.15 K.

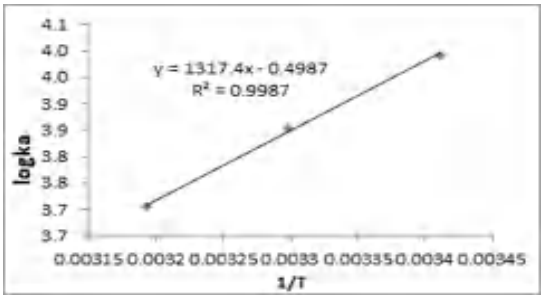

Fig.5: Plot of logK_a vs 1/T for the interaction of β-CD with ISD.

Table 6: Association constants obtained by the Benesi−Hildebrand method (K_a) from UV-Visible study, Fluorescence study and ITC study along with corresponding thermodynamic parameters of Indigosulfonic Acid dipotassium Salt-β-cyclodextrin inclusion complexes at 293.15K[a], 303.15K[a] and 313.15K[a].

Method	K_a**(10^{3}M^{-1})**			ΔG^0 **(kJmol^{-1})**	ΔH^0 **(kJ mol^{-1})**	ΔS^0**(Jmol^{-1}) K^{-1}**
	293.15K	303.15K	313.15K			
UV-Vis Spectroscopy	9.82	7.13	5.07	-2.38	-5.23	-9.55
Fluorescence Spectroscopy	9.51	-	-	-	-	-
ITC study	8.70±1.98			-3.203	-1.60±0.23	5.38

3.3. Fluorescence study: With the help of fluorescence study we can evaluate the binding constant by observing the reasonable change in the fluorescence emission spectrum due to some sort of interactions between β-CD and ISD.

The modified Stern-Volmer equation (equation 4) was employed to determine the extent of interaction (association constant K_a) between the host and guest molecule used in this experiment,

$$\frac{F_0}{\Delta F} = \frac{1}{F_q.K_a.[\mathrm{Q}]} + \frac{1}{F_q} \quad (4)$$

Where, ΔF is the difference in fluorescence at a concentration [Q] in absence and presence of cyclodextrin. K_a, the quenching constant, is equivalent to the association constant. F_q is the fraction of fluorescence accessible to the quencher (here cyclodextrin). From the plot of $F_0/\Delta F$ vs 1/[Q] the binding constant was calculated[44-46].

The concentration of ISD was kept constant at 0.5μM while the concentrations of β-CD varied from 0.2 μM to 0.8 μM. **(Table7, Fig.6).** From fluorescence study, the association constant was found to be 9.51x10^3 at 298.15K, which is comparable to the association constant obtained from the UV-Visible spectroscopy at 293.15K**(Table7).**

Table 7: Data for calculation of Association Constant using fluorescence spectroscopic study

Fo	F	ΔF= Fo-F	1/[β-CD] /M-1	1/ΔF	Intercept	Slope	K_a /M^{-1}
987921.44	1028281.44	40360.00	50000.00	2.48E-05			
987921.44	1038976.82	51055.38	33333.33	1.96E-05			
987921.44	1052248.39	64326.95	25000.00	1.55E-05	3.8E-06	4E-10	9512.25
987921.44	1067024.89	79103.46	20000.00	1.26E-05			
987921.44	1080453.77	92532.33	16666.67	1.08E-05			
987921.44	1092249.02	104327.58	14285.71	9.59E-06			
987921.44	1101122.40	113200.96	12500.00	8.83E-06			

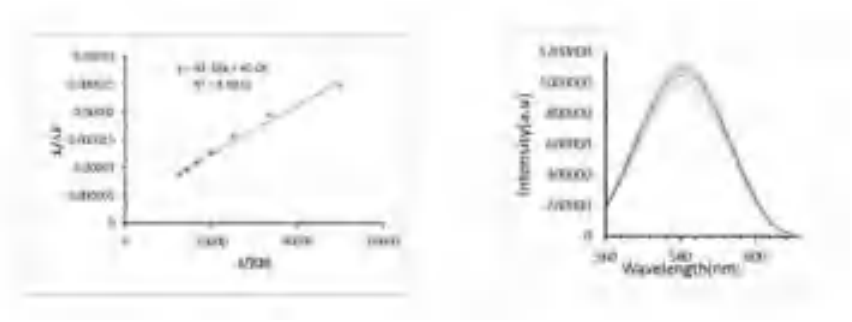

Fig.6: Plot of 1/ΔF (ΔF is the absorbance difference of guest in presence and absent of CD) Vs 1/[CD] ([CD] is the concentration of CD) from the Stern-Volmer equation and fluorescence spectra of Indigosulfonic Acid Dipotassium salt and β-Cyclodextrin at different molar concentration.

3.4. Calorimetric characterization of complexation: In order to calculate the weak binding constants and the corresponding thermodynamic parameters for the host-guest inclusion complex with high accuracy, we have applied Isothermal titration calorimetry (ITC) method. This analytical method is used to determine binding constants ranging from 10^8 to 10^2 M^{-1} [47].It has become an effective method for directly determining the thermodynamic parameters instead of the previously used van't Hoff equation methodology, ITC method is more precise in terms of the determination of thermodynamic parameters [48]. The ITC diagrams of ISD binding to β-CD are given in **Fig. 7.**

From the plot of ITC, of ISD and Beta CD, the upper graph denotes heat release upon each injection of ISD to the sample cell i.e. in Beta CD [49]. The heat release is generally due to complexation of the guest molecule with the host until saturation is achieved that means guest molecules are getting associated to the specific number of the host molecules. It has been observed that the process of inclusion of ISD inside the β-CD is exothermic in nature and the magnitude of the heat evolved during the inclusion process decreases gradually with each injection until complete saturation is achieved.

The extent of the host-guest inclusion is supported by the structural orientation of cyclodextrin molecule which makes the non-polar part of the guest molecule to enter into the hollow cavity of CD molecule, thus the inclusion complex gets stability [42].Another driving force for inclusion process can be attributed to the fact of releasing the water molecules from the hydrophobic cavity into the bulk and hence the total entropy of the system gets increased [50]. The incorporation of the guest molecule takes place from the wider rim of the β-CD molecule, as evident from NOESY spectrum.

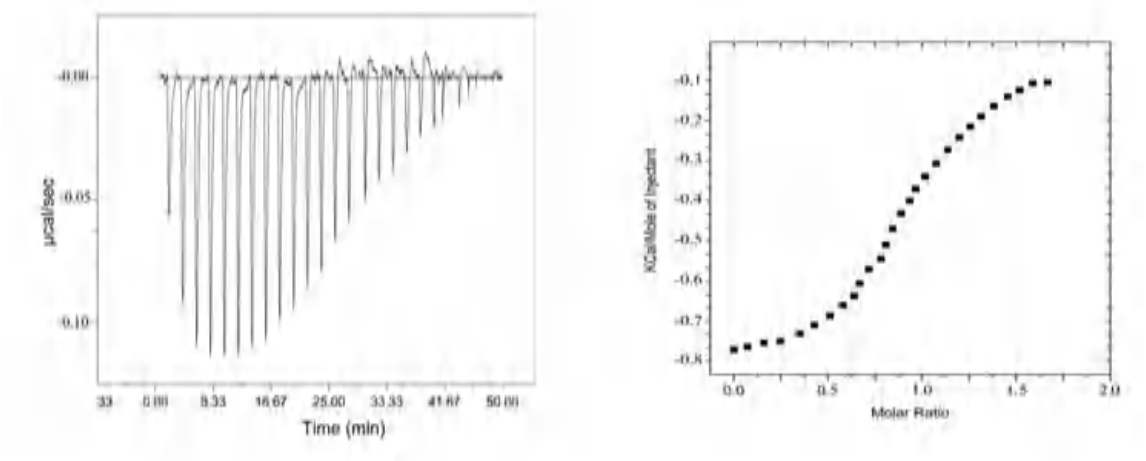

Fig.7: Representative ITC(Isothermal Titrtion Calorimetry) profiles for the titration of ISD(Indigosulfonic Acid Dipotassium salt) (500mM) with β-CD (50 mM) at 298.15 K. figure above represent the raw data for the continuous injection of β-CDs(β-Cyclodextrin) into the ISD(Indigosulfonic Acid dipotassium Salt), after correction of heat of dilution. Figure below is the binding isotherm fitted to the raw data and the bottom panels show the integrated heat data after correction of heat of dilution.

The heats of binding were plotted as a function of the molar ratio of [CD/ISD]. The binding parameters like the stoichiometry of binding (N^c), the equilibrium binding constant (K), enthalpy of complexation (ΔH^0) and standard changes in free energy (ΔG^0) and entropy (ΔS^0) were estimated from ITC data on the basis of fitting the data according to the independent binding model. The values of thermodynamic parameters, particularly ΔH^O and ΔS^O**(Table 6),** shows that of the complexation deals with non-covalent forces in solvent medium, e.g. electrostatic, hydrophobic, van der Waals, and H-bonding interaction. The complexation process was found to be exothermic ($\Delta H^0<0$) and spontaneous ($\Delta G^0<0$) with positive entropic contribution. The negative value of ΔH^0 indicates heat evolution during the inclusion phenomenon while positive entropy changes (ΔS^0) usually arise from the translational and conformational freedoms of host and guest upon complexation.

Negative Gibbs energy indicates that inclusion process is a spontaneous one under experimental conditions; $-T\Delta S^0$, denotes that inclusion of ISD in the CDs is accompanied by displacement of water molecules from the CD cavity. On the other hand, comparatively it has been observed that smaller $-T\Delta S^0$ terms are associated with larger CD cavities [51].Every peak shown in the binding isotherm indicates a single injection of the guest molecule into the host solution. The exothermicity of the calorimetry peaks **(Fig. 7)** arises because of the considerable interaction between ISD and β-CD molecule. The stoichiometry (N^c) of the inclusion phenomena using ITC analysis is determined from the value of number of binding sites. We obtained the value very close to 1 (Table 8), which clearly indicates 1:1 stoichiometry, which is in good agreement with the 1:1 stoichiometric ratio obtained from the Benesi-Hildebrand plot analysis of the UV-Visible spectroscopic data.

The principal forces involved are van der Waals and hydrophobic interactions. Hydrophobic interactions are entropy driven ($|H^0|<|T\Delta S^0|$), whereas van der Waals interactions are essentially enthalpy driven processes, [52, 53]. From the data obtained, it has been found that the binding of ISD with β-CDs are entropy driven as the enthalpy value of the interaction is smaller with respect to the entropy of the interaction ($|H^0|<|T\Delta S^0|$). This indicates hydrophobic interactions predominate over major van der Waal's interactions in this case.

Table 8: Value indicating the Binding sites obtained from Isothermal Titration Calorimetric study.

Temperature(K)	Number of binding sites(N^C)
298.15	0.954±0.0693

3.5. FT-IR SPECTROSCOPY

During inclusion procedure, if the guest molecule gets inserted into the hollow cavity of CD molecule some changes in stretching frequencies of the concerned spectral bands will take place, in other words either the spectral bands will get shifted from their previous positions or two spectral bands get merged or widening of bands happen. From the FTIR spectral pattern, we found some bands were absent and some got shifted from its earlier positions in the inclusion complex **(Table 9, Fig.8).** In the IC the bands due to the O-H stretching, stretching of –C-H from $–CH_2$, bending of C-O-C of β-CD are found shifted from 3406.34 cm^{-1} to 3458.65 cm^{-1}, 2944.46 cm^{-1} to 2934.45cm^{-1}, 1163.56cm^{-1} to 1152.45cm^{-1}. On the other hand, band at 1631.15 cm^{-1} for the Stretching due to conjugated C=O was found shifted to 1661.53 cm^{-1} and stretching due to C-N was shifted from 1420.43 cm^{-1} to 1464.32 cm^{-1}. In pure CD bending of –C-H from $–CH_2$ and bending of O-H at 1403.38 cm^{-1} were found absent. In the guest molecule, stretching due to aliphatic N-H bond at 3446.17 cm^{-1}, out of plane C-H bending at 820.27cm-^{1} and broad band due to bending of N-H bond at 674.07 cm^{-1} were found absent in the FT-IR spectra of ISD-CD IC.

Table 9: Data obtained from FT-IR spectroscopic study of β-CD, ISD and β-CD+ISD.

Groups	Wave number(Cm^{-1})		
	β-CD	ISD	ISD-β-CD
stretching of O-H	3406.34		3458.65
stretching of –C-H from $–CH_2$	2944.46		2934.45
bending of –C-H from $–CH_2$ and bending of O-H	1403.38		
bending of C-O-C	1163.56		1152.45
vibration involving α-1,4 linkage	958.23		957.34
Stretching due to Aliphatic N-H bond		3446.17	
Stretching due to conjugated C=O		1631.15	1661.53
Stretching due to C-N		1420.43	1464.32
Out of plane C-H bending		820.27	
Broad band due to bending of N-H bond		674.07	

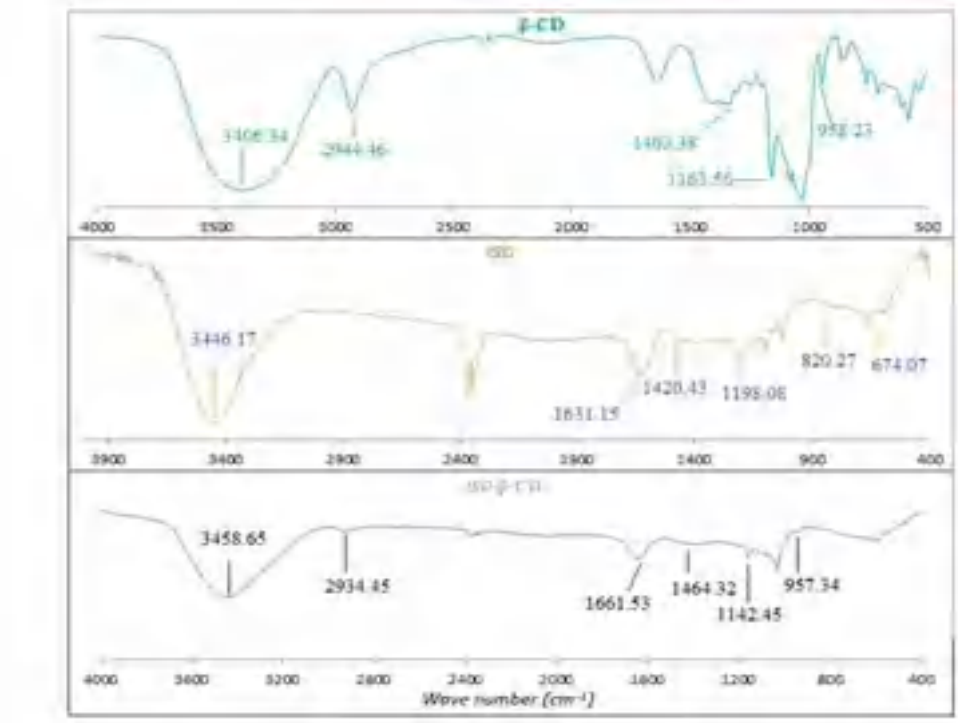

Fig.8: FT-IR spectra of β-Cyclodextrin, pure Indigosulfonic acid dipotassium salt and ISD-β-Cyclodextrin inclusion complex.

3.6.^{1}H NMR AND 2D NOESY spectral analysis of solid inclusion complex: The inclusion complex formation between β-CD and ISD can be established with thehelp of ^{1}H NMR study. The change in chemical shifts values of the protons of inclusion complex is of main interest here. The H3, H5 protons of β-CD situated in the interior hydrophobic cavity where H3 is at the wider rim and H5 is at the narrower rim. The chemical shift values obtained from the ^{1}H-NMR spectroscopic analysis were recorded **(table10 and Fig.9).**

Table 10: The chemical shift values of β-CD, pure ISD and ISD-β-CD IC obtained from ^{1}H- NMR spectroscopy.

β-CD(400 MHz, Solvated in D_2O) δ /ppm	3.48–3.53 (6H,t, J = 9.2 Hz), 3.56–3.59 (6H, dd, J = 9.6, 3.2 Hz), 3.73–3.78 (18H,m), 3.87–3.92 (6H, t, J = 9.2 Hz), 5.00–5.01 (6H, d, J = 3.6 Hz).
ISD	6.85-6.87(2H,d,J=6.8Hz),7.65-7.67(2H,d,J=7.6Hz),7.92(2H,s)
ISD-β-CD IC	3.42-3.48 (6H, t, J = 9.2 Hz), 3.51-3.57 (6H, dd, J =9.6, 3.2 Hz), 3.53-3.59 (18H, m), 3.63-3.67 (6H, t, J=9.2 Hz), 5.01-5.02 (6H, d, J = 3.6 Hz), 0.95(3H, s);6.87-6.90(2H,d,J=6.8Hz),7.69-7.72(2H,d,J=7.6Hz),7.98(2H, s).

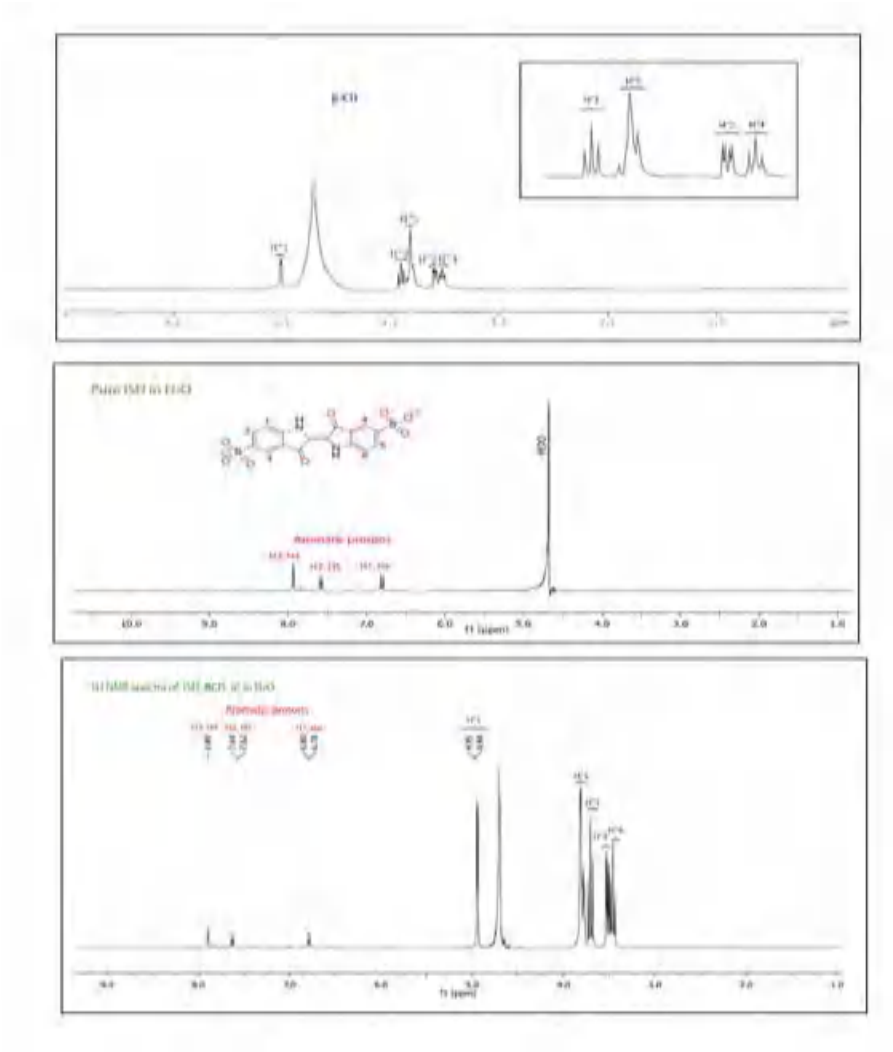

Fig.9: ^{1}H NMR spectra of β-Cyclodextrin, pure Indigosulfonic acid dipotassium salt and β-CD-ISD inclusion complex.

From the data tabulated in the **table 10** it is seen that H3 proton experiences more interaction compared to H5 proton. The more up field shift of the H3 proton of β-CD in the inclusion complex than the H5 proton clearly suggest that insertion occurs through the wider rim **(Table 11).** The other protons are at the same position as in the pure β-CD. So, from the chemical shifts values of the interacting protons (mainly H3 and H5) we can come to the conclusion that the guest molecule is entering towards the hydrophobic cavity from the hydrophilic environment[54,55]. This, in fact, supports the association constant values obtained from UV-Vis, fluorescence and ITC studies.

Table 11: Change in chemical shifts (ppm) of the H3 and H5 protons of β-cyclodextrin molecule in host-guest complexes in D_2O.

Protons of CD	ISD+β-CD
H3	0.24
H5	0.19

DOI:10.24214/jcbps.A.11.2.30423.]

In NOE spectroscopy the two protons at 0.4 nm apart in space can cause nuclear overhauser effect [36].It is an imperative method to interpret the extent of interaction among the host (β-cyclodextrin) and guest (ISD) molecules when two protons are in close proximity (3-5Å).Then the appearance of an NOE cross peak can be detected among the relevant protons in the NOESY spectrum. The existence of the host-guest interaction in ISD-β-CD inclusion complex can be proved by Nuclear Overhauser Effect measurements (NOESY spectrum) in D_2O medium. The NOESY spectrum of the IC shows significant NOE cross-peaks between the H''3 and H''5 protons of cyclodextrin and the aromatic protons (H1, H2, H3, H4, H5, H6) of ISD molecule **(Fig.10).** These results obtained satisfactorily coincide with the tentative complex structure given in **fig.11,** indicating the partial inclusion of dye molecule into the cavity of Cyclodextrin. Such observation strongly supports the existence of the non-covalent type of interaction in the complexation of ISD by the β-CD molecule.

The NOE cross-peaks between aromatic protons of ISD (circled in the **Fig. 10)** and H"5, H"3 protons of CD was observed implying complete insertion of non-polar part of ISD into the β-CD cavity. The NOESY spectrum also specified the insertion of the non-polar part of the ISD into the β-CD cavity by the interaction between H1, H2, H3 protons of the guest molecule and H"3, H"5 from the CD, which completely supports the shift of H"3 and H"5 protons in the 1H-NMR spectroscopic study.

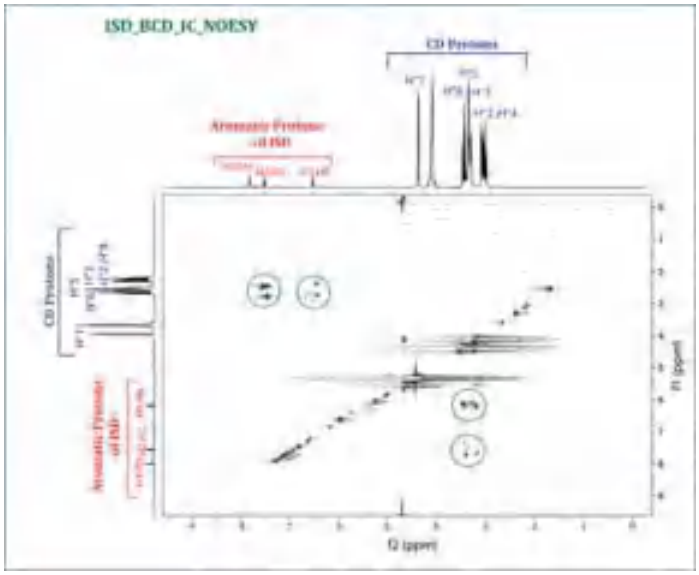

Fig.10:2D NOESY NMR spectra of ISD-β-Cyclodextrin inclusion complex.

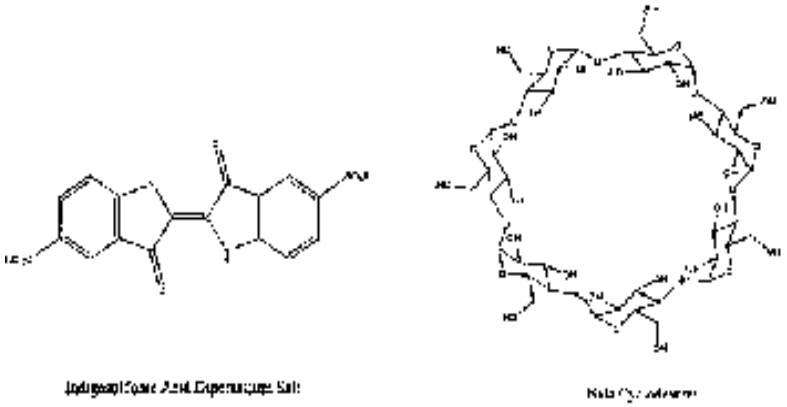

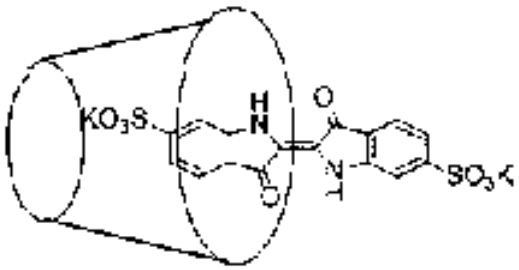

Inclusion Complexation through the wider rim

Fig 11: Structures of Indigosulfonic Acid Dipotassium Salt and β-Cyclodextrin and their schematic representation of inclusion.

3.7. Structural Effect of Cyclodextrin: The formation of host-guest IC is mainly focused on the structural combination of both the molecules. ICs are formed only when there is the stronger association between the guest and host molecules over other forces. The complexation strength depends on the factors such as the size of the guest molecule, the van der Waals interactions, the release of water molecules, hydrogen bonding, charge transfer interactions, hydrophobic interactions, the release of conformational strain etc. Here, the hydrophobic part of the dye molecule enters inside the hydrophobic cavity of the CD molecule during the formation of the inclusion complex and it is stated that no covalent bond forms or breaks in the system of IC[8, 56].

The interesting fact is that the cavity of the CD molecule is blocked by water molecules but this is unfavourable. When the hydrophobic part of the guest molecule enters inside the hollow cavity of CD, the water molecules are easily replaced. It is clear that the hydrophobic interaction predominates here. However, entropy of the system increases due to the elimination of the water molecules to the bulk as seen from the ITC experiment, which helps the process of formation of the ICs to be spontaneous. The size of the guest molecule or more specifically the hydrophobic part of the guest molecule, which enters into the CD cavity, is another determining factor for the formation of the IC. The hydrophobic part of ISD fits better inside β-CD by relieving the ring strain of the CD as well as lowering the energy of the system. Encapsulation of a single ISD molecule sterically blocks the side of the wider rim inhibiting other molecule to enter inside the cavity, which is reflected in the UV-Vis study of Job plot.

3.8. SEM Study: Scanning Electron Microscope study is a qualitative method to figure out the morphological changes of the starting compound and the inclusion complex attained by the complexation by host β-CD molecule.**Fig.12** shows the micro images of A, B and C. The surface morphology of the three components namely β-cyclodextrin (host), ISD (guest) and their inclusion complex were studied by scanning electron microscope. The surface morphology of β-CD appears as flat configuration having a regular arrangement of fine lines whereas pure ISD is found to have thread/flakes like morphology. ISD.β-CD inclusion complex appears like irregular shaped crystals [the surface looks like crystals (though no real crystals are there) here only the surface morphology is considered], in which the original morphology of both of the starting compounds gets disappeared.Those changes on the surface structure of the isolated compounds indicate the establishment of interactions with a new phase formation.

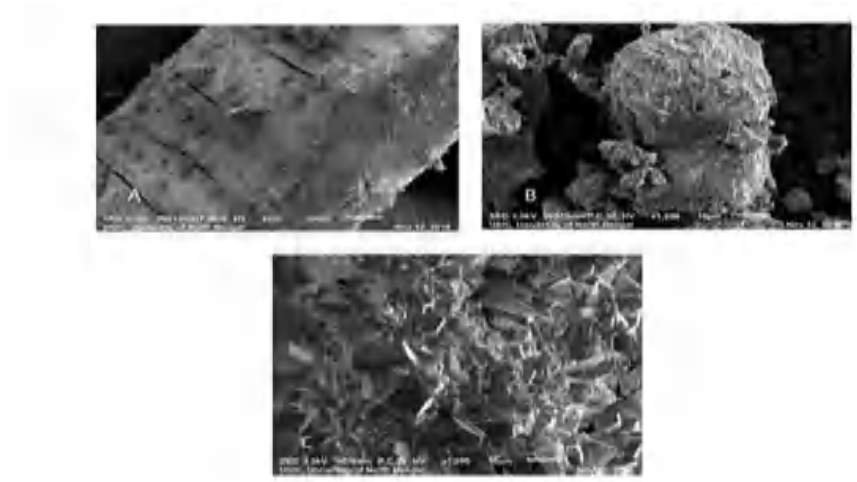

Fig.12: SEM images of (A) pure β-Cyclodextrin, (B) pure Indigosulfonic acid Dipotassium Salt and (C) ISD.β-CD inclusion complex.

CONCLUSION

In this study we have successfully characterised the inclusion of the dye molecule Indigosulfonic Acid Dipotassium Salt inside the naturally occurring oligosaccharide β-CD molecule. The IC was characterised using various thermodynamic as well as spectroscopic methods. The negative value of ΔG of the process, the high association constant from UV-Vis and ITC study of the inclusion show that the IC formed is more stable compared to the pure ISD. The higher stability may be the main reason for the controlled release of the ISD. The inclusion complex found to have higher solubility in water compared to the free ISD. Thus it may reduce the toxic effect generated from colouring foods and drugs. Moreover its controlled release inside the body may reduce the toxicity. As cyclodextrins have very low toxicity, it might be anticipated that the inclusion process makes the overall moiety (IC) of very low toxicity. This study may further open scopes for scientific and industrial research in future.

ACKNOWLEDGEMENTS

All the authors have extreme gratitude to the Special Assistance Scheme, Department of Chemistry, and NBU for instrumental and financial support. Prof. M.N. Roy is also grateful to the UGC-BSR (Basic Scientific Research) for the one-time grant award. Authors would also like to acknowledge USIC, NBU for doing SEM.

REFERENCES

1. J. Carrazana, B. Reija, P.R. Cabrer, W. Al-Soufi, M. Novo, J.V. Tato, Complexation of Methyl Orange with ß-cyclodextrin: Detailed Analysis and Application to Quantification of Polymer-bound Cyclodextrin, Supramolecular Chemistry 16(8) (2004) 549-559.
2. S. Saha, T. Ray, S. Basak, M.N. Roy, NMR, surface tension and conductivity studies to determine the inclusion mechanism: thermodynamics of host–guest inclusion complexes of natural amino acids in aqueous cyclodextrins, New Journal of Chemistry 40(1) (2016) 651-661.

3. M.L. Bender, M. Komiyama, Cyclodextrin chemistry, Springer Science & Business Media2012.
4. J.H. Fendler, Membrane mimetic chemistry: characterizations and applications of micelles, microemulsions, monolayers, bilayers, vesicles, host-guest systems, and polyions, Wiley New York1982.
5. J.L. Atwood, J.E.D. Davies, D.D. MacNicol, Inclusion compounds, Academic Press1984.
6. K. Kalyanasundaram, Photochemistry in microheterogeneous systems, Elsevier2012.
7. Y. Izadmanesh, J.B. Ghasemi, Thermodynamic study of β-cyclodextrin-dye inclusion complexes using gradient flow injection technique and molecular modeling, SpectrochimicaActa Part A: Molecular and Biomolecular Spectroscopy 165 (2016) 54-60.
8. B.K. Barman, A. Dutta, M.N. Roy, Sustenance of Inclusion Complexes of Ionic Liquid with Cyclic Oligosaccharide Molecules in Liquid and Solid Phases by Diverse Approaches, ChemistrySelect 3(26) (2018) 7527-7534.
9. S. Barman, B.K. Barman, M.N. Roy, Preparation, characterization and binding behaviors of host-guest inclusion complexes of metoclopramide hydrochloride with α-and β-cyclodextrin molecules, Journal of Molecular Structure 1155 (2018) 503-512.
10. L. Liu, Q.-X. Guo, Use of quantum chemical methods to study cyclodextrin chemistry, Journal of inclusion phenomena and macrocyclic chemistry 50(1-2) (2004) 95-103.
11. E. Kompantseva, M. Gavrilin, L. Ushakova, β-Cyclodextrin derivatives and their applications in pharmacology (a review), Pharmaceutical chemistry journal 30(4) (1996) 258-262.
12. C. Yañez, M. Araya, S. Bollo, Complexation of herbicide bentazon with native and modified β-cyclodextrin, Journal of Inclusion Phenomena and Macrocyclic Chemistry 68(1-2) (2010) 237-241.
13. P. Persico, C. Carfagna, Cosmeto-Textiles: State of the art and future perspectives, Advances in Science and Technology, Trans Tech Publ, 2013, pp. 39-46.
14. T. Wang, M. Wang, C. Ding, J. Fu, Mono-benzimidazole functionalized β-cyclodextrins as supramolecular nanovalves for pH-triggered release of p-coumaric acid, Chemical Communications 50(83) (2014) 12469-12472.
15. H. Zhou, T. Yamada, N. Kimizuka, Supramolecular thermo-electrochemical cells: enhanced thermoelectric performance by host–guest complexation and salt-induced crystallization, Journal of the American Chemical Society 138(33) (2016) 10502-10507.
16. L. Stricker, E.-C. Fritz, M. Peterlechner, N.L. Doltsinis, B.J. Ravoo, Arylazopyrazoles as light-responsive molecular switches in cyclodextrin-based supramolecular systems, Journal of the American Chemical Society 138(13) (2016) 4547-4554.
17. M. Xue, W. Wei, Y. Su, D. Johnson, J.R. Heath, Supramolecular probes for assessing glutamine uptake enable semi-quantitative metabolic models in single cells, Journal of the American Chemical Society 138(9) (2016) 3085-3093.
18. P. Díez, A. Sánchez, M. Gamella, P. Martínez-Ruíz, E. Aznar, C. De La Torre, J.R. Murguía, R. Martínez-Máñez, R. Villalonga, J.M. Pingarr n, Toward the design of smart delivery systems controlled by integrated enzyme-based biocomputing ensembles, Journal of the American Chemical Society 136(25) (2014) 9116-9123.

19. Y.L. Sun, Y.W. Yang, D.X. Chen, G. Wang, Y. Zhou, C.Y. Wang, J.F. Stoddart, Mechanized Silica Nanoparticles Based on Pillar [5] arenes for On-Command Cargo Release, Small 9(19) (2013) 3224-3229.
20. Y. Zhou, L.L. Tan, Q.L. Li, X.L. Qiu, A.D. Qi, Y. Tao, Y.W. Yang, Acetylcholine-triggered cargo release from supramolecular nanovalves based on different macrocyclic receptors, Chemistry–A European Journal 20(11) (2014) 2998-3004.
21. H. Li, D.-X. Chen, Y.-L. Sun, Y.B. Zheng, L.-L. Tan, P.S. Weiss, Y.-W. Yang, Viologen-mediated assembly of and sensing with carboxylatopillar [5] arene-modified gold nanoparticles, Journal of the American Chemical Society 135(4) (2013) 1570-1576.
22. Z. Zhang, G. Wu, J. Gao, T. Song, Inclusion complex of a Bcl-2 inhibitor with cyclodextrin: characterization, cellular accumulation, and in vivo antitumor activity, Molecular Pharmaceutics 7(4) (2010) 1348-1354.
23. G. Yu, K. Jie, F. Huang, Supramolecular amphiphiles based on host–guest molecular recognition motifs, Chemical reviews 115(15) (2015) 7240-7303.
24. E. Iglesias, Inclusion complexation of novocaine by β-cyclodextrin in aqueous solutions, The Journal of organic chemistry 71(12) (2006) 4383-4392.
25. J. Liu, W.E. Hennink, M.J. Van Steenbergen, R. Zhuo, X. Jiang, Versatile supramolecular gene vector based on host–guest interaction, Bioconjugate Chemistry 27(4) (2016) 1143-1152.
26. Z. Aytac, Z.I. Yildiz, F. Kayaci-Senirmak, N.O. San Keskin, S.I. Kusku, E. Durgun, T. Tekinay, T. Uyar, Fast-dissolving, prolonged release, and antibacterial cyclodextrin/limonene-inclusion complex nanofibrous webs via polymer-free electrospinning, Journal of agricultural and food chemistry 64(39) (2016) 7325-7334.
27. X. Chen, Z. Liu, S.G. Parker, X. Zhang, J.J. Gooding, Y. Ru, Y. Liu, Y. Zhou, Light-induced hydrogel based on tumor-targeting mesoporous silica nanoparticles as a theranostic platform for sustained cancer treatment, ACS applied materials & interfaces 8(25) (2016) 15857-15863.
28. Z.-Q. Shi, Y.-T. Cai, J. Deng, W.-F. Zhao, C.-S. Zhao, Host–guest self-assembly toward reversible thermoresponsive switching for bacteria killing and detachment, ACS applied materials & interfaces 8(36) (2016) 23523-23532.
29. H. Dong, Y. Wei, W. Zhang, C. Wei, C. Zhang, J. Yao, Y.S. Zhao, Broadband tunablemicrolasers based on controlled intramolecular charge-transfer process in organic supramolecular microcrystals, Journal of the American Chemical Society 138(4) (2016) 1118-1121.
30. H. Li, F. Li, B. Zhang, X. Zhou, F. Yu, L. Sun, Visible light-driven water oxidation promoted by host–guest interaction between photosensitizer and catalyst with a high quantum efficiency, Journal of the American Chemical Society 137(13) (2015) 4332-4335.
31. M. Šuleková, M. Smrčová, A. Hudák, M. Heželová, M. Fedorová, Organic colouring agents in the pharmaceutical industry, Folia Veterinaria 61(3) (2017) 32-46.
32. A. Dąbrowski, Adsorption—from theory to practice, Advances in colloid and interface science 93(1-3) (2001) 135-224.
33. A. Reife, Dyes, environmental chemistry, Kirk-OthmerEncyclopedia of Chemical Technology (2000).

34. M. Irimia-Vladu, E.D. Głowacki, P.A. Troshin, G. Schwabegger, L. Leonat, D.K. Susarova, O. Krystal, M. Ullah, Y. Kanbur, M.A. Bodea, Indigo-A natural pigment for high performance ambipolar organic field effect transistors and circuits, Advanced Materials 24(3) (2012) 375-380.

35. J. Seixas de Melo, A. Moura, M. Melo, Photophysical and spectroscopic studies of indigo derivatives in their keto and leuco forms, The Journal of Physical Chemistry A 108(34) (2004) 6975-6981.

36. S. Saha, A. Roy, M.N. Roy, Mechanistic Investigation of Inclusion Complexes of a Sulfa Drug with α-and β-Cyclodextrins, Industrial & Engineering Chemistry Research 56(41) (2017) 11672-11683.

37. Y. Yang, Q. Hu, Q. Zhang, K. Jiang, W. Lin, Y. Yang, Y. Cui, G. Qian, A large capacity cationic metal–organic framework nanocarrier for physiological pH responsive drug delivery, Molecular pharmaceutics 13(8) (2016) 2782-2786.

38. F. Cramer, W. Saenger, H.-C. Spatz, Inclusion compounds. XIX. 1a The formation of inclusion compounds of α-cyclodextrin in aqueous solutions. Thermodynamics and kinetics, Journal of the American Chemical Society 89(1) (1967) 14-20.

39. A. Roy, S. Saha, B. Datta, M.N. Roy, Insertion behavior of imidazolium and pyrrolidinium based ionic liquids into α and β-cyclodextrins: mechanism and factors leading to host–guest inclusion complexes, RSC Advances 6(102) (2016) 100016-100027.

40. J.V. Caso, L. Russo, M. Palmieri, G. Malgieri, S. Galdiero, A. Falanga, C. Isernia, R. Iacovino, Investigating the inclusion properties of aromatic amino acids complexing beta-cyclodextrins in model peptides, Amino Acids 47(10) (2015) 2215-2227.

41. J.S. Renny, L.L. Tomasevich, E.H. Tallmadge, D.B. Collum, Method of continuous variations: applications of job plots to the study of molecular associations in organometallic chemistry, AngewandteChemie International Edition 52(46) (2013) 11998-12013.

42. S. Saha, A. Roy, K. Roy, M.N. Roy, Study to explore the mechanism to form inclusion complexes of β-cyclodextrin with vitamin molecules, Scientific reports 6 (2016) 35764.

43. M. Shah, V. Shah, A. Ghosh, Z. Zhang, T. Minko, Molecular inclusion complexes of β-cyclodextrin derivatives enhance aqueous solubility and cellular internalization of paclitaxel: Preformulation and in vitro assessments, Journal of pharmaceutics & pharmacology 2(2) (2015) 8.

44. H.A. Benesi, J. Hildebrand, A spectrophotometric investigation of the interaction of iodine with aromatic hydrocarbons, Journal of the American Chemical Society 71(8) (1949) 2703-2707.

45. N. Roy, R. Ghosh, K. Das, D. Roy, T. Ghosh, M.N. Roy, Study to synthesize and characterize host-guest encapsulation of antidiabetic drug (TgC) and hydroxy propyl-β-cyclodextrin augmenting the antidiabetic applicability in biological system, Journal of Molecular Structure 1179 (2019) 642-650.

46. V.D. Suryawanshi, L.S. Walekar, A.H. Gore, P.V. Anbhule, G.B. Kolekar, Spectroscopic analysis on the binding interaction of biologically active pyrimidine derivative with bovine serum albumin, Journal of pharmaceutical analysis 6(1) (2016) 56-63.

47. G. Wenz, C. Strassnig, C. Thiele, A. Engelke, B. Morgenstern, K. Hegetschweiler, Recognition of Ionic Guests by Ionic β-Cyclodextrin Derivatives, Chemistry–A European Journal 14(24) (2008) 7202-7211.

48. G.A. Holdgate, W.H. Ward, Measurements of binding thermodynamics in drug discovery, Drug discovery today 10(22) (2005) 1543-1550.

49. B. Roy, P. Guha, P. Nahak, G. Karmakar, S. Maiti, A.K. Mandal, A.G. Bykov, A.V. Akentiev, B.A. Noskov, K. Tsuchiya, Biophysical Correlates on the Composition, Functionality, and Structure of Dendrimer–Liposome Aggregates, ACS Omega 3(9) (2018) 12235-12245.

50. H. Shekaari, F. Jebali, Volumetric and conductometric studies of some amino acids in aqueous ionic liquid, 1-hexyl-3-methylimidazolium chloride solutions at 298.15 K, Physics and Chemistry of Liquids 49(5) (2011) 572-587.

51. N.A. Todorova, F.P. Schwarz, The role of water in the thermodynamics of drug binding to cyclodextrin, The Journal of Chemical Thermodynamics 39(7) (2007) 1038-1048.

52. M. Rekharsky, Y. Inoue, Microcalorimetry in Cyclodextrins and Their Complexes: Chemistry, Analytical Methods, Applications, Wiley–VCH Verlag GmbH & Co. KGaA (2006) 215-222.

53. A. Cooper, C.M. Johnson, J.H. Lakey, M. Nöllmann, Heat does not come in different colours: entropy–enthalpy compensation, free energy windows, quantum confinement, pressure perturbation calorimetry, solvation and the multiple causes of heat capacity effects in biomolecular interactions, Biophysical chemistry 93(2-3) (2001) 215-230.

54. B.K. Barman, B. Rajbanshi, A. Yasmin, M.N. Roy, Exploring inclusion complexes of ionic liquids with α-and β-cyclodextrin by NMR, IR, mass, density, viscosity, surface tension and conductance study, Journal of Molecular Structure 1159 (2018) 205-215.

55. M.N. Roy, A. Roy, S. Saha, Probing inclusion complexes of cyclodextrins with amino acids by physicochemical approach, Carbohydrate polymers 151 (2016) 458-466.

56. D. Ekka, M.N. Roy, Molecular interactions of α-amino acids insight into aqueous β-cyclodextrin systems, Amino Acids 45(4) (2013) 755-777.

57. V. Balzani and E Scandola Supramolecular Photochemistry, Ellis Horwood, New York, 1991, pp. 288-318.

58. Synthesis of a New Indigo Vat Dye 1Nwokonkwo D. C. and 2Okafor C. O. 1Department of Industrial Chemistry, Faculty of Sciences, Ebonyi State University Abakaliki, Nigeria. 2Department of Pure and Industrial Chemistry,University of Nigeria, Nsukka, Nigeria.

Corresponding author: Mahendra Nath Roy

1Department of Chemistry, University of North Bengal, Darjeeling-734013, India.

mahendraroy2002@yahoo.co.in,Tel: +91 353 2776381, Fax: +91 353 2699001.

Online publication Date: 10.04.2021

Synthesis and Characterization of Inclusion Complex of DL-Aminoglutethimide with β-Cyclodextrin and Its Innovative Application in Biological System: Computational and Experimental Investigations

[1]Samapika Ray, [1]Niloy Roy, [2]Biraj Kumar Barman, [1]Paramita Karmakar, [1]Pranish Bomzan, [1]Biplab Rajbanshi, [3]Ankita Dutta, [3]Anoop Kumar and Mahendra Nath Roy[1*]

[1]Department of Chemistry, University of North Bengal, Darjeeling 734013, India

[2]Departmet of Chemistry, Parimal Mitra Smriti Mahavidyalaya, Malbazar, Jalpaiguri, India

[3]Department of Biotechnology, University of North Bengal, Darjeeling 734013, India

---

(**Accepted in ACS Omega**)

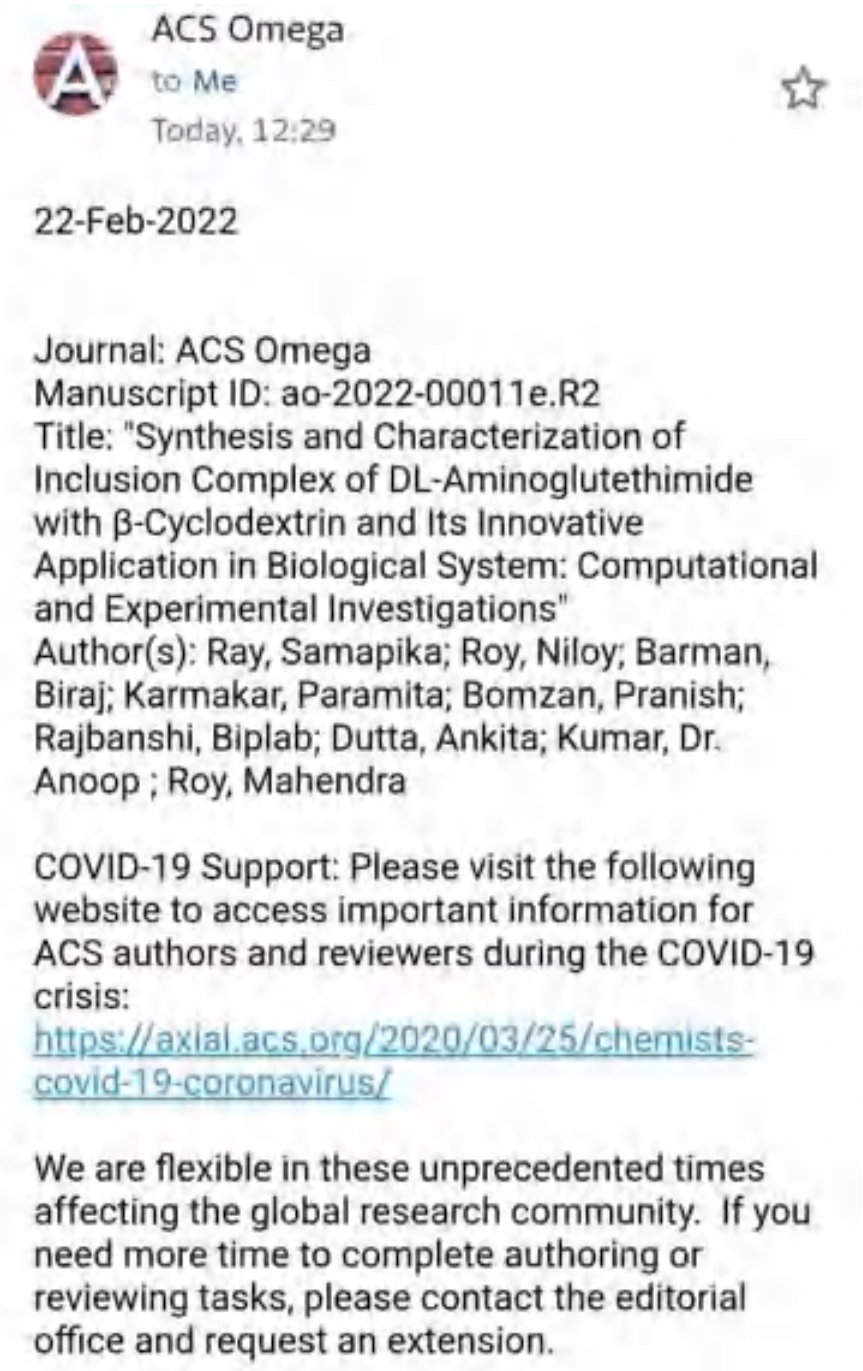

ACS Omega
to Me
Today, 12:29

22-Feb-2022

Journal: ACS Omega
Manuscript ID: ao-2022-00011e.R2
Title: "Synthesis and Characterization of Inclusion Complex of DL-Aminoglutethimide with β-Cyclodextrin and Its Innovative Application in Biological System: Computational and Experimental Investigations"
Author(s): Ray, Samapika; Roy, Niloy; Barman, Biraj; Karmakar, Paramita; Bomzan, Pranish; Rajbanshi, Biplab; Dutta, Ankita; Kumar, Dr. Anoop ; Roy, Mahendra

COVID-19 Support: Please visit the following website to access important information for ACS authors and reviewers during the COVID-19 crisis:
https://axial.acs.org/2020/03/25/chemists-covid-19-coronavirus/

We are flexible in these unprecedented times affecting the global research community. If you need more time to complete authoring or reviewing tasks, please contact the editorial office and request an extension.

Dear Dr. Roy:

Thank you for submitting your manuscript to ACS Omega.

We are pleased to inform you that your manuscript ao-2022-00011e.R2 is about to be accepted for publication in ACS Omega. Prior to formal acceptance please perform the following formatting changes:

- In case your current addresses differ from the research affiliations they should be included as footnotes. (affiliations in the system and MS must match)
- Please update and label the abstract upon submission of your revised manuscript to match the manuscript file.

- The following formats for journal (1) and book (2) entries must be used in the references:
(1) Doe, J. S.; Smith, J.; Roe, P. Syntheses and biological activities of rebeccamycin analogues. Introduction of a halogenoacetyl substituent. J. Am. Chem. Soc.(in italic) 1968 (bold), 90 (in italic), 8234−8241.
(2)Fierke, C. A.; Hammes, G. G. Transient kinetic approaches to enzyme mechanisms. In Contemporary Enzyme Kinetics and Mechanism, 2nd ed.; Purich, D., Ed.; Academic Press: New York, 1996; pp 1−35.

← Roy, Mahendra ao-2022-00011e....

York, 1996; pp 1−35.
For journal articles published online ahead of print or online only, the DOI should be used:
2. Liu, C.; Yang, S. Synthesis of angstrom-scale anatase titania atomic wires. ACS Nano 2009, DOI: 10.1021/nn900157r.

PLEASE NOTE: Please do not highlight the changes. Please do not make other changes since the manuscript is checked as is. Please do not remove or add any references, just make he asked corrections to existing ones

To revise your manuscript, log into ACS Paragon Plus with your ACS ID at http://acsparagonplus.acs.org/ and select "My Authoring Activity". There you will find your manuscript title listed under "Revisions Requested by Editorial Office." Your original files are available to you when you upload your revised manuscript. If you are replacing files, please remove the old version of the file from the manuscript before uploading the new file. Please upload manuscript file that is free of any annotations or highlights.

Funding Sources: Authors are required to report ALL funding sources and grant/award numbers relevant to this manuscript. Enter all sources of funding for ALL authors relevant to this